



Norwegian University of Life Sciences
Faculty of Science and Technology
Department of Building- and Environmental Technology

Philosophiae Doctor (PhD)
Thesis 2023:16

Microplastics in stormwater runoff: Measuring tire wear particles (TWP) concentration in the road environment and effect of treatment systems

Mikroplast i veiavrenning: Måling av konsentrasjon av dekkslitasjepartikler (DSP) i veimiljøet og renseeffekt i anlegg for overvann

Demmelash Mengistu

Microplastics in stormwater runoff: Measuring tire wear particles (TWP) concentration in the road environment and effect of treatment systems

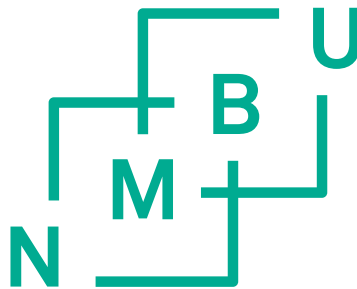
Mikroplast i veiavrenning: Måling av konsentrasjon av dekkslitasjepartikler (DSP) i veimiljøet og renseeffekt i anlegg for overvann

Philosophiae Doctor (PhD) Thesis

Demmelash Mengistu

Norwegian University of Life Sciences
Faculty of Science and Technology
Department of Building- and Environmental Technology

Ås (2023)



Supervision team

Prof. **Arve Heistad**, Ph.D. (Main supervisor)

Faculty of Science and Technology (RealTek)
Norwegian University of Life Sciences,
Ås, Norway.

Post-doc. **Vegard Nilsen**, Ph.D. (Co-supervisor)

Faculty of Science and Technology (RealTek)
Norwegian University of Life Sciences,
Ås, Norway.

Research Scientist **Claire Coutris**, Ph.D. (Co-supervisor)

Division of environment and natural resources
Norwegian Institute of Bioeconomy Research
Ås, Norway.

Prof. emeritus **Knut Kvaal**, (Co-supervisor)

Faculty of Science and Technology (RealTek)
Norwegian University of Life Sciences,
Ås, Norway.

Evaluation Committee

Senior Research Scientist, **Christian Vogelsang**, Ph.D. (First opponent)

Norwegian institute for water research
Oslo, Norway.
christian.vogelsang@niva.no

Associate Prof. **Åsmund Rinnan**, Ph.D. (Second opponent)

Faculty of Science
University of Copenhagen,
Frederiksberg, Denmark.
aar@food.ku.dk

Associate Prof. **Nazli Pelin Kocaturk Schumacher**, Ph.D. (Committee coordinator)

Faculty of Science and Technology (RealTek)
Norwegian University of Life Sciences,
Ås, Norway.
pelin.kocaturk.schumacher@nmbu.no

Summary

Tire wear particles (TWP) are a major source of microplastics that are mainly transported by stormwater from roads to the environment. Their risk has not yet been sufficiently evaluated, mainly because of the lack of suitable analytical methods for identifying and measuring their environmental concentrations. However, the ecotoxicological effects of TWP or chemical substances present in, or on, the particles are widely reported. For example, recent findings attributed the mass mortality of coho salmon (*Oncorhynchus kisutch*) in the Pacific Northwest region of the USA to the acute toxicity of a by-product of a tire manufacturing additive. Acute toxicity to other fish species such as brook trout (*Salvelinus fontinalis*) and rainbow trout (*Oncorhynchus mykiss*) is also reported. Moreover, TWP are persistent in the environment while their generation is increasing, which calls for action to limit their environmental spread. Conversely, stormwater management solutions are becoming a growing fixture in the road environment for their multipurpose role in controlling peak runoff and reducing pollution. However, knowledge of the effect of stormwater management solutions in removing TWP is limited.

The overall goal of this Ph.D. study was to introduce a suitable analytical method for detecting and quantifying TWP in the environment and measuring the actual concentrations of TWP in sediments of stormwater management solutions associated with roads.

Three study sites and laboratory experiments were used as data sources for the studies included in this thesis (Papers I–IV). Simultaneous thermal analysis (STA) and Fourier transform infrared spectroscopy (FTIR) were used to analyze the samples, and parallel factor analysis (PARAFAC) was used for data analysis. Analysis of variance (ANOVA) and t-tests were used for statistical analysis.

In the first part, the laboratory study introduced a method that detected the presence of rubber materials (RM) in formulated sediment spiked with tire granules (TGIS, Paper I). The combination of STA, FTIR, and PARAFAC enhanced the identification of TWP in formulated sediment. The method appeared to aggregate all likely RM (butadiene rubber (BR), styrene-butadiene rubber (SBR), ethylene propylene diene monomer (EPDM), and natural rubber (NR)) present in the spiked tire granules, which is a good attribute given that TWP in road environments originate from different types of tires, whose rubber compositions are varied. The method estimated unknown concentrations of RM by including a minimum of one sample with known RM concentration (reference sample) in the analysis setup (Paper I). However, it is uncertain if the results from the small data size used in the linearity analysis could be applied to environmental samples. It is also uncertain if using a fixed ratio of RM to TWP in the reference sample estimates unknown concentrations accurately since a wide range of ratios has been reported in the literature. Therefore, the method was further improved to suit the estimation of RM in environmental samples with a method detection limit (MDL) of 0.7 mg/g (Paper II). The improved method used the proportionality relationship between component score from

PARAFAC model and sample mass loss during heating in the STA following Beer–Lambert’s law.

In the second part, we measured TWP concentrations in stormwater treatment solutions; gully pots in Paper II, and bioretention cells in Paper III. The study demonstrated that stormwater management solutions retain TWP. Concentrations of TWP ranging between 0.1 and 15% were measured in gully pots’ sediments (Paper II). The study revealed the association between TWP concentrations, traffic density, and braking/acceleration intensity. The study demonstrated the potential of gully pots to act as temporary sinks. The study further demonstrated that another stormwater management solution, bioretention cells constructed with engineered soil, retain TWP (Paper III). TWP were detected in all size fractions of the bioretention soil. It appears particle sizes and locations of the inlet (entry point of road runoff to the bioretention cell) influenced TWP concentrations in the bioretention cell.

In the third part, we tested the removal efficiency of engineered soil in laboratory column experiments and found very high TWP retention of TWP >25 μm (Paper III). The observed high removal efficiency in the laboratory test and measured TWP concentrations in functional bioretention cells showed the potential of bioretention cells in removing >25 μm TWP from stormwater runoff and limiting their spread in the environment.

In the fourth part, we assessed TWP concentrations in soil along the racetrack at Rudskogen motorsport center (Paper IV). The study demonstrated the presence of large pieces of tires (4–9 cm) and two different microplastics, namely RM, and tire reinforcement microplastics (TRMP). The distance from the edge of the racetrack and locations along the racetrack has shown to influence RM and TRMP concentrations.

Finally, the thesis recommends future research in applying high-resolution STA to further improve the quantification method. Establishing a linear range between scores and concentrations is also recommended to reduce uncertainty in estimates. Studying TWP retention in gully pots in settings where gully pot operations and environmental conditions are controlled is recommended to conclusively determine the influence of traffic conditions. It is also recommended to study the vertical distribution of TWP in the bioretention soil and conduct a long-term assessment of TWP concentrations in the influent and effluent. The thesis further recommends studies on the mass transport in the environment, degradation impacts on TWP concentration over time, the removal efficiency of sweeping, and analysis of finer particles <25 μm to fill the knowledge gaps on the fate of TWP in the environment.

Notwithstanding these future research needs, this thesis contributes to the improvement of measuring environmental concentrations of TWP and filling the knowledge gaps with respect to

stormwater management solutions' effect, which has implications for controlling and monitoring TWP in the environment and designing stormwater management solutions.

Sammendrag

Dekkslitasjepartikler (DSP) er en viktig kilde til mikroplast, som hovedsakelig transporteres med overvann til miljøet. Likevel er risikoen ved DSP ikke tilstrekkelig evaluert, hovedsakelig på grunn av utilstrekkelige analytiske metoder for å identifisere og måle konsentrasjoner i miljøet. Toksiske effekter er imidlertid ofte rapportert ved at DSP selv eller de kjemiske stoffene i eller på partiklene har negative miljøpåvirkninger. Nylige studier tilskrev massedødeligheten av cohokals (*Oncorhynchus kisutch*) i Stillehavet, Norvest i USA til den akutte toksisiteten av et biprodukt lekket ut fra DSP. Akutt toksisitet for andre fiskearter som bekkerøye (*Salvelinus fontinalis*) og regnbueørret (*Oncorhynchus mykiss*) er også rapportert. DSP-dannelsen øker og DSP er et bestandig materiale, noe som krever tiltak for å begrense spredningen i miljøet. På den annen side er lokal overvannsdiskonering i ferd med å bli et vanlig element i veimiljøet, og kan både kontrollere spissavrenning og redusere forurensning. Kunnskapen om virkningen av løsninger for overvannshåndtering i å fjerne DSP er imidlertid begrenset.

Det overordnede målet for denne Ph. D. studien var å introdusere en adekvat analytisk metode for å identifisere og kvantifisere DSP i miljøet og måle konsentrasjoner i sedimenter av lokal overvannsdiskonering og i jord assosiert med veier.

Tre studiesteder og laboratorieeksperimenter ble brukt som datakilder for studiene inkludert i denne oppgaven (Artikler I–IV). Simultan termisk analysator (STA) og Fourier transform infrarød spektroskopi (FTIR) ble brukt til å analysere prøver, og parallellfaktoranalyse (PARAFAC) ble brukt for dataanalyse. Tilsvarende ble variansanalyse (ANOVA) og t-tester brukt for statistisk analyse.

I den første delen introduserte studien en metode som påviste tilstedeværelsen av gummimateriale (GM) i komponert jord tilsatt dekkgranulat (Artikkel I). Kombinasjonen av STA, FTIR, og PARAFAC forbedret identifikasjon av GM. Metoden detekterer alle former for GM i dekk, noe som er en god egenskap gitt at DSP i veimiljøer stammer fra forskjellige typer dekk med variert gummisammensetning. Metoden estimerte ukjente konsentrasjoner av GM ved å inkludere minst én prøve med kjent GM-konsentrasjon i analyseoppsettet (Artikkel I). Det er imidlertid usikkert om resultatene fra den lille datamengden som ble brukt i linearitetsanalysen kan brukes på miljøprøver. Det er også usikkert om et fast forholdstall mellom GM og DSP estimerer konsentrasjoner nøyaktig, siden et bredt spekter av forholdstall er rapportert i litteraturen. Derfor ble metoden ytterligere forbedret for å passe til estimeringen av GM i miljøprøver med en metodetetsjonsgrense (MDL) på 0,7 mg/g (Artikkel II).

I andre del målte vi DSP-konsentrasjoner i anlegg for overvann; sandfang i Artikkel II og regnbed i Artikkel III. Studien viste at DSP ble holdt tilbake i disse anleggene. Konsentrasjoner fra under 0,1 til 15% ble målt i sandfangsedimenter. Studien avdekket sammenhengen mellom DSP-konsentrasjoner og trafikk tetthet og bremse-/akselerasjonsintensitet. Andre faktorer, som lokalmiljø og tømmeffrekvens, som ikke er evaluert i denne studien, kan ha påvirket konsentrasjonen av DSP. Selv om denne studien ikke målte renseeffekten til sandfang, på grunn

av mangelen på DSP-konsentrasjon i innkommende og utgående overvann samtidig, fungerte anlegget som midlertidiglager. Studien viste videre at et annet anlegg med konstruert jord holder tilbake DSP (regnbed, Artikkel III). DSP ble påvist i alle størrelsesfraksjoner av regnbedsjord. Det ser ut til at partikkelstørrelser og plassering av innløpet (inngangspunktet for veiavrenning til regnbed) påvirket DSP-konsentrasjoner i regnbed. Imidlertid har ikke prosesser som kan redusere akkumulering, slik som nedbrytning og romlig bevegelse av DSP langs dybden, blitt studert.

I den tredje delen testet vi fjerningseffektiviteten til konstruert jord i kolonneeksperimenter og fant svært høy retensjon av DSP >25 μm (Artikkel III). Den observerte høye fjerningseffektiviteten i laboratorietesten og målte DSP-konsentrasjoner i anlegget viste potensialet til å fjerne >25 μm DSP fra overvannsavrenning og begrense spredningen av DSP i miljøet.

I fjerde del vurderte vi DSP-konsentrasjoner i jord langs motorsportbanen ved Rudskogen motorsportsenter (Artikkel IV). Studien viste at både større biter av dekk (4–9 cm) og to forskjellige mikroplaster (GM, og dekkforsterkningsmikroplast (DFMP)) var til stede langs banen. Avstanden fra kanten av banedekket og posisjonen langs banen har vist seg å påvirke DSP- og DFMP-konsentrasjonene.

Til slutt anbefaler oppgaven fremtidig forskning innen anvendelse av høyoppløselig STA for å forbedre kvantifiseringsmetoden ytterligere. Det anbefales også å etablere et lineært område mellom PARAFAC-skår og konsentrasjon for å redusere usikkerhet i estimater. Det anbefales å studere DSP-konsentrasjoner i sandfang i omgivelser hvor drift og miljøforhold er kontrollert for å bestemme påvirkningen av trafikkforholdene. Det er også anbefalt å studere vertikal fordeling av DSP i jord i regnbed og å gjennomføre langtids vurdering av DSP-konsentrasjon i innløp og utløp. Avhandlingen anbefaler videre studier av massetransport i miljøet, nedbrytningseffekter på DSP-konsentrasjoner over tid, fjerningseffektiviteten ved feiing og analyse av partikler <25 μm for å fylle kunnskapshullene om DSP i miljøet.

Til tross for disse fremtidige forskningsbehovene, bidrar resultatene fra denne avhandlingen til å forbedre måling av miljøkonsentrasjoner av DSP og fylle kunnskapshullene med hensyn til effekten av lokal overvannsdisponering, noe som har implikasjoner for kontroll, overvåking av DSP i miljøet, samt for utforming av løsninger for lokal overvannsdisponering.

Dedication

This thesis is dedicated to my mother, Tirunesh Tolesa Ido. She was my lifelong counselor and an inspirational mom. May her memory forever be a comfort and a blessing.

Foreword

After modeling and mapping potential drainage routes in 2017, we found that roads and associated ditches are important pathways to convey stormwater in Ås municipality. While discussing further work on the same theme with my former colleague Lars Buhler, the water quality issue, and the performance of roadside infrastructures with respect to pollutant removal stood out. However, pollutants originating from roads and entering the sewerage system are an issue at the interface between the water and road sections' responsibility area which was a challenge to justify resources allocation. Later the same year, the Research Council of Norway announced a call under the Public Sector Ph.D. Scheme with the intention to expand research activities in the public sector. Ås municipality responded to the call with the aim to promote collaboration between academia and generate knowledge that is relevant and applicable. Upon being granted the award, Ås municipality signed an implementation agreement with the Norwegian university of life sciences (NMBU) with the arrangement that the Ph.D. candidate accesses office space, academic network, and other resources at the Science and Technology faculty. The faculty offered supervision to ensure academic quality, while Ås municipality led the project to ensure the relevance of the research work. Cooperation was later expanded to include the Norwegian institute of bio-economy (NIBIO), which offered laboratory access and supervision. The grant condition was to allocate 75% of the candidate's time to the project while 25% was allocated to regular work. During the implementation, we revised the project and narrowed the study scope to "microplastics in stormwater runoff" to sharpen its scientific delivery. During the implementation years, the world has experienced the *covid-19* pandemic followed by a lockdown, which caused a delay in project completion. Nonetheless, we published four original and new articles in international journals for open access and wider circulation. With the results achieved, I believe that the Ph.D. project generated new insights into microplastics where there is a great need for knowledge. This thesis is based on those articles and presents a summary of the knowledge generated by the Ph.D. project.

Ås, February 2023

Demmelash Mengistu

Acknowledgments

This Ph.D. study has become a reality with the support of many people who deserve thank you. First of all, I would like to express my deepest gratitude to my lead supervisor prof. Arve Heistad for his willingness to support initiating this project. Arve, you make things happen, this study would have been impossible without your help. Thank you for the trust and confidence you have placed in me. Your support and guidance were unwavering throughout. I want to express my gratitude to my co-supervisor Vegard Nilsen for helping sharpen my research work on microplastics from the road environment and for critical reviews of the manuscripts. I appreciated your effort in engaging other students in this research area and raising funds for the research expenses, particularly on TWP from the racetrack. I would also like to extend my sincere gratitude to my co-supervisor Claire Coutris for her guidance in planning experiments, critical review of the manuscripts, recommending seminars to attend, and financing the experiments in gully pot and bioretention work. Your analytical approach and eye for detail have helped me a lot in preparing manuscripts. I communicate scientific work better now because of you. My sincere appreciation to co-supervisor Knut Kvaal for introducing me to the world of mathematical decomposition.

I am grateful to Monica Fongen for the analysis of samples and discussion on infrared and heating temperature of materials. Special thanks to Belachew G. Zeleke for his encouragement and willingness to read my drafts and Trond Knapp Haraldsen for his assistance in collecting samples.

I would like to thank my former and current colleagues at Ås Kommune, the engineering (technical) unit, particularly Jan Fredrik Årseth and Lars Buhler for initiating the project and coordinating communication between the Norwegian University of Life Sciences (NMBU) and the Research Council of Norway. I would also like to thank Anette Bjerke for facilitating the administration work, especially at the end of the project when an extension of the project period was needed because of the *covid-19* pandemic. I would also like to extend my thanks to Lillann Skuterud for her input in the project proposal, Dag Svenning for collecting traffic density data, and Dagfinn Fossum for preparing test samples.

I would also like to thank the Research Council of Norway (Norges forskningsråd) for financial support of the project through a public sector Ph.D. scheme.

Special thank you to the Ejersa group, my extended family in Norway, for your encouragement and support throughout the study period. I am grateful for the all-nighter waves of laughter,

debates, and discussions on various topics at the birthday parties, holiday gatherings, and outings at cabins.

I thank my family for their encouragement and support from near and far. A special thank you to my dear Meseret Guluma for your unreserved support and love. Your can-do attitude is contagious. To Naol Demmelash, thank you for being the person to turn to first with software issues. You are my inspiration son! Thanks to my brother, Tekalign Mengistu, for being the anchor of our family.

Finally, for all of you whom I have not mentioned by name here, know that I appreciate your support and encouragement!

Demmelash Mengistu

List of Figures

Figure 1. Raw FTIR spectra (4000-600 cm^{-1}) of formulated sediment spiked with tire granules.....	10
Figure 2 . FTIR dataset arranged in a three-way structure and decomposed into three PARAFAC components.	12
Figure 3. Estimated efficiencies of a gully pot trap particles	16
Figure 4. Study framework of the thesis	20
Figure 5. Overview of (a) sampling sites and gully pots.....	22
Figure 6. Left picture: bioretention cell located between the road and sidewalk	23
Figure 7. Overview of the Rudskogen racetrack with sampling locations.....	24
Figure 8. Experimental setup of the thesis	27
Figure 9. Raw FTIR spectra (4000-400 cm^{-1}) of formulated sediment spiked with tire granules.....	29
Figure 10. Schematic presentation of the steps involved in PARAFAC analysis	30
Figure 11. (a) TGA weight loss and (b) DTGA curves for NR/SBR blends of different elastomer components.....	31
Figure 12. Infrared spectrum of a NR/SBR (40/60) blend	32
Figure 13. Mass loss/sample (left Y-axis) and PARAFAC scores.....	35
Figure 14. Loadings of the PARAFAC model for tire granules only	36
Figure 15. Loadings of the PARAFAC model for tire granule-only.....	37
Figure 16. Mass loss/sample (left Y-axis) and PARAFAC scores.....	39
Figure 17. (a) FTIR spectra and (b) pyrolysis temperature profile indicating rubber materials (RM)	40
Figure 18. FTIR spectra of component 1	41
Figure 19. Partial least square (PLS) linear regression of scores	43
Figure 20. Tire wear particle (TWP) concentrations in bioretention soil	47
Figure 21. Marbles observed on the grass along the Rudskogen racetrack.....	51
Figure 22. Racetrack: Concentrations of microplastics in soil size fractions.....	52
Figure 23. Racetrack: Concentrations of a) rubber materials (RM) and b) tire reinforcement microplastics (TRMP) in the soil size fraction 50–1000 μm	54

List of Tables

<i>Table 1. General ingredients of tires</i>	3
<i>Table 2. Proportion (by mass) of soil fraction in bulk soil</i>	25
<i>Table 3. Concentrations of rubber materials (RM) and tire wear particles (TWP) in gully pot sediments</i>	45
<i>Table 4. Tire wear particle (TWP > 25 µm) concentrations in the influent (gully pot water) and columns effluent (C₁-C₃)</i>	49
<i>Table 5. Tire wear particles (TWP) retained by columns</i>	50

List of Acronyms

AADT	Average annual daily traffic
BR	Butadiene rubber
DTGA	Differential Thermogravimetric Analysis
EDXS	Energy dispersive X-ray spectroscopy
EEMs	Excitation-emission matrices
EPDM	Ethylene propylene diene monomer
FTIR	Fourier Transform InfraRed
GC-MS	Gas chromatography-Mass spectroscopy
GESAMP	Joint Group of Experts on Scientific Aspects of Marine
IC	Inward cornering
IR	InfraRed
LOQ	Limit of quantification
LS	Long straight
MDL	Method detection limit
NCBA	N-cyclohexyl-2-benzothiazolamine
NIST	National Institute for Standards and Technology
NR	Natural rubber
OC	Outward cornering
OECD	The Organization for Economic Co-operation and Development
PARAFAC	Parallel factor analysis
PBR	Poly-butadiene rubber
PLS	Partial least square
PPD	P-phenylenediamine
RDI	Rain detachment index
RM	Rubber material
RMSEC	Root mean square error of calibration
RMECV	Root mean square error of cross-validation
SAPEA	Science advice for policy by European academies
SBR	Styrene butadiene rubber
SBS	Styrene-butadiene-styrene
SD	Standard deviation
SF	Start/Finish
STA	Simultaneous Thermal Analysis
TED	Thermal extraction desorption
TG	Tire granules
TGA	Thermogravimetric analysis
TGIS	Tire granules spiked formulated soil
TGO	Tire granule-only
TRMP	Tire reinforcement microplastics

TRWP	Tire and road wear particle
TWP	Tire wear particles
WWTPs	Wastewater treatment plants

List of publications

This thesis is based on the appended four papers. The papers are published for open access and are reproduced for use in the thesis.

Paper I

Mengistu, D., Nilsen, V., Heistad, A., & Kvaal, K. (2019) 'Detection and quantification of tire particles in sediments using a combination of simultaneous thermal analysis, fourier transform infra-red, and parallel factor analysis', *International Journal of Environmental Research and Public Health*, 16, no. 18: 3444. <https://doi.org/10.3390/ijerph16183444>

Paper II

Mengistu, D., Heistad, A., & Coutris, C. (2021) 'Tire wear particles concentrations in gully pot sediments', *Science of the Total Environment*, 769, 144785. <https://doi.org/10.1016/j.scitotenv.2020.144785>

Paper III

Mengistu, D., Coutris, C., Paus, K. H., & Heistad, A. (2022) 'Concentrations and retention efficiency of tire wear particles from road runoff in bioretention cells', *Water* 14, 3233. <https://doi.org/10.3390/w14203233>

Paper IV

Mengistu, D., Nilsen, V., Coutris, C., Amdal, H., & Heistad, A. (2023) 'Microplastics concentration in soil along a racetrack'. *Water Air Soil Pollut* 234, 9. <https://doi.org/10.1007/s11270-022-06008-7>

Table of contents

Summary.....	ii
Sammendrag	vi
Dedication	viii
Foreword.....	x
Acknowledgments	xii
List of Figures	xiv
List of Tables.....	xv
List of Acronyms	xvi
List of publications	xviii
Table of contents	xx
1. Introduction	1
1.1. Definition and properties of tire wear particles	2
1.1.1. Chemical components	3
1.1.2. Shape	4
1.1.3. Size.....	4
1.1.4. Density	4
1.1.5. Degradation.....	5
1.1.6. Environmental risk	5
1.2. Measuring concentrations of tire wear particles in the environment	6
1.2.1. Curing agents as markers	7
1.2.2. Thermal analysis of rubber material.....	7
1.2.3. Fourier–Transform Infra-Red spectroscopy analysis of rubber materials	9
1.2.4. Parallel factor analysis for rubber material identification and quantification	10
1.3. Concentration of tire wear particles in stormwater runoff from roads	13
1.3.1. Factors influencing generation of tire wear particles.....	13
1.3.2. Precipitation.....	14
1.4. Stormwater treatment and tire wear particles retention.....	14
1.4.1. Gully pots as tire wear particles sink.....	15

1.4.2.	Deposition of tire wear particles along roadside soil	17
2.	Thesis objectives and framework of the study	19
3.	Materials and methods.....	21
3.1.	Study sites	21
3.2.	Experimental setup, sample preparation, and sampling.....	25
3.3.	Sample analysis.....	28
3.3.1.	Simultaneous thermal analysis	28
3.3.2.	Fourier transform infra-red spectroscopy.....	28
3.4.	Data preparation and parallel factor analysis model	28
3.4.1.	Data preparation.....	28
3.4.2.	PARAFAC model	29
3.4.3.	Rubber material identification.....	30
3.4.4.	Estimation of concentrations and statistical analysis.....	32
4.	Results and discussion.....	35
4.1.	A new method for detecting and estimating the quantity of tire wear particles in environmental samples.....	35
4.1.1.	Identifying tire wear particles in environmental samples.....	35
4.1.2.	Measuring tire wear particle concentrations	41
4.2.	Tire wear particle concentrations in stormwater treatment solutions	44
4.2.1.	Tire wear particle concentrations in gully pot sediments	44
4.2.2.	Tire wear particle concentrations in bioretention cell soil	45
4.3.	Tire wear particles removal efficiency of engineered soil	48
4.3.1.	Retention efficiency of the engineered soil.....	48
4.3.2.	Vertical Distribution of TWP in the Columns.....	49
4.4.	Microplastics deposition in soil along a racetrack	50
4.4.1.	Effect of racetrack alignment and distance from the edge.....	53
4.4.2.	Environmental impact.....	54
5.	General discussion.....	57
6.	Conclusion and future research	61

7. References	63
8. Appended Papers	75

1. Introduction

Plastic pollution in the environment has been recognized since the 1970s (Andersson-Sköld *et al.*, 2020). Alarming findings, such as “the Great Pacific Garbage Patch” (Moore *et al.*, 2001; Law *et al.*, 2010; Eriksen *et al.*, 2013), have also been reported. However, according to Bradley (2019), it was the “Blue Planet II” documentary in 2018 that revealed the extent of plastic pollution, which focused public attention and action on large-scale plastic waste. In her article about tire abrasion published in *WaterBriefing*, Bradley (2019) writes that “now we understand the plastic pollution we can see, we must work harder to understand, manage and prevent the plastic pollution that can't be seen,” pointing to potentially more harmful effects of microplastics on ecosystems and humans. Microplastics have become ubiquitous in the environment, raising exposure concern to human beings (Leslie *et al.*, 2022). Recent scientific studies showed that microplastics enter the human gastrointestinal, respiratory, and circulatory systems (Schwabl *et al.*, 2019; Jenner *et al.*, 2022; Leslie *et al.*, 2022) with potential health effects (Choi *et al.*, 2020; Fleury and Baulin, 2021). Uptake by plants, e. g., carrots, were also reported (Dong *et al.*, 2021).

Tire and road wear particles (TRWP) generated by abrasion at the interface between tires and roads during driving are considered a major sources of microplastics in the environment (Kreider *et al.*, 2009). Many research works and reports have been published on the emission factors, annual emissions, and environmental concentrations of TRWP since 1974 (Wik and Dave, 2009; Baensch-Baltruschat *et al.*, 2020). However, scientific knowledge and research on TRWP are patchy and insufficient to translate into significant public awareness on a scale similar to that of larger plastics (Bradley, 2019). A good example is that drivers check tread depth for safety reasons, yet most never think about lost material (Bradley, 2019).

Globally, road traffic is continuously increasing, leading to higher emissions of TWP (definition is presented in section 1.1), which is persistent as a polymer and may take decades to decompose entirely (Ojeda, 2013). In Norway, more than 7000 tons of annual tread emissions are estimated (Vogelsang *et al.*, 2018), which are mainly transported by stormwater (Jan Kole *et al.*, 2017; Johannessen *et al.*, 2021; Tian *et al.*, 2021). However, the actual concentrations measured in different environmental matrices are inconsistent (Eisentraut *et al.*, 2018; Dröge and Tromp, 2019; Klöckner *et al.*, 2019; Leads and Weinstein, 2019) mainly because of the lack of adequate analytical methods, which are limiting factors in risk assessments (SAPEA, 2019; Baensch-Baltruschat *et al.*, 2020).

While very few studies (e.g., Tamis *et al.*, 2021) assessed the environmental risk posed by TWP and other associated chemical substances, research on the toxicity of TWP and their constituents is growing (e.g., Gualtieri *et al.*, 2005; European Union, 2008; Wagner *et al.*, 2018; Halle *et al.*, 2020; Longhin, Mantecca and Gualtieri, 2020; Tamis *et al.*, 2021; Tian *et al.*, 2021). The toxic effects of leachate, spiked sediment, and elutriates from tire tread particles have been demonstrated in aquatic organisms in the literature (Wik and Dave, 2005, 2006; Villena *et al.*, 2017; Khan *et al.*,

2019). These effects include acute (Wik and Dave, 2005, 2006; Khan *et al.*, 2019) and chronic (Villena *et al.*, 2017; Khan *et al.*, 2019) toxicities. In addition to chemicals leaching from TWP, their transformation products have also shown acute toxicity. Even though degradation of TWP in the environment is not well understood, one recent study showed that a low concentration (0.8 µg/L) of 6-ppd-quinone is a likely cause for the mass mortality of coho salmon (*Oncorhynchus kisutch*) (Tian *et al.*, 2021). This by-product has shown acute toxicity to other fish species such as brook trout (*Salvelinus fontinalis*) and rainbow trout (*Oncorhynchus mykiss*) (Brinkmann *et al.*, 2022).

Notwithstanding the uncertainty in translating laboratory findings into effects in the natural environment (SAPEA, 2019), there is a growing evidence of TWP' negative impacts (Tamis *et al.*, 2021; Tian *et al.*, 2021), which together with increasing generation and persistence in the environment call for measures to limit their spread in the environment (Andersson-Sköld *et al.*, 2020).

Stormwater is reported to transport TWP to receiving water bodies (Jan Kole *et al.*, 2017; Johannessen *et al.*, 2021; Tian *et al.*, 2021). Historically, stormwater management has involved directly removing surface water through a series of pipes to reduce local flooding, and wastewater treatment plants (WWTP), which might also remove TWP as particles. However, because of climate change and urbanization, stormwater volumes are becoming more critical, leading to significant loads of pollutants, including TWP, to receiving water bodies (Dale *et al.*, 2017; U. S. Environmental Protection Agency, 2021; Skaaraas *et al.*, 2015). Currently, environmentally conscious approaches are becoming a growing fixture in the road environment because of their multipurpose role in controlling peak runoff and reducing pollution from stormwater. These stormwater management practices show clear convergence with the need to limit the spread of TWP. However, the effects of roadside infrastructures on retaining TWP are not yet widely understood. This was a practical experience for us in the Water and sewer section at Ås municipality. After modeling stormwater sewer capacity and mapping potential flood conveyance routes in 2017, we were left with one question: "how do the roadside infrastructures perform with respect to TWP removal?".

This thesis is motivated by the lack of suitable analytical methods required to measure the environmental concentration of TWP and the knowledge gap in the effect of treatment solutions. The thesis introduced a new TWP measurement method (Papers I and II). The method was then applied to measure the actual TWP concentrations in the treatment facilities and test the treatment efficiencies of stormwater management solutions. These included gully pots (Paper II) as a traditional stormwater management approach and bioretention cells (Paper III) representing a more recent approach. A racetrack (Paper IV) was also included in the study due its potential of generating high amounts of TWP.

1.1. Definition and properties of tire wear particles

TWP are defined as microplastics, mainly because of the high (40–60%) content of natural or synthetic polymers in vehicle tires (Verschoor, 2015; Hartmann *et al.*, 2019; Jekel, 2019). Additional

criteria for defining TWP as microplastics include properties such as solidity—melting and glass temperatures above 20 °C, insolubility—solubility less than 1 mg/L at 20 °C— (Jekel, 2019), and particle size. Size and other particle properties are important parameters in determining the fate of TWP in the environment (Wagner *et al.*, 2018) and are presented in more detail below.

1.1.1. Chemical components

TWP result from car tire abrasion, consist of complex mixtures of various chemicals, such as rubber, fillers, reinforcement agents, processing aids, accelerators and retarders, adhesives, and activators used in the manufacturing process (Grigoratos and Martini, 2014). Although the composition of a specific tire depends on its model and manufacturer, the general components of common vehicle tires are listed in Table 1 (Wagner *et al.*, 2018).

Table 1. General ingredients of tires adopted from (Wagner *et al.*, 2018).

Category	Content (wt %)	Ingredients
Rubber/Elastomer	40–60	butadiene rubber (BR), styrene-butadiene rubber (SBR), ethylene propylene diene monomer (EPDM), and natural rubber (NR)
Reinforcing agent (filler)	20–35	Carbon black, silica, and silanes
Process oils	15–12	mineral oils
Textile and metals	5–10	
Vulcanization agent	1–2	ZnO, S, Se, and Te Thiazoles, organic peroxides, and nitro compounds
Additives	5–10	Preservatives (halogenated cyanoalkanes), antioxidants (amines and phenols), desiccants (calcium oxides), plasticizers (aromatic and aliphatic esters), and processing aids (mineral oils and peptisers)

The different notations used to describe tire particles should be understood as follows: **TG** describes tire granules/crumb rubber processed from scrap tires by a granulator. **RM** represent rubber materials/elastomer fraction of a tire, while **TWP** represent tire wear particles with all tire ingredients (Table 1). **TRWP** represent tire wear particles generated during driving and contain road wear in addition to the tire ingredients.

The characteristics of TRWP are different from those of the TWP (Panko *et al.*, 2013) mainly because of physicochemical changes that occur at the interface of tires and road, either due to heat and friction or via incorporation of material from the road surface. TWP are seldom reported in the environment as they heteroaggregate to form TRWP (Cadle and Williams, 1978; Adachi and Yoshiaki, 2004; Kreider *et al.*, 2009). Therefore, TRWP may be more suitable when referring to TWP in the environment (Baensch-Baltruschat *et al.*, 2020). TRWP contain substances used in

manufacturing, such as Zn, Si, and S, as well as other metals, such as Al, Ca, Cu, Fe, Mg, Ti, and Ni (Kwak *et al.*, 2013; Wagner *et al.*, 2018) and a large variety of other organic compounds, such as n-alkanes, n-alkanoic acids, and natural resins (Kreider *et al.*, 2009). Some of these chemical compounds, such as 6-ppd, anthracene, fluoranthene, naphthalene, and benzo (a)pyrene, are among the priority substances in the field of water policy (European Union, 2008). The other important aspect related to the chemical composition of TRWP is the transformation products of leaching chemicals, such as 6-ppd to 6-ppd-quinone in the environment (Tian *et al.*, 2021).

1.1.2. Shape

TRWP are elongated or sausage-like in shape (Cadle and Williams, 1978; Adachi and Yoshiaki, 2004; Kreider *et al.*, 2009; Sommer *et al.*, 2018). The aspect ratio varies depending on the sample studied; for example, Kreider *et al.* (2009) reported an aspect ratio of 0.63, whereas Sommer *et al.* (2018) reported an average aspect ratio of 0.36.

1.1.3. Size

A 5 mm upper limit is widely used for microplastics after an international research workshop on the occurrence, effects, and fate of microplastic marine debris in 2008 (Arthur, Baker and Bamford, 2009). This size is assumed to be ingestible by biota, causing ecological impact and physical blockade of the gastrointestinal tract. Others recommend a more rigorous scientific definition of micrometer range for microplastics, e.g., between 1 and 1,000 μm (Hartmann *et al.*, 2019), 0.1–1,000 μm (GESAMP, 2015) and 10–1,000 μm (Eisentraut *et al.*, 2018). TRWP size distribution in road dust or in the environment can differ depending on many variables including factors influencing TRWP generation (presented in section 1.3.1.), tire composition, as well as analysis method of TRWP (Kovochich *et al.*, 2021). According to Kreider *et al.* (2009), the TRWP size distribution of an on-road drive ranges from 4 μm to 280 μm , with a mode centered at approximately 50 μm and 25 μm by volume and particle number, respectively. In a study of characterizing individual TRWP in road dust, tunnel dust, and sediment, Kovochich *et al.* (2021) found average TRWP size of 158 μm by number and 224 μm by volume. The study reported larger TRWP average size, 267 μm , by number and 506 μm by volume in environmental sediment. Generally, the main parts of the tread wear are coarse particles (>10 μm) (Panko *et al.*, 2013; Jan Kole *et al.*, 2017), while a substantial amount (ca. 0.1–10%) are fine particles (<10 μm) and airborne (Grigoratos and Martini, 2014).

1.1.4. Density

The density of TRWP is essential for their transport in the environment because it affects the settling velocity and their travel distance in water (Siegfried *et al.*, 2017). Low densities will lead to long ranges of transport in surface waters and negligible settling rates (Jekel, 2019). The particle density of TRWP was estimated to be 1.8 g cm^{-3} because of aggregation of tread (1.18 g cm^{-3}) (Unice *et al.*, 2019) and a roadway pavement material (2.4 g cm^{-3}) (Kreider *et al.*, 2009; Unice, Kreider and Panko, 2012; Panko *et al.*, 2013). However, size of encrustation is fluctuating, and

different studies have reported that environmental substances make up a varying share of TRWP. For example, Kreider *et al.* (2009), Panko *et al.* (2013), and Unice *et al.* (2012) used 50% road mineral encrustation content, whereas Sommer *et al.* (2018) used a 10–50% estimate. Another study, Klöckner *et al.* (2021) estimated 25% mineral encrustation in the tunnel dust TRWP. This makes determination of TRWP density challenging. Klöckner *et al.* (2021), who fractionated TRWP in highway tunnel road dust <1mm, reported that density of TRWP was mostly (ca. 2/3) in the range of <1.7 g/cm³, while rest was in the range >1.7 g/cm³. However, tunnel road dust may not have similar characteristics with road dust for direct comparison. Jung and Choi, (2022), who studied road dust near a bus stop, reported that TRWP to be <1.7 g/cm³.

1.1.5. Degradation

According to a review of studies on TWP degradation (Baensch-Baltruschat *et al.*, 2020), photo- and biodegradation appear to be the two main degradation pathways in the environment. However, they reported no quantitative study to indicate the TWP degradation rate in the environment, except for Cadle and Williams (1978), who observed a half-life of 70 weeks. Another review (Wagner *et al.*, 2018) supports the slow degradation of TWP in the environment because of its rubber polymer and carbon black constituents. The effect of tire additives on slowing the biological degradation processes, as reported by Stevenson, Stallwood and Hart (2008), also suggests the persistence potential of TWP in the environment.

1.1.6. Environmental risk

Even though TWP are major sources of microplastics in the environment, their environmental risk assessments are limited. To my knowledge there is only one recent study (Tamis *et al.*, 2021), which assessed risk posed by TWP from stormwater runoff in Europe and reported a significant dose-related effects for specific organisms the in surface water and sediment. Moreover, studies on concentration of TWP in aquatic and terrestrial environment are few and those which exist have reported very different values in different environmental matrixes (Dröge and Tromp, 2019; Eisentraut *et al.*, 2018; Klöckner *et al.*, 2019; Leads and Weinstein, 2019). These inconsistencies, which are mainly attributed to lack of adequate analytical method (Rødland *et al.*, 2021), make risk assessment uncertain as the quality of assessment is determined by its weakest piece of evidence (SAPEA, 2019).

On the other hand, several studies demonstrated the toxicity of TWP or their constituents. For example, laboratory studies have proved TWP or their constituents to be toxic (Gualtieri *et al.*, 2005; Halle *et al.*, 2020; Longhin *et al.*, 2020; Tamis *et al.*, 2021; Tian *et al.*, 2021; Wagner *et al.*, 2018, Wik and Dave, 2009). Some of the organic chemical compounds present in TWP, such as (N-(1,3-dimethylbutyl)-N'-phenyl-1,4-phenylenediamine (6-PPD), Anthracene, Fluoranthene, Naphthalene, Benzo(a)pyrene) are listed as priority substances in the field of water policy

(European Union, 2008; Tamis *et al.*, 2021). The other important aspect in relation to identification of toxic substances are transformation products of chemicals leaching from TWP in the environment such as 6ppd-quinone (Tian *et al.*, 2021).

Toxic effects of leachate, spiked sediment and elutriates from tire tread particles were demonstrated by laboratory studies using test organisms (small crustaceans, some algae, fish, and tadpoles) (Capolupo *et al.*, 2020; Khan *et al.*, 2019; Villena *et al.*, 2017; Wik and Dave, 2006, 2005), whereas no toxic effects were seen in others (Panko *et al.*, 2013; Redondo-Hasselerharm *et al.*, 2018). The studied effects include acute toxicity (e.g. LC₅₀ was reported when *Hyallolela azteca* were exposed to 3426 ± 172 particles mL⁻¹ (Khan *et al.*, 2019); while EC₅₀ was reported for *Daphnia magna* at concentrations ranging from 500 to >10000 mg/l (Wik and Dave, 2006, 2005)). Chronic toxicity (e.g. impact on growth, development, and survival, deformity, death, reduced number offspring when *Hyallolela azteca* was exposed to 500-2000 particles mL⁻¹) (Khan *et al.*, 2019) and population decline when *Aedes albopictus* and *Aedes triseriatus* were exposed to 500-100000 mg/L tire leachate (Villena *et al.*, 2017).

The concentrations reported in those studies are within the range of TWP concentrations found on road surface or near road and in river sediments (Wagner *et al.*, 2018). The concentrations seem high compared to measured environmental concentrations beyond 30 m from roads, in road runoff and river water (Wagner *et al.*, 2018). However, recent studies showed that a very low concentration (LC₅₀ ≈ 0.8 µg/l) of 6ppd-quinone to be the cause of mass mortality of coho salmon (Tian *et al.*, 2021). Acute toxicity to other fish species such as brook trout (*Salvelinus fontinalis*) and rainbow trout (*Oncorhynchus mykiss*) is also reported at concentrations (LC₅₀ value ≤ 1 µg/l) (Brinkmann *et al.*, 2022). However, the toxicity reported might be species-specific as Arctic char (*Salvelinus alpinus*), white sturgeon (*Acipenser transmontanus*) or even other salmon species tested like (chum salmon, *Oncorhynchus keta*) found to be tolerant to 6ppd-quinone at concentration that was lethal to coho (Brinkmann *et al.*, 2022; McIntyre *et al.*, 2021).

Despite the fact that toxic effects have been reported on only a few species, which may also be specific to those species, the presence of TWP or their constituents in the environment at concentrations that cause lethal effects is a concern. This is specially worrying as emissions continue to increase, which justifies studying TWP in the environment.

1.2. Measuring concentrations of tire wear particles in the environment

Measuring the environmental concentrations of TWP is relevant for exposure assessment to determine environmental risk and evaluate the efficiency of control measures. A common technique applied in microplastic monitoring, visual identification supported by a stereo

microscope and vibrational spectroscopic methods, such as Fourier transform infrared (FTIR) spectroscopy, does not work for TWP because of absorption of IR light by dark color of the particles (Eisentraut *et al.* 2018; Wagner *et al.* 2018). Instead, indirect methods were applied to determine the amount of TWP in environmental samples. The indirect methods involve the determination of markers that are either additives or rubber (styrene-butadiene rubber, SBR or natural rubber, NR) constituents of tires. A reliable marker should fulfil the following criteria (Unice, Kreider and Panko, 2013; Wagner *et al.*, 2018; Klöckner *et al.*, 2019):

- i) it is specific to tire,
- ii) it is present in all tire brands in comparable proportion,
- iii) not easily separated from tire in the environment, for example by leaching
- iv) be easily and precisely detectable.

The methods used currently are highlighted in the following sections, along with their limitations in measuring TWP in the environment.

1.2.1. Curing agents as markers

Tire manufacturing involves a curing process, a reaction between the elastomer and other vulcanization chemicals that give the tires strength and elastic properties (Coran, 2013). The main elements used in the vulcanization process and considered as markers for TWP are Zn, S, and a variety of organic compounds, such as benzothiazoles, 2-(4-morpholinyl) benzothiazole (24MoBT), and N-cyclohexyl-2-benzothiazolamine (NCBA) (Kumata *et al.*, 2000; Adachi and Yoshiaki, 2004). Energy-dispersive X-ray spectroscopy (EDXS) has been used to detect TWP in road dust and tire debris produced in the laboratory based on its Zn content (Camatini *et al.*, 2001; Adachi and Yoshiaki, 2004). Nonetheless, because organic Zn is also emitted from other traffic-related sources and non-traffic-related sources, it is regarded as not very specific to tire wear, leading to overestimation of TWP concentrations (Hillenbrand *et al.*, 2005; Panko *et al.*, 2013; Unice, Kreider and Panko, 2013; Padoan, Romè and Ajmone-Marsan, 2017; Wagner *et al.*, 2018). NCBA is not a specific marker, as it is also found in antifreeze leakages in automobile radiators (Kumata *et al.*, 2000). In addition, benzothiazoles are prone to leaching in aqueous environments (Unice, Kreider and Panko, 2013). Therefore, the presence of Zn and benzothiazoles is not a positive proof of the existence of tire rubber particles. To date, no other curing agent has been reported to fulfil the requirements for a reliable marker in all media.

1.2.2. Thermal analysis of rubber material

Rubber material (RM) is the major component of TWP, the rest being fillers, reinforcement materials, plasticizers, vulcanization agent, and antiaging chemicals (Fernández-Berridi *et al.*, 2006; Kreider *et al.*, 2009; Jusli *et al.*, 2014). Thermoanalytical methods, which decompose the structure of the rubber polymer are widely used in identification and quantification. Polymer-specific degradation products are identified by gas chromatography-mass spectrometry (GC-MS)

(Unice, Kreider and Panko, 2012; Eisentraut *et al.*, 2018; Wagner *et al.*, 2018). The appropriate markers are dipentene and isoprene for NR (Unice, Kreider and Panko, 2012; Eisentraut *et al.*, 2018; Wagner *et al.*, 2018), whereas styrene, butadiene, and vinyl cyclohexene are used as markers for SBR (Unice *et al.*, 2012; Wagner *et al.*, 2018). Pyrolysis-GC-MS system was used in the publication of the International Organization for Standardization (ISO) technical specifications ISO/TS 21396:2017(E) for quantifying TRWP in soil and sediments (ISO, 2017). However, Eisentraut *et al.* (2018) identified oligomers of isoprene in the degradation products of plant material, which can give false positives or overestimate the amount of TWP when the TED-GC-MS system is used. Conversely, (Rauert *et al.*, 2021) reported potential underestimation of TRWP when the ISO method was used, mainly because of the assumption that the total mass of RM content in all tire treads is 50% and varying ratios between different RM present in tires. Determining RM in tires is challenging due to variations in types and brands. Despite numerous studies, there is still uncertainty in the field. Tires consist of natural rubber (NR, polyisoprene) and synthetic rubbers like styrene butadiene rubber (SBR) and butadiene rubber (BR). These two polymers are also the main components in heavy vehicles, which were previously thought to primarily contain NR (Rauert *et al.*, 2021). Unice *et al.* (2012) estimated that the total polymer composition of all tread types was 50%, with 44% SBR in passenger vehicle tires and 45% NR in heavy vehicle tires while the rest is attributed to other rubber types. Grigoratos and Martini (2014) reported that the composition of passenger car tires was 41%, with 40% NR, 30% SBR, 20% BR, and 10% other rubbers. Another study Vogelsang *et al.* (2018) reported a total composition range of 40-60% RM in tires, with 36-54% SBR and NR/PBR while other rubber types contribute 4-6%. These inconsistent ratios make it difficult to accurately estimate TWP concentration using specific rubber markers, unless a comprehensive and diverse sample set of tires is used, including tires from various locations and purposes to account for geographical and seasonal differences. Alternatively, using reference tires relevant to each study area as suggested by Rødland *et al.* (2021).

Thermogravimetric analysis (TGA) is another widely used technique for characterizing the RM constituents in tires. This technique is used to determine the composition of materials that exhibit weight loss due to decomposition by measuring the change in material mass with respect to temperature and time (Mohomed, 2016). Derivative thermogravimetric analysis (DTGA) is particularly valuable because it generates elastomer identification peaks (Fernández-Berridi *et al.*, 2006). However, this technique also has its limitations: it works well when the DTGA curves of each elastomer are separated, but standard TGA falls short in this respect as it scans broader weight losses, resulting in overlapping signals with multiple peaks (Mohomed, 2016). In this study, simultaneous thermal analysis (STA), which simultaneously generates mass loss data, time, and temperature, was employed. The instrument specifications and analytical setup are presented in the methodology section.

1.2.3. Fourier–Transform Infra-Red spectroscopy analysis of rubber materials

Infrared radiation (IR) refers to the electromagnetic spectrum between the visible and microwave regions in the wavenumber range of 4,000 cm^{-1} –400 cm^{-1} . The infrared range is of practical interest in organic chemistry. Organic molecules absorb and convert IR energy into molecular vibrations, which appear in bands. The frequency or wavelength of absorption depends on the molecular structure of the studied substance, and the band position is proportional to the vibrational energy. IR spectroscopy is one of the oldest techniques for molecular-level characterization of materials, and it has been extensively used to study polymers (Litvinow and De, 2002; Silverstein *et al.*, 2015). The actual spectra were translated to Fourier transform infrared (FTIR) for presentation and to facilitate the matching of an unknown spectrum against a reference sample. A sharp and weak peak at approximately 3,016 cm^{-1} (C=C double bond) and strong peaks at approximately 2,925 and 2,850 cm^{-1} (C–H stretch of saturated hydrocarbons) are indicative of organic substances (Silverstein *et al.*, 2015). The diagnostic bands for the SBR and NR pyrolysis products correspond to the vibrations of the aromatic groups of polystyrene at 750 and 700 cm^{-1} , respectively, and the vibrations of the vinyl groups (990 and 910 cm^{-1}) and trans at 960 cm^{-1} of butadiene (Fernandez-Berridi *et al.*, 2006). Quantitative analysis is possible from the FTIR spectra using Beer–Lambert’s law (Litvinow and De, 2002), following the relationship (eq. 1) between the concentration of the polymer and the amount of radiation absorbed:

$$A = \varepsilon * c * l \quad (1)$$

A = absorbance

ε = a constant called the absorptivity or extinction coefficient $\text{M}^{-1}\text{cm}^{-1}$

c = concentration (molar, M)

l = is the thickness of the sample cell (cm)

An absorbance versus concentration calibration curve can be formed to determine the concentration of the unknown component (Litvinow and De, 2002).

However, FTIR lacks the specificity that certain groups of atoms (functional groups) generate bands at or near the same frequency, necessitating other techniques to support identification (Silverstein *et al.*, 2015). In addition, FTIR spectra are not suitable for identifying and quantifying TWP without further treatment of the data generated using this technique (Litvinow and De, 2002). In this study, FTIR spectra generated after heating samples in STA showed overlapping signals. For example, FTIR spectra of formulated sediment spiked with tire granules (TGIS, Paper I) showed multiple peaks (Fig. 1) indicating the presence of water (peaks above 3400 and around 1500 cm^{-1}), organic compounds (strong peaks close 3000 cm^{-1}) and carbon dioxide (strong peak

around 2300 cm^{-1}) on the same spectra showing the challenge of identifying and quantifying independent chemical components.

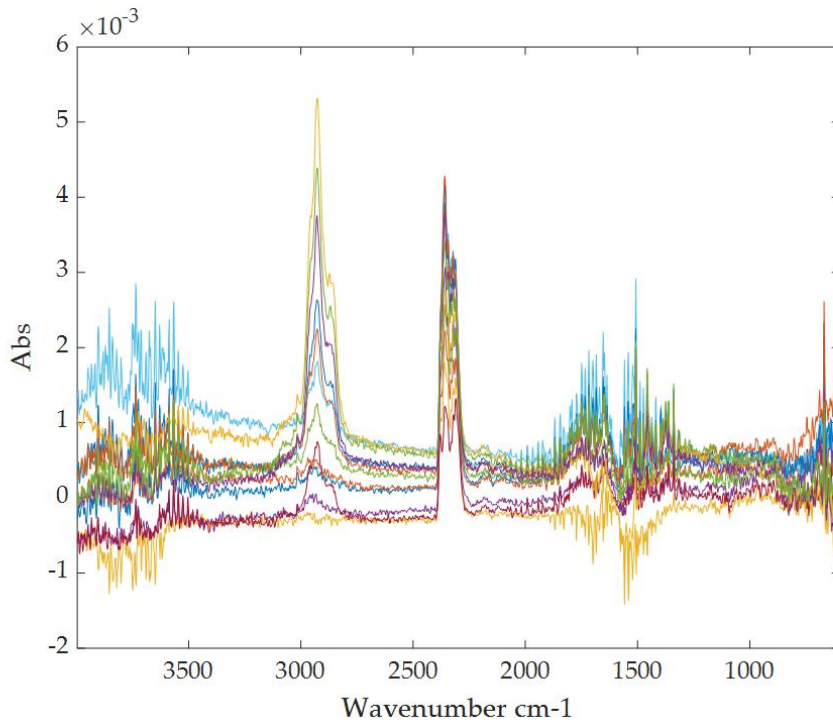


Figure 1. Raw FTIR spectra ($4000\text{-}600\text{ cm}^{-1}$) of formulated sediment spiked with tire granules (TGIS, Paper 1)

1.2.4. Parallel factor analysis for rubber material identification and quantification

Owing to the existence of multiple substances, which generate overlapping signals (e. g. FTIR of TGIS, Fig. 1), in soil/sediment samples, identifying and quantifying RM through thermal and FTIR analysis is a challenge as discussed in section 1.2.2. & 1.2.3. PARAFAC has shown great versatility in this respect to resolve multi-component data into underlying analytes. PARAFAC is a multi-way data decomposition method that facilitates the identification and quantification of underlying signals, called components (Murphy *et al.*, 2013). The method, originating from psychometrics (Bro, 1997), has been applied to many research fields, including the environment and a wide range of data types, such as spectral Nuclear magnetic resonance, GC-MS, and FTIR. For example, the PARAFAC model was applied to fluorescence EEMs of natural organic matter with samples, excitation wavelength, and emission wavelength forming the three-way array (Murphy *et al.*, 2013). Another example is the application of PARAFAC to FTIR of milk products

reported in Baum *et al.* (2016) with samples, absorption wavenumber, and evolution time forming the three-way array. The algorithms used in PARAFAC are based on alternating least squares (ALS). The PARAFAC model of a three-way dataset decomposes the data into components and a residual array, as shown in eq. 2 (Murphy *et al.*, 2013). PARAFAC has demonstrated great versatility in resolving the multicomponent matrix into underlying analytes (Baum *et al.*, 2016) and offers a reliable foundation for estimating the quantity of components based on Beer-Lambert's law (Murphy *et al.*, 2013; Melville, Lucieer and Aryal, 2018). This method assumes:

- 1) tri-linearity—the same number of components underlies the chemical variation in each dimension of the dataset. In a PARAFAC model, tri-linearity refers to the fact that each component of the model can be represented as a matrix product of three vectors. The tri-linearity property allows for the modeling of multi-way arrays, in a compact and interpretable form.
- 2) variability—signals or intensities of the chemical components are different; this means the values in the components are expected to vary across the different modes of the tensor. In other words, the variability assumption states that the patterns in the data tensor can be explained by a limited number of underlying components.
- 3) additivity—the total signal is sum of a fixed number of components (Murphy *et al.*, 2013). In other words, this property states that the low-rank approximations of a multi-way array can be obtained by adding together the low-rank approximations of the individual modes.

Choosing the correct number of components for the model and acquiring the appropriate signal-to-noise ratio of the spectral data are critical for the analysis (Bro, 1997). Diagnostic tools for determination of the number of components are presented below in section 1.2.4.1). The second and third assumptions constitute Beers' law, and PARAFAC components that do not conform to this law are not meaningful (Murphy *et al.*, 2013).

$$X_{ijk} = \sum_{f=1}^F a_{if} b_{jf} c_{kf} + e_{ijk}, \quad (2)$$

Murphy *et al.* (2013) defines eq (2), "where $i = 1, \dots, I$; $j = 1, \dots, J$; $k = 1, \dots, K$ x_{ijk} is the data point corresponding to the i^{th} sample at the j^{th} variable on mode 2 and at the k^{th} variable on mode 3, and e_{ijk} is the residual representing the variability not accounted for by the model." According to Murphy *et al.* (2013), in a valid model, the components have direct chemical interpretation and a_{if} is directly proportional to the concentration of the f^{th} analyte of sample i , and the vector b_f with elements b_{jf} is a scaled estimate of the wavenumber cm^{-1} of the f^{th} analyte. Similarly, vector c_f with elements c_{kf} is proportional to the specific mass loss rate of the f^{th} analyte. Unknown concentrations of an analyte can then be estimated from PARAFAC model scores, which are

represented by a_{if} if at least one sample with a known concentration is included in the analysis setup (Murphy *et al.*, 2013), while vectors b_f and c_f are used for identification of the analytes. The application of PARAFAC for identifying and quantifying RM in environmental samples has not been tested previously. This study introduces the method presented in Paper I.

This equation is graphically illustrated in Fig. 2 for three components ($f = 3$).

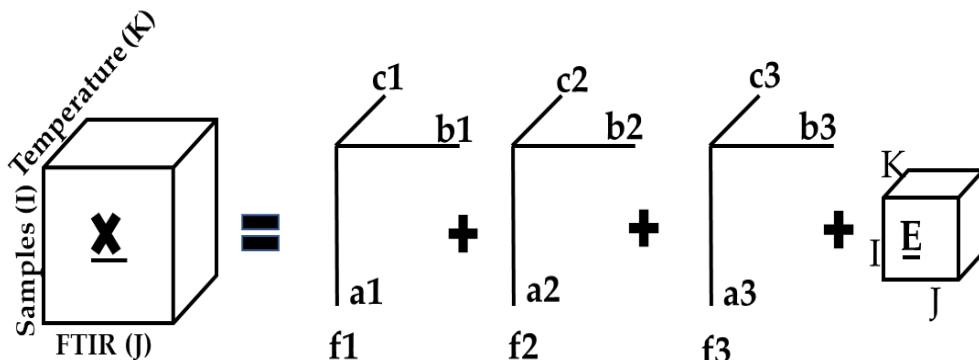


Figure 2 . FTIR dataset arranged in a three-way structure and decomposed into three PARAFAC components.

1.2.4.1. Diagnostic tools for assessment of the PARAFAC model

Core consistency

In PARAFAC model, core consistency is the most important and effective tool for determining the appropriate number of components (Bro and Kiers, 2003; Rinnan, 2004). The appropriate number is the largest number beyond which adding other components does not improve the fit considerably (Bro and Kiers, 2003). A core consistency is expressed in percentage (%) and is always less than or equal to 100 %, however it should not be close to zero or negative as this implies invalid model. Core consistency is not always a reliable diagnostic for the number of PARAFAC components as it tends to protect overfitting than underfitting (Murphy, *et al.* 2013) and should be supported by other tools. Explained variance and uniqueness are among other useful tools in this respect (Rinnan, 2004).

Split-half analysis

Split-half analysis is another diagnostic tool to assess the reliability of the PARAFAC model at the selected number of components. It involves dividing the data into two halves and comparing the similarity between loadings from each half. The loadings of the two models would be similar if the appropriate number of components has been selected (Rinnan, 2004). However, the split

should be performed cautiously as similar samples in the same split would affect the results. The split-half analysis results close to 100 % indicate a high similarity.

Multiple diagnostic tools that could estimate the correct number of components to build more robust model were proposed by Rinnan (2004). However, only some of the diagnostics accessible from the PARAFAC model analysis window (core consistency, variation per component, residuals, and split-half analysis) were utilized in this thesis.

1.3. Concentration of tire wear particles in stormwater runoff from roads

Once generated, TWP are transported to terrestrial or aquatic environments through different pathways. A notable amount (0.1–10%) of TWP becomes airborne, while the majority is deposited on the road or the side soil (Panko *et al.*, 2013; Jan Kole *et al.*, 2017). Seasonal road operation activities such as snow removal and street sweeping remove a limited amount of particles deposited on the road (Björklund, Strömvall and Malmqvist, 2011; Janhäll *et al.*, 2016). Most of particles deposited on the road or side soil are washed off and transported with surface runoff depending on the precipitation intensity (Vogelsang *et al.*, 2018; Wik and Dave, 2009). Many local factors influence the amount of TWP deposited and transported by runoff (presented in 1.3.1 and 1.3.2), indicating the challenge of predicting their concentration profiles. For example, according to Wik and Dave (2009), TWP concentrations may range from 0.3 to 197 mg/L in stormwater runoff.

1.3.1. Factors influencing generation of tire wear particles

A passenger car tire is estimated to emit approximately 10–30% of its tread weight into the road environment before it is worn out (Grigoratos and Martini, 2014; Parker-Jurd *et al.*, 2019). Estimate of wear rate in Norway varies between 132 and 600 mg/vkm depending on vehicle types (Vogelsang *et al.*, 2018). Some of the factors affecting wear rate are listed below (a–d):

a) Tire characteristics

Different types of tire wear at different rates owing to their chemical composition and pattern of the tread, which vary depending on their use. For example, as cited in Vogelsang *et al.* (2018), LeMaitre *et al.* (1998) found that winter tires wear more than summer tires. Tire manufacturers also use customized compositions to optimize the tire characteristics within each category (Andersson-Sköld *et al.*, 2020). The most important tire characteristics that affect wear are the size, tread depth, construction, pressure and tread temperature, chemical composition, accumulated mileage, and wheel alignment (Jekel, 2019).

b) Vehicle characteristics

Weight, load distribution, driving wheel location, engine power, electronic braking systems, suspension type, and state of maintenance all affect the wear rate. For example, Chen and Prathaban's (2013) modeling study showed the effect of load on wear and demonstrated that a

higher load increased wear. Similarly, heavy-duty vehicles emit more TWP per distance driven compared to light-duty vehicles and passenger cars (Grigoratos and Martini, 2014).

c) Road surface characteristics

Road material, texture, pattern, porosity, condition, and wetness affect tire wear. For example, concrete pavements produce lower wear emissions of particulate matter (PM₁₀) than other types of pavements (Grigoratos and Martini, 2014). Road surfaces influence tire wear mainly through their micro- and macrotextures. Large variations in tire wear were observed owing to different road surfaces, where the wear on rough, harsh surfaces was approximately thrice as severe as that on smooth, polished surfaces (Lowne, 1970).

d) Vehicle operation

There is correlation between vehicle speed and tire wear (Gustafsson *et al.*, 2008; Snilsberg, 2008). Generally, drivers can increase their tire wear by speeding, fast acceleration, braking, and high cornering speeds. Increased wear rates may also occur because of steering system misalignment and incorrect tire pressures (Boulter, 2006; Pohrt, 2019).

1.3.2. Precipitation

Deposited particles are washed off the road with runoff when the precipitation intensity exceeds a certain limit, defined by the rainfall detachment index (RDI) (Brodie and Porter, 2006). According to Brodie and Porter (2006), the transported amount increases linearly with the rainfall intensity up to a maximum, where it levels off. Climate change might contribute to the further mobilization of TWP, as it is expected to increase the intensity and frequency of rainfall and snowmelt, producing a high amount of stormwater (Skaaraas *et al.*, 2015; Dale *et al.*, 2017; U. S. Environmental Protection Agency, 2021).

1.4. Stormwater treatment and tire wear particles retention

Owing to the increasing trend in TWP emissions, their persistence in the environment, and their potential risk, it is important to take measures to limit the spread of TWP (Andersson-Sköld *et al.*, 2020). Two general approaches of reducing TWP discussed in Andersson-Sköld *et al.*, (2020): 1) source reducing measures, which are mainly addressing factors affecting TWP generation presented in section 1.3.1. These measures are related to individual choices and drivers' behavior like usage of studded tires, correct tire pressure, long lasting tire, speed and driving behavior, total vehicle km, choice of vehicle. Source reducing measures are also related to the vehicles and tires industry advancement to manufacture less wearing tires and lighter vehicles. 2) dispersal reducing measures, which are mainly related to stormwater management as physical removal by street sweeping and snow removal are not considered to be significant (Janhäll *et al.*, 2016). Although not explicitly designed for TWP retention, several stormwater management systems are suitable for pollutants (Vogelsang *et al.*, 2018). Traditionally Waste Water Treatment Plants receive a significant amount of stormwater from urban areas (Verschoor *et al.*, 2016), which might

be efficient in removing TWP due to their performance on other particles larger than 30 μm (Vogelsang *et al.*, 2018). Recently, wet and dry ponds, infiltration basins, ditches, and constructed wetlands are becoming a common stormwater management facilities (Jotte, Raspati and Azrague, 2017). Some of the systems have shown promising results. For example, TRWP retention in bioretention indicated removal efficiencies of over 70% in stormwater runoff (Lange *et al.*, 2021, 2022). However, the retention of TWP have not been widely studied in many systems, including gully pots, bioretention cell, and roadside soil.

1.4.1. Gully pots as tire wear particles sink

Gully pots are small sedimentation basins embedded in the ground, usually connected to stormwater pipes. The primary objective gully pots is retaining the solids in stormwater runoffs to prevent clogging of the sewerage system (Lindholm, 2015; Wei *et al.*, 2021). They are fitted along the road at about 60–70 m distance apart to reduce the hydraulic loading during heavy precipitations. The minimum diameter of a typical gully pot in Norway is 1 m while its outlet is at 100 cm from the bottom (Lindholm, 2015). Frequent emptying, when they are approximately 50% filled, is recommended to maintain adequate retention (Lindholm, 2015; Wei *et al.*, 2021).

The fraction of solids captured by gully pots has been studied extensively, and retention efficiencies of 20–50% depending on emptying frequency are reported (Lindholm, 2015). Others, such as Butler and Karunaratne (1995), give less credit to retained sediment height and present influent flow rate and particle diameter as primary factors for trap efficiency. Fig. 3 shows the estimated efficiency of a gully pot in retaining particles with respect to diameter and influent flow velocity. There is a positive correlation between particle diameter and trap efficiency because larger particles settle faster. The expected retention efficiency for particles $<50 \mu\text{m}$ is very low, even at low influent velocities suggesting the inefficiency of gully pots in retaining TWP, given that a significant share of TRWP are in the size range of 50 μm or less (Kreider *et al.*, 2009).

The retention of particles is also affected by increases in flow velocity into gully pots. According to Lindholm (2015), the two-year recurrence precipitation intensity for Oslo, Blindern was determined to be significantly greater than the maximum inflow capacity of a gully pot (25 l/s).. In other words, the critical value (28 l/s*ha) that a gully pot can receive is six times lower than the inflow a two-year recurrence rain can generate in 5 minutes. The precipitation intensity that generates this critical value is so small that it occurs multiple times annually (Lindholm, 2015), suggesting less potential for removing particles and TWP in gully pots. TWP concentration in gully pot sediments is discussed in detail in Paper II.

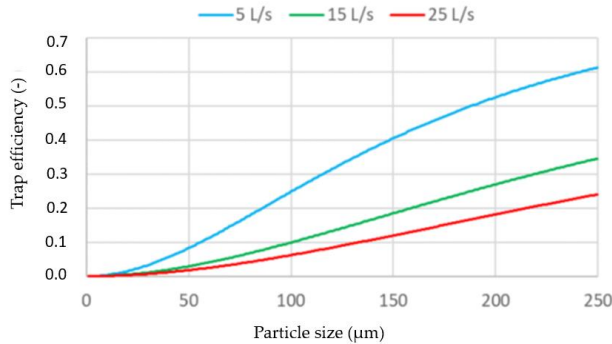


Figure 3. Estimated efficiencies of a gully pot trap particles with diameters between 1 μm and 350 μm and a density of 1.7 g/cm^3 when the influent flow velocity to the gully pot is 5–25 L/s. Adapted from (Vogelsang *et al.*, 2018)

Bioretention cells as tire wear particles retention measure

Bioretention cells (also known as rain gardens) are widely used to manage stormwater from road runoff (Paus *et al.*, 2014; Kratky *et al.*, 2017; Ding *et al.*, 2019). The objectives of bioretention cells are to reduce peak runoff, increase groundwater recharge, enhance the aesthetics of the community (Khan *et al.*, 2013), and improve runoff water quality through infiltration, sedimentation, and sorption processes (Kim *et al.*, 2003; LeFevre *et al.*, 2015; Paus *et al.*, 2016, 2013). Their pollutant (e.g., petroleum hydrocarbons) removal capabilities have been reported in many studies (e.g., LeFevre *et al.*, 2012 a,b). Although their pollutant removal efficiencies vary depending on site characteristics, design, implementation, and climatic conditions (Brown and Hunt, 2012; Roy-Poirier, 2010), bioretention cell have been shown to effectively retain sediments (Gilbreath *et al.*, 2019).

Their use is not limited by climatic conditions, as studies have proven the practical application of bioretention cell under cold climatic conditions (air temperature between -5 and +5 $^{\circ}\text{C}$) (Khan *et al.*, 2013; Ding *et al.*, 2019). Engineered soils with high infiltration capacity and high organic matter content are critical for bioretention to infiltrate water, retain moisture for dry periods, set conditions for plant growth, and remove pollutants (Paus *et al.*, 2013). However, because the infiltration capacity is reduced at lower temperatures, engineered soil at least four times higher than that designed for warmer climates (100 mm/h at 25 $^{\circ}\text{C}$) is recommended in cold climatic regions (Paus *et al.*, 2016).

Optimal hydrological performance is only a part of the equation for bioretention to function as a treatment facility. Soil with good plant growth properties is important. Although satisfactory hydrological and pollutant removal functions of bioretention cell have been reported (Gilbreath *et al.*, 2019), the establishment of vegetation has been challenging. For example, Tahvonon (2018)

found that engineered soil that worked best in surface water management was not optimal for plant growth. The lack of nutrients was one of the main reasons for the limited plant growth, which was significantly improved by the addition of garden compost.

Treatment of runoff in bioretention cells removes TWP, likely through physical straining (Smyth *et al.*, 2021). However, removal efficiency can be affected by TWP size, as demonstrated by Gilbreath *et al.* (2019), who studied rubber fragments $\geq 125 \mu\text{m}$ and showed decreasing removal efficiency with decreasing size. This can be problematic for efficient TWP retention by bioretention cells because significant amounts of smaller TRWP ($\leq 50 \mu\text{m}$) have been found in road dust (Kreider *et al.*, 2009; Klöckner *et al.*, 2021). Therefore, TRWP in engineered soil, including TRWP $< 50 \mu\text{m}$ and removal efficiency, is the topic covered in Paper III.

1.4.2. Deposition of tire wear particles along roadside soil

Road verges outside urban centers, which are grassy or filled with soil or gravel, transport rain and meltwater away from the road by either direct infiltration or through the stormwater conveying system to a nearby recipient or local treatment facilities (Vegdirektoratet, 2014). Although verges are not a treatment system, wear particles can be retained by the soil and vegetation within the verge (Åstebøl and Hvitved-Jacobsen, 2014). TRWP have been found at highly variable concentrations along roads ranging from 0.6 to 117 mg/g dry weight (Cadle and Williams, 1978; Fauser, 1999; Vogelsang *et al.*, 2018). The concentration of TRWP is expected to decrease exponentially with distance (Wagner *et al.*, 2018), with 80% of the wear particles found within 5 m from the road (Cadle and Williams, 1978).

The soil along the racetracks may receive high amounts of TWP generated by the high-speed, fast acceleration and retardation, and increased cornering speeds, which, according to Pohrt (2019), leads to increased tire wear. High deposition might be possible as Dahl *et al.* (2006), who studied the effects of speed on tire wear generation in a laboratory road simulator found speed to be the main factor in particle generation. Therefore, it is expected that motor racing, which is a frequent activity in a relatively small space might lead to high deposition of TWP in the soil along the racetrack.

Racecar tires have components similar to road cars, such as NR, SBR, carbon black or silica, sulfur, zinc oxide, antioxidants, and antiozonants (Wik and Dave, 2009; Grigoratos and Martini, 2014; Formula 1, 2021a). Despite these similarities, race and road tires are very different and probably generate different TWP, as road tires are made to last 40,000–50,000 km (Grigoratos and Martini, 2014; Parker-Jurd *et al.*, 2019), whereas Formula1 tires are designed to last for a maximum of 200 km (Formula 1, 2021b). There are few prior studies on the deposition and concentrations of TWP along racetracks, and this is the topic of Paper IV.

2. Thesis objectives and framework of the study

This thesis was motivated by the lack of a suitable analytical methods for measuring the environmental concentrations of TWP and a knowledge gap on the effect of stormwater management solutions. The specific objectives of this study were as follows:

- Develop a method for detecting and quantifying TWP in complex environmental samples, such as soils and sediments (Papers I and II).
- Measure TWP concentrations in stormwater treatment solutions, namely gully pots (Paper II) and bioretention cell (Paper III).
- Evaluate the efficiency of the treatment solution (bioretention cell, Paper III) in retaining TWP.
- Measure the deposition of TWP in soil along a racetrack and evaluate the effect of distance from the edge and racetrack alignment on TWP concentrations (Paper IV).

Fig. 4 provides a general overview of the thesis and the logical connections between the background, methods, objectives, and implications of the thesis.

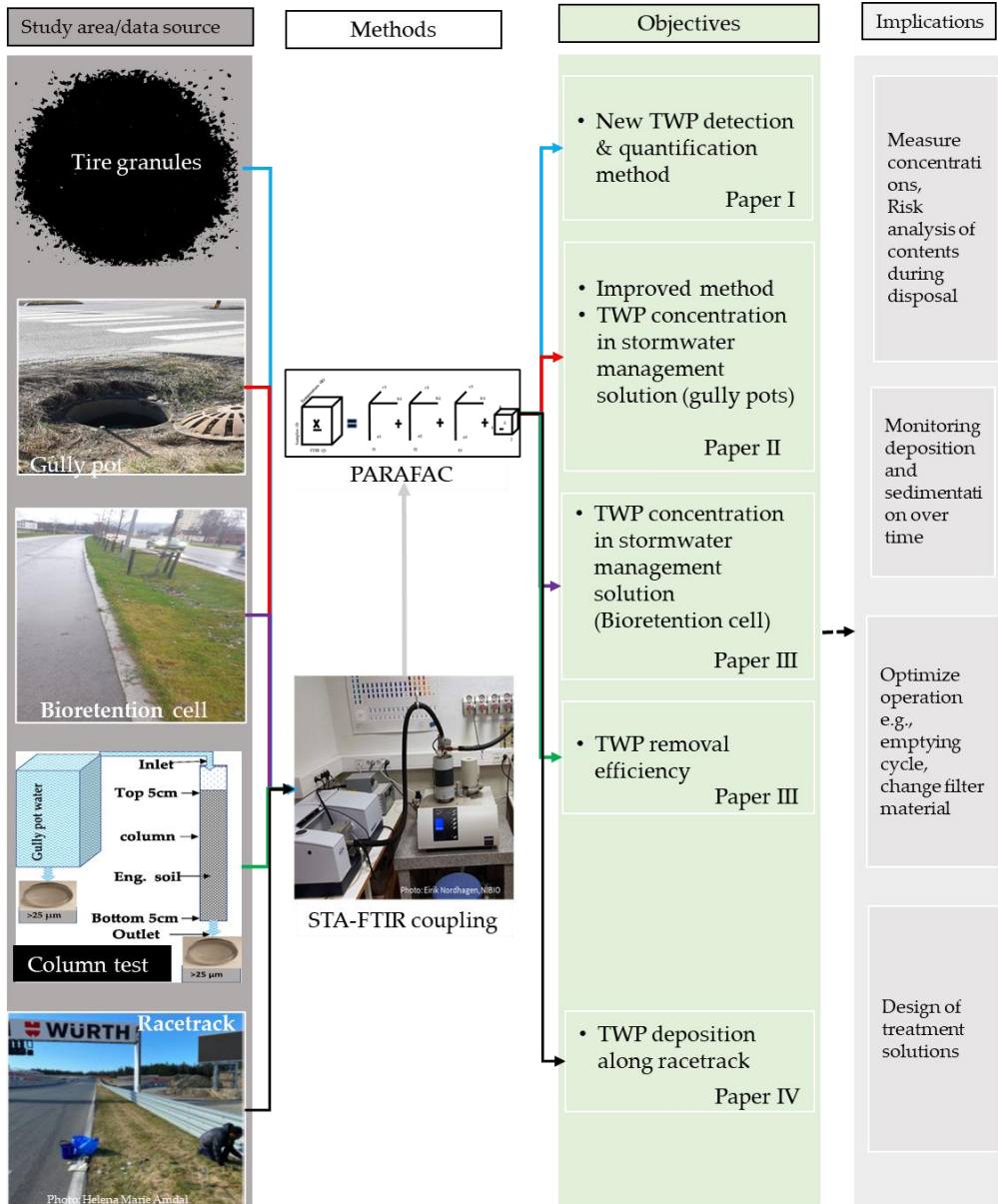


Figure 4. Study framework of the thesis. Similar colored lines connect the data sources to specific objective/Papers. Data sources and objectives are connected through STA/FTIR-PARAFAC which are connected by grey line. Implications of the results of the studies included in this thesis are shown by a dotted arrow. Implications are not matched one-to-one as results in one study might have different implications.

3. Materials and methods

3.1. Study sites

Laboratory experiments and field studies were conducted to introduce a new method of quantification and to measure TWP concentrations in the sediments/soils of the treatment solutions. Three sites were selected for this study.

1. Ten gully pots at five sites (Fig. 5) in a municipality of Southern Norway (Ås, N59.660, E10.784) were selected to measure TWP concentrations in gully pot sediments (Paper II). The sites were selected for expected varying TWP generating factors such as traffic density and street characteristics. Streets at the selected sites had a speed limit of 30 km/h, which is common in built-up areas and town centers in Norway. The traffic density in these streets was recorded using radar from Amparo solutions during June and July 2020. Unfortunately, information on gully pot maintenance was unavailable at the time of the study.
2. To evaluate if a bioretention cells established with engineered soil retain TWP, soil samples were collected from two positions in a bioretention cell (i.e. close to the inlet and 5 m away, each position represented by 3 sampling points) in a municipality of Southern Norway (Drammen, along county road FV282, between N59.737, E10.201 and N59.734, E10.206) (Paper III). The bioretention cell was established in 2019 using engineered soil (70% sand, 30% compost) and designed to optimize hydrological conditions, pollutant removal, and plant growth (Haraldsen, Gamborg and Vike, 2019). The bioretention cell is located on the street with a speed limit of 50 km/h and a traffic density of 20,800 annual average daily traffic (AADT) (Statens Vegvesen, 2020). It receives road runoff through several standardized inlets fitted to the side curb, a 13 cm high structure separating the driveway from the bioretention cell (Fig. 6). These inlets operate only during warmer seasons and are closed during the cold winter season (December–March) (Haraldsen, Gamborg and Vike, 2019).
3. The study of TWP concentrations in gully pots sediments (Paper II) indicated the influence of driving patterns. As a high speed, high braking and acceleration are associated with a diving pattern to generate high wear, a leading motorsport facility in Norway (Rudskogen) was selected to quantify the amount of TWP deposited in soils adjacent to the racetrack. Four locations were selected at the Rudskogen Motorsports Center (Fig. 7) to measure TWP concentrations along the racetrack (Paper IV). The racetrack is located in a municipality of Southeastern Norway (Rakkestad, N59.368, E11.262). The main racetrack is a 3 km long asphalt with an elevation difference of 43 m, and 14 corners. Verges along the racetrack were grass-covered, gravel, or paved. The width of the verge varied from 2.8 m to 40 m.

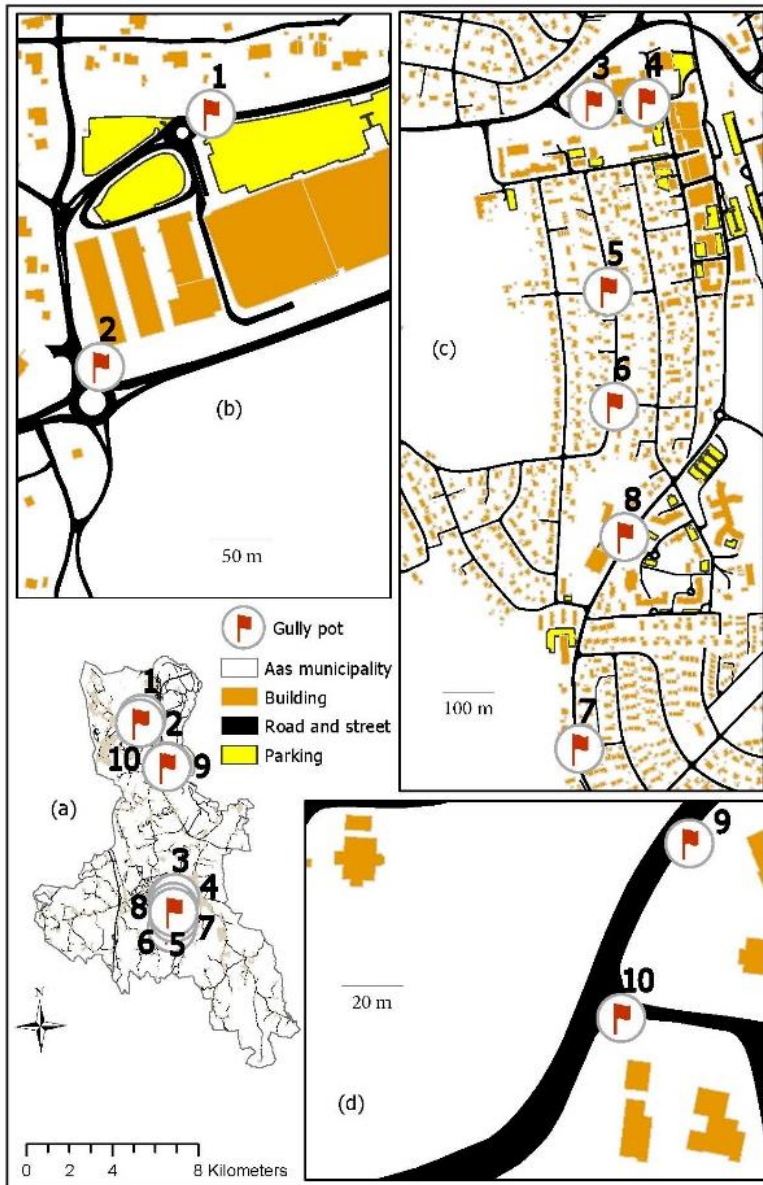


Figure 5. Overview of (a) sampling sites and gully pots (b) gully pots at site Sjoskogenveien (1, 2), (c) gully pots at sites Raadhusplassen (3, 4), Maaltrøstveien (5, 6), and Brekkeveien (7, 8), (d) gully pots at site Nordbyveien (9, 10). Reprinted from Mengistu, Heistad and Coutris (2021).



Figure 6. Left picture: bioretention cell located between the road and sidewalk . Right picture: inlets specially designed and fitted to the side curb bring road runoff to the bioretention cell. (a) A 13 cm high side curb separates the road from the bioretention cell, (b) sampling spot in front of an inlet.

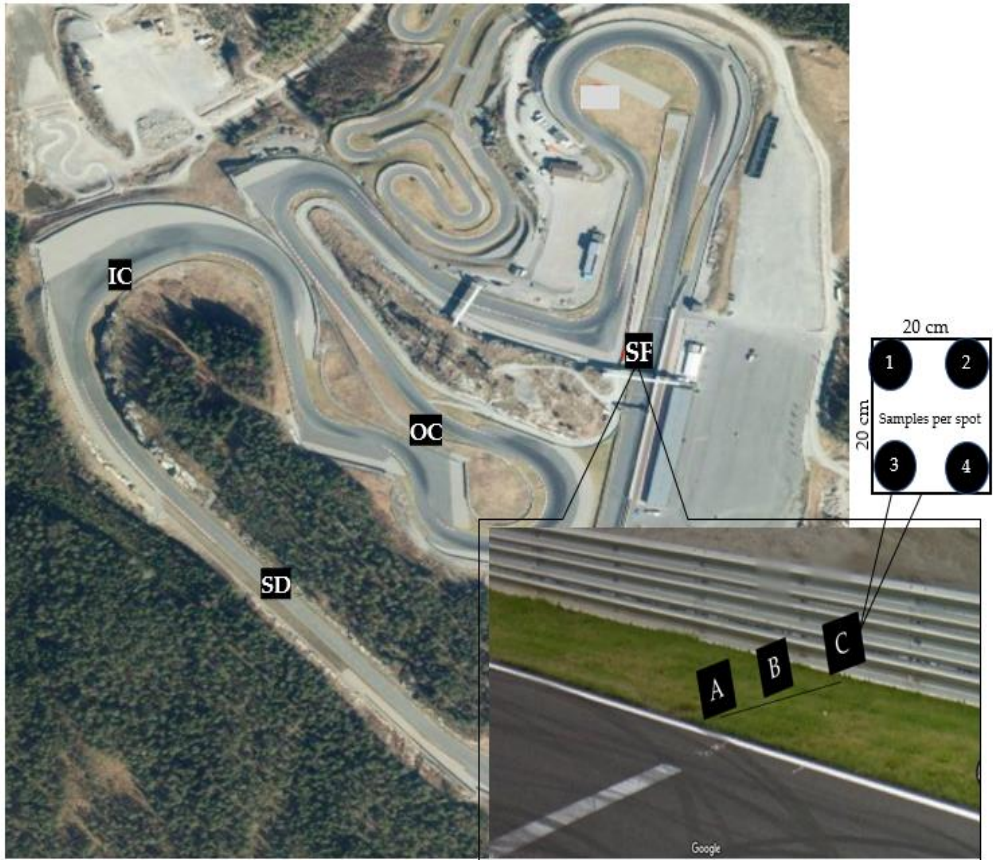


Figure 7. Overview of the Rudskogen racetrack with sampling locations (SF) start/finish, (LS) long straight, (IC) inward corner, and (OC) outward corner. Inset map: Sampling spots at the start/finish at distances A (0–20 cm), B (100–120 cm), and C (260–280 cm) away from the edge of the racetrack.

3.2. Experimental setup, sample preparation, and sampling

The experimental setup used in this study is presented in Fig. 8. For the experiment in Paper I, tire granules (TG) were collected from Ragn-Sells, a producer who removes gravel, spikes and other metal residues and grinds discarded tires from Norway and Sweden for reuse, e.g., in artificial turf. The TG samples of four different masses (0.5, 1, 2.5, and 5 mg) were placed in crucibles in two replicates, as a reference for the identification and quantification of TWP. These samples contain TG only and designated as TGO. Another set of samples were prepared by spiking 50 mg of formulated sediment with the four different masses of TG. The formulated sediment has a composition of 5% organic matter, 75% quartz sand, and 20% kaolinite clay (OECD, 2010). The spiked samples were designated as TGIS. TGIS (50 mg) from each of the four concentrations was placed in separate aluminum crucibles in three replicates for heating to study if the method identify and quantify TWP from sediments.

For Paper II, 500 mL of wet sediment was collected from each gully pot (10 in total from five study sites) using a spade. The samples were consistently taken from the top of the sediment accumulated under the standing water, in an attempt to account for the most recent contaminations. All samples were oven dried at 105 °C, crushed, homogenized with a mortar and pestle, and sieved at 5 mm to exclude materials beyond the defined microplastic range. A standard natural soil, LUFA 2.2 (LUFA Speyer, Germany), was included in the experimental setup as a rubber-free control. From each sample, a subsample of 80 mg of dry sediment was collected in three replicates for analysis to obtain a total of 33 samples.

For Paper III, topsoil (0–5 cm) was collected using a soil sampling tube from six different locations: three spots, each located in front of three different inlets, and three 5 m away from these inlets. The samples were oven-dried at 105 °C for 24 h. Samples collected at the inlets were mixed and homogenized using a Kenwood kitchen blender KMM770 for 5 min at high speed to prepare composite sample A. The three samples taken 5 m away from the inlets were mixed and homogenized similarly, resulting in composite B. Both A and B were sifted using a vibratory sieve shaker (Retac 3D, Retsch, Germany) with stainless steel mesh sizes of 50, 100, and 500 µm to form four different size fractions, as shown in Table 2. From each sample, a subsample of 80 mg of dry sediment was collected in triplicate for analysis.

Table 2. Proportion (by mass) of soil fraction in bulk soil collected from a bioretention cell in Drammen, southern Norway, close to the inlet (entry point of road runoff, A) and 5 m away from the inlet (B).

Soil size fraction (µm)	Proportion in bulk soil (%)	
	A	B
<50	3.8	3.3
50–100	24.6	22.6
100–500	35.6	39.0
500–5000	36.0	35.1

In addition, (for Paper III), engineered soil was composed of medium sand, silty sand, and garden compost (collected from Lindum AS, Norway), mixed in a proportion of 8:15:6 by mass. This engineered soil was recommended by (Haraldsen, Gamborg and Vike, 2019) because of its infiltration efficiency and quality in promoting plant growth. Three similar cylindrical columns (C_1 , C_2 , C_3 , diameter 3.8 cm, surface area 11.34 cm², height 50 cm) were filled with 40 cm of engineered soil. The bottom of the column was sealed with a lid with two small openings (diameter of 5 mm) to release the effluent water. The openings were connected to a 20 L water container to collect the effluent. Road runoff collected from gully pots served as influent to the columns. Standing water and sediments from the gully pots (120 L from Sjoskogenveien and 100 L from Raadhusplassen) were collected and stored in a cold room. Using Watson peristaltic pumps, road runoff was applied to three columns (C_1 , C_2 , and C_3). The pumps were calibrated to yield a hydraulic load of 3.7 mm/min for 10 min (total water height of 37 mm). The rate and duration were chosen as to represent Norwegian water quality design rain (Paus, 2018) for a cell size collecting and treating runoff from a catchment 10 times the size of the cell area. The pumps were programmed for 10 min on and 30 min off (10 min application, 30 min rest). The resting period was later prolonged (up to 4 h), as the high particle loads caused soil clogging and reduced infiltration. Influent water (6 L) and all effluent from the columns (C_1 , C_2 , C_3) were filtered through a 25 μ m mesh. The retained particles were analyzed for TWP concentrations in the influent and effluent to estimate the removal efficiency. To assess the spatial distribution of retained TWP in the column, soil samples were collected from the top and bottom 5 cm of the three columns, which were then density-separated by 1.8 g/cm³ ZnCl₂ solution and filtered through a 25 μ m mesh. Density separation was required to concentrate TWP in the samples to aid detection by excluding denser particles through settling, while TRWP with estimated density of 1.8 g cm³ float in ZnCl₂ solution. Filtration ensured measurement of similar size (>25 μ m) in all samples to help comparison.

For Paper IV, four sampling locations were selected to represent different racetrack alignments where TWP generation and transportation from the track surface to the verges was assumed to occur at different rates following linear speeding, radial acceleration, and braking. TWP generation is assumed to occur at different rates at selected locations, following linear speed, radial acceleration, and braking. The selected sampling locations (SF, LS, IC, and OC) are shown in Fig. 7. At each sampling location, three different spots with an area of 20 × 20 cm² each and sample center distances from the edge of the racetrack (10 cm, 110 cm, and 270 cm, respectively) were selected. Four samples from the topsoil (0–5 cm depth) were collected from each spot using a soil corer and mixed to form composite samples. Twelve composite samples were oven-dried at 105 °C overnight and then homogenized with a blender for approximately 15 s. Larger particles were removed by sifting with a 5 mm mesh before a subsample of 10 g was sieved with three different mesh sizes (1,000 μ m, 50 μ m, and 25 μ m). From each sample, a subsample of 80 mg of dry sediment was collected in triplicate for analysis.

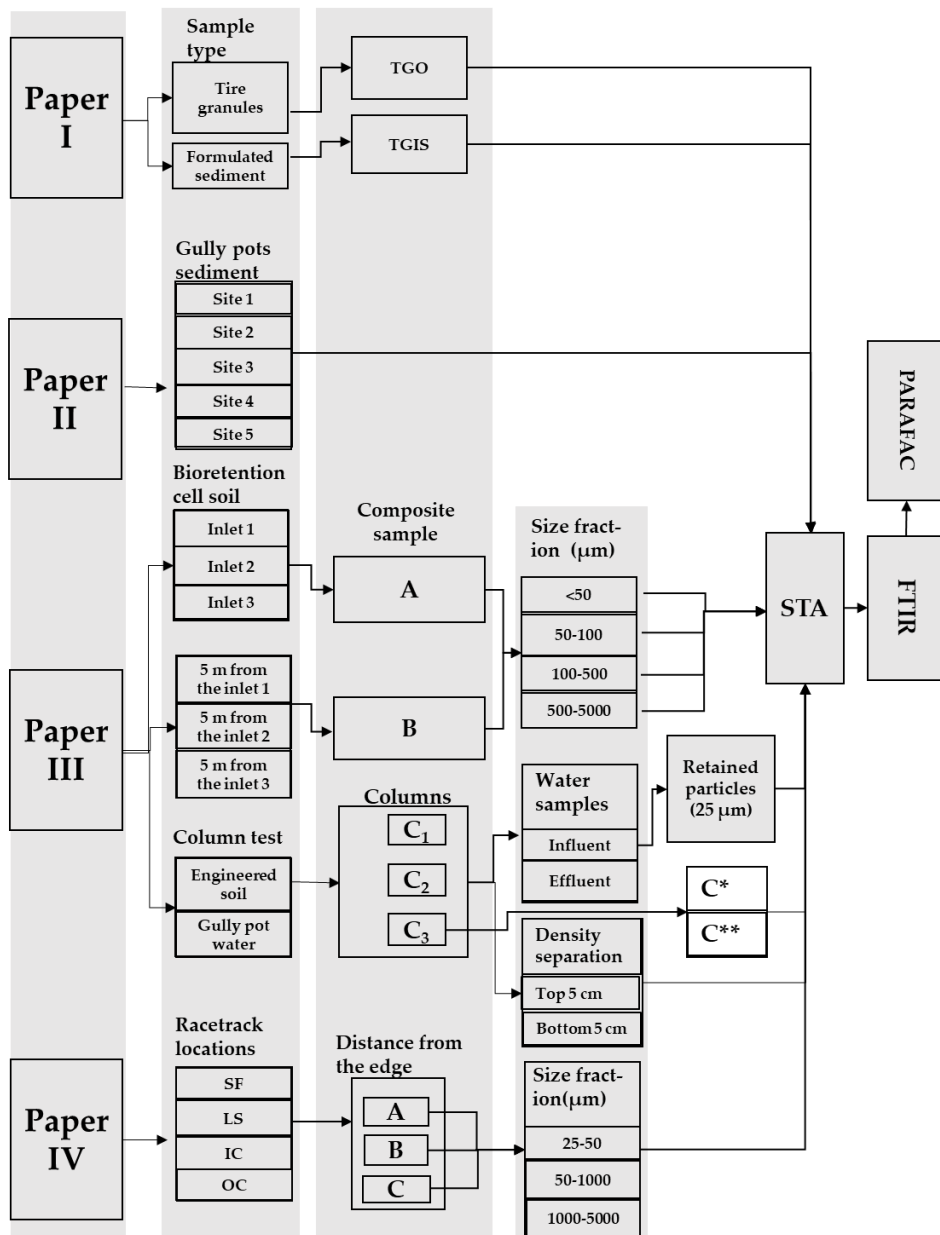


Figure 8. Experimental setup of the thesis . TGO: tire granules only samples, TGIS: formulated sediment spiked with tire granules. Sampling locations of the gully pots: sites 1-5. Bioretention cell: A is a sampling position at the inlet of road runoff to the bioretention cell, while B is a sampling position 5 m away from the inlet. Size fraction shows the size ranges (<50, 50-100, 100-500, and 500-5000 μm) of the bioretention soil in A and B. Column test: C₁-C₃ are the three columns used in the TWP retention efficiency test. C* are additional samples from C₃ without any treatment. C** are additional samples from (C₃) which received only filtration treatment. Influent is the gully pot water used in the experiment, while Effluent is the water passed through the column. Racetrack locations: SF is start/finish, LS is long straight, IC is inward corner, and OC is outward corner. Distance from the edge of racetrack: A (0–20 cm), B (100–120 cm), and C (260–280 cm). Size fraction shows the size ranges (25-50, 50-1000, and 1000-5000 μm) of the soil along racetrack. STA: simultaneous thermal analysis. FTIR: Fourier infrared transform spectroscopy. PARAFAC: parallel factor analysis.

3.3. Sample analysis

3.3.1. Simultaneous thermal analysis

The samples were heated in a simultaneous thermal analyzer STA 449 F1 Jupiter, with carrier type S (Netzsch, Germany), from 40 to 800 °C at a rate of 10 °C/min under a protective nitrogen atmosphere (flow rate 20 mL/min). The evolved gases were continuously purged into the FTIR using nitrogen as the carrier gas (at 50 mL/min). The thermogravimetric unit in the STA registered changes in the sample mass (balance resolution of 25 ng) every 13 s during the heating process, resulting in 333 mass measurements at 333 temperature ramps per sample. The sample mass change registration was adjusted to 6.83 s, which resulted in 613 (Paper II) and 666 (Papers III-IV) mass measurements and temperature ramps.

3.3.2. Fourier transform infra-red spectroscopy

A Bruker Tensor 27 FTIR spectrometer with an external gas cell (Bruker, USA) was used to obtain FTIR spectra of the gas evolved in the STA. The average signal of 16 scans, with a wavenumber range of 4000–400 cm^{-1} , was collected at a resolution of 1.93 cm^{-1} during the heating process, generating 1,762 signal points. Each scan took 13 s, resulting in 333 spectra per sample. After the study published in Paper I, the number of scans was reduced from 16 to 8, the time between scans was reduced to 6.83 s, and the spectra number increased to 613 (Paper II), and 666 (Papers II, III, and IV), in order to remove some artifacts observed in Paper I.

3.4. Data preparation and parallel factor analysis model

3.4.1. Data preparation

With visual evaluation of the TGIS FTIR (Paper I), the signals appeared to be intense between 600 and 400 cm^{-1} (Fig. 9). Modelling with the full range of spectra (4000–400 cm^{-1}) did not result in meaningful loadings possibly due to Rayleigh scattering, which are not desirable in PARAFAC modelling (Rinnan, 2004; Thygesen *et al.*, 2004). To prepare the data for the PARAFAC model, we first removed spectral data below 600 cm^{-1} (See Fig. 1, section 1.2.3. for FTIR spectra 4000–600 cm^{-1}). Murphy *et al.* (2013) should be referred to for more information on the Rayleigh scattering. Then, synchronizing the programmed time and temperature in the STA and FTIR, a three-way dataset was formed, as described in Fig. 2 (section 1.2.4.). The datasets had 8 samples \times 1762 Wavenumber (cm^{-1}) and 333 Temperature ($^{\circ}\text{C}$) in Paper I (TGO), 12 samples \times 1762 Wavenumber (cm^{-1}) and 333 Temperature ($^{\circ}\text{C}$) in Paper I (TGIS), 33 samples \times 1762 Wavenumber (cm^{-1}) and 613 Temperature ($^{\circ}\text{C}$) in Paper II, 56 samples \times 1762 Wavenumber (cm^{-1}) and 666 Temperature ($^{\circ}\text{C}$) in Papers III and IV.

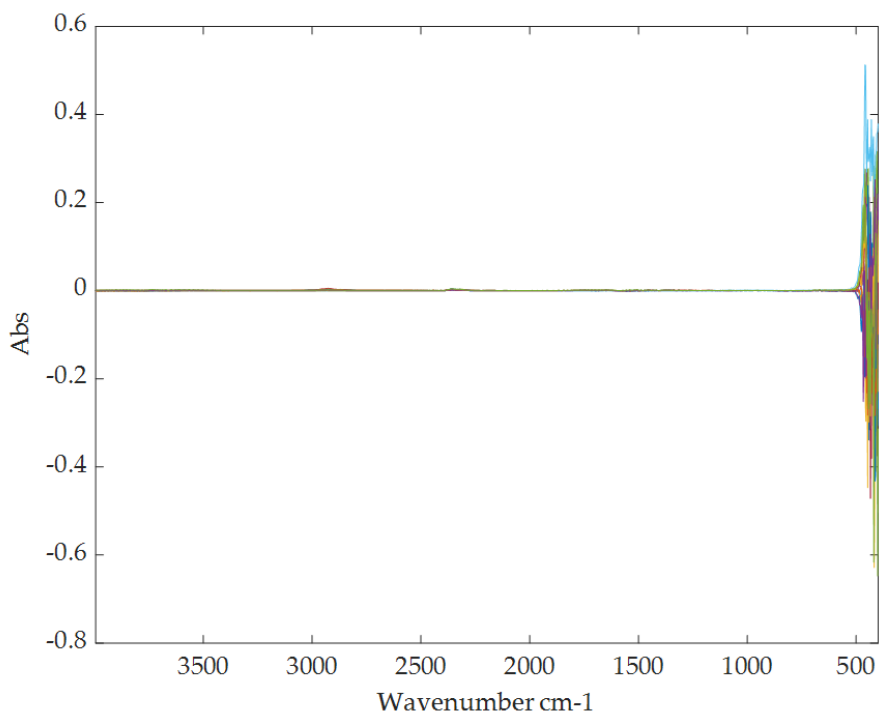


Figure 9. Raw FTIR spectra (4000-400 cm^{-1}) of formulated sediment spiked with tire granules (TGIS, Paper I)

3.4.2. PARAFAC model

PARAFAC models were built using components in MATLAB (The MathWorks, Inc., R2018a, Natick, USA) and a PLS Toolbox for MATLAB version 8.6 & 9.0 (Eigenvector Research, Inc., Wenatchee, USA). Throughout this thesis, the PARAFAC models were first run without preprocessing starting by two components and increasing until the core consistency reaches unacceptable level (close to zero). Then, one of the preprocessing (normalization was applied only to samples in Paper II) was applied to improve the model fit followed by evaluation of the results using visual inspection of the loadings, core consistency, variation per component and split-half analysis. The applied preprocessing showed meaningful results (interpretable loadings) only when applied to mode 2 (FTIR).

The various steps involved in the PARAFAC analysis are shown in Fig. 10.

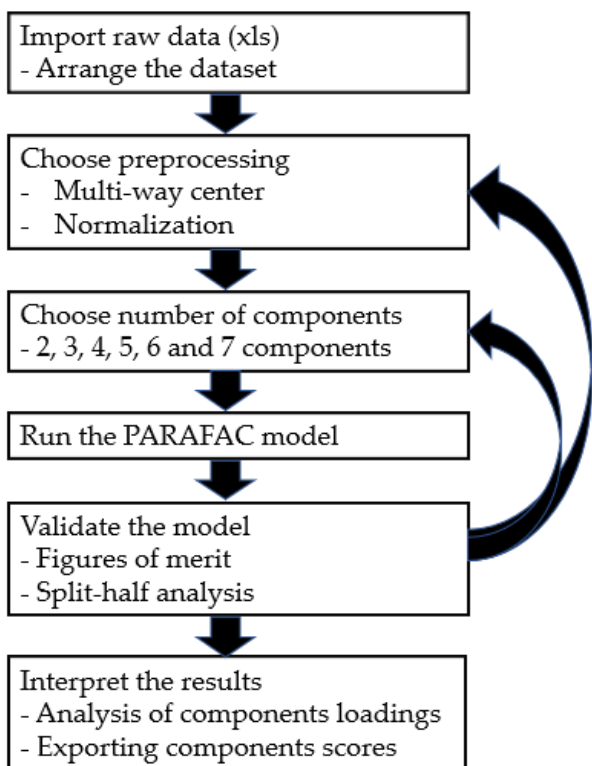


Figure 10. Schematic presentation of the steps involved in PARAFAC analysis of STA-FTIR data of sediment samples. Default split-half analysis was used in the study. The back arrows symbolize the repetition of component modification and preprocessing performed after a PARAFAC model run to identify the proper number of components. Reused from Mengistu, Heistad and Coutris (2021).

The validity of the PARAFAC model was evaluated using figures of merit (core consistency, variation per component, and residuals) and split-half analysis, as detailed in the appended papers. Finally, the model with the most components and best figures of merit was selected. The PARAFAC model generates Mode 1 scores, Mode 2 loadings, and Mode 3 loadings for each component (trilinear components). In this analysis, Mode 2 represents the FTIR spectra and is therefore referred to as the FTIR spectra in this thesis, while Mode 3 represents the mass loss rate at a given temperature and is referred to as the pyrolysis temperature. FTIR spectra and pyrolysis temperatures were used to identify the components in the samples, more specifically, to determine if RM were present in the samples. Scores were used to estimate concentrations, as described in section 1.2.4 of this thesis.

3.4.3. Rubber material identification

FTIR spectra (wavenumber cm^{-1}) and pyrolysis temperatures ($^{\circ}\text{C}$) of components were visually evaluated against the FTIR spectra and DTGA of markers of rubber constituents (NR and synthetic rubber) of tires (section 1.2.2 & 1.2.3 of this thesis) for detecting the presence of RM.

As one spectroscopic method may not reliably identify a substance, FTIR spectra and pyrolysis temperatures were used concurrently. In addition to positive matching, identification was strengthened by the exclusion of components that did not resemble RM, such as degradation products of organic substances (water, carbon dioxide, monomers, dimers, and oligomers) that may be generated during heating.

See Fig. 11 a and b for the mass loss and DTGA curves of various SBR/NR blends relevant to car tires.

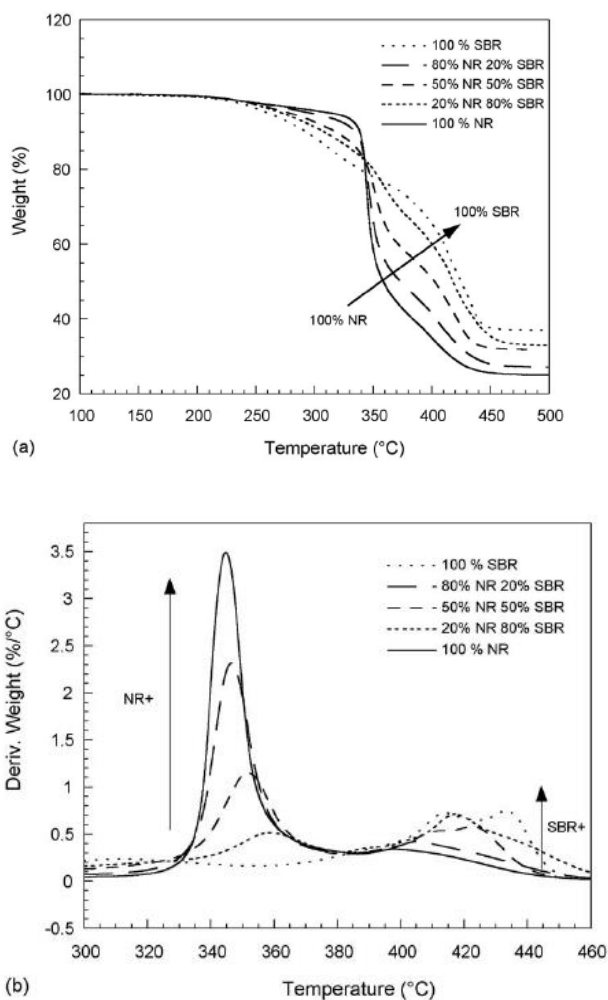


Figure 11. (a) TGA weight loss and (b) DTGA curves for NR/SBR blends of different elastomer components obtained using high-resolution thermogravimetric analysis at a heating rate of 40 °C/min. Adopted from (Fernandez-Berridi et al., 2006) with permission from Elsevier.

An example of the FTIR spectrum of the rubber blend (40/60 NR/SBR) is shown in Fig. 12.

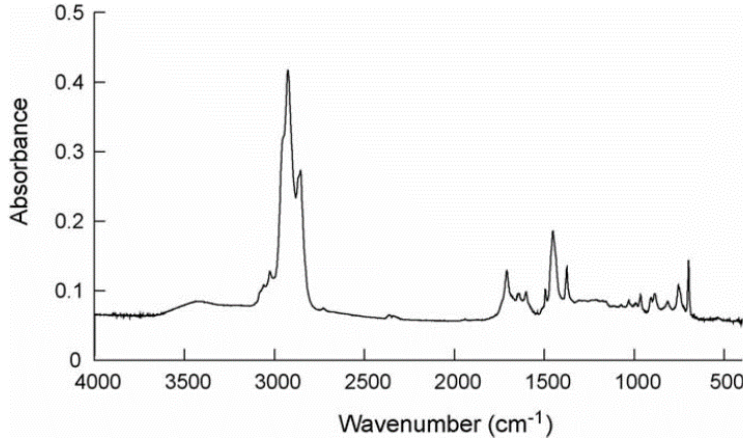


Figure 12. Infrared spectrum of a NR/SBR (40/60) blend . Adopted from Fernandez-Berridi *et al.* (2006) with permission from Elsevier.

3.4.4. Estimation of concentrations and statistical analysis

Calibration with known measured concentrations

After the RM component was identified, the measured quantity of TGs before heating (RM concentrations) was calibrated against scores from the PARAFAC model using PLS regression analysis (Paper I). The producer ratio (58%, RM/TG by mass) was used for calibration. The soundness of the model fit and the estimation accuracy of unknown concentrations (if at least one sample with known RM concentration is added to the analysis setup) was tested by R^2 and the root mean square error of validation (RMSECV) as shown in eq. 3 (Baum *et al.*, 2016). The RMSECV % was calculated by dividing RMSECV by the mean of the sample values.

$$RMSECV = \sqrt{\frac{\sum_{l=1}^L (y_l - \hat{y}_l)^2}{L}}, \quad (3)$$

y_l = predicted TWP quantity of the l th sample not included in the calibration and \hat{y}_l = known tire quantity of the l th sample. L = number of samples

Estimation of concentrations from mass loss during heating samples

When no sample with known RM concentrations was included in the analysis (Papers II, III, and IV), eq. 4 was used. The basic principles for this approach are the additivity assumption of the PARAFAC model and the Beer–Lambert law (Murphy *et al.*, 2013). This method has the advantage of not requiring a known concentration of RM in the analysis setup. The estimated RM concentrations from Papers II–IV were calibrated against the respective scores from the three PARAFAC models (one from each study) to test linearity.

$$C_{RM} = (ml \times a_{if}) / (m \times S_i), \quad (4)$$

Where C_{RM} = concentration of RM in a sample (mg/g)

ml = sample mass loss in STA (mg)

m = initial sample dry mass (g)

a_{if} = score of components identified as RM in sample i

S_i = sum of scores of all components of sample i

Differences in TWP concentrations were tested by one-way analysis of variance (the assumptions of normality and homoscedasticity were tested by normal probability plot and Levene's test, respectively, and fulfilled), followed by a Tukey pairwise comparison in gully pots, and a t-test in bioretention cell and column experiments. The level of significance was set to 0.05.

4. Results and discussion

This chapter summarizes the main findings from Papers I–IV.

4.1. A new method for detecting and estimating the quantity of tire wear particles in environmental samples

4.1.1. Identifying tire wear particles in environmental samples

A new method (Paper I) was developed to identify and quantify TWP in environmental samples by combining two instruments (STA and FTIR) with the PARAFAC model. After heating the TGO samples in STA, a high average mass loss (69%) was registered. The mass loss increased with increasing TGO sample mass (Fig. 13). The mass loss was 11 percentage points higher than the producer’s account of the RM content (58%) in tire granules (Ragnsells, 2018). Tire granule producers applied the International Federation of Association of Football (FIFA) test method, which attributes all mass loss between 300 and 650 °C to RM (FIFA, 2015), and seems to overestimate rubber content, suggesting the presence of additional substances in the evolved gas.

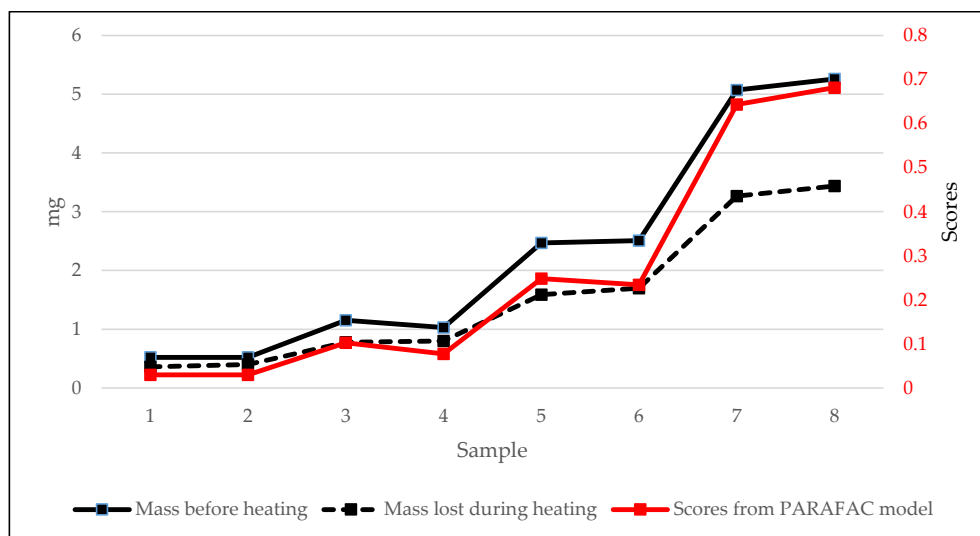


Figure 13. Mass loss/sample (left Y-axis) and PARAFAC scores (right Y-axis) increased with increasing tire granules (TGO).

The mixed substances were then resolved by fitting a PARAFAC model to this multi component dataset. The model decomposed the TGO dataset into three components and revealed relatively “pure” and interpretable underlying substances. The FTIR spectra of the second component (Fig. 14a) showed a sharp and weak peak at approximately 3,016 cm^{-1} (a typical C=C double bond) and strong peaks at approximately 2,925 and 2,850 cm^{-1} (C–H stretch of saturated hydrocarbons), indicating the presence of organic substances (Silverstein *et al.*, 2015). Other peaks in the fingerprint area ($<1,500 \text{ cm}^{-1}$) were difficult to interpret but showed similarities with the FTIR spectra of tires shown in Fig. 12 in this thesis and reported in the

literature (Gunasekaran, Natarajan and Kala, 2007; Cambridge Polymer Group, 2014) conforming to the presence of RM in TGO. This was further supported by the pyrolysis temperature of the same component (Fig 14b), showing peaks similar (if the STA-FTIR coupling is factored in) to the pyrolysis temperature of the tires/rubber blend shown in Fig. 11b in this thesis and other literature (Jasminská, Brestovič and Čarnogurská, 2013; Januszewicz *et al.*, 2017). The scores of the component increased with increasing measured mass of TGO (Fig. 10), suggesting that this component was RM.

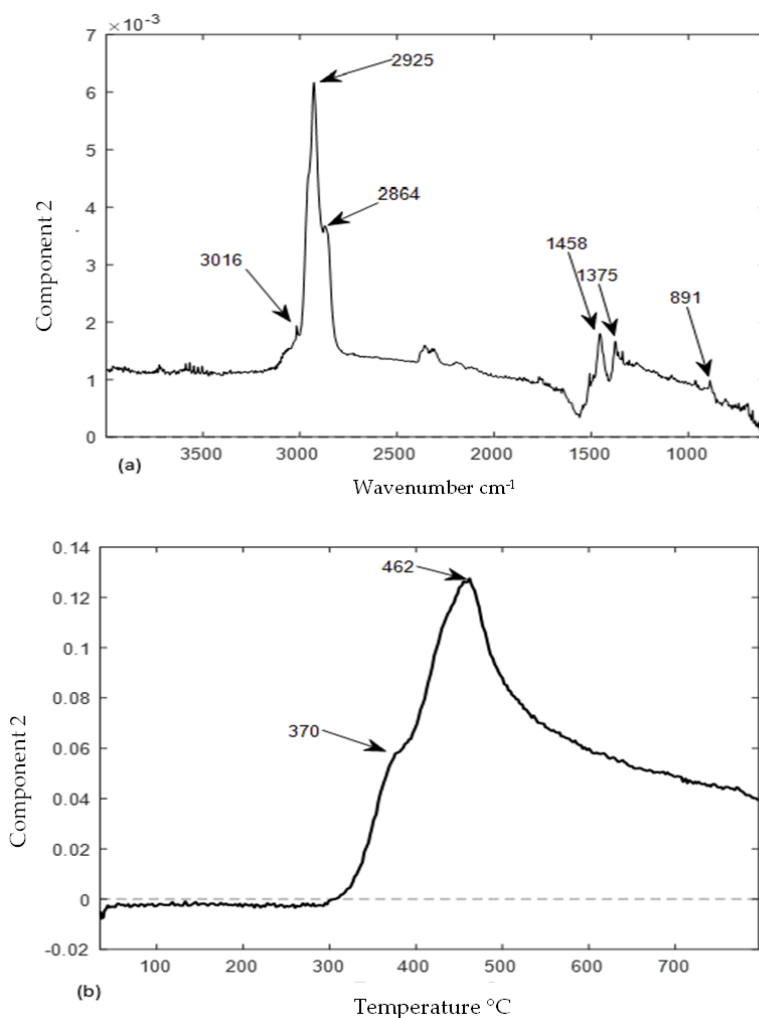


Figure 14. Loadings of the PARAFAC model for tire granules only (TGO). (a) FTIR spectrum of component 2, (b) pyrolysis temperature profile of component 2. A sharp and weak peak at around 3016 cm^{-1} ($\text{C}=\text{C}$ double bond) and strong peaks at approximately 2,925 and 2,850 cm^{-1} ($\text{C}-\text{H}$ stretch of saturated hydrocarbons) are indicative of organic substances (Silverstein *et al.*, 2015). Diagnostic bands for SBR and NR pyrolysis products are those which correspond to the out of plane bending vibrations of aromatic $=\text{C}-\text{H}$ and $\text{C}=\text{C}$ groups of polystyrene at 750 and 700 cm^{-1} , respectively, and the out of plane bending vibrations of $=\text{C}-\text{H}$ of vinyl groups (990 and 910 cm^{-1}) and *trans* groups $-\text{CH}=\text{CH}-$ at 960 cm^{-1} of butadiene.

The FTIR spectra of the first and third components of the TGO (Fig. 15) showed very different peaks than the FTIR spectra of the RM. Both components showed similar FTIR spectra (Fig. 15a and c), which resembled the spectrum of water in the gaseous phase and carbon dioxide (NIST Chemistry WebBook, SRD 69, 2011). However, the pyrolysis temperatures of the two components were different (Fig. 15b and d), suggesting that PARAFAC decomposed components based on their pyrolysis temperature, even if they represented the same substance (water in the vapor phase and carbon dioxide) in the two components. The segregation of components with similar spectra into different components violated the basic assumption of PARAFAC decomposition, which states that the signals between two chemical components should not be identical. However, it helped differentiate the sources of the substances under study. For example, the pyrolysis temperature spectrum of Fig. 12d showed features similar to those of cellulose and lignin pyrolysis temperatures (Shen *et al.*, 2013; Kawamoto, 2017), whereas Fig. 15b showed no specific peak, suggesting an artifact of water vapor generated during the STA–FTIR transfer process.

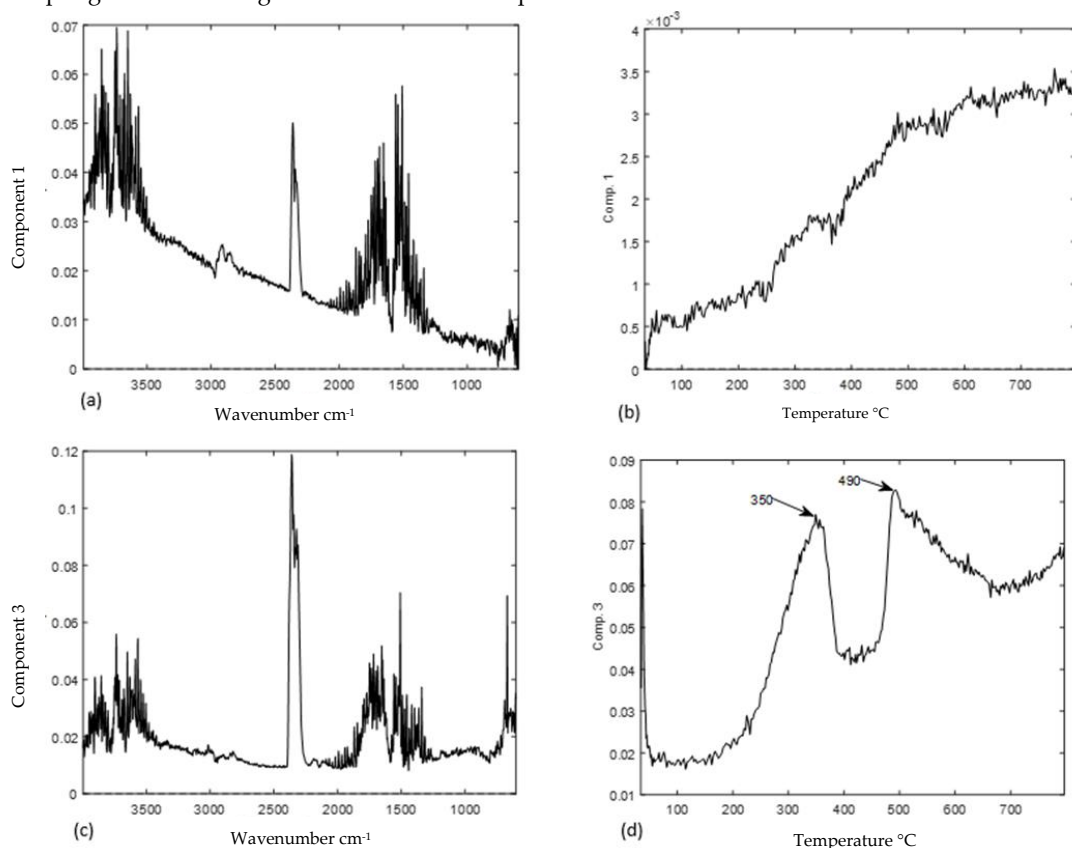


Figure 15. Loadings of the PARAFAC model for tire granule-only (TGO) samples. (a) FTIR spectrum of component 1, (b) pyrolysis temperature profile of component 1, (c) FTIR spectrum of component 3, (d) pyrolysis temperature profile of component 3.

TGIS lost an average of 8% of its original mass during heating. The lower mass loss compared to TGO was expected, given that TGIS samples contained a maximum of 15% of decomposable materials (spiked tire granules and organic matter in formulated sediment).

The PARAFAC model fitted to the TGIS data yielded three components. After evaluating the FTIR spectra and pyrolysis temperature profile, one of the components showed profiles similar to those of the components identified as RM in the TGO. In addition, the scores of this component showed an increasing trend with the tire granule percentage in TGIS (Fig. 16), similar to that observed in TGO. Therefore, the spectra and mass loss increase in TGIS indicated that RM were identifiable in the formulated soil using the new method.

The FTIR spectra and pyrolysis temperature profiles of the first and third components of TGIS showed profiles and peaks similar to those of the other components in the TGO. They presented a negative confirmation that these two components did not represent RM.

Environmental samples used in Papers II, III, and IV appeared to lose variable percentages (2–50%) of their original mass during heating, likely depending on the quantity of degradable substances present in the samples. PARAFAC models fitted to the data resulted in two components in Paper II and three components in Papers III and IV. One of the components in all models showed an FTIR spectrum similar to that of the RM components in the TGO and TGIS (Fig. 17a). However, the pyrolysis temperature profile of this component (Fig. 17b) lacked a peak at approximately 370 °C observed in the TGO and TGIS spectra (Fig. 13b). This difference might be attributed to the difference in relative concentrations of the different types of polymers in the tires. Fernández-Berridi *et al.* (2006), who experimented with NR and SBR, found that NR pyrolyzed at temperatures 70–90 °C lower than SBR. Tire body parts contain different types of polymers depending on the function required. For example, a sidewall contains more oxidation-resistant polymers, whereas a tread requires abrasion-resistant polymers. In tire granules (e.g., in TGO and TGIS samples), all body parts (all polymer types in the tire) may be available, whereas TWP is assumed to hold mostly tread, justifying the overlapped peak in samples collected from roadsides. Similar finding was reported in Haydary *et al.* (2008). Samples from sites receiving runoff water from sports arena, such as football turfs where tire granules are applied, may show pyrolysis temperature profiles similar to those observed in TGO and TGIS. Despite the difference in the intensity of pyrolysis temperature peaks, the PARAFAC model identified all RM as a single component in tire granules and TGIS, showing its potential in accounting for polymers associated with tires in the environment, irrespective of their relative ratio in the tire production process and type of tires used. Aggregation is against the basic definition of PARAFAC modeling and prevents the identification of the individual polymer types (SBR, NR, and EPDM) in the environment. However, aggregation seems to be a convenient attribute, given that TWP in environmental samples originate from different types of tires whose polymer composition is under commercial confidentiality. One of the three components of the PARAFAC model from Paper

IV showed FTIR peaks typical for hydrocarbons ($2,927$ and $2,850\text{ cm}^{-1}$) with other peaks at approximately $1,500$ and 700 cm^{-1} . The pyrolysis temperature of the component indicated the highest degradation at $456\text{ }^{\circ}\text{C}$ with another broad peak at $610\text{ }^{\circ}\text{C}$ (range of $500\text{--}700\text{ }^{\circ}\text{C}$). This component may have originated from the decomposition of other microplastics such as polyester, as it is one of the common reinforcement synthetic fabrics in the tire industry, fitted under treads (Tian, Wang and Wei, 2019). The synthetic fibers in the soil along the racetrack are plausible because of the observed removal of pieces of tires from the tread, which might have exposed the underlying reinforcement materials. Although determining the identity of the component with certainty is difficult, the component showed similar FTIR and the pyrolysis temperature to that of polyester presented in (Bautista *et al.*, 2017). However, further studies using GC-MS may help achieve more precise identification. This study used tire reinforcing microplastics (TRMP) to refer to this component.

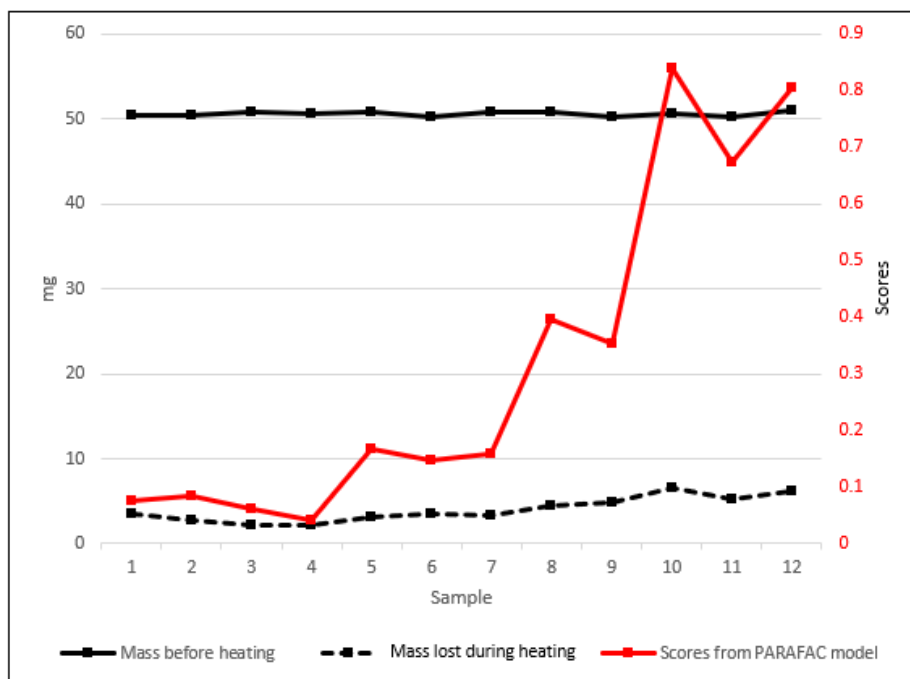


Figure 16. Mass loss/sample (left Y-axis) and PARAFAC scores (right Y-axis) increased with increasing tire granules concentrations in formulated sediment (TGIS)

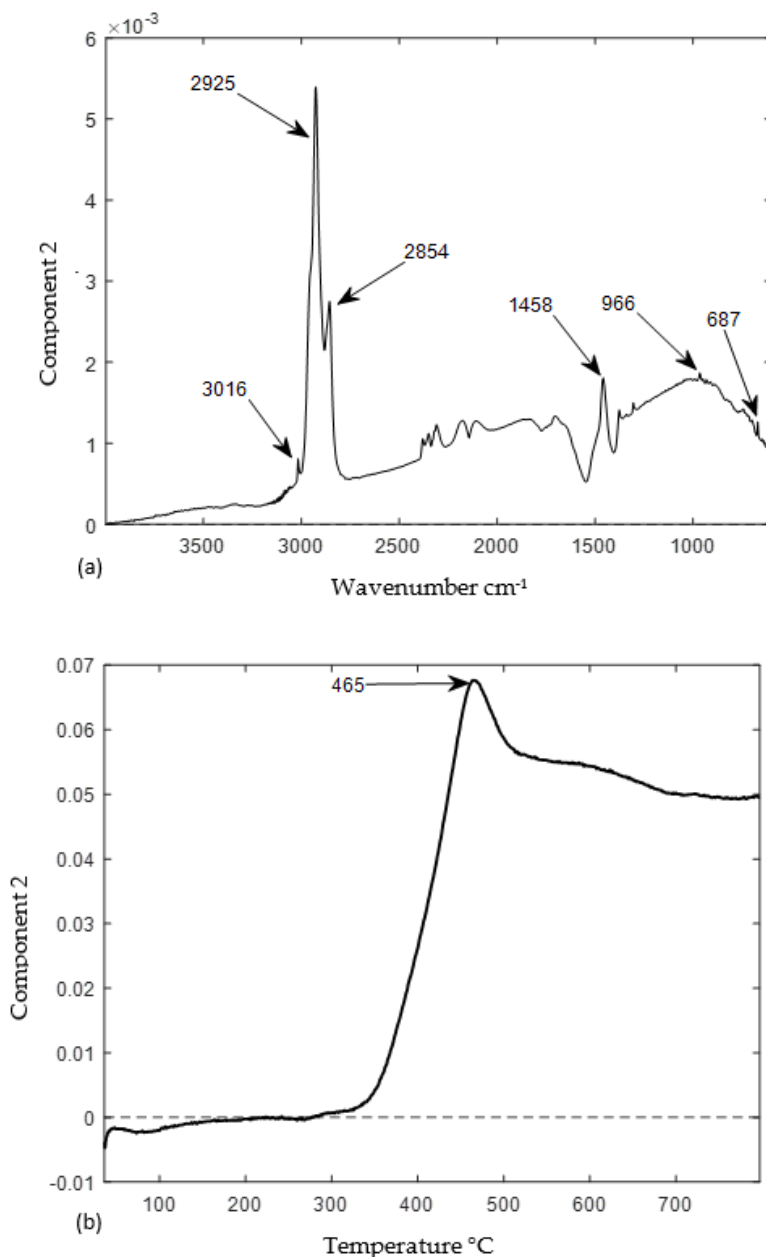


Figure 17. (a) FTIR spectra and (b) pyrolysis temperature profile indicating rubber materials (RM)

Another interesting point to be discussed here is that the FTIR spectrum of one of the components (non-RM) from the environmental samples in Papers II, III, and IV (Fig. 18) showed additional peaks than those observed for similar components of TGO and TGIS. These additional peaks appeared in the region typically assigned to hydrocarbons, yet merged with the FTIR spectra showing water and carbon dioxide. Evaluation of the pyrolysis temperature

profile of the components revealed that these additional peaks were generated at the pyrolysis temperature for plant materials (Shen *et al.*, 2013; Kawamoto, 2017) and bitumen (Mohomed, 2016). Earlier studies (Eisentraut *et al.*, 2018) reported the interference of organic substances from environmental samples with the pyrolysis products of TWP. The advantage of the PARAFAC model is demonstrated here by separating all degradation products of environmental substances (water, carbon dioxide, dimers, and oligomers from plant materials) from RM and retaining substances that have similar pyrolysis temperatures.

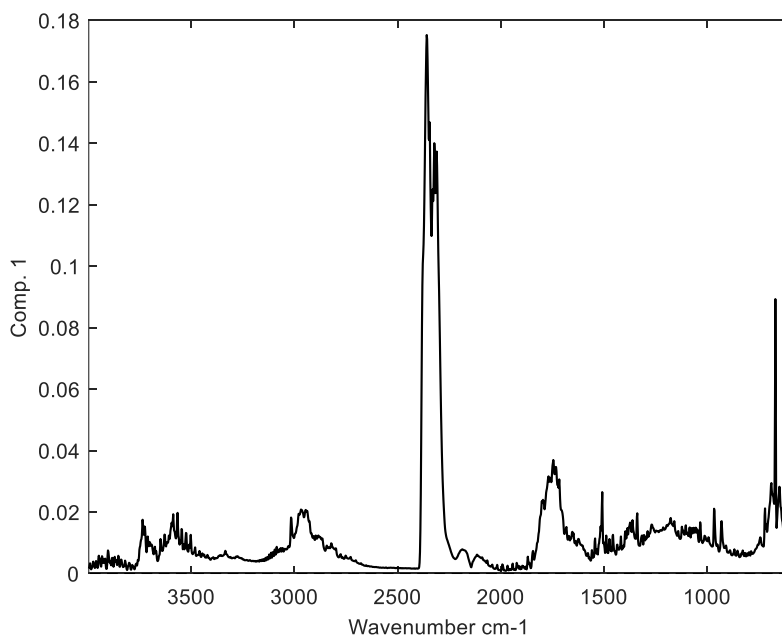


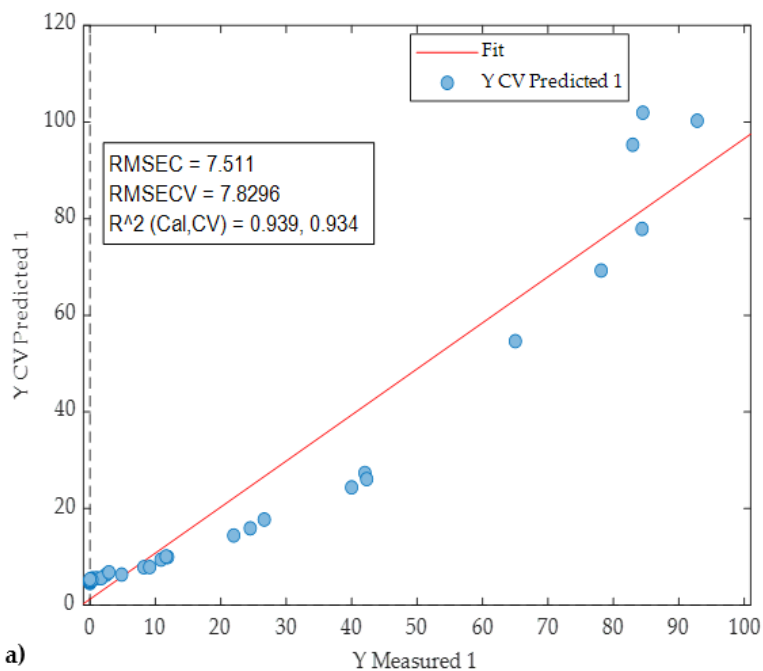
Figure 18. FTIR spectra of component 1 (Papers II, III and IV) showed additional peaks than observed on similar components of TGO and TGIS.

4.1.2. Measuring tire wear particle concentrations

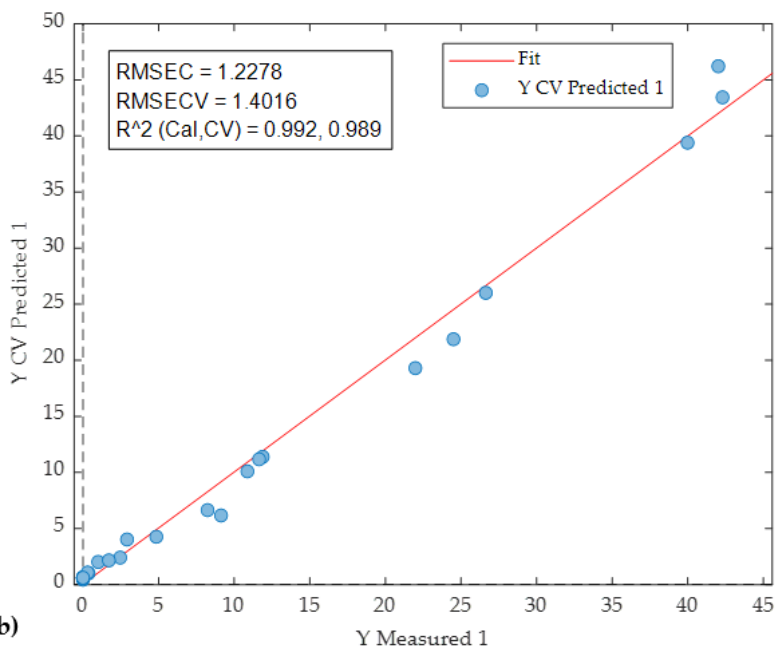
In Paper I, after a component was identified as RM, calibrating its PARAFAC scores against known quantities before heating resulted in a strong correlation in TGO ($R^2 = 0.98$, RMECV = 12%) and in TGIS ($R^2 = 0.92$, RMECV = 10%). This level of fit supports the proportional relationship between score and concentration (Murphy *et al.*, 2013). Therefore, the regression fit implies that if a sample with a known quantity of RM is added to the analysis setup, it is possible to estimate unknown RM concentrations in environmental samples (Bro, 1997). However, given the multiple sources of uncertainty in the spectroscopic analysis, the results may have also been overestimated by bias from the small sample size used in the study. In addition to measurement and instrument errors, uncertainty could be introduced from the transformation of the chemical parameters into physical parameters (RM transformed to spectra in this study) for qualitative and quantitative analyses. This transformation is

influenced by sample impurities, volume, concentration, and temperature (Dobiliene, Raudiene and Žilinskas, 2008). In addition, the applicability of estimating RM and TWP using a fixed ratio (58%) is uncertain when a wide range of RM to TWP ratios (40–60%) is presented in the literature (e.g., Grigoratos and Martini, 2014; Wik and Dave, 2009). Therefore, an alternative approach, estimating RM concentrations based on mass loss and scores from the PARAFAC model, was introduced in Paper II. The method detection limit (MDL) was 0.7 mg RM per g dry sediment (Paper II). Although high compared to the MDL in methods using pyrolysis–GC/MS, it is suitable to determine RM concentrations in soil and sediments from stormwater management solutions, even without pre-processing of samples.

A spike recovery analysis indicated a high but acceptable recovery rate of 123%. The calibration between the estimated RM concentrations and scores ($n = 33$) showed a strong correlation ($R^2 = 0.93$, RMECV = 7.8 mg/g (34%), Fig. 19a). The uncertainty appears to be high, which might be due to the inherent limitation in Beer-Lambert's law. As reported in (Mayerhöfer, Pipa and Popp, 2019) the linear behavior of correlations is limited to specific ranges. Removal of the highest six estimates resulted in a lower (14%) RMECV (Fig. 19b), which supports this suggestion. Although calibration is not required to determine unknown RM concentrations in the alternative approach (used in Papers II, III, and IV), it is critical to determine the operating range of linearity between concentrations and scores in future studies. Even though, a fixed ratio of RM to TWP not needed to estimate RM in the method presented here, it continues to be a challenge to estimate TWP concentrations in environmental samples once RM concentrations were determined. A recent study (Rødland *et al.*, 2021) recommended large scale tire survey or locally adapted values to generate a more representative proportion of RM in tires, and reduce uncertainty in quantifying TRWP in the environment. The method presented in Paper II is adaptable and can be applied to determine TWP concentrations in environmental samples with RM content values higher or lower than the 58% used in the current study, including those generated by large scale surveys.



a)



b)

Figure 19. Partial least square (PLS) linear regression of scores of samples used in Paper II against their estimated concentrations of rubber materials (RM) (a) all samples analyzed (b) samples with estimated RM concentration < 45 mg/g. Y measured is RM calculated from PARAFAC model scores and mass loss, Y CV is predicted RM when one of the samples is missing.

In conclusion, this study introduced and demonstrated a novel method to detect and estimate concentrations of RM in tire granules, formulated sediments, gully pot sediments and bioretention and racetrack side soils. The method consists of two steps, first utilizing a combination of instruments (STA and FTIR) to generate the data matrices, and then utilizes PARAFAC for the data analysis. The STA and FTIR provided suitable data for the PARAFAC, which successfully decomposed the overlying components into different components, including the rubber materials, tire reinforcement microplastics, and other compounds as well as artifacts. The RM concentration estimation was improved in Paper II by using mass loss in the STA and scores from PARAFAC model. The model appeared to perform well, spike analysis showed good recovery rate, and provided a feasible way to apply FTIR to RM. The method needed no prior sample preparation or establishment of RM to TWP ratio or between different RM in tires, which has been a challenge when using pyrolysis-GC-MS method. The prediction accuracy of the method may be improved with a higher resolution STA instrument, which generates gases based on the degradation rate of substances. It is also very critical to determine a linearity range between scores and concentrations to reduce uncertainty in concentration estimates of the method.

4.2. Tire wear particle concentrations in stormwater treatment solutions

4.2.1. Tire wear particle concentrations in gully pot sediments

This study revealed the presence of RM and TWP in gully pot sediments after concurrent evaluation of the FTIR spectra and pyrolysis temperatures of the valid PARAFAC model (Paper II).

RM and TWP concentrations in gully pot sediments (in mg/g sediment dry weight) are presented in Table 3 and were found to differ significantly across gully pots ($F_{10,32} = 194.6$, $P < 0.001$). Traffic density and driving patterns appeared to influence TWP concentrations, as concentrations were highest at sites where AADT was high and at locations where braking and acceleration intensity were expected to be high (parking lot and roundabouts).

In addition, TWP concentrations were significantly different in the two gully pots at the same site, indicating a possible effect of the microenvironment on the mobilization of TWP entering the gully pots. The microenvironment affects the concentration of TWP in stormwater and the volumetric velocity of the stormwater entering the gully pots, influencing the retention efficiency (Lindholm, 2015), and thus also TWP concentrations in gully pot sediments. However, the influence of other factors not explicitly evaluated in this study, such as management activities, cannot be excluded.

The presence of TWP at concentrations reaching 150 mg/g, i.e., 15%, in the sediment indicated that gully pots could serve as temporary sinks to protect recipient water from pollution.

Table 3. Concentrations of rubber materials (RM) and tire wear particles (TWP) in gully pot sediments (mg/g sediment dry weight). Results provided as mean and standard deviation (SD), n = 3 per gully pot and control. Means with different letters are statistically different (Tukey, $p < 0.05$).

Site	Gully pot ID	RM (mg/g sediment dw)		TWP (mg/g sediment dw)	
		Mean	SD	Mean	SD
Sjoskogenveien	1	86.7	a 5.3	149.6	a 9.1
	2	41.4	b 1.3	71.4	b 2.2
	3	24.4	c 2.3	42.0	c 4.0
Raadhusplassen	4	75.8	a 9.9	130.7	a 17.0
	5	0.8	d 1.4	1.4	d 2.4
Maaltrøstveien	6	1.6	d 2.8	2.8	d 4.8
	7	0.5	d 0.5	0.8	d 0.9
Brekkeveien	8	5.8	d 5.0	10.0	d 8.7
	9	11.5	d 0.5	19.8	d 0.9
Nordbyveien	10	1.5	d 1.5	2.7	d 2.5
	Control	LUFA soil	0.1 d 0.2	0.2 d 0.3	

To conclude, the new method introduced in the in Paper I and improved in Paper II, was used to identify RM signals, and estimate their concentrations in the gully pot sediments. Concentrations of TWP in the studied gully pot sediments ranged from below 0.1% to 15%, showing the potential of gully pots to act as temporary sinks for TWP. The highest TWP concentrations were found at sites with higher traffic density and braking/acceleration intensity. However, to conclusively determine the influence of traffic conditions on TWP retention in gully pots, the approach should be applied in settings where gully pot emptying frequency and all other TWP generating, and mobilization factors are controlled. For sediments with low TWP concentrations (<1 mg/g), density separation might be an interesting pre-step to concentrate TWP in samples and could also help to clarify the amount of TWP in different density classes. Another interesting pre-step might be mechanical sieving of the samples, which could also be helpful to understand capture efficiency by size in gully pots. Improving laboratory equipment and analytical procedures is another area to consider, where the use of high-resolution STA, for instance, might help individual polymer detection by improving separation between closely occurring mass loss events. Finally, by enabling quantification of TWP in gully pot sediments, the approach supports environmental monitoring of TWP and safe disposal of gully pot sediments, which is critical for environmental pollution management.

4.2.2. Tire wear particle concentrations in bioretention cell soil

Bioretention cell built with engineered soil showed retention of TWP in all the soil size fractions considered in this study. The finest soil fraction (<50 μm) contained the highest

concentrations of TWP at both the inlet (A) and 5 m away from the inlet (B) samples (54.3 ± 9.0 and 45.5 ± 8.9 mg/g, respectively), compared to other size fractions.

However, normalized TWP concentrations (i.e., factored by soil size proportion and total TWP concentrations in soil; Fig. 20) showed that TWP concentrations in the finer soil fraction ($<50 \mu\text{m}$) constituted only 7% of the total TWP concentration and were lower than those in the coarser soil fractions by a factor of 2–7, regardless of the sampling distance from the inlet. The differences across size fractions were statistically significant ($F_{3,16} = 20.7$, $P < 0.001$), except in B, where the difference between $<50 \mu\text{m}$ and $100\text{--}500 \mu\text{m}$ was not significant. This was related to the mass of the engineered soil in this fraction (3.8 and 3.3% in A and B, respectively; Table 2) compared with the other three coarser fractions.

Studies on the size distribution of TWP retained by bioretention are scarce. However, the results of the present study were in contrast with those of Klöckner *et al.* (2020), who covered size ranges up to $500 \mu\text{m}$ and found a decreasing trend in TRWP concentrations with increasing sediment grain size in a sedimentation basin. The observed trend in the TRWP concentration in the sedimentation basin differed from that found in the street dust analyzed in the same study, which showed no clear trend with size. Klöckner *et al.* (2020) attributed the observed change in TRWP from coarse in runoff to fine in the sedimentation basin to processes such as the easy transportability of finer particles, sedimentation of coarse particles before entering the sedimentation basin, and mechanical degradation of coarse particles. The present study, with bioretention cell close to the road, may not be affected by the processes listed above and may receive similar TRWP as present in road dust, suggesting that significant amounts of TRWP below $100 \mu\text{m}$ enter the bioretention cell. Another study by Eisentraut *et al.* (2018), covering size ranges similar to those of the present study (but with a lower limit at $10 \mu\text{m}$), showed no clear trend but a relatively higher SBR (a TWP marker) concentration in street runoff in the size fraction $500\text{--}5000 \mu\text{m}$ than in the size fraction $100\text{--}500 \mu\text{m}$. However, the studied matrices, street runoff in Eisentraut *et al.* (2018), and bioretention soil in the current study were different and thus not directly comparable.

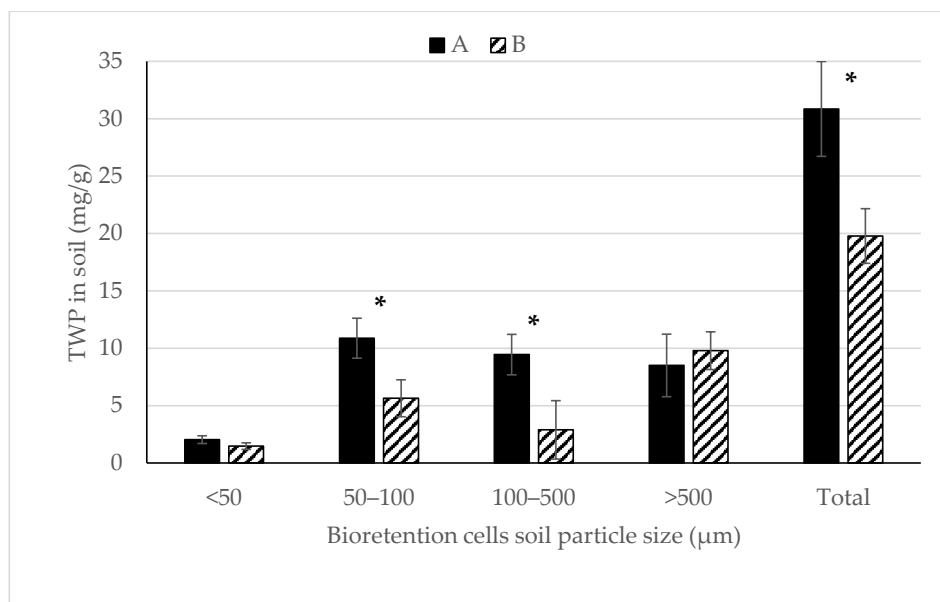


Figure 20. Tire wear particle (TWP) concentrations in bioretention soil (mg/g, mean and one standard deviation, $n=3$) factored by soil size proportion and total TWP concentrations, at the inlet (A), and 5 m away from it (B). Asterisks indicate significant differences between A and B (t -test, $p < 0.05$).

Retention efficiency could not be assessed because of a lack of data on incoming and outgoing flow and TWP concentrations. Therefore, it was unclear if the low contribution from the size range $<50 \mu\text{m}$ was attributable to a lower share of small-sized TWP entering the bioretention cell or if the bioretention cell was less efficient in retaining the finer TWP, as reported by Gilbreath *et al.* (2019). The latter seems plausible for two reasons. First, field and road simulator studies have reported that significant amounts of TWP are found in the size range of $50 \mu\text{m}$ and lower (Kreider *et al.*, 2009; Klöckner *et al.*, 2021). Second, the primary retention mechanism in bioretention cell is physical straining (Smyth *et al.*, 2021), which may allow the transfer of finer TWP down the soil profile or farther away with stormwater. Studies related to the retention efficiency of TWP in bioretention cell are scarce for direct comparison, and few available studies are based on particle counts. For example, Gilbreath *et al.* (2019) observed up to 100% retention of microplastic particles (including rubbery fragments) larger than $500 \mu\text{m}$. The retention efficiency decreased to 55% for the size fraction between $125\text{--}355 \mu\text{m}$, which supports the suggestion that finer TWP may have moved down or away with stormwater.

Total TWP concentrations in mg per g soil dry weight (all soil fractions considered) were $30.9 \pm 4.1 \text{ mg/g}$ (mean \pm standard deviation, SD) at the inlet and $19.8 \pm 2.4 \text{ mg/g}$ 5 m away from the inlet. These concentrations were thrice and twice higher than the average TWP concentrations, respectively, reported by Unice *et al.* (2013) in roadside soils in the Seine River watershed, France. The slightly lower TWP concentrations reported by Unice *et al.* (2013) may be

attributed to the fact that the roadside soil was sampled at a depth of 0–15 cm (while 0–5 cm in the present study) and further away from the road edge (3–15 m). However, other factors not specified in the study (e.g., traffic density and service time) make comparison difficult. Baensch-Baltruschat *et al.* (2020) estimated an average TWP concentration of 20.2 mg/g in roadside soil collected at 0–10 cm depth and 0.5 m away from the edge of federal roads in Germany, with an average traffic density of 24,000. This was consistent with the TWP concentrations observed in the present study. Although these studies had different TWP-generating conditions and treatment systems compared with the present study, the results indicated that roadside bioretention systems retain TWP. Expectedly, we also showed that the total TWP concentrations in soil, while in the same order of magnitude, were significantly higher at the inlet than at 5 m away from it (t-test, $P = 0.03$).

In this study, assessment of a functional bioretention cell demonstrated the presence of TWP in the top 5 cm of soil in all soil size fractions (<50 μm , 50–100 μm , 100–500 μm , >500 μm). TWP concentration was affected by the position of the inlet fitted to the roadside curb, as TWP concentrations at the inlet were higher (30.9 ± 4.1 mg/g) than those observed 5 m away from the inlet (19.8 ± 2.4 mg/g). The study demonstrated that bioretention cells built with engineered soils not only transport high amounts of runoff water but also have shown to retain TWP, demonstrating their potential as control measures along roads. However, it would be interesting to study the vertical distribution of TWP in the bioretention soil to better understand their fate. Furthermore, conducting a long-term assessment of TWP concentrations in the influent and effluent of bioretention cells in the field will provide valuable information on the retention efficiency. Studying the degradation processes of TWP in stormwater management solutions and in the environment is also crucial in order to understand the retention efficiency and accumulation of TWP.

4.3. Tire wear particles removal efficiency of engineered soil

4.3.1. Retention efficiency of the engineered soil

An average of 12.8 ± 2.1 L of gully pot water with a TWP concentration of 77.2 ± 4.8 mg/L passed through each column (Table 4). However, clogging was observed after one week of infiltration, suggesting that the initial resting period was insufficient for the hydraulic load and therefore increased. Particle deposition, which was expected to be high in gully pot water, likely the cause of the clogging. Alem *et al.* (2013) demonstrated clogging at the top of a column owing to particle deposition. Similarly, Conley *et al.* (2020) found a high infiltration decline due to clogging caused by sediment accumulation. However, the results of this study should be interpreted cautiously because a year and a half worth of rainfall was applied for 2 weeks in the column experiment. Furthermore, the absence of freeze-thaw cycles and vegetation in the columns may have made the soil more prone to clogging than what is typically observed in operative bioretention cell. Vegetation plays a crucial role in bioretention because their

roots enhance infiltration, and their leaves promote interception and the transport of water through evapotranspiration (Tahvonen, O., 2018).

TWP concentrations are listed in Table 4. The overall TWP removal efficiency was $99.6 \pm 0.5\%$ for particles $>25 \mu\text{m}$. This level of removal is high compared with that reported in a few available studies on the removal efficiency of microplastics (including rubber fragments) by bioretention cell (Gilbreath *et al.*, 2019; Lange *et al.*, 2021a; Lange *et al.*, 2021b; Smyth *et al.*, 2021). However, these studies were field bioretention cell functioning for 2–3 years during the study with configurations different from the column test in the current study, either in the catchment area they serve or soil composition.

The results of these experiments imply that bioretention cell are efficient at retaining TWP $>25 \mu\text{m}$. However, only 7% of $<50 \mu\text{m}$ TWP was observed in the top 5 cm of the functional bioretention cell, requiring a further study on the retention performance of finer TWP ($<25 \mu\text{m}$).

Table 4. Tire wear particle (TWP $> 25 \mu\text{m}$) concentrations in the influent (gully pot water) and columns effluent (C₁-C₃).

Sample	Column	Water (L)	Retained particles $>25 \mu\text{m}$ (mg/L)	TWP concentration (mg/L)		Removal efficiency (%)	
				Mean	SD	Mean	SD
Influent			366.7	79.9	4.9		
Effluent	C ₁	13.8	40.6	0.1	0.1	99.9	0.1
	C ₂	10.3	117.3	0.8	0.2	99.0	0.2
	C ₃	14.2	12.5	0.1	0.0	99.9	0.0

4.3.2. Vertical Distribution of TWP in the Columns

In this study, a test with samples that received no pretreatment, C3*, showed a TWP concentration of $5.0 \pm 1.4 \text{ mg/g}$ in the top 5 cm of the column, while the TWP concentration in the bottom 5 cm was below the MDL (Table 5). The relatively high TWP concentration in the top 5 cm seems to originate mainly from the deposition of finer particles ($<25 \mu\text{m}$), as wet sieving of the same sample with a $25 \mu\text{m}$ mesh (C3**) showed a reduction in TWP concentration (Table 5). It is likely that these fine particles also contributed to the observed reduction in infiltration in the columns.

Table 5. Tire wear particles (TWP) retained by columns, in mg/g soil dw) in the 0–5 cm (Top 5 cm) and 35–40 cm (Bottom 5 cm) soil layers of bioretention columns C1–C3, following ZnCl₂ density separation of soil samples. In column C3, TWP concentrations were also determined without prior filtration nor density separation (C3*), and with filtration only (C3**). N/A: not available.

Column	Top 5 cm		Bottom 5 cm	
	Mean	SD	Mean	SD
C ₃ *	5.0	1.4	0.0	0.0
C ₃ **	1.0	1.7	N/A	N/A
C ₁	0.9	1.0	0.4	0.5
C ₂	0.8	0.3	0.9	0.5
C ₃	0.6	0.7	0.4	0.2

TWP concentrations, determined in samples pretreated with density separation and filtration, in the top 5 cm (0.7 ± 0.7 mg/g) and bottom 5 cm (0.6 ± 0.4 mg/g) showed no statistically significant difference (t-test, $p = 0.21$). Considering the mass balance in the influent and effluent, sample pretreatment by density separation may have underestimated TWP concentrations due to unrecovered particles with higher density (>1.8 g/cm³). The results suggests that while sample preparation by density separation using ZnCl₂ is a common practice in microplastics and TRWP analysis, it is not optimal for TRWP, as it fails to recover TRWP denser than 1.8 g/cm³. Although comparing TWP concentrations at the top and bottom of the columns provided valuable results, further studies looking at TWP concentrations over the entire soil profile would enable mass balance and thereby a better understanding of TWP fate in bioretention cells.

The column experiment, despite the varying concentrations of total solid particles >25 μm in the effluent, showed high retention efficiency ($>99\%$) of TWP > 25 μm in engineered soil consisting of sand, silty-sand, and garden compost. Surface clogging and limited infiltration were observed during the experiment, which was attributed to a high particle load in a short time. A long-term study on a vegetated bioretention cell may provide more realistic wetting and drying conditions and particle loadings from the road environment to better explain the TWP dynamics in bioretention cells. The observed high concentrations of TWP <25 μm in the top 5 cm of the engineered soil suggests the entry of a high proportion of finer TWP to the bioretention system (Table 5). This warrants further study on the fate of TWP < 25 μm and their retention by bioretention cells, especially since our results on a large-scale functional bioretention cell showed that TWP in the finer soil fraction (<50 μm) only represented 7% of the top 5 cm of soil.

4.4. Microplastics deposition in soil along a racetrack

Marbles, which are pieces of rubber shredded from tires of different sizes and shapes, were observed in the grass around the racetrack (Fig. 21). Some have sausage-like shapes, typical

for micro-size TWP from roads (Kreider *et al.*, 2009; Sommer *et al.*, 2018). Their scorched surface and unusually large size (4–9 cm) compared with that of TWP from road traffic may be attributed to the harsh driving conditions that generate high heat, and the type of tire (soft tire) used in racing vehicles.



Figure 21. Marbles observed on the grass along the Rudskogen racetrack . Photo: Helena Marie Amdal

The visually undetectable microplastics along the racetrack were analyzed by fitting a PARAFAC model with three components to the FTIR data from all the samples in this study. RM and tire reinforcement microplastics (TRMP) were detected in all soil size fractions considered in this study, with the highest concentrations being in the soil fraction 1000–5000 μm (Fig. 22a and b). Mean concentrations in the soil size fraction of 50–1000 μm were also notable, whereas very little were observed in the finer fraction (25–50 μm).

This finding contradicts the TWP size distributions reported in many road and tunnel dust studies, which reported higher concentrations in the finer size range (e.g., Klöckner *et al.*, 2021; Kreider *et al.*, 2009). However, this is not unexpected, given the driving behavior and tires used in racing.

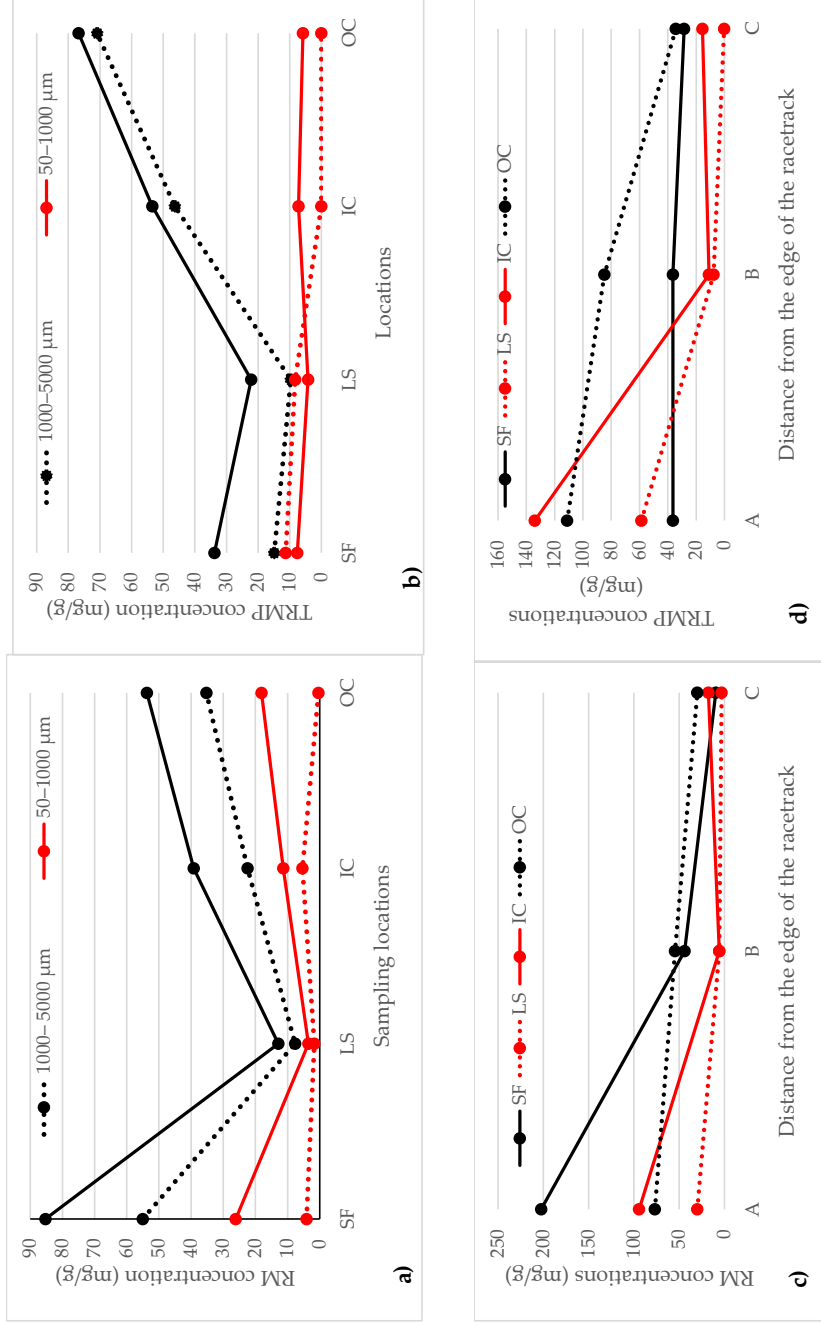


Figure 22. Racetrack: Concentrations of microplastics in soil size fractions (25–50 μm , 50–1000 μm , and 1000–5000 μm) at different locations (start/finish (SF), long straight (LS), outward corner (OC), and inward corner (IC)) along the Rudsøgen racetrack. (a) Concentrations of rubber materials (RM) in mg/g dry soil weight. (b) Concentrations of tire reinforcement microplastics (TRMP) in mg/g dry soil weight. Distances from the edge of the racetrack: A (0–20 cm), B (100–120 cm), C (260–280 cm). Concentrations of rubber material (RM) in mg/g soil dry weight are shown in a) and c), while concentrations of tire reinforcement microplastics (TRMP) in mg/g soil dry weight are shown in b) and d).

4.4.1. Effect of racetrack alignment and distance from the edge

All size fractions considered (including mean concentrations of 50–1000 μm), the RM concentrations were 2.5–17 times higher 20 cm from the edge of the racetrack than further away for all locations, suggesting that TWP were mainly deposited within a 20 cm distance from the edge of the track. The highest RM concentration (202.4 mg/g, Fig. 22c) was observed at SF, followed by IC (94.2 mg/g), and lowest at LS (29.9 mg/g). The concentration decrease with distance was notable, even though the distance was only 2.8 m. Since, according to Grigoratos and Martini (2014) and Wik and Dave (2009), RM makes only 40–60 % of tires, the results indicate a deposition of higher mass of TWP by a factor of two, which suggests that soil along the racetrack acts as a TWP sink. These results agree with the findings of (Cadle and Williams, 1978), who reported an exponential decrease in TRWP concentrations with distance from the edge of the road. The concentration levels at SF and IC were higher than the highest RM concentration in gully pot sediments reported in Paper II. Similarly, a decreasing concentration trend with increasing distance from the edge of the racetrack was observed for the TRMP (Fig. 22d). The average RM concentration of the three distances and the three size fractions, at each location showed the highest RM concentration at SF, followed by OC, while LS showed the lowest concentration for RM. For TRMP, the highest concentration was measured at OC, followed by IC, whereas the lowest was measured at LS.

RM concentrations in the soil size fraction 50–1000 μm showed statistically significant differences between the four locations ($F_{3,24} = 10.56$, $p < 0.001$), and the three distances from the edge of the racetrack ($F_{2,24} = 19.24$, $p < 0.001$) (Fig. 23a). Considering that cornering and start/finish are associated with high TWP generation, this finding agrees with that of Pohrt (2019), who reported that high speed, fast acceleration and retardation, and increased cornering speeds lead to increased tire wear. Only 36% of the samples with soil size 50–1000 μm showed detectable TRMP, suggesting that TRMP were mainly coarse in size (1000–5000 μm). The differences in mean TRMP concentrations between locations ($F_{3,24} = 0.18$, $p = 0.91$) and distances ($F_{2,24} = 1.56$, $p = 0.23$) were not statistically significant (Fig. 23b).

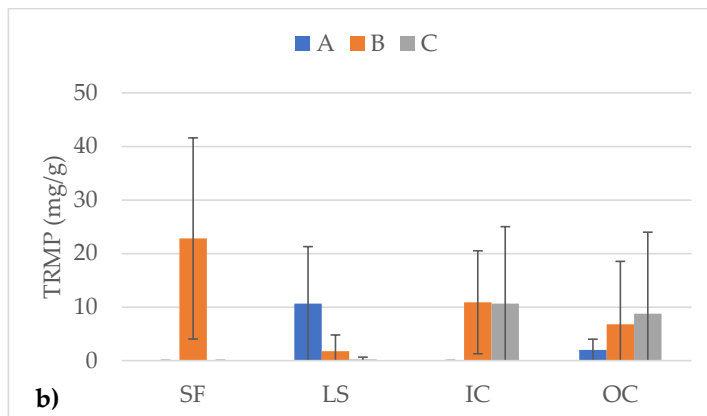
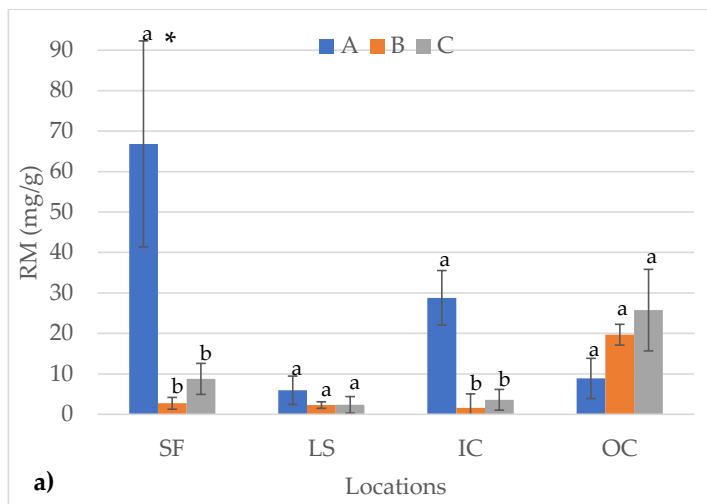


Figure 23. Racetrack: Concentrations of a) rubber materials (RM) and b) tire reinforcement microplastics (TRMP) in the soil size fraction 50–1000 μm at different locations (start/finish-SF, long straight-LS, inward corner-IC, and outward corner-OC) along the Rudskogen racetrack. Different letters indicate a statistically significant difference between the mean RM concentrations at various distances from the edge of the racetrack: A (0-20 cm), B (100-120 cm), and C (260-280 cm). Asterisks indicate a statistically significant difference between the mean concentrations of RM at the four locations (Tukey, $p < 0.05$). Results are presented as mean with standard deviation (error bar).

4.4.2. Environmental impact

Deposition of TWP along the racetrack poses environmental risk if exposed to flooding as stormwater is reported to transport TWP to receiving water bodies (Jan Kole *et al.*, 2017; Johannessen *et al.*, 2021; Tian *et al.*, 2021). While acute and chronic toxic effects of TRWP are widely reported in laboratory tests (Khan, Halle and Palmqvist, 2019), some recent field studies (e.g., Tamis *et al.*, 2021) have demonstrated the environmental risk posed by TWP and other associated chemical substances from stormwater runoff in Europe. In addition, by-

products of tire manufacturing additives are reported to be acutely toxic to some species. For example, the mass mortality of coho salmon (*Oncorhynchus kisutch*) in the streams of the Pacific Northwest region of the USA is attributed to 6ppd-quinone (a transformation product of N-(1,3-dimethylbutyl)-N-phenyl-p-phenylenediamine (6PPD)) (Tian *et al.*, 2021). Acute toxicity to other fish species such as brook trout (*Salvelinus fontinalis*) and rainbow trout (*Oncorhynchus mykiss*) is also reported (Brinkmann *et al.*, 2022).

However, the toxicity reported might be species-specific as Arctic char (*Salvelinus alpinus*), white sturgeon (*Acipenser transmontanus*) or even other salmon species tested like (chum salmon, *Oncorhynchus keta*) found to be tolerant to 6ppd-quinone (Brinkmann *et al.*, 2022; McIntyre *et al.*, 2021). From the results presented in the present study, high inflow of microplastics into rivers might be possible as mass flux studies (Unice *et al.*, 2019) in watersheds show that 50 % of generated TRWP in roads reach freshwater systems. It is possible that toxic effects could be observed in rivers receiving stormwater from the present study area as sweeping —the only treatment measure in racetrack— according to Janhäll *et al.*, (2016) is not considered effective in removing the finer microplastic particles. However, sweeping after the races may remove more TWP than reported in literatures (Björklund, Strömvall and Malmqvist, 2011; Janhäll *et al.*, 2016) because of the high fraction of large size microplastics particles observed in this study. Future study on concentrations of microplastics from racetrack dust before and after sweeping as well as concentrations along the route to rivers should be considered to better understand the annual flux.

In summary, this study demonstrated the presence of microplastics (RM and TRMP) in the soil along a racetrack. Although the two different types of microplastics were found together in most samples, the correlation observed between RM and TRMP concentrations was weak, suggesting the effect of track alignment on the type of microplastics abraded. Racetrack locations also affected TWP deposition, with the highest RM concentrations observed in soil alongside the Start/ Finish area. Distance from the edge of the racetrack affected the concentrations of RM and TRMP, as concentrations decreased with increased distance, when all size fractions were considered. However, additional studies are required to quantify the generation of microplastics during racing, and to assess the efficiency of sweeping in removing microplastics from racetracks. Mechanism of spread of microplastics and mass transport from the racetrack to the environment should also be studied to understand potential environmental effects. Despite those gaps, the initial results of this study suggest that motorsport is of concern in terms of microplastics release to the environment.

5. General discussion

Quantifying RM/TWP through chemical analysis, particularly using FTIR, is not well established (Litvinow and De, 2002). However, some studies (e.g., Fernández-Berridi *et al.*, 2006; Mohomed, 2016) have applied the simultaneous use of FTIR and DTGA to identify polymers in “pure” tire samples. This thesis applied the simultaneous approach to environmental samples after subjecting the data to the PARAFAC model. The results from Paper I indicated that the method introduced in this thesis detected the presence of RM in formulated sediment spiked with tire granules and in other environmental samples. The markers selected (RM) inherently fulfil some of the qualities of a reliable marker. For example RM are not expected to easily transform while the TWP reside in the environment because of slow degradation (Cadle and Williams, 1978; Stevenson, Stallwood and Hart, 2008; Wagner *et al.*, 2018), and RM are present at higher concentration in tires (up to 60%) than in environmental matrices (Wagner *et al.*, 2018). The method improved the analytical accessibility and specificity of the marker by generating FTIR spectra and pyrolysis temperature profiles for the same component to facilitate concurrent evaluation and enhanced identification, which would otherwise have been a challenge using one spectroscopic method. However, the standard STA used in this thesis aggregated all RM in the samples, as opposed to the high-resolution STA, which enabled segregation between different polymer types (Fernández-Berridi *et al.*, 2006). Given that TWP in road environments originate from different types of tires (summer and winter tires, heavy-duty vehicles, and passenger car tires), whose polymer composition is under commercial confidentiality, aggregation might be a convenient attribute. The aggregation may also have helped detect different polymers present in smaller quantities, which otherwise would have been undetectable individually. Conversely, the aggregation might contribute to the overestimation of TWP as other sources; for example, polymer-modified bitumen, albeit in small quantities (Vogelsang *et al.*, 2018), were reported to generate RM (Rødland *et al.*, 2021). STA/TGA works well when the DTGA curves of each elastomer are separated, but standard TGA falls short in this respect as it scans broader weight losses, resulting in overlapping signals with multiple peaks (Mohomed, 2016). In Hi-Res TGA the heating rate of the sample material is dynamically and continuously modified in response to changes in the rate of decomposition of the material so as to maximize weight change resolution. This approach allows very high heating rates to be used in regions where no weight changes occur, whereas heating rate is decreased when a weight change is detected. This method gives narrower and more intense derivative weight loss peaks with the result of a greater resolution from competing and overlapping weight losses.

The results of Paper I and II indicated that the introduced method is suitable for estimating RM in environmental samples with no pre-processing of samples collected from stormwater management solutions. However, a fixed ratio of rubber to tire continued to be a challenge to estimate TWP concentrations in environmental samples once RM concentrations were

determined. A recent study (Rødland *et al.*, 2021) recommended large scale tire survey or locally adapted values to generate a more representative proportion of RM in tires, and reduce uncertainty in quantifying TRWP in the environment. The method introduced in the present study (Paper II) is valid for estimation of TWP concentrations in environmental samples at any rubber content defined values.

Papers II and III showed that stormwater management solutions retained TWP. In Paper II, TWP concentrations ranging from below 0.1% to 15% were measured in gully pots sediments. This study revealed an association between TWP concentrations, traffic density, and braking/acceleration intensity. Other factors such as the microenvironment and emptying frequency, which were not evaluated in this study, might have influenced the concentration of TWP. Although this study did not consider the retention efficiency of gully pots because of the lack of data on TWP concentrations in the incoming and outgoing stormwaters simultaneously, it demonstrated the potential of gully pots to act as temporary sinks. Knowledge of TWP concentrations in gully pots offers valuable information to road managers to optimize operations and support the safe disposal of sediments, which is critical for environmental pollution management.

The results from Paper III showed that bioretention cell constructed with engineered soil retained TWP. TWP were detected in all size fractions of the bioretention soil (<50, 50–100, 100–500, and 500–5000 μm). A laboratory column test (Paper III) showed high TWP >25 μm removal using engineered soil composed for bioretention. The measured TWP concentrations in the functional bioretention cell and the observed high removal in the laboratory test showed the potential of bioretention cell to remove >25 μm TWP from stormwater runoff and limit their spread in the environment. This presents a good opportunity for retaining TWP in facilities designed for other purposes, at a time when specific policy recommendations to limit TWP spread in the environment are nonexistent (Vogelsang *et al.*, 2018), and evidence of environmental risk is growing (Tamis *et al.*, 2021; Tian *et al.*, 2021).

The engineered soil composed for bioretention cells along traffic roads may also be considered for other high TWP generating areas such as racetracks. Even though the mechanisms of generation and transportation to the roadside are different, high RM concentrations (up to 20.2%) were estimated in the top 5 cm soil within 20 cm distance from the edge of the track at the SF location (Paper IV). The results from Paper IV also showed that large pieces of tires (4–9 cm), which are unusual sizes for TWP in traffic roads, were observed visually along the racetrack. The large pieces might breakdown to finer TWP mechanically or to constituent chemicals through photo and biodegradation (Baensch-Baltruschat *et al.*, 2020) overtime. In addition to RM, other microplastics (TRMP) were observed at all locations studied along the racetrack. Concentrations of these two types of microplastics were affected by the distance from the edge of the racetrack and sample locations. The findings of this study could be of interest to racetrack managers in terms of planning microplastic management solutions. Even

though additional studies are required to map environmental effect and policy measures, our initial results suggest that motor sport is a concern in terms of microplastics release to the environment.

6. Conclusion and future research

This thesis aims to address the lack of a suitable analytical method for measuring the environmental concentrations of TWP and filling the knowledge gap on the effect of stormwater management solutions. The thesis introduced a new method for identifying and estimating the total rubber materials present in samples without a need to preprocess samples. The STA and FTIR provided suitable data for the PARAFAC, which successfully decomposed the overlying signals into different components, including the rubber materials and other compounds as well as artifacts. The RM concentration estimation using mass loss in the STA and scores from PARAFAC model needed no prior knowledge of rubber ratios to tire or between different rubber types in tires. This thesis demonstrated that stormwater management solutions along roads (gully pots and bioretention cells) retain TWP. Traffic density and driving patterns appeared to influence concentrations of TWP in gully pots while inlet position affected concentrations in the bioretention cells. The engineered soil used in bioretention cells has shown to be particularly efficient in retaining TWP larger than 25 μm . Additionally, the study showed that soil along racetrack deposited two different types of microplastics, which have been influenced by the location of the racetrack and distance from the edge.

Future research should focus on several key areas to improve our understanding of TWP concentrations in the environment. Firstly, improving laboratory equipment and analytical procedures is an area to consider for the method introduced in this thesis, where the use of high-resolution STA, for instance, might help individual polymer detection by improving separation between closely occurring mass loss events. A linearity range between scores and concentrations should be established to reduce uncertainty in concentration estimates of the PARAFAC model. Secondly, TWP retention in gully pots should be studied in settings where gully pot emptying frequency and all other TWP generating, and mobilization factors are controlled to conclusively determine the influence of traffic conditions. It is also recommended to study the vertical distribution of TWP in the bioretention soil and conduct a long-term assessment of TWP concentrations in the influent and effluent. The thesis further recommends studies on TWP mass transport in the environment, degradation impacts on TWP concentration over time, the removal efficiency of sweeping, and analysis of particles $<25 \mu\text{m}$ to fill the knowledge gaps on the fate of TWP in the environment.

Notwithstanding these future research needs, this thesis contributes to the improvement of methods to identify and measure environmental concentrations of TWP. It also fills the knowledge gap with respect to stormwater management solutions' effect, which has implications for the control and monitoring of TWP and other microplastics in the environment and for designing stormwater management solutions.

7. References

- Adachi, K. and Yoshiaki, T. (2004) 'Characterization of heavy metal particles embedded in tire dust', *Environment International*, 30(8), pp. 1009–1017. doi: 10.1016/j.envint.2004.04.004.
- Alem, A. *et al.* (2013) 'Filtration of kaolinite particles in a saturated porous medium: Hydrodynamic effects', *Hydrogeology Journal*, 21(3), pp. 573–586. doi: 10.1007/s10040-012-0948-x.
- Amdal, H. M. (2021) *Dekkslitasjepartikler fra motorsportbaner: En første kartlegging og mulige tiltak [Tire wear particles from racetracks: A first assessment and possible measures]*. Norwegian University of Life Sciences (NMBU). Available at: <https://hdl.handle.net/11250/2833780>.
- Andersson-Sköld, Y. *et al.* (2020) *Microplastics from tyre and road wear - A literature review*. Linköping. Available at: www.vti.se.
- Arthur, C., Baker, J. and Bamford, H. (2009) 'Proceedings of the international research workshop on the occurrence, effects, and fate of microplastic marine debris', in *NOAA Technical Memorandum NOS-OR&R-30*, p. 530.
- Åstebøl, S. O. and Hvitved-Jacobsen, T. (2014) *Vannbeskyttelse i vegplanlegging og vegbygging (Rapport nr. 295), Statens vegvesens rapporter*. Oslo. Available at: https://www.vegvesen.no/_attachment/1160093/binary/1086413?fast_title=Vannbeskyttelse+i+vegplanlegging+og+vegbygging.
- Baensch-Baltruschat, B. *et al.* (2020) 'Tyre and road wear particles (TRWP) - A review of generation, properties, emissions, human health risk, ecotoxicity, and fate in the environment', *Science of the Total Environment*, 733, p. 137823. doi: 10.1016/j.scitotenv.2020.137823.
- Baum, A. *et al.* (2016) 'Rapid quantification of casein in skim milk using Fourier transform infrared spectroscopy, enzymatic perturbation, and multiway partial least squares regression: Monitoring chymosin at work', *Journal of Dairy Science*, 99(8), pp. 6071–6079. doi: 10.3168/jds.2016-10947.
- Bautista, Y. *et al.* (2017) 'Thermal degradation mechanism of a thermostable polyester stabilized with an open-cage oligomeric silsesquioxane', *Materials*, 11(22). doi: 10.3390/ma11010022.
- Björklund, K., Strömvall, A. M. and Malmqvist, P. A. (2011) 'Screening of organic contaminants in urban snow', *Water Science and Technology*, 64(1), pp. 206–213. doi: 10.2166/wst.2011.642.
- Boulter, P. G. (2006) *A Review of Emission Factors and Models for Road Vehicle Non-Exhaust Particulate Matter*, TRL published project report PPR065. Available at: <https://trl.co.uk/reports/PPR065>.
- Bradley, J. (2019) *Tyre abrasion – the dark side of microplastics pollution*, *WaterBriefing*. Available at: <https://www.waterbriefing.org/home/water-issues/item/15892-tyre-abrasion—the-dark-side-of-microplastics-pollution>.
- Brinkmann, M. *et al.* (2022) 'Acute toxicity of the tire rubber-derived chemical 6PPD-quinone to four fishes of commercial, cultural, and ecological importance', *Environmental Science and*

Technology Letters, 9(4). doi: 10.1021/acs.estlett.2c00050.

Bro, R. (1997) 'PARAFAC. Tutorial and applications', *Chemometrics and Intelligent Laboratory Systems*, 38(2), pp. 149–171. doi: 10.1016/S0169-7439(97)00032-4.

Bro, R., Kiers, H.A.L. (2003) 'A new efficient method for determining the number of components in PARAFAC models', *J. Chemom.* 17, 274–286. doi.org/10.1002/cem.801

Brodie, I. M. and Porter, D. M. (2006) *Investigation of stormwater particles generated from common urban surfaces, USQ*. University of Southern Queensland. Available at: <https://eprints.usq.edu.au/3558/>.

Brown, R. A. and Hunt, W. F. (2012) 'Improving bioretention / bio filtration performance with restorative maintenance', *Water Science & Technology*, 65(2), pp. 361–367. doi: 10.2166/wst.2012.860.

Butler, D. and Karunaratne, S. H. P. G. (1995) 'The suspended solids trap efficiency of the roadside gully pot', *Water Research*, 29(2). doi: 10.1016/0043-1354(94)00149-2.

Cadle, S. H. and Williams, R. L. (1978) 'Gas and particle emissions from automobile tires in laboratory and field studies', *Journal of the Air Pollution Control Association*, 28(5), pp. 502–507. doi: 10.1080/00022470.1978.10470623.

Camatini, M. *et al.* (2001) 'Microcharacterization and identification of tire debris in heterogeneous laboratory and environmental specimens', *Materials Characterization*, 46, pp. 271–283. doi: 10.1016/S1044-5803(00)00098-X.

Cambridge Polymer Group (2014) 'Car tire composition analysis by TGA-FTIR'. Boston: Cambridge Polymer Group, pp. 1–9. Available at: <http://www.campoly.com>.

Capolupo, M. *et al.* (2020) 'Chemical composition and ecotoxicity of plastic and car tire rubber leachates to aquatic organisms', *Water Research*, 169, p. 115270. doi: 10.1016/j.watres.2019.115270.

Charles, J. *et al.* (2009) 'FTIR and thermal studies on nylon-66 and 30% glass fibre reinforced nylon-66', *E-Journal of Chemistry*, 6(1), pp. 23–33. doi: 10.1155/2009/909017.

Chen, Z. and Prathaban, S. (2013) *Modeling of tyre parameters' influence on transport productivity for heavy trucks*. Chalmers University of Technology. Available at: <https://hdl.handle.net/20.500.12380/191805>.

Choi, D. *et al.* (2020) 'In vitro chemical and physical toxicities of polystyrene microfragments in human-derived cells', *Journal of Hazardous Materials*, 400. doi: 10.1016/j.jhazmat.2020.123308.

Conley, G. *et al.* (2020) 'Quantifying clogging patterns of infiltration systems to improve urban stormwater pollution reduction estimates', *Water Research*, 7, p. 100049. doi: 10.1016/j.wroa.2020.100049.

Dahl, A. *et al.* (2006) 'Traffic-generated emissions of ultrafine particles from pavement-tire interface', *Atmospheric Environment*, 40(7), pp. 1314–1323. doi: 10.1016/j.atmosenv.2005.10.029.

Dale, M. *et al.* (2017) 'New climate change rainfall estimates for sustainable drainage', *Proceedings of the Institution of Civil Engineers: Engineering Sustainability*, 170(4), pp. 214–224.

doi: 10.1680/jensu.15.00030.

Ding, B. *et al.* (2019) 'Bioretention cells under cold climate conditions : Effects of freezing and thawing on water infiltration , soil structure , and nutrient removal', *Science of the Total Environment*, 649, pp. 749–759. doi: 10.1016/j.scitotenv.2018.08.366.

Dobiliene, J., Raudiene, E. and Žilinskas, R. P. (2008) 'Uncertainty of spectrometric analysis', *Proceedings of the 12th IMEKO TC1 Education and Training in Measurement and Instrumentation and TC7 Measurement Science Joint Symposium on 'Man, Science and Measurement' 2008*, pp. 117–123.

Dong, Y. *et al.* (2021) 'Uptake of microplastics by carrots in presence of As (III): Combined toxic effects', *Journal of Hazardous Materials*. doi: 10.1016/j.jhazmat.2021.125055.

Dröge, R. and Tromp, P. (2019) *Measurements of organic micropollutants, microplastics and associated substances from road transport*. Available at: <https://www.microproof-cedr.nl/deliverables.php>.

Eisentraut, P. *et al.* (2018) 'Two birds with one stone - Fast and simultaneous analysis of microplastics: Microparticles derived from thermoplastics and tire wear', *Environmental Science and Technology Letters*, 5(10), pp. 608–613. doi: 10.1021/acs.estlett.8b00446.

Eriksen, M. *et al.* (2013) 'Plastic pollution in the South Pacific subtropical gyre', *Marine Pollution Bulletin*, 68(1–2), pp. 71–76. doi: 10.1016/j.marpolbul.2012.12.021.

European Commission directorate-general for research and innovation (2019) *Environmental and health risks of microplastic pollution*. Luxembourg. doi: 10.2777/65378.

European Union (2008) *Environmental quality standards, Official Journal of the European Union*. The European Union. Available at: <https://eur-lex.europa.eu/legal-content/EN/TXT/?uri=CELEX:32008L0105>.

Fausser (1999) *Particulate air pollution with emphasis on traffic generated aerosols*. Technical University of Denmark. Denmark. Forskningscenter Risoe. Risoe-R, No. 1053(EN)

Fernández-Berridi, M. J. *et al.* (2006) 'Pyrolysis-FTIR and TGA techniques as tools in the characterization of blends of natural rubber and SBR', *Thermochimica Acta*, 444(1), pp. 65–70. doi: 10.1016/j.tca.2006.02.027.

FIFA (2015) *Handbook of test methods, quality programme for football turf*. Zurich: Federation Internationale de Football Association.

Fleury, J. B. and Baulin, V. A. (2021) 'Microplastics destabilize lipid membranes by mechanical stretching', *Proceedings of the National Academy of Sciences of the United States of America*, 118(31). doi: 10.1073/PNAS.2104610118.

Formula 1 (2021a) *Tire compound*. Available at: http://www.formula1-dictionary.net/tire_compound.html (Accessed: 12 September 2021).

Formula 1 (2021b) *What is the most important part of a racing car?* Available at: http://www.formula1-dictionary.net/most_important.html (Accessed: 12 September 2021).

GESAMP (2015) *Sources, fate and effects of microplastics in the marine environment: A global*

assessment. Exeter. Available at: www.imo.org.

Gilbreath, A. *et al.* (2019) 'Multiyear water quality performance and mass accumulation of PCBs, mercury, methylmercury, copper, and microplastics in a bioretention rain garden', *J. Sustainable Water Built Environ.*, 5(4). doi: 10.1061/JSWBAY.0000883.

Grigoratos, T. and Martini, G. (2014) *Non-exhaust traffic related emissions. Brake and tyre wear PM*, JRC SCIENCE AND POLICY REPORTS. Luxembourg. doi: 10.2790/21481.

Gualtieri, M. *et al.* (2005) 'Toxicity of tire debris extracts on human lung cell line A549', *Toxicology in Vitro*, 19(7), pp. 1001–1008. doi: 10.1016/j.tiv.2005.06.038.

Gunasekaran, S., Natarajan, R. K. and Kala, A. (2007) 'FTIR spectra and mechanical strength analysis of some selected rubber derivatives', *Spectrochimica Acta - Part A: Molecular and Biomolecular Spectroscopy*, 68(2), pp. 323–330. doi: 10.1016/j.saa.2006.11.039.

Gustafsson, M. *et al.* (2008) 'Properties and toxicological effects of particles from the interaction between tyres, road pavement and winter traction material', *Science of the Total Environment*, 393(2–3). doi: 10.1016/j.scitotenv.2007.12.030.

Halle, L. L. *et al.* (2020) 'Ecotoxicology of micronized tire rubber: Past, present and future considerations', *Science of the Total Environment*, 706, p. 135694. doi: 10.1016/j.scitotenv.2019.135694.

Haraldsen, T. K., Gamborg, M. and Vike, E. (2019) *Utvikling av jordblandinger til regnbed i Drammen Pottforsøk med periodevis vannmetning og uttørring*. Available at: https://nibio.brage.unit.no/nibio-xmlui/bitstream/handle/11250/2581065/NIBIO_RAPPORT_2019_5_1.pdf?sequence=1&isAllowed=y.

Hartmann, N. B. *et al.* (2019) 'Are we speaking the same language? Recommendations for a definition and categorization framework for plastic debris', *Environmental Science and Technology*, 53(3), pp. 1039–1047. doi: 10.1021/acs.est.8b05297.

Hillenbrand, T. *et al.* (2005) *Einträge von Kupfer, Zink und Blei in Gewässer und Böden*, Umweltbundesamt. Available at: <http://www.umweltbundesamt.de>.

ISO (2017) *Rubber – Determination of mass concentration of tire and road wear particles (TRWP) in soil and sediments – Pyrolysis-GC/MS method*. Available at: <https://www.iso.org/obp/ui/#iso:std:iso:ts:21396:ed-1:v1:en> (Accessed: 16 August 2020).

Jan Kole, P. *et al.* (2017) 'Wear and tear of tyres: A stealthy source of microplastics in the environment', *International Journal of Environmental Research and Public Health*, 14(10). doi: 10.3390/ijerph14101265.

Janhäll, S. *et al.* (2016) *Utvärdering av städmaskiners förmåga att reducera vägdammsförrådet i gatu- och tunnelsemiljöer i Trondheim*. Available at: <http://vti.diva-portal.org/smash/get/diva2:899278/FULLTEXT01.pdf>.

Januszewicz, K. *et al.* (2017) 'Physicochemical problems of mineral processing thermogravimetric analysis/pyrolysis of used tyres and waste rubber', *Physicochem. Probl. Miner. Process*, 53(2), pp. 802–811. doi: 10.5277/ppmp170211.

- Jasminská, N., Brestovič, T. and Čarnogurská, M. (2013) 'The effect of temperature pyrolysis process of used tires on the quality of output products', *Acta Mechanica et Automatica*, 7(1), pp. 20–25. doi: 10.2478/ama-2013-0004.
- Jekel, M. (2019) 'Scientific Report on tyre and road wear particles, TRWP, in the aquatic environment', *REPORT - European Tyre & Rubber Manufacturers Association (ETRMA)*, pp. 1–35. Available at: <https://www.tyreandroadwear.com/news/scientific-report-on-tyre-and-road-wear-particles-trwp-in-the-aquatic-environment/>.
- Jenner, L. C. *et al.* (2022) 'Detection of microplastics in human lung tissue using μ FTIR spectroscopy', *Science of the Total Environment*, 831, p. 154907. doi: 10.1016/j.scitotenv.2022.154907.
- Johannessen, C. *et al.* (2021) 'The Tire Wear Compounds 6PPD-Quinone and 1,3-diphenylguanidine in an urban watershed', *Archives of Environmental Contamination and Toxicology*, pp. 2–10. doi: 10.1007/s00244-021-00878-4.
- Jotte, L., Raspati, G. and Azrague, K. (2017) *Review of stormwater management practices, Klima 2050*. Thondheim.
- Jung, U. and Choi, S.S. (2022) 'Classification and Characterization of Tire-Road Wear Particles in Road Dust by Density' *Polymers*, 14. doi.org/10.3390/polym14051005
- Jusli, E. *et al.* (2014) 'Chemical properties of waste tyre rubber granules', *Advanced Materials Research*, 911(April), pp. 77–81. doi: 10.4028/www.scientific.net/amr.911.77.
- Kawamoto, H. (2017) 'Lignin pyrolysis reactions', *Journal of Wood Science*, 63(2), pp. 117–132. doi: 10.1007/s10086-016-1606-z.
- Khan, F. R., Halle, L. L. and Palmqvist, A. (2019) 'Acute and long-term toxicity of micronized car tire wear particles to *Hyalella azteca*', *Aquatic Toxicology*, 213, p. 105216. doi: 10.1016/J.AQUATOX.2019.05.018.
- Khan, U. T. *et al.* (2013) 'Bioretention cell efficacy in cold climates: Part 2 – water quality performance', *Can. J. Eng.*, 1233, pp. 1222–1233. doi: 10.1139/I2012-111.
- Kim, H., Seagren, E. A. and Davis, A. P. (2003) 'Engineered bioretention for removal of nitrate from stormwater runoff', *Water Environment Research*, 75(4), pp. 355–367. doi: 10.2175/106143003X141169.
- Klößner, P. *et al.* (2019) 'Tire and road wear particles in road environment – Quantification and assessment of particle dynamics by Zn determination after density separation', *Chemosphere*, 222, pp. 714–721. doi: 10.1016/j.chemosphere.2019.01.176.
- Klößner, P. *et al.* (2020) 'Characterization of tire and road wear particles from road runoff indicates highly dynamic particle properties', *Water Research*, 185. doi: 10.1016/j.watres.2020.116262.
- Klößner, P. *et al.* (2021) 'Comprehensive characterization of tire and road wear particles in highway tunnel road dust by use of size and density fractionation', *Chemosphere*, 279, p. 130530. doi: 10.1016/J.CHEMOSPHERE.2021.130530.
- Kovochich, M. *et al.* (2021) 'Characterization of individual tire and road wear particles in

environmental road dust, tunnel dust, and sediment'. *Environ. Sci. Technol. Lett.* 8, 1057–1064. doi.org/10.1021/acs.estlett.1c00811

Kratky, H. *et al.* (2017) 'A critical literature review of bioretention research for stormwater management in cold climate and future research recommendations', 11(4), pp. 1–15. doi: 10.1007/s11783-017-0982-y.

Kreider, M. L. *et al.* (2009) 'Physical and chemical characterization of tire-related particles: Comparison of particles generated using different methodologies', *Science of The Total Environment*, 408(3), pp. 652–659. doi: 10.1016/j.scitotenv.2009.10.016.

Kumata, H. *et al.* (2000) 'Historical trends of N-cyclohexyl-2-benzothiazolamine, 2-(4-morpholinyl)benzothiazole, and other anthropogenic contaminants in the urban reservoir sediment core', *Environmental Science and Technology*, 34(2). doi: 10.1021/es990738k.

Kwak, J. H. *et al.* (2013) 'Characterization of non-exhaust coarse and fine particles from on-road driving and laboratory measurements', *Science of the Total Environment*, 458–460, pp. 273–282. doi: 10.1016/j.scitotenv.2013.04.040.

Lange, K. *et al.* (2021) 'Removal of rubber, bitumen and other microplastic particles from stormwater by a gross pollutant trap - bioretention treatment train', *Water Research*, 202(July), p. 117457. doi: 10.1016/j.watres.2021.117457.

Lange, K. *et al.* (2022) 'Occurrence and concentration of 20–100 µm sized microplastic in highway runoff and its removal in a gross pollutant trap – bioretention and sand filter stormwater treatment train', *Science of the Total Environment*, 809. doi: 10.1016/j.scitotenv.2021.151151.

Law, K. L. *et al.* (2010) 'Plastic Accumulation in the North Atlantic Subtropical Gyre', *Science*, 329, pp. 1185–1188. doi: 10.1126/science.1192321.

Leads, R. R. and Weinstein, J. E. (2019) 'Occurrence of tire wear particles and other microplastics within the tributaries of the Charleston harbor estuary, South Carolina, USA', *Marine Pollution Bulletin*, 145(June), pp. 569–582. doi: 10.1016/j.marpolbul.2019.06.061.

LeFevre, G. H. *et al.* (2015) 'Review of dissolved pollutants in urban storm water and their removal and fate in bioretention cells', *Journal of Environmental Engineering*, 141(1), p. 04014050. doi: 10.1061/(asce)ee.1943-7870.0000876.

LeFevre, G. H., Hozalski, R. M. and Novak, P. J. (2012) 'The role of biodegradation in limiting the accumulation of petroleum hydrocarbons in raingarden soils', *Water Research*, 46(20), pp. 6753–6762. doi: 10.1016/j.watres.2011.12.040.

Lefevre, G. H., Novak, P. J. and Hozalski, R. M. (2012) 'Fate of naphthalene in laboratory-scale bioretention cells: Implications for sustainable stormwater management', *Environmental Science and Technology*, 46(2), pp. 995–1002. doi: 10.1021/es202266z.

Leslie, H. A. *et al.* (2022) 'Discovery and quantification of plastic particle pollution in human blood', *Environment International*, (March), p. 107199. doi: 10.1016/j.envint.2022.107199.

Lindholm, O. (2015) 'Forurensingstilførsler fra veg og betydningen av å tømme sandfang', *Vann*, (01), pp. 93–100. Available at: https://vannforeningen.no/wp-content/uploads/2015/06/2015_924560.pdf.

Litvinow, V. M. and De, P. P. (2002) *Spectroscopy of rubber and rubbery materials*. Shawbury: Rapra Technology Limited.

Longhin, E. M., Mantecca, P. and Gualtieri, M. (2020) 'Fifteen years of airborne particulates in vitro toxicology in milano: Lessons and perspectives learned', *International Journal of Molecular Sciences*. doi: 10.3390/ijms21072489.

Lowne, R. W. (1970) 'The effect of road surface texture on tyre wear', *Wear*, 15, pp. 57–70. doi: 10.1016/0043-1648(70)90186-9.

Mayerhöfer, T. G., Pipa, A. V. and Popp, J. (2019) 'Beer's Law-why integrated absorbance depends linearly on concentration', *ChemPhysChem*, pp. 2748–2753. doi: 10.1002/cphc.201900787.

McIntyre, J. K. *et al.* (2021) 'Treading water: Tire wear particle leachate recreates an urban runoff mortality syndrome in coho but not chum salmon', *Environmental Science and Technology*, 55(17), pp. 11767–11774. doi: 10.1021/acs.est.1c03569.

Melville, B., Lucieer, A. and Aryal, J. (2018) *Principles of fluorescence spectroscopy*. Third Edit, Springer. Third Edit. Edited by J. R. Lakowicz. New York: Springer Science+Business Media, LLC. doi: 10.3390/rs10020308.

Mengistu, D., Heistad, A. and Coutris, C. (2021) 'Tire wear particles concentrations in gully pot sediments', *Science of the Total Environment*, 769, p. 144785. doi: 10.1016/j.scitotenv.2020.144785.

Mohomed, K. (2016) 'Thermogravimetric analysis (TGA) theory and applications', *TA Instruments*, pp. 4–235. Available at: <http://webcache.googleusercontent.com/search?q=cache:2tG2B4rkrtwJ:www.tainstruments.com/wp-content/uploads/CA-2016-TGA.pdf+&cd=20&hl=en&ct=clnk&client=firefox-b>.

Moore, C. J. *et al.* (2001) 'A comparison of plastic and plankton in the North Pacific Central Gyre', *Marine Pollution Bulletin*, 42(12), pp. 1297–1300. doi: 10.1016/S0025-326X(01)00114-X.

Murphy, K. R. *et al.* (2013) 'Fluorescence spectroscopy and multi-way techniques. PARAFAC', *Analytical Methods*, 5(23), pp. 6557–6566. doi: 10.1039/c3ay41160e.

Natalia, J., Tomas, B. and Maria, C. (2013) 'The Effect of temperature pyrolysis process of used tires on the quality of output products', *Acta Mechanica et Automatica*, 7(1). doi: 10.2478/ama-2013-0004.

NIST Chemistry WebBook, SRD 69 (2011) *National standards and technology, US department of Commerce*. Available at: <https://webbook.nist.gov/cgi/inchi?ID=C7732185&Type=IR-SPEC&Index=0> (Accessed: 24 July 2019).

Oecd (2010) 'Sediment-water chironomid life-cycle toxicity test using spiked water or spiked sediment', *GUIDELINES*. OECD, p. 29. doi: 10.1787/9789264090910-en.

Ojeda, T. (2013) 'Polymers and the environment', in *Polymer Science*. IntechOpen. doi: <http://dx.doi.org/10.5772/51057>.

Padoan, E., Romè, C. and Ajmone-Marsan, F. (2017) 'Bioaccessibility and size distribution of metals in road dust and roadside soils along a peri-urban transect', *Science of the Total*

Environment, 601–602, pp. 89–98. doi: 10.1016/j.scitotenv.2017.05.180.

Panko, J. M. *et al.* (2013) 'Measurement of airborne concentrations of tire and road wear particles in urban and rural areas of France, Japan, and the United States', *Atmospheric Environment*, 72, pp. 192–199. doi: 10.1016/j.atmosenv.2013.01.040.

Parker-Jurd, F. N. F. *et al.* (2019) *Investigating the sources and pathways of synthetic fibre and vehicle tyre wear contamination into the marine environment*, The Department for Environment Food and Rural Affairs. London.

Paus, A. *et al.* (2013) 'Forslag til dimensjonering og utforming av regnbed for norske forhold', *Vann*.

Paus, A. K. H. (2018) 'Forslag til dimensjonerende verdier for trinn 1 i Norsk Vann sin tretrinns strategi for håndtering av overvann', *Vann*, 1.

Paus, K. H. *et al.* (2014) 'Assessment of the hydraulic and toxic metal removal capacities of bioretention cells After 2 to 8 years of service', *Water and air pollut.* doi: 10.1007/s11270-013-1803-y.

Paus, K. H., Muthanna, T. M. and Braskerud, B. C. (2016) 'The hydrological performance of bioretention cells in regions with cold climates: Seasonal variation and implications for design', *Hydrology Research*, 47(2), pp. 291–304. doi: 10.2166/nh.2015.084.

Paus, K. and Muthanna, T. M. (2015) 'The hydrological performance of bioretention cells in regions with cold climates : Seasonal variation and implications for design suggestions for designing and constructing bioretention cells for a nordic climate Forslag til dimensjonering og utforming av', (October). doi: 10.2166/nh.2015.084.

Pohrt, R. (2019) 'Tire wear particles hot spots- Review of influencing factors', *Mechanical Engineering*, 17(1). doi: <https://doi.org/10.22190/FUME190104013P>.

Ragn-sells (2018) *Gummigranulat*. Available at: https://www.ragnsells.no/globalassets/norge/dokumenter/dekkgjenvinning/rs_pb_granulat_fin_v5-2018-01-16.pdf (Accessed: 2 August 2018).

Rauert, C. *et al.* (2021) 'Challenges with quantifying tire road wear particles: Recognizing the need for further refinement of the ISO technical specification', *Environmental Science & Technology Letters*, 8(3), pp. 231–236. doi: 10.1021/acs.estlett.0c00949.

Rinnan, A., 2004. Application of PARAFAC on spectral data. Fac. Sci. The Royal Veterinary and Agricultural University.

Rødland, E. S. *et al.* (2021) 'A novel method for the quantification of tire and polymer-modified bitumen particles in environmental samples by pyrolysis gas chromatography mass spectroscopy', *Journal of Hazardous Materials*, 423(July 2021). doi: 10.1016/j.jhazmat.2021.127092.

Redondo-Hasselerharm, P. E. *et al.* (2018) 'Ingestion and Chronic Effects of Car Tire Tread Particles on Freshwater Benthic Macroinvertebrates', *Environmental Science and Technology*, 52(23), pp. 13986–13994. doi: 10.1021/acs.est.8b05035.

Rødland, E. S. *et al.* (2022) 'A novel method for the quantification of tire and polymer-modified

bitumen particles in environmental samples by pyrolysis gas chromatography mass spectroscopy', *Journal of Hazardous Materials*, 423(August 2021). doi: 10.1016/j.jhazmat.2021.127092.

Roy-poirier, A. (2010) *Review of bioretention system research and design : Past , present , and future*. Queen's University. doi: 10.1061/(ASCE)EE.1943-7870.0000227.

SAPEA (2019) *A scientific perspective on micro-plastics in nature and society*. Berlin. doi: 10.26356/microplastics.

Schwabl, P. *et al.* (2019) 'Detection of various microplastics in human stool', *Annals of Internal Medicine*, 171(7). doi: 10.7326/m19-0618.

Shen, D. *et al.* (2013) 'The overview of thermal decomposition of cellulose in lignocellulosic biomass', in *cellulose - Biomass Conversion*. doi: 10.5772/51883.

Siegfried, M. *et al.* (2017) 'Export of microplastics from land to sea. A modelling approach', *Water Research*, 127, pp. 249–257. doi: 10.1016/j.watres.2017.10.011.

Silverstein, M. R. *et al.* (2015) *Spectrometric identification of organic compounds*. Eighth. Edited by K. Joan, Y. Jennifer, and O. Mary. Hoboken, New Jersey: John Wiley & Sons., Inc.

Skaaraas, H. *et al.* (2015) 'Overvann i byer og tettsteder, som problem og ressurs', *NOU: Norges offentlige utredninger*. Available at: <https://www.regjeringen.no/contentassets/e6db8ef3623e4b41bcb81fb23393092b/201520150016000dddpdfs.pdf>.

Smyth, K. *et al.* (2021) 'Bioretention cells remove microplastics from urban stormwater', *Water Research*, 191. doi: 10.1016/j.watres.2020.116785.

Snilsberg, B. (2008) *Pavement wear and airborne dust pollution in Norway: Characterization of the physical and chemical properties of dust particules*. Norwegian University of Science and Technology. Available at: <https://ntnuopen.ntnu.no/ntnu-xmlui/handle/11250/235839>.

Sommer, F. *et al.* (2018) 'Tire abrasion as a major source of microplastics in the environment', *Aerosol and Air Quality Research*, 18(8), pp. 2014–2028. doi: 10.4209/aaqr.2018.03.0099.

Statens Vegvesen (2020) *Vegkart*. Available at: [https://vegkart-2019.atlas.vegvesen.no/#kartlag:geodata/hva:\(~\(farge:'0_0,id:643\)\)/hvor:\(kommune:\(~602\)\)/@243508,6627176,8/vegobjekt:1007532883:40a744:643](https://vegkart-2019.atlas.vegvesen.no/#kartlag:geodata/hva:(~(farge:'0_0,id:643))/hvor:(kommune:(~602))/@243508,6627176,8/vegobjekt:1007532883:40a744:643) (Accessed: 21 March 2021).

Stevenson, K., Stallwood, B. and Hart, A. G. (2008) 'Tire rubber recycling and bioremediation: A review', *Bioremediation Journal*, 12(1), pp. 1–11. doi: 10.1080/10889860701866263.

Tahvonen, O. (2018) 'Adapting bioretention construction details to local practices in Finland', *Sustainability*, 10(276). doi: 10.3390/su10020276.

Tamis, J. E. *et al.* (2021) 'Environmental risks of car tire microplastic particles and other road runoff pollutants', *Microplastics and Nanoplastics*, 1(1), pp. 1–17. doi: 10.1186/s43591-021-00008-w.

Thygesen, L.G. *et al.* (2004) 'Stabilizing the PARAFAC decomposition of fluorescence spectra by insertion of zeros outside the data area' *Chemom. Intell. Lab. Syst.* 71, 97–106.

doi.org/10.1016/j.chemolab.2003.12.012

Tian, L., Wang, D. and Wei, Q. (2019) 'Study on dynamic mechanical properties of a nylon-like polyester tire cord', *Journal of Engineered Fibers and Fabrics*, 14(1800). doi: 10.1177/1558925019868807.

Tian, Z. *et al.* (2021) 'A ubiquitous tire rubber-derived chemical induces acute mortality in coho salmon', *Science*, 371(6525), pp. 185–189. doi: 10.1126/science.abd6951.

U. S. Environmental Protection Agency (2021) *The effect of climate change on water resources and programs*. Available at: <https://https://cfpub.epa.gov/watertrain/> (Accessed: 24 October 2021).

Unice, K. M. *et al.* (2019) 'Characterizing export of land-based microplastics to the estuary - Part II: Sensitivity analysis of an integrated geospatial microplastic transport modeling assessment of tire and road wear particles', *Science of the Total Environment*, 646, pp. 1650–1659. doi: 10.1016/j.scitotenv.2018.08.301.

Unice, K. M., Kreider, M. L. and Panko, J. M. (2012) 'Use of a deuterated internal standard with pyrolysis-GC/MS dimeric marker analysis to quantify tire tread particles in the environment', *International Journal of Environmental Research and Public Health*, 9(11), pp. 4033–4055. doi: 10.3390/ijerph9114033.

Unice, K. M., Kreider, M. L. and Panko, J. M. (2013) 'Comparison of tire and road wear particle concentrations in sediment for watersheds in France, Japan, and the United States by quantitative pyrolysis GC/MS analysis', *Environmental Science and Technology*, 47(15), pp. 8138–8147. doi: 10.1021/es400871j.

Vegdirektoratet (2014) *Vegbygging, Håndbok N200*. Oslo: Statens Vegvesen.

Verschoor, A. *et al.* (2016) *Emission of microplastics and potential mitigation measures, REPORT - RIVM Report 2016-0026*. Bilthoven. Available at: <https://www.rivm.nl/dsresource?objectid=dad60794-a4a2-44f9-8416-624cfbc4861e&type=org&disposition=inline>.

Verschoor, A. J. (2015) *Towards a definition of microplastics: Considerations for the specification of physico-chemical properties, RIVM Letter report*. Bilthoven. doi: 10.1080/0449010X.1964.10703070.

Villena, O. C. *et al.* (2017) 'Effects of tire leachate on the invasive mosquito *Aedes albopictus* and the native congener *Aedes triseriatus*', *PeerJ*, 2017(9), pp. 1–15. doi: 10.7717/peerj.3756.

Vogelsang, C., Lusher, A.L., Dadkhah, M.E., Sundvor, I., Umar, M., Ranneklev, S.B., Eidsvoll, D. and Meland, S. (2018) *Microplastics in road dust – characteristics, pathways and measures*. Oslo. doi: 10.1097/nnr.0000000000000034.

Wagner, S. *et al.* (2018) 'Tire wear particles in the aquatic environment - A review on generation, analysis, occurrence, fate and effects', *Water Research*, 139(March), pp. 83–100. doi: 10.1016/j.watres.2018.03.051.

Wei, H. *et al.* (2021) 'An assessment of gully pot sediment scour behaviour under current and potential future rainfall conditions', *Journal of Environmental Management*, 282(June 2020), p. 111911. doi: 10.1016/j.jenvman.2020.111911.

Wik, A. (2008) *When the rubber meets the road - Ecotoxicological Hazard and Risk Assessment of Tire*

Wear Particles, THESIS PhD. Available at:
<http://gupea.ub.gu.se/handle/2077/17762>
http://gupea.ub.gu.se/bitstream/2077/17762/1/gupea_2077_17762_1.pdf
<https://gupea.ub.gu.se/handle/2077/17762>.

Wik, A. and Dave, G. (2005) 'Environmental labeling of car tires—toxicity to *Daphnia magna* can be used as a screening method', *Chemosphere*, 58(5), pp. 645–651. doi: 10.1016/J.CHEMOSPHERE.2004.08.103.

Wik, A. and Dave, G. (2006) 'Acute toxicity of leachates of tire wear material to *Daphnia magna*—Variability and toxic components', *Chemosphere*, 64(10), pp. 1777–1784. doi: 10.1016/J.CHEMOSPHERE.2005.12.045.

Wik, A. and Dave, G. (2009) 'Occurrence and effects of tire wear particles in the environment – A critical review and an initial risk assessment', *Environmental Pollution*, 157(1), pp. 1–11. doi: 10.1016/J.ENVPOL.2008.09.028.

8. Appended Papers

Paper I

Paper II

Paper III

Paper IV

Appended Papers

Mengistu, D., Nilsen, V., Heistad, A., & Kvaal, K. (2019) 'Detection and quantification of tire particles in sediments using a combination of simultaneous thermal analysis, fourier transform infra-red, and parallel factor analysis', *International Journal of Environmental Research and Public Health*, 16, no. 18: 3444. <https://doi.org/10.3390/ijerph16183444>



Article

Detection and Quantification of Tire Particles in Sediments Using a Combination of Simultaneous Thermal Analysis, Fourier Transform Infra-Red, and Parallel Factor Analysis

Demmelash Mengistu ^{1,2,*}, Vegard Nilsen ¹, Arve Heistad ¹ and Knut Kvaal ¹

¹ Faculty of Science and Technology, Norwegian University of Life Sciences, 1430 Ås, Norway; vegard.nilsen@nmbu.no (V.N.); arve.heistad@nmbu.no (A.H.); knut.kvaal@nmbu.no (K.K.)

² The Municipality of Ås, Myrveien 16, 1430 Ås, Norway

* Correspondence: demmelash.mengistu@nmbu.no

Received: 28 August 2019; Accepted: 12 September 2019; Published: 17 September 2019



Abstract: Detection and quantification of tread wear particles in the environment have been a challenge owing to lack of a robust method. This study investigated the applicability of a combination of Simultaneous Thermal Analysis (STA), Fourier Transform Infra-Red (FTIR), and Parallel Factor Analysis (PARAFAC) in the detection and quantification of tire particles from formulated sediments. FTIR spectral data were obtained by heating 20 samples in STA. Among the 20 samples, 12 were tire granules in formulated sediments (TGIS) containing 1%, 2%, 5%, and 10% by mass of tire granules, while the remaining eight contained 0.5, 1, 2.5, and 5 mg of tire granules only (TGO). The PARAFAC models decomposed the trilinear data into three components. Tire rubber materials in tire granules (RM) and a combination of water and carbon dioxide were the components identified in all samples. The linear regression analysis of score values from the PARAFAC models showed that the RM quantity predicted were comparable to measured values in both TGIS and TGO. Decomposing the overlying components in the spectral data into different components, and predicting unknown quantity in both sample types, the method proves robust in identifying and quantifying tire particles from sediments.

Keywords: detection; quantification; PARAFAC; FTIR; microplastics; tire particles; sediment; method

1. Introduction

Tread wear particles has become an environmental concern because of their significant global microplastics contribution [1,2]. Vehicle tires release about 11.5% of mass during their service life [3,4]. The considerable amount of particles released to the environment is composed of many chemicals, including natural and synthetic rubber polymers, fillers, reinforcing agents, processing aids, accelerators and retarders, adhesives and activators [5]. Tread wear particles generated during driving by rolling shear of tread against pavement [6] picks more substances from the road surface and other traffic related emissions [1]. These particles are deposited along roadsides with wildly varying quantity. Parts of the tread wear particles enter the marine environment [7] and spread even to the remote areas [2]. Tread wear particles are recognized as threat to human health and marine and terrestrial organisms. Adverse health and environmental effects from airborne particulate matters of tire wear are reported in [1,8] while other studies (e.g., [2]) included potential adverse effects from terrestrial and aquatic environment. However, quantification of tread wear particles and the associated risks remains unanswered [2]. In fact, quantification is a common challenge for emerging pollutants such as graphene nanoparticles [9].

The failure to detect and accurately quantify tread wear particles arises from lack of a robust method to detect tire particles in the environment [1,6]. Methods applied to detect microplastics in the environment or analytical methods established for single polymer particle detection are not suitable for identification of tread wear particles [1,6], because the use of these methods requires a challenging extraction step and extensive pretreatment [10]. Work on indirect methods of detection through markers could not establish dependable markers from additives in the tire making process [6]. However, studies have reported that component analysis methods are reliable to detect polymers in the environment [11,12]. Rubber material, which is the core component in tires [13], therefore, makes a good candidate for component analysis to determine the presence and to estimate the quantity of tread wear particles in sediments and soils [6]. Simultaneous Thermal Analysis (STA) or application of Thermal Gravimetric Analysis (TGA) and Differential Scanning Calorimetry (DSC), are standard tools in compositional analysis of multi-component materials like tire [14,15]. Simultaneous Thermal Analysis, besides its comparatively lesser time and sample preparation demands, gives information on two physical processes, mass change and heat flow, on the same sample simultaneously [16]. However, physical properties alone are not sufficient in identifying chemical components [16]. Coupling the STA to Fourier Transform Infra-Red (FTIR) spectroscopy provides additional and powerful information about the chemical properties of materials [17,18]. Nevertheless, direct application of this method, on complex matrices like sediments and soils where the quantity of tread wear particles is expected to be low, is unreliable [6]. One factor limiting the effectiveness of the method is the generation of overlying components in the TGA [14] which gives non-conclusive FTIR matches referenced to the usually pure compound in the library [19]. Quantitative analysis through calibration curve is also impossible because of the overlying components [11].

Mathematical tensor decomposition methods can resolve FTIR spectra with overlying components. Parallel Factor Analysis (PARAFAC) has shown great versatility in this respect in resolving the multi-component matrix into underlying analytes [20] and offers a reliable foundation to estimate quantity of the components based on Beer-Lambert's law [21,22]. The method requires tri-linearity—the same number of components underlie the chemical variation in each dimension of the dataset; variability—no identical signals or co-varying intensities between two chemical components; and additivity—the total signal is due to the linear superposition of a fixed number of components [22]. Choosing the right number of components for the model and acquisition of appropriate signal-to-noise ratio of spectral data is critical for the analysis [23].

The objective of this study is to introduce a new method for detecting and estimating quantity of rubber materials from formulated sediment (RM) for possible application in the detection and quantification of tread wear particles from soil and sediment.

2. Materials and Methods

2.1. Tire Granules

Three different sizes of tire granules (<1.2 mm, 1–2.8 mm, 2.5–4 mm) were obtained from Ragn-Sells, a producer and distributor of tire granules by grinding discarded tires in Norway and Sweden [24]. The source of the granules is coded as plastic and rubber (1912 04) in the European waste code. The product specification states that the tire granules contain 58% elastomer designated as Styrene-Butadiene Rubber (SBR). Styrene butadiene rubber (SBR) is a synthetic rubber. However, it represents all rubber materials in tires in the manufacturers' context. The SBR content of the tire granules is estimated with similar method to the International Federation of Association of Football (FIFA) test Method 11, Thermal Gravimetric Analysis [25]. The producer's specification was not verified by independent study and the rubber material in tire granules (RM) is relatively high compared to 40–50% rubber materials in tires estimated by [26–28]. However, we used the stated proportion to represent all RM in this experiment.

2.2. Formulated Sediment

To ensure experiment repeatability and knowledge of particle size and content in the samples, sediment was formulated according to OECD guidelines [29] for the testing of chemicals with composition of 5% organic matter, 75% quartz sand, and 20% kaolinite clay. Finally, water-equivalent to 50% by volume of the formulated sediment was added to the mix [29]. Organic matter used in the sediment preparation is a conifer bark (EAN: 7058782362833) obtained from a plant shop (Plantasjen). Quartz sand (0.2–0.4 mm) and kaolinite clay (CAS: 1332-58-7) were obtained from Radasand and VWR respectively.

2.3. Sample Preparation

We prepared two types of samples for the experiment (Table 1) using Mettler Toledo XP205 DeltaRange analytical balance. The first sample type was tire granules in formulated sediment (TGIS). We prepared TGIS by placing a 1000 mg of formulated sediment in four small beakers of size 20 mL each. A total of 10, 20, 50, and 100 mg of finely ground tire granules (<1.2 mm was selected for this experiment [24]) were added to the four beakers in random order giving four (1%, 2%, 5%, and 10%) rubber material concentrations named RM1, RM2, RM3, RM4. We shook each beaker by hand for a proper mix. We then collected 50 mg of TGIS from each beaker and placed in separate aluminum crucibles in three replicates. Based on a 58% ratio, the collected 50 mg samples formed four classes of rubber materials in tire granules (RM) equivalent to 0.29 mg in 1% TGIS, 0.58 mg in 2% TGIS, 1.45 mg in 5%TGIS, and 2.9 mg in 10% TGIS. The second sample type contained tire granules only (TGO). We used TGO to test if the detection and quantification of RM from TGIS and TGO is comparable. We prepared TGO samples by placing 0.5, 1, 2.5, and 5 mg of tire granules in separate aluminum crucibles in two replicates. The second sample type corresponded to the rubber material quantities in TGIS. The samples were assigned identification numbers. Total sample was limited to 20 because of the high cost of data generation and limited budget. Two replicates were enough for TGO since homogeneity is assumed.

Table 1. Sample type, class, mass, rubber material quantity, number of replicates, and identification number. Sample type: TGIS = Tire granules in sediment, TGO = Tire granule only. Rubber materials (RM) = rubber materials: RM1 = samples with rubber material concentration of 0.29 mg, RM2 = samples with rubber material concentration of 0.58 mg, RM3 = samples with rubber material concentration of 1.45 mg, RM4 = samples with rubber material concentration of 2.90 mg.

RM	RM Quantity (mg)	Sample Type	Sample Mass (mg)	Number of Replicates	Identification Number
RM1	0.29	TGIS	50	3	1, 2, 3
		TGO	0.5	2	1, 2
RM2	0.58	TGIS	50	3	4, 5, 6
		TGO	1	2	3, 4
RM3	1.45	TGIS	50	3	7, 8, 9
		TGO	2.5	2	5, 6
RM4	2.90	TGIS	50	3	10, 11, 12
		TGO	5	2	7, 8

2.4. Experimental Flow and Procedure

Figure 1 presents the flow of the experiment.

Simultaneous Thermal Analysis: The experiment was conducted at the Norwegian Institute of Bioeconomy Research (NIBIO)—a laboratory which is primarily set for the analysis of wood and wood products. We placed crucibles with samples on automatic sample changer and fed to the Simultaneous Thermal Analyzer-STA 449 F1 Jupiter (Netzsch, Selb, Germany), type S, for heating according to pre-programmed arrangement. The heating process was programmed to progress at the rate of 10 °C/min temperature rise from 4 to 800 °C in a N₂ (20 mL/min) protective gas environment.

Evolved gases were purged to the attached FTIR instrument by N₂ gas (50 mL/min) every 2.28 °C increase on average. See [30] for more information on STA. Weight loss of samples were registered in percentage as the heating progressed. We converted the weight loss to mg per temperature ramp by multiplying original sample mass with percentage difference between consecutive temperature ramps.

Fourier Transform Infra-Red (FTIR) (Bruker, Billerica, MA, USA): We used Bruker TENSOR 27 with external gas cell FTIR to scan the spectra of the evolved gases. The average signal of 16 scans of FTIR spectra in the wavenumber range of 600–4000 cm⁻¹ was collected with a resolution of 1.9 cm⁻¹ during the heating process.

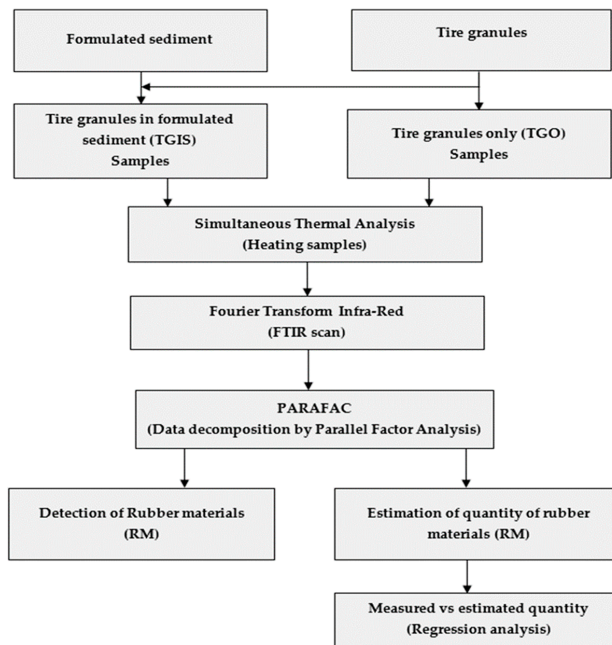


Figure 1. Graphical presentation of flow of the experiment (sample preparation and sampling, sample heating, Fourier Transform Infra-Red (FTIR) scanning, data decomposition, rubber material detection (RM), estimation of quantity of rubber materials (RM), and regression analysis).

2.5. Data and the PARAFAC Model

We obtained two sets of data per sample from STA and FTIR instruments. The STA data included temperature ramp and percentage mass loss. The FTIR data contained wavenumber cm⁻¹ and absorbance intensity. The first task was to assign temperature ramp from the STA data to the FTIR data. The data were handled using MATLAB (The MathWorks Inc., R2018a, Natick, MA, USA). PARAFAC models were built using Partial least squares (PLS) Toolbox for MATLAB version 8.6; Eigenvector Research Inc. (Wenatchee, WA, USA) [31].

FTIR data from each sample was represented by a matrix (Wavenumber cm⁻¹ × Temperature °C), representing spectral wavenumbers and heating ramp along their dimensions. As all FTIR data were measured using a similar temperature ramp, individual matrices could be stacked to form a three-way data structure of Samples (S), wave numbers (W), and temperature ramps (T). This gave a trilinear data of 12 and eight samples × 1672 wavenumber cm⁻¹ × 333 temperature steps (spectra), making it suitable for a multiway analysis [20].

Two PARAFAC models were applied to the trilinear data to decompose into sets of scores and loadings, a procedure similar to [23,32]. Each data point in the dataset (X_{SWT}) can then be described according to the [22] equation (Equation (1))

$$X_{SWT} = \sum_{f=1}^F a_{Sf} b_{Wf} c_{Tf} + e_{SWT}, \quad (1)$$

where: $S = 1-12$ in TGIS, and $1-8$ in TGO, $W = 1-1672$, $T = 1-333$; f represents a PARAFAC component and each component has 12 and 8 a -values (scores); one for each sample. Each component has 1672 b -values; one for each wavenumber and 333 c -values; one for each temperature ramp. e_{SWT} is the residual, representing the variability not accounted for by the model. Several number of possible components (2, 3, 4, 8) were tested and the best number of components to use was selected based on model diagnostics; namely residuals, the core consistency and fit values. See [33] for information on core consistency and model fit. A preprocessing of multiway centering along mode 2 was used in TGO and no preprocessing was needed in TGIS.

PARAFAC was preferred because it can find pure spectra from overlying components and residuals if the right component number is used in the model [23]. Mode loadings of the PARAFAC model offer reliable information because b and c in Equation (1) are scaled estimates of the component at specific FTIR spectrum and temperature respectively.

2.6. Rubber Material Identification

Loadings of the PARAFAC model carry fingerprint information about the substances under evaluation. Wavenumber cm^{-1} and temperature loadings of a component were evaluated against the fingerprint markers of rubber constituents (natural rubber and synthetic rubber) of tire (Tables 2 and 3) for detection of the presence of RM in TGIS and TGO.

Table 2. Tire rubber material identification wavenumber cm^{-1} . Polymers: NR = Natural Rubber, SBR = Styrene Butadiene Rubber, EPDM = Ethylene Propylene Diene Monomer.

Polymer	Functional Group	Wavenumber cm^{-1}	Reference
NR, SBR, EPDM	Methyl	2964	Gunasekaran, Natarajan, and Kala, [18]
NR	Methylene	2950, 2853	Gunasekaran, Natarajan, and Kala, [18]
NR, SBR, EPDM	OH	3470	Gunasekaran, Natarajan, and Kala, [18]
EPDM		1076	V. M. LiPtvinow and P. P. De, [11]
SBR	Polystyrene	750, 700	Fernández-Berridi et al. and Gunasekaran, Natarajan, and Kala, [14,18]
EPDM	Propylene	1461, 1376	Gunasekaran, Natarajan, and Kala, (2007) [18]
SBR	Vinyl	990, 910	Fernández-Berridi et al. and Gunasekaran, Natarajan, and Kala, [14,18]
SBR	Butadiene	960	Gunasekaran, Natarajan, and Kala, [18]
NR, EPDM	Ethylene	722, 815	Fernández-Berridi et al. [14]
EPDM, (NR)	Alkyl	2929, 2856	Fernández-Berridi et al. and Gunasekaran, Natarajan, and Kala, [14,18]
NBR	Alkyl	2230	Gunasekaran, Natarajan, and Kala, [18]

Table 3. Rubber materials pyrolysis degradation temperature in °C. Polymers: NR = Natural Rubber, SBR = Styrene Butadiene Rubber, EPDM = Ethylene Propylene Diene Monomer.

Polymer	Temperature (°C)	Reference
NR, SBR, EPDM	376–476, 400–550	Januszewicz, Klein, Klugmann-Radziemska, and Kardas, and M. Engineering and S. Republi, [5,34]
NR	350	Fernández-Berridi et al. [14]
NR, SBR, EPDM	300–500	Fernández-Berridi et al. [14]
SBR	424	Fernández-Berridi et al. [14]

2.7. Quantity Estimation

Quantity of RM can be estimated from PARAFAC scores which is represented by a_{sf} in Equation (1) [22]. We calibrated the score values of TGIS and TGO samples against measured RM using PLS linear regression to assess the estimation performance. The regression was used in reverse to predict the quantity from score values of the PARAFAC model. The root mean square error of cross-validation (RMSECV) was calculated by Equation (2) [20].

$$RMSECV = \sqrt{\frac{\sum_{l=1}^L (y_l - \hat{y}_l)^2}{L}}, \quad (2)$$

where y_l = predicted tire quantity of the l th sample not included in the calibration; and \hat{y}_l = known tire quantity of the l th sample. L = number of sample.

3. Results

3.1. Sample Weight Loss in Simultaneous Thermal Analysis (STA)

Gases evolved from samples because of degradation during heating in the STA. Purging the evolved gases to FTIR created weight loss in all samples. The weight loss as a function of temperature is presented in Figure 2. Weight loss is observed at temperature range of 200–650 °C with peak loss rate around 370, 420, and 510 °C in tire granules in formulated sediment (TGIS) samples. The weight loss shows a narrow range (200–490 °C) with peak in loss rate around 370 and 420 °C in tire granules only (TGO) samples. The area under the weight loss curves and the peaks of the curves are higher in higher rubber materials in tire granules (RM) quantity classes indicating increased degradation with increased RM quantity. The wider temperature range and the higher degradation intensity in TGIS samples compared to the TGO samples shows generation of additional gases from organic substances in TGIS. All weight loss curves show jagged structure indicating existence of noise in the data.

3.2. Landscape Surfaces of FTIR Data

The FTIR data of evolved gases were assessed for intuitive understanding of the underlying components of the samples. Landscape surfaces of 20 FTIR data from TGIS and TGO are presented in Figure 3. Samples presented in each row have equal amount of tire granules (see Table 1). However, the landscapes show variation between the first three samples in TGIS and the next two samples in TGO containing equal amount of tire granules. The variation in landscape surfaces is detectable visually in the lower quantity profiles. Spectral intensity increases in all samples (except number 7) with increased amount of RM. Multiple peaks are observed in all of the landscape surfaces of the FTIR data.

3.3. The PARAFAC Model and Results

Following several runs using different number of components, PARAFAC models with three components explained most of the variation in the data and thus deemed appropriate for our data

to decompose the FTIR spectral data of both TGIS and TGO. The models captured 89.5% and 90% of explained variations in TGIS and TGO respectively. Low residuals in both sample types, except for sample number 10 in TGIS where a higher value is observed (Figure 4a,b). No variation is observed between model fit (the percentage of variations explained by each component) and unique fit (model fit of a component that is not shared by other components) in TGO (Figure 4d) while variation is observed between model fit and unique fit in component 2 and 3 in TGIS (Figure 4c). The models attained a very high core consistency, indicating a super diagonal core tensor G (Figure 4e,f). See [31] for information on core consistency and model fit.

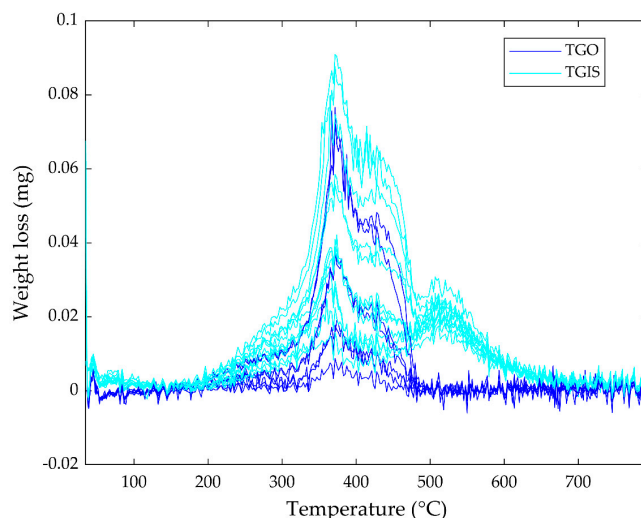


Figure 2. Weight loss (mg) of all 20 samples during heating in the Simultaneous Thermal Analysis (STA) instrument. TGO = Tire granules only, TGIS = Tire granules in formulated sediment.

The models with three components better exposed the differences between the components visibly, either in structure or in values of the components. Landscape surfaces of the three components are presented in Figure 5 in a rearranged order than how they appeared in the respective models. The surfaces display distinct appearance in structure from the landscape surfaces of the raw data.

Landscape surfaces of the three components from the PARAFAC model of TGIS corresponds to landscape surfaces of the components of TGO, except component 2 where the appearance looks different (Figure 5c,d). Landscape surfaces of component 1 in TGIS and TGO (Figure 5a,b) display a similar structure with a structure in the raw data that gained increased visibility with increase in RM.

Two loadings and a score occurred in each component in both PARAFAC models (Equation (1)). The wavenumber cm^{-1} loadings are expressed by mode 2, and the temperature loadings are expressed by mode 3 while scores are expressed by mode 1.

Wavenumber cm^{-1} loadings: Wavenumber cm^{-1} reveals the chemical properties of components as it carries fingerprint information about the substances under evaluation. Figure 6a,b show the wavenumber cm^{-1} of component 1 represented by mode 2 loadings of the models of TGIS and TGO respectively. The two loadings exhibit similar peaks around 2950, 2853, 1450, 1370, 960, and 890 cm^{-1} . The wavenumber cm^{-1} loadings of TGIS shows a peak around 2350 cm^{-1} (red circle in Figure 6a) that was not seen in TGO loadings. The wavenumber cm^{-1} loadings of component 2 of TGIS and TGO show peaks at around 3735, 3560, 2356, 1510, and 670 (Figure 7a,b). The wavenumber cm^{-1} loadings of component 2 of TGO shows a peak around 2900 cm^{-1} (red circle in Figure 7b) that was not seen in TGIS loadings. Wavenumber loadings of component 3 of both TGIS and TGO exhibit similar peaks with component 2 wavenumber cm^{-1} loadings (Figure 8a,b).

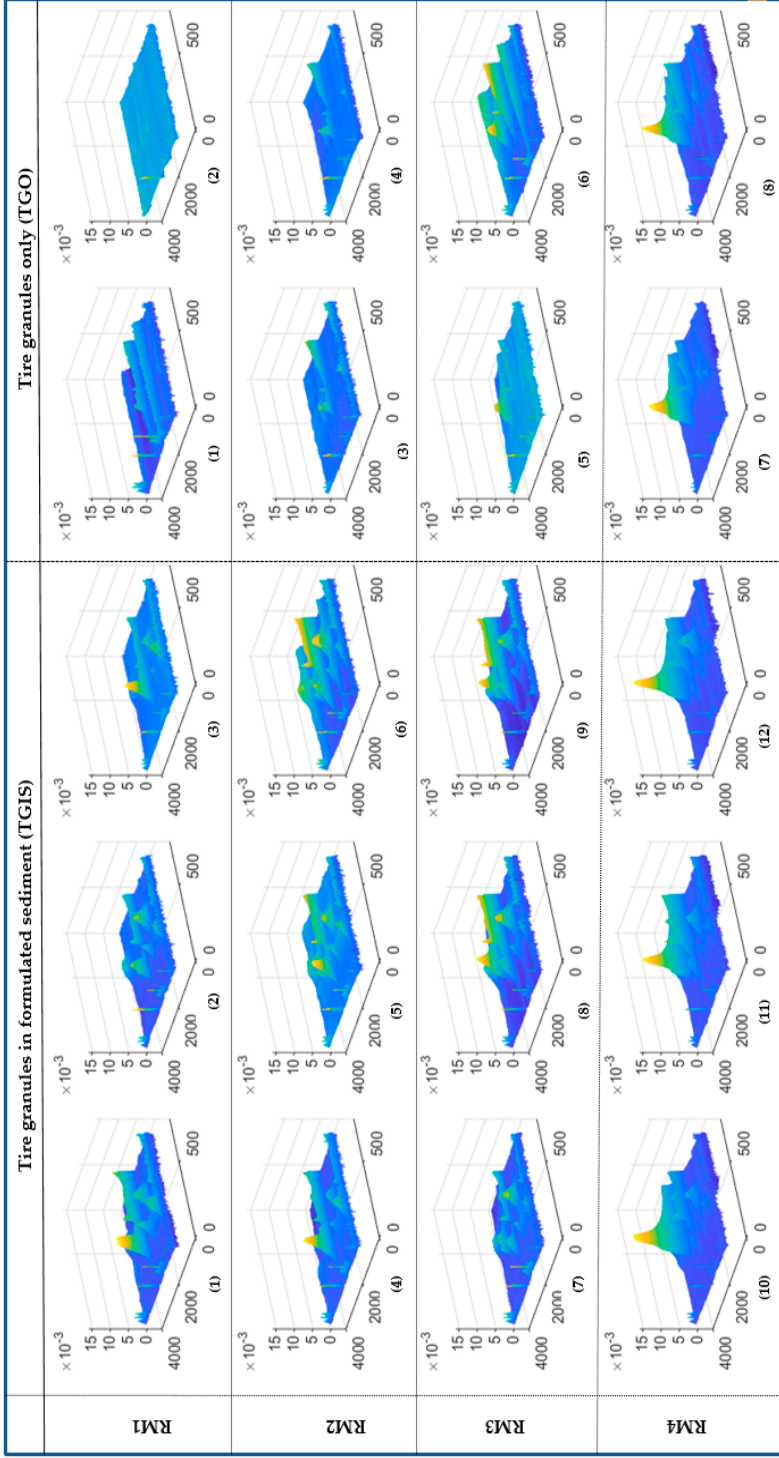


Figure 3. Landscape surfaces of the 20 raw FTIR spectral data. The first three columns in the figure are spectral data of samples in tire granules in formulated sediments (TGIS). The last two columns represent samples in tire granules only (TGO). The RM amount remain similar within rows and increase along the columns. The X-axis represent wavenumber (0–4000 cm^{-1}), Y-axis represent temperature (0–800 $^{\circ}\text{C}$), and z-axis represent intensity of the spectra (absorbance).

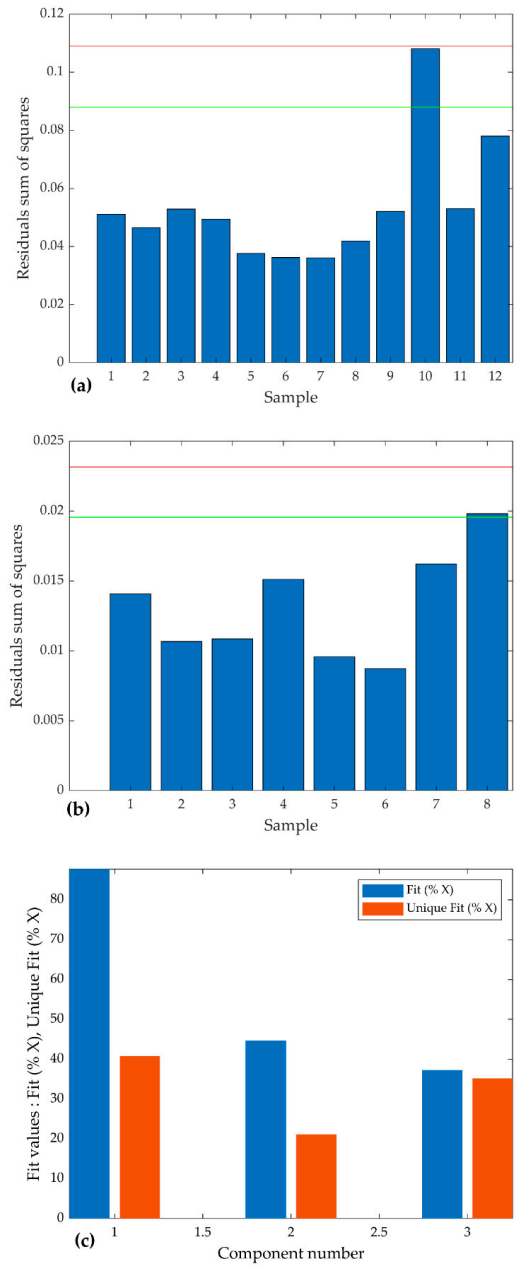


Figure 4. Cont.

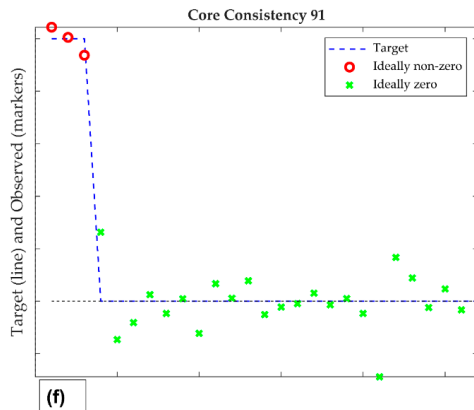
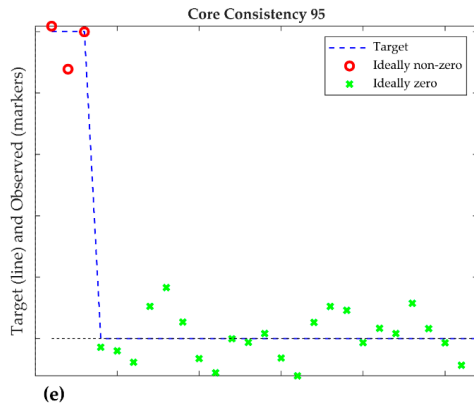
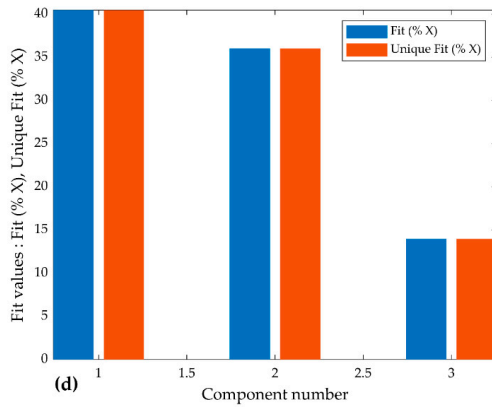


Figure 4. Diagnostic of the Parallel Factor Analysis (PARAFAC) models. (a) Residuals sum of squares of TGIS, (b) residuals sum of squares of TGO, (c) model fit and unique fit of component in TGIS, (d) model fit and unique fit of components in TGO, (e) core consistency of TGIS, and (f) core consistency of TGO.

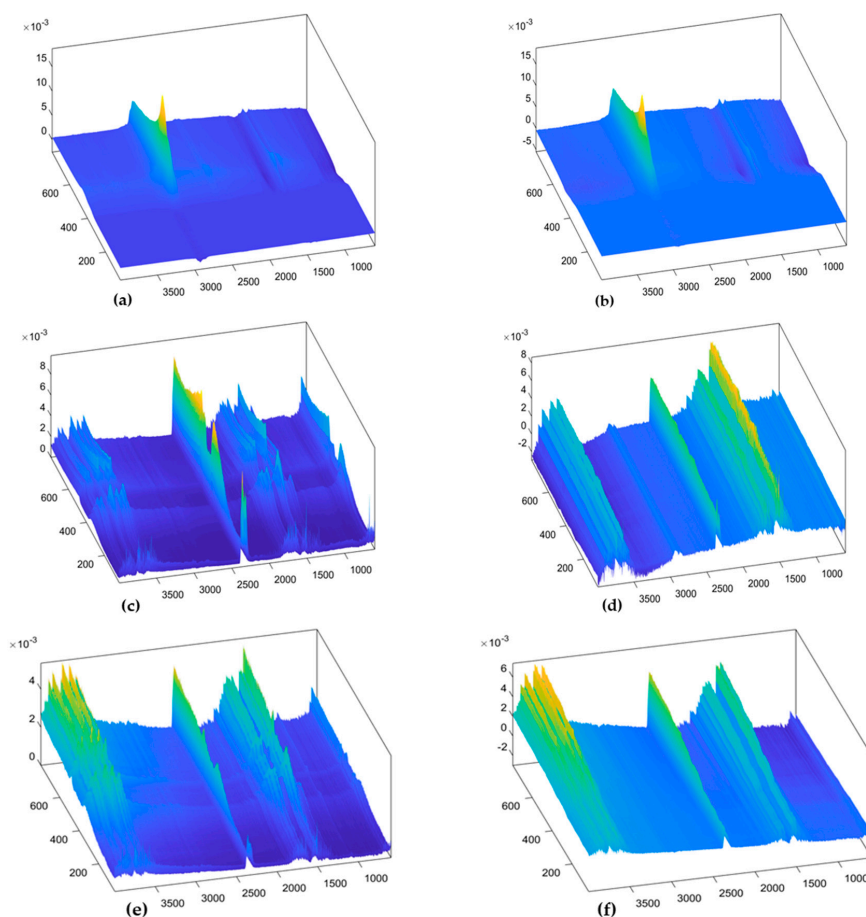


Figure 5. Loading surfaces of the three components of the PARAFAC models. (a) Component 1 of TGIS, (b) component 1 of TGO, (c) component 2 of TGIS, (d) component 2 of TGO, (e) component 3 of TGIS, and (f) component 3 of TGO. X-axis indicates wavenumber in cm^{-1} , Y-axis indicates temperature in $^{\circ}\text{C}$, Z-axis indicates component value.

Temperature ($^{\circ}\text{C}$) loadings: Mode 3 loadings show temperature in $^{\circ}\text{C}$ at which the components are generated during heating of the samples. Temperature loadings of component 1 start rising at a temperature around 300°C and reaches maximum at a temperature around 450°C in both TGIS and TGO (Figure 6c,d). The loadings of component 2 of TGIS, peaks at a temperature around 350 and 490°C (Figure 7c). Temperature loadings of component 2 of TGO increases with temperature (Figure 7d). Component 3, which have similar wavenumber cm^{-1} loadings with component 2, shows continuously increasing temperature loadings in both TGIS and TGO (Figure 8c,d). Temperature loadings peaks observed in component 1 in both TGIS and TGO correspond to the maximum weight loss in the STA instrument (Figure 2). Component 2 in TGIS also showed maximum peaks in the range where maximum weight loss was observed.

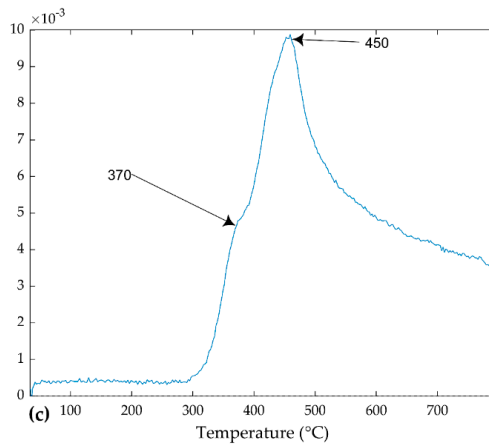
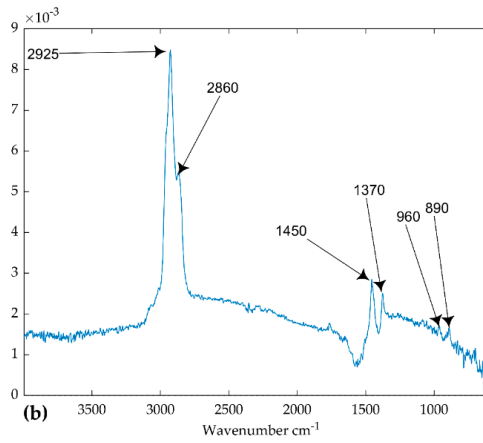
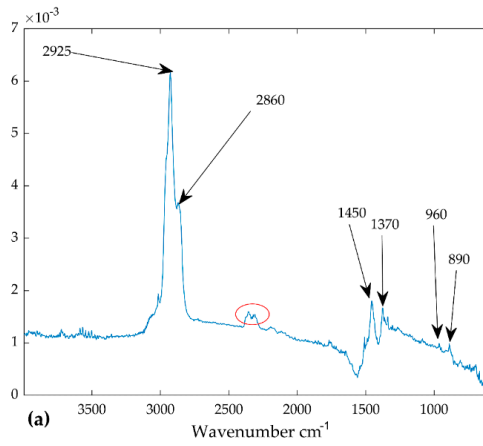


Figure 6. Cont.

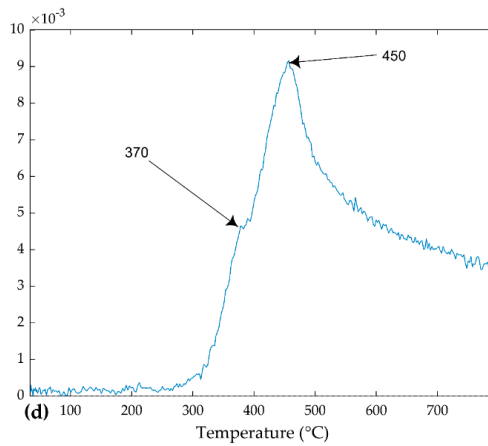


Figure 6. Loadings of the PARAFAC model. (a) Mode 2 loadings of component 1 (TGIS), (b) mode 2 loadings of component 1 (TGO), (c) mode 3 loadings of component 1 (TGIS), and (d) mode 3 loadings of component 1 (TGO). Y-values are scaled values of the components. The red circle in (a) shows a peak that is not seen in (b).

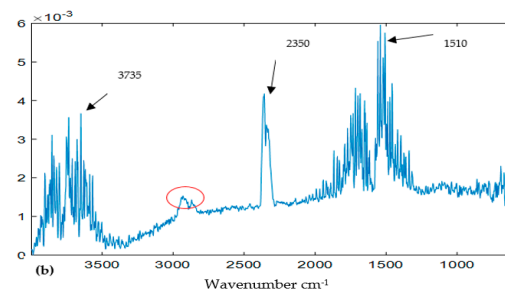
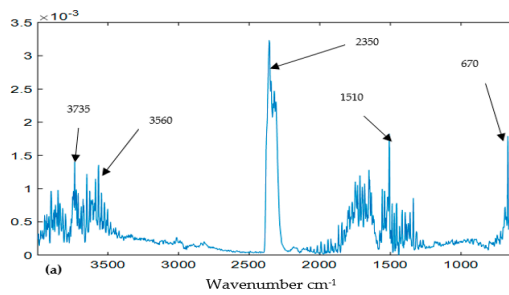


Figure 7. Cont.

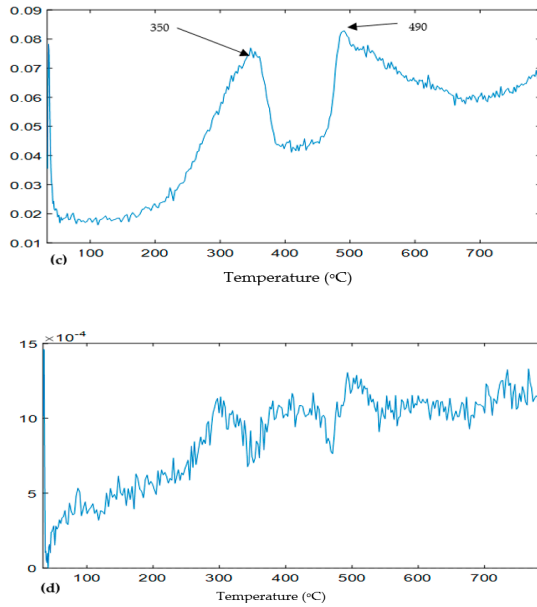


Figure 7. Loadings of the PARAFAC model. (a) Mode 2 loadings of component 2 (TGIS), (b) mode 2 loadings of component 2 (TGO), (c) mode 3 loadings of component 2 (TGIS), and (d) mode 3 loadings of component 2 (TGO). X-values are wavenumber cm^{-1} in (a,b) and temperature $^{\circ}\text{C}$ in (c,d). Y-values are scaled values of the components. The red circle in (b) shows a peak not seen in (a).

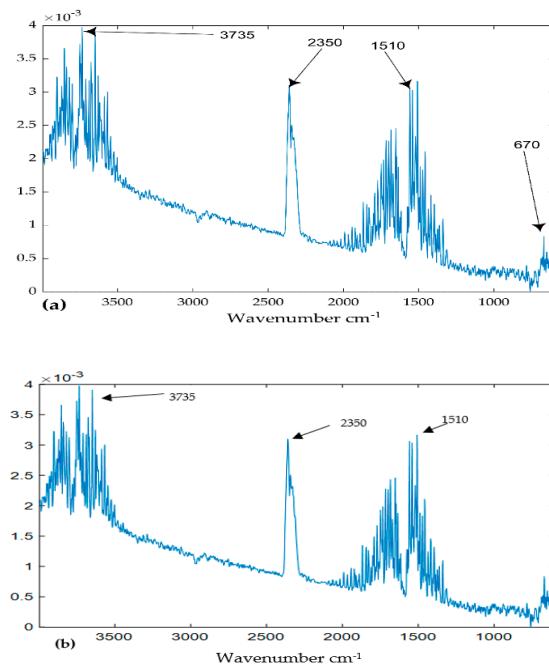


Figure 8. Cont.

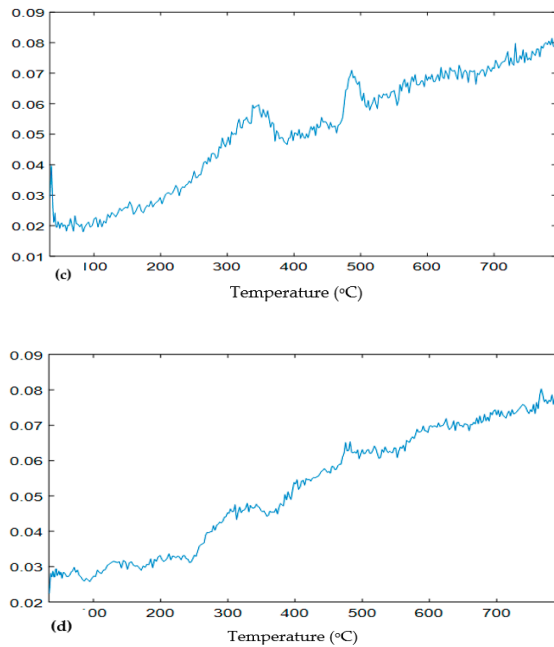


Figure 8. Loadings of the PARAFAC model. (a) Mode 2 loadings of component 3 (TGIS), (b) mode 2 loadings of component 3 (TGO), (c) mode 3 loadings of component 3 (TGIS), and (d) mode 3 loadings of component 3 (TGO). X-values are wavenumber cm^{-1} in (a,b) and temperature $^{\circ}\text{C}$ in (c,d). Y-values are scaled values of the components.

Sample scores: Figure 9 shows scores of the components which indicate the relative quantity of each component in each sample. Scores of component 1 (Figure 9a,b) show the systematic relation between score values and increased RM in both TGIS and TGO. Score values increased with increased RM quantity. Scores of the second component are shown in Figure 9c,d. Relative quantity of component 2 decreased with increased RM quantity in both TGIS and TGO. Scores of the third component are shown in Figure 9e,f. No systematic relation is observed between increase in amount of RM and variation in score values in both TGIS and TGO.

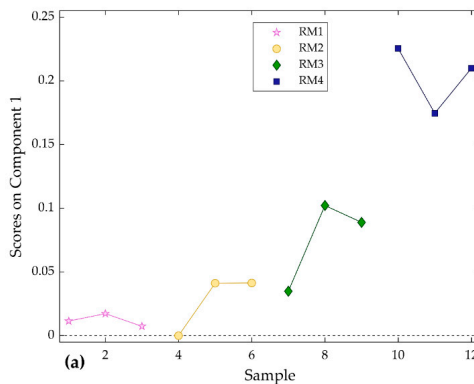


Figure 9. Cont.

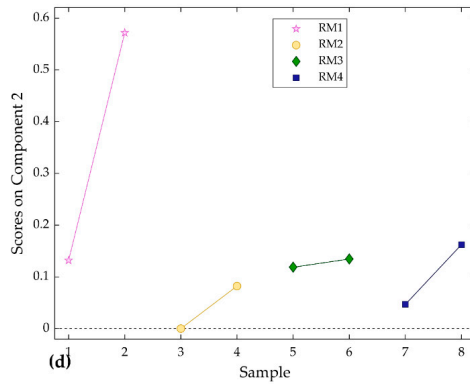
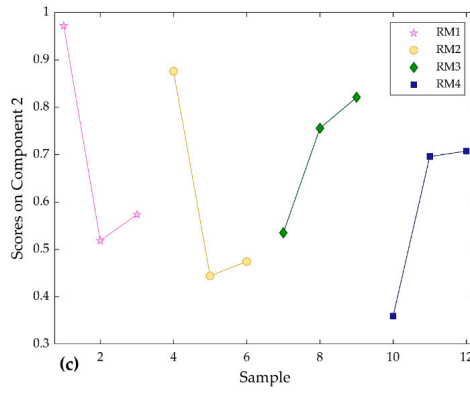
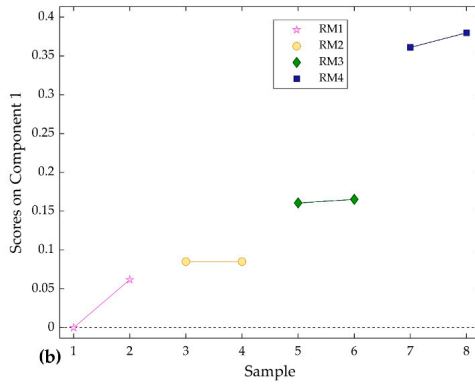


Figure 9. Cont.

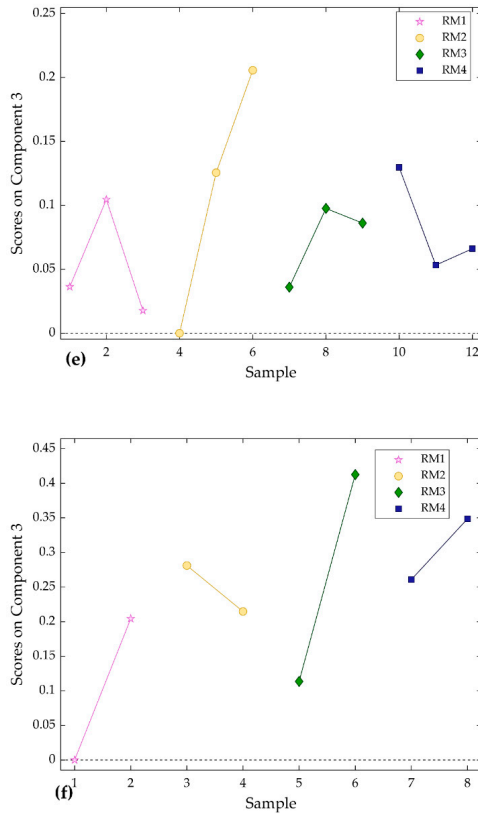


Figure 9. Scores of the two PARAFAC models with three components. (a) Scores of component 1 (TGIS), (b) scores of component 1 (TGO), (c) scores of component 2 (TGIS), (d) scores of component 2 (TGO), (e) scores of component 3 (TGIS), and (f) scores of component 3 (TGO).

Quantity estimation: following assessment of the score values, the component which showed increased score with increased RM were analyzed by PLS linear regression. Unknown quantity of component 1 was predicted for each sample (Figure 10) using score values of the component from PARAFAC models and measured values of RM (Table 1). The regression analysis showed $R^2 = 0.92$ and 0.98 , and RMSECV (Equation (2)) = 0.36 and 0.22 mg for TGIS and TGO respectively (Figure 10a,b).

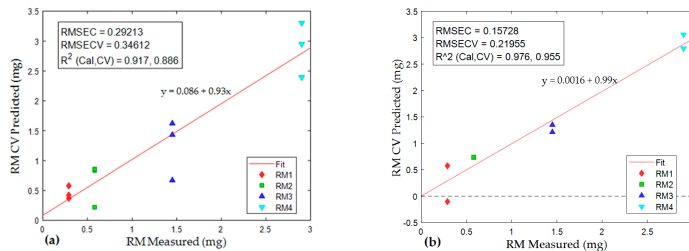


Figure 10. Partial least squares (PLS) linear regression of score values of samples in TGIS and TGO against measured values of RM. (a) Regression of TGIS samples, (b) regression of TGO samples. X-axis represents measured RM, Y-axis represents predicted RM. In the regression equation, y = predicted rubber materials (RM), x = measured rubber materials (RM).

4. Discussion

4.1. Decomposition of Overlying Components

According to different thermogravimetric analysis [5,14,17], rubber and tires degrade at pyrolysis temperature range of 340–550 °C. The wide degradation temperature range (20–650 °C) observed in this experiment, indicates the presence of more chemical substances than only rubber materials in tire granules (RM) in the evolved gases. The presence of multiple peaks in the landscape surfaces of the FTIR data of the evolved gases also points to the existence of overlying components.

The PARAFAC models resolved the components in this experiment. The models demonstrated good performance in capturing 89.5% and 90% of explained variations in tire granules in formulated sediment (TGIS) samples and tire granules only (TGO) samples respectively. A very high core consistency and small difference between components' fit and unique fit means that PARAFAC model of TGO is highly stable. Models with similar performance [22,33] are considered to be unique and appropriate. The PARAFAC model of TGIS demonstrated similar performance with the exception of model unique fit diagnostics, which showed significant data points sharing between component 2 and component 3. Little or no difference between model fit and unique fit of component 1 in both models indicates the component being resolved uniquely. Decomposing the FTIR data with good diagnostic values conforms to the basic assumptions of the PARAFAC model. However, the models violate the non-covariability assumption because of the appearance of two substances with identical wavenumber cm^{-1} loadings in components 2 and 3 in both TGIS and TGO. These two substances are identified together likely due to generation of two substances that vary at similar intensities during the heating process (this point is discussed in the next section). The covariability phenomenon may have also happened to the rubber materials with similar spectral properties like natural rubber and synthetic rubber polymers present in tires [2,5,6] and yet identified as one component in the model. Despite this limitation, the PARAFAC models demonstrated good performance in accounting for differences between substances having similar chemical properties by keeping components 2 and 3 apart because of their difference in degradation temperatures. As a result, the models successfully resolved the overlying components into groups of three substances, which are discussed in the next section.

4.2. Identification of Components

The great advantage of coupling STA to FTIR is that it provides both physical and chemical properties for concurrent interpretation [11]. It permits compound analysis for fingerprint identification. Application of PARAFAC enhances the identification and quantification of substances by decomposing overlying components [22]. In this experiment, the PARAFAC models generated loadings. The loadings were matched against established fingerprint markers from Tables 1 and 2 for assessment of chemical and physical properties of the three different components, which are discussed below.

Component 1: mode 2 loadings of the PARAFAC models in this experiment represent spectra of components, which reveal the fingerprint markers of substances. The mode 2 loadings of component 1 of both TGIS and TGO matched the identification marker wavenumbers cm^{-1} of rubber materials in tire (Table 2). Wavenumber cm^{-1} 2925, 2850, 1450, and 1377 are markers for ethylene propylene diene monomer (EPDM) while 960 and 890 are fingerprint markers for styrene butadiene rubber and butadiene in natural rubber respectively. Studies on FTIR spectra and rubber properties by [35,36] found similar wavenumber cm^{-1} peaks to identify natural and synthetic rubber.

Mode 3 loadings of the PARAFAC models provide information on the degradation temperature of components. The temperature loadings of component 1 shows a peak around 370 °C and shows a maximum peak at 450 °C in both TGIS and TGO. These temperature peaks are attributable to rubber material degradation (Table 3). Different studies have established a similar temperature range for rubber degradation. For example, the application note of Cambridge Polymer Group [17] states degradation temperature range of 340–550 °C with maximum degradation rate at 370 °C for natural rubber and 463 °C for styrene butadiene rubber. A study by [14] found tire degradation temperature in

the range of 300–500 °C with maximum at 350 °C for natural rubber and 420 °C for styrene butadiene rubber. A similar temperature range (376.9–476.9 °C) is established by [5].

Component 2: assessment of component 2 showed no match with wavenumber cm^{-1} of tire materials in Table 2. The component in both models showed identification spectral peaks around wavenumber cm^{-1} 3735, 3560, and 1510 which are attributable to water in gaseous phase. It showed additional high peaks on the same spectra at 2350 and 670. These frequencies according to [37] are fingerprint markers to water and carbon dioxide substances.

Temperature loadings of component 2, peaks around 350 and 490 °C in TGIS. These peaks are closer to the of the three weight loss peaks observed in Figure 2. Similar temperature ranges are found to be typical for pyrolysis degradation of cellulose and lignin by [38,39] indicating component 2 stemmed mainly from plant material in TGIS. The corresponding component in TGO with no specific peak indicates the water vapor was released from the degradation of substances in tire granules.

Component 3: the wavenumber cm^{-1} of component 3 is similar to the wavenumber cm^{-1} of component 2 indicating water in gaseous phase in both TGIS and TGO albeit with low intensity at 2350 cm^{-1} . The temperature loadings of component 3 increase continuously with temperature in both TGIS and TGO. This component is separated from component 2—which has wavenumber cm^{-1} —due to its temperature loadings pattern. It is plausible therefore to suggest that component 3 is an artifact generated in the STA instrument during heating process rather than coming from the samples. The presence of data noise displayed by jagged loadings (components 2 and 3) and the possibility of condensation at sub-ambient temperature in purging process [40] supports the suggestion that the component may be external to the samples.

Therefore, the PARAFAC models separated rubber materials (RM) from other substances (water and carbon dioxide) in the FTIR data and facilitated the detection of RM in TGIS and TGO by both chemical and thermal properties. The fingerprint markers indicated that natural rubber (butadiene) and synthetic rubber (styrene butadiene rubber and ethylene propylene diene monomer) constitutes the identified RM. Ethylene propylene diene monomer (EPDM), a component of a tire sidewall, is an important marker in the identification. However, natural rubber (NR) and styrene butadiene rubber (SBR) could be the defining rubber materials for tread wear particles in the environment where the particles originate mainly from the tire thread.

4.3. Estimation of Quantity of Components

Quantifying tread wear particles through chemical analysis, particularly the use of FTIR, is not well established. Some [41] suggested FTIR as an alternative to be tested; while other studies [11] reported the inapplicability of FTIR in tire wear particles identification because of overlying components. However—in the PARAFAC model—if a component is identified as a specific chemical analyte, its quantity can be determined by adding a known quantity of the same chemical analyte—following Beer-Lambert's law [22]. The rubber material component in this model represents all rubber materials in tire granules (RM). Calibrating the scores of the component identified as RM in TGIS and TGO against measured RM resulted in strong correlation between measured and predicted values in both TGIS and TGO. The goodness-of-fit test showed RMSECV of 0.36 and 0.22 mg in TGIS and TGO respectively. The regression analysis showed that predicted RM quantity were comparable to measured values in both TGIS and TGO indicating the possibility of estimating unknown quantity of RM by adding a known quantity of TGO.

Given a RM content of tire granules of 58%, estimation of quantity of tire granules is straightforward. As a result, the method effectively estimated quantity of tire particles from formulated sediments. The method can be applied to environmental samples to detect and quantify tread wear particles from soil and sediment. This offers environmental regulators and road authorities a new method that avoids extensive extraction and pretreatment steps common in microplastics analysis. With further development and attachment of PARAFAC to the FTIR analysis, the method can be automated for faster analysis of tread wear particles in soil and sediment samples.

5. Conclusions

This study introduced and demonstrated a new method to detect and eventually estimate quantity of tire particles in formulated sediments. The method consists of two steps, first utilizing a combination of instruments (STA and FTIR) to generate the data matrices, and then utilizes PARAFAC for the data analysis. In the current study, the STA and FTIR provided suitable data for the PARAFAC, which successfully decomposed the overlying components into different components, including the rubber materials and other compounds as well as artifacts. Otherwise, this would have been a challenge under conventional analytical methods. The prediction accuracy of the method may be improved with a laboratory designed to analyze rubber materials. A higher resolution STA instrument, which generates gases based on the degradation rate of substances and reduces artifacts, may also improve the prediction accuracy.

Author Contributions: Conceptualization, D.M.; Analysis, D.M., K.K.; Supervision, A.H. and V.N.; Writing—original draft, D.M.; Writing—review and editing, D.M., A.H., V.N., K.K.

Funding: The municipality of Ås and The Research Council of Norway financed this research.

Acknowledgments: The authors wish to thank Belachew Gizachew Zeleke for comments on the draft manuscript.

Conflicts of Interest: The authors declare no conflict of interest.

References

1. Panko, J.M.; Chu, J.; Kreider, M.L.; Unice, K.M.; Unice, K. Measurement of airborne concentrations of tire and road wear particles in urban and rural areas of France, Japan, and the United States. *Atmos. Environ.* **2013**, *72*, 192–199. [[CrossRef](#)]
2. Jan Kole, P.; Löhr, A.J.; Van Belleghem, F.G.A.J.; Ragas, A.M.J. Wear and tear of tyres: A stealthy source of microplastics in the environment. *Int. J. Environ. Res. Public Health* **2017**, *14*, 1265. [[CrossRef](#)] [[PubMed](#)]
3. Blok, J. Environmental exposure of road borders to zinc. *Sci. Total Environ.* **2005**, *348*, 173–190. [[CrossRef](#)] [[PubMed](#)]
4. Verschoor, A.J. Towards a Definition of microplastics. *RIVM Lett. Rep.* **2015**, *116*, 13–15.
5. Januszewicz, K.; Klein, M.; Klugmann-Radziemska, E.; Kardas, D. Physicochemical Problems of Mineral Processing Thermogravimetric analysis/pyrolysis of used tyres and waste rubber. *Physicochem. Probl. Miner. Process* **2017**, *53*, 802–811. [[CrossRef](#)]
6. Wagner, S.; Hüffer, T.; Klöckner, P.; Wehrhahn, M.; Hofmann, T.; Reemtsma, T. Tire wear particles in the aquatic environment—A review on generation, analysis, occurrence, fate and effects. *Water Res.* **2018**, *139*, 83–100. [[CrossRef](#)] [[PubMed](#)]
7. Bergmann, M.; Gutow, L.; Klages, M. *Marine Anthropogenic Litter*; Springer: Berlin/Heidelberg, Germany, 2015.
8. Grigoratos, T.; Martini, G. Brake wear particle emissions: A review. *Environ. Sci. Pollut. Res.* **2015**, *22*, 2491–2504. [[CrossRef](#)] [[PubMed](#)]
9. David, G.G., Jr.; Adeleye, A.S.; Sung, L.; Ho, K.T.; Robert, M.; Petersen, E.J.; Division, E.; Agency, E.P.; Division, A.E. Detection and Quantification of Graphene-Family Nanomaterials in the Environment. *EPA Public Access.* **2019**. [[CrossRef](#)]
10. Fischer, M.; Scholz-Böttcher, B.M. Microplastics analysis in environmental samples—Recent pyrolysis-gas chromatography-mass spectrometry method improvements to increase the reliability of mass-related data. *Anal. Methods* **2019**, *11*, 2489–2497. [[CrossRef](#)]
11. Litvinow, V.M.; De, P.P. *Spectroscopy of Rubber and Rubbery Materials*; iSmithers Rapra Publishing: Shawbury, UK, 2002.
12. Unice, K.M.; Kreider, M.L.; Panko, J.M. Use of a Deuterated Internal Standard with Pyrolysis-GC/MS Dimeric Marker Analysis to Quantify Tire Tread Particles in the Environment. *Int. J. Environ. Res. Public Health* **2012**, *9*, 4033–4055. [[CrossRef](#)]
13. Thorpe, A.; Harrison, R.M. Sources and properties of non-exhaust particulate matter from road traffic: A review. *Sci. Total Environ.* **2008**, *400*, 270–282. [[CrossRef](#)] [[PubMed](#)]
14. Fernandez-Berridi, M.J.; González, N.; Mugica, A.; Bernicot, C. Pyrolysis-FTIR and TGA techniques as tools in the characterization of blends of natural rubber and SBR. *Thermochim. Acta* **2006**, *444*, 65–70. [[CrossRef](#)]

15. Dümichen, E.; Eisentraut, P.; Bannick, C.G.; Barthel, A.-K.; Braun, U.; Senz, R. Fast identification of microplastics in complex environmental samples by a thermal degradation method. *Chemosphere* **2017**, *174*, 572–584. [CrossRef] [PubMed]
16. Akinade, K.A.; Campbell, R.M.; Compton, D.A.C. The use of a simultaneous TGA/DSC/FT-IR system as a problem-solving tool. *J. Mater. Sci.* **1994**, *29*, 3802–3812. [CrossRef]
17. Cambridge Polymer Group. *Car Tire Composition Analysis by TGA-FTIR*; Cambridge Polymer Group: Cambridge, UK, 2014.
18. Gunasekaran, S.; Natarajan, R.; Kala, A. FTIR spectra and mechanical strength analysis of some selected rubber derivatives. *Spectrochim. Acta Part A Mol. Biomol. Spectrosc.* **2007**, *68*, 323–330. [CrossRef] [PubMed]
19. Gary, L.; Wen Jing, Z.W. Identification of Unknown Mixtures of Materials from Biopharmaceutical Manufacturing Processes by Microscopic-FTIR and Library Searching. *Am. Pharm. Rev.* **2011**, *14*, 60.
20. Baum, A.; Hansen, P.; Nørgaard, L.; Sørensen, J.; Mikkelsen, J. Rapid quantification of casein in skim milk using Fourier transform infrared spectroscopy, enzymatic perturbation, and multiway partial least squares regression: Monitoring chymosin at work. *J. Dairy Sci.* **2016**, *99*, 6071–6079. [CrossRef] [PubMed]
21. Melville, B.; Lucieer, A.; Aryal, J. Assessing the Impact of Spectral Resolution on Classification of Lowland Native Grassland Communities Based on Field Spectroscopy in Tasmania, Australia. *Remote Sens.* **2018**, *10*, 308. [CrossRef]
22. Murphy, K.; Stedmon, C.A.; Graeber, D.; Bro, R. Fluorescence spectroscopy and multi-way techniques. PARAFAC. *Anal. Methods* **2013**, *5*, 6557. [CrossRef]
23. Rasmus, B. PARAFAC. Tutorial and applications. *Chemom. Intell. Lab. Syst.* **1997**, *38*, 149–171. [CrossRef]
24. Ragn-Sells Däckåtervinning AB. 2018. Available online: https://www.ragnsells.no/globalassets/norge/dokumenter/dekkgjenvinning/rs_pb_granulat_fin_v5-2018-01-16.pdf (accessed on 8 June 2019).
25. FIFA. *Handbook of Test Methods*; FIFA: Zurich, Switzerland, 2015.
26. Sommer, F.; Dietze, V.; Baum, A.; Sauer, J.; Gilge, S.; Maschowski, C.; Gieré, R. Tire Abrasion as a Major Source of Microplastics in the Environment. *Aerosol Air Qual. Res.* **2018**, *18*, 2014–2028. [CrossRef]
27. Jusli, E.; Nor, H.M.; Jaya, R.P.; Zaiton, H.; Haron, Z. Chemical Properties of Waste Tyre Rubber Granules. *Adv. Mater. Res.* **2014**, *911*, 77–81. [CrossRef]
28. Formela, K.; Cysewska, M.; Haponiuk, J. The influence of screw configuration and screw speed of co-rotating twin screw extruder on the properties of products obtained by thermomechanical reclaiming of ground tire rubber. *Polim. Polym.* **2014**, *59*, 170–177. [CrossRef]
29. OECD. *OECD Sediment-Water Chironomid Life-Cycle Toxicity Test Using Spiked Water or Spiked Sediment*; OECD: Paris, France, 2010.
30. Netzsch. *Thermal Analysis Methods (Part 1): TG, DSC, STA, EGA Practical Applications of Thermal Analysis Methods in Material Science*; Netzsch: Selb, Germany, 2012.
31. Wise, B.M.; Gallagher, N.B.; Windig, W.; Bro, R.; Shaver, J.M.; Koch, R.S. Chemometrics Tutorial for PLS – Toolbox and Solo. *Eig. Res. Inc.* **2006**, *3905*, 102–159.
32. Baum, A.; Hansen, P.W.; Meyer, A.S.; Mikkelsen, J.D. Simultaneous measurement of two enzyme activities using infrared spectroscopy: A comparative evaluation of PARAFAC, TUCKER and N-PLS modeling. *Anal. Chim. Acta* **2013**, *790*, 14–23. [CrossRef]
33. Bro, R.; Kiers, H.A.L. A new efficient method for determining the number of components in PARAFAC models. *J. Chemom.* **2003**, *17*, 274–286. [CrossRef]
34. Engineering, M.; Republi, S. The Effect of Temperature Pyrolysis Process. *Siendo* **2001**. [CrossRef]
35. Delva, L.; Verberckmoes, A.; Cardon, L.; Ragaert, K. The use of rubber as a compatibilizer for injection moulding of recycled post-consumer mixed polyolefines. In Proceedings of the 2nd International Conference WASTES: Solutions, Treatments and Opportunities, Braga, Portugal, 11–13 September 2013; pp. 689–694.
36. Mente, P.; Motaung, T.E. Natural Rubber and Reclaimed Rubber Composites—A Systematic Review. *Polym. Sci.* **2016**, *2*, 1–19. [CrossRef]
37. NIST Chemistry WebBook, SRD 69. National Institute of Standards and Technology, U.S. Department of Commerce, 2011. Available online: <https://webbook.nist.gov/cgi/inchi?ID=C7732185&Type=IR-SPEC&Index=0> (accessed on 24 July 2019).
38. Kawamoto, H. Lignin pyrolysis reactions. *J. Wood Sci.* **2017**, *63*, 117–132. [CrossRef]
39. Shen, D.; Xiao, R.; Gu, S.; Zhang, H. The Overview of Thermal Decomposition of Cellulose in Lignocellulosic Biomass. In *Cellulose Biomass Conversion*; IntechOpen: Rijeka, Croatia, 2013.

40. Menczel, J.D.; Alcon, L.; Prime, R.B. *Thermal Analysis of Polymers: Fundamentals and Applications*; John Wiley & Sons., Inc.: Hoboken, NJ, USA, 2009.
41. Vogelsang, C.; Lusher, A.L.; Dadkhah, M.E.; Sundvor, I.; Umar, M.; Ranneklev, S.B.; Eidsvoll, D.; Meland, S. *Microplastics in Road Dust—Characteristics, Pathways and Measures*; Norwegian Environment Agency: Trondheim, Norway, 2018.



© 2019 by the authors. Licensee MDPI, Basel, Switzerland. This article is an open access article distributed under the terms and conditions of the Creative Commons Attribution (CC BY) license (<http://creativecommons.org/licenses/by/4.0/>).

Mengistu, D., Heistad, A., & Coutris, C. (2021) 'Tire wear particles concentrations in gully pot sediments', *Science of the Total Environment*, 769, 144785.
<https://doi.org/10.1016/j.scitotenv.2020.144785>



Tire wear particles concentrations in gully pot sediments

Demmelash Mengistu^{a,*}, Arve Heistad^a, Claire Coutris^b

^a Norwegian University of Life Sciences (NMBU), Faculty of Science and Technology, Ås, Norway

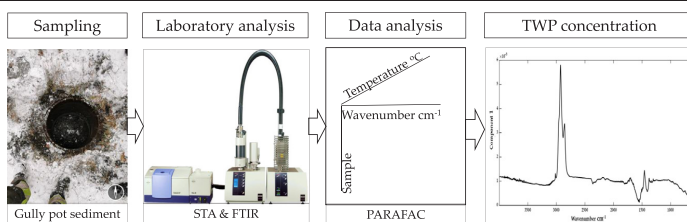
^b Norwegian Institute of Bioeconomy Research (NIBIO), Division of Environment and Natural Resources, Ås, Norway



HIGHLIGHTS

- Combining STA, FTIR and PARAFAC enables TWP quantification in environmental samples.
- No sample pretreatment is required and all particles sizes are included.
- TWP made up to 15% of gully pot sediments.

GRAPHICAL ABSTRACT



ARTICLE INFO

Article history:

Received 17 October 2020

Received in revised form 19 December 2020

Accepted 21 December 2020

Available online 14 January 2021

Editor: Shuzhen Zhang

Keywords:

Road runoff

Tire wear particles

Thermogravimetry

FTIR

PARAFAC

ABSTRACT

While tire wear and tear is known to be a major source of microplastics in the environment, its monitoring is still hampered by the lack of analytical methods able to provide concentrations in environmental matrices. Tire wear particles (TWP) present in road runoff enter the drainage system through gully pots, built to prevent sediment deposition in the drainage system, and eventually protect downstream receiving waters. The aim of this study was to detect and quantify TWP in gully pot sediments, by using a novel method combining Simultaneous Thermal Analysis (STA), Fourier Transform Infrared (FTIR) spectroscopy and Parallel Factor Analysis (PARAFAC). The method was applied to samples from five sites in Southern Norway, characterized by different traffic densities and patterns. The method involved no sample pretreatment, the whole sediment sample was submitted to thermal decomposition in STA, and gases generated during pyrolysis were continuously transferred to FTIR. The FTIR data were arranged in a trilinear multi-way dataset (samples \times IR spectra wavenumber \times pyrolysis temperature) and then analyzed by PARAFAC. The results showed that TWP concentrations in gully pots varied greatly across sites, ranging from below 1 mg TWP/g sediment in streets with the lowest traffic densities, to 150 mg TWP/g sediment at the most trafficked study site. The results also indicated that other traffic conditions, such as driving patterns influence TWP concentrations. Finally, by enabling quantification of TWP in gully pot sediments, the approach presented here supports environmental monitoring of TWP and safe disposal of gully pot sediments, which is critical for environmental pollution management.

© 2021 The Author(s). Published by Elsevier B.V. This is an open access article under the CC BY license (<http://creativecommons.org/licenses/by/4.0/>).

1. Introduction

Road runoffs are found to contain substantial amounts of contaminants (Birch and Scollen 2003; Lindholm 2015) including tire wear particles (TWP) originating from vehicle tires (Andersson-Sköld et al. 2020). TWP is one of the major sources of microplastics in the

environment, and average emission per capita is estimated to be 0.81 kg/year worldwide and 0.9 kg/year in Norway (Kole et al. 2017; Vogelsang et al. 2018). In addition to potential adverse effects on human health, TWP could also affect aquatic and terrestrial ecosystems, where their main entrance way is through runoff (Kole et al. 2017; Wagner et al. 2018). Inflowing of TWP into water bodies begins with road runoff entering the drainage system through gully pots (Bolognesi et al. 2008). Gully pots are built to retain solids in the runoff and prevent or reduce sediment deposition in the drainage system and

* Corresponding author at: Kajaveien 5, NO-1432 Ås, Norway.
E-mail address: demmelash.mengistu@nmbu.no (D. Mengistu).

eventually protect the downstream receiving waters (Bolognesi et al. 2008; Karlsson and Viklander 2008; Lindholm 2015). Accumulation of TWP in gully pots is influenced by road deposition, particle size and density, stormwater inflow intensity (e.g. mobilization) and design of the gully pots (Bolognesi et al. 2008). Earlier studies (Kole et al. 2017; Panko et al. 2013) estimated that the major part of generated TWP would be coarse in size ($>10\ \mu\text{m}$), and deposited on or close to the road. This presents a high potential for TWP entering gully pots. However, the spread of TWP in the environment and the properties governing spreading processes are not adequately studied (Wagner et al. 2018). For example, the density of TWP is reported to be in the range of 1.13 to $1.16\ \text{g}/\text{cm}^3$ (Rhodes et al. 2012), while tires' main constituent part, carbon black (ca. 40%) (Roy et al. 2004), has a density of $1.8\ \text{g}/\text{cm}^3$ and styrene butadiene rubber (SBR) has a density of $0.94\ \text{g}/\text{cm}^3$ (CAS 2020). The lower densities of TWP compared to other road derived particles (e.g. asphalt $2.36\ \text{g}/\text{cm}^3$, quartz $2.65\ \text{g}/\text{cm}^3$ or limestone $2.0\ \text{g}/\text{cm}^3$ (CAS 2020; Rumble, 2017)) suggest that TWP have a high potential to be transported over longer distances. However, studies reported that TWP aggregate with higher density particles in the road environment due to heat and friction created during driving (Kreider et al. 2010; Järnskog et al. 2020; Kole et al. 2017; Sommer et al. 2018; Wagner et al. 2018). This heteroaggregation would increase density and subject TWP to sedimentation.

The solids retained in gully pots build up overtime, necessitating a regular emptying to avoid clogging of the drainage system (Bolognesi et al. 2008). For safe disposal of gully pot sediments, it is critical to be able to quantify the environmental contaminants they may contain, including TWP. However, TWP monitoring in gully pots remains a challenge, mainly due to the lack of widely applicable, easy and inexpensive analytical methods (Järnskog et al. 2020).

While commonly used in microplastics studies, vibrational spectroscopic methods, such as Fourier transform infrared (FTIR) spectroscopy, have been found inapt for the analysis of TWP (Eisenbraut et al. 2018; Wagner et al. 2018). Although attenuated total reflectance (ATR)-FTIR could be used for larger ($>0.5\ \text{mm}$) TWP particles (Fernández-Berridi et al. 2006; Manohar et al. 2017), the requirements of the methods (e.g. placing each isolated particle onto a glass slide, to bring it in close contact with the germanium crystal of the ATR objective), make its application challenging for TWP under $0.5\ \text{mm}$. In addition, although μ -FTIR methods use polymer specific absorption patterns of irradiated infrared and present unambiguous detection possibility for a range of microplastics (John 2000), their applicability to TWP analysis fails for three main reasons. First, extensive sample preparation is needed, usually including digestion of matrix compounds and density separation. Second, the methods encounter optical challenges from the filler components in TWP, especially carbon black, which causes near-complete absorption of IR light (Eisenbraut et al. 2018; Wagner et al. 2018). Third, FTIR works best with pure substances. The existence of multiple components in environmental samples makes the method unable to detect TWP in gully pot sediments (Litvinov and De 2002). Chromatography, including pyrolysis gas chromatography-mass spectrometry (Py-GC/MS) and thermal extraction desorption (TED)-GC/MS, is presented as an alternative approach to resolve many of the problems encountered by FTIR alone (Eisenbraut et al. 2018; Unice et al. 2012). Chromatography is proved to be effective in quantifying TWP polymers at a low limit of detection, and an international standard method, the ISO 21396 (ISO 2017) has been developed based on Py-GC/MS. However, the method requires deuterated internal standard procedure and establishing international market share of styrene butadiene rubber (SBR) and natural rubber (NR), which adds complexity and uncertainty. In addition, the lack of dependable marker that is specific and consistently available in all types of tires, while at the same time absent from non-contaminated (background) environmental matrices, is another problem associated with these methods. This is particularly true when the environmental matrix is suspected to develop decomposition products interfering with the chosen marker for elastomers. For

example, Unice et al. (2012) reported that the presence of monomers and dipentene in environmental samples could positively bias measured TWP concentrations. Another study, using TED-GC/MS, reported the impossibility of analyzing NR in environmental samples due to interference of dimers and higher oligomers originating from the decomposition of plant materials (Eisenbraut et al. 2018).

Combining the advantages of FTIR and thermal methods has been recently reported as a good method to analyze TWP in environmental samples (Mengistu et al. 2019). The method uses first pyrolysis in simultaneous thermal analysis (STA) before FTIR scanning of pyrolysis products. The method adds a temperature dimension to create a multi-way dataset suitable to Parallel Factor Analysis (PARAFAC). PARAFAC is a powerful tool improving the application of spectroscopic methods to environmental samples and has been extensively used in food and environmental sciences (Andersen and Bro 2003; Murphy et al. 2013). It decomposes the data into underlying chemical components with estimates of spectra and concentration (Andersen and Bro 2003). Quantification is facilitated by using mass loss during pyrolysis in conjunction with scores of components from a PARAFAC model. However, no study using the method to analyze TWP in environmental samples has yet been reported.

This study addresses unanswered questions regarding TWP quantification in the environment, and its objectives are to (1) evaluate whether gully pots retain TWP from road runoff, by using a novel method combining STA, FTIR and PARAFAC, and (2) determine TWP concentrations in gully pot sediments.

2. Materials and methods

2.1. Study area

TWP concentrations in gully pot sediments were studied at 5 sites (4 municipal streets and a parking lot) in a municipality of Southern Norway (Ås, N59.660, E10.784, Fig. 1). Each site was represented by two gully pots. The characteristics of the selected sites are described in Table 1. All the selected streets had a speed limit of $30\ \text{km}/\text{h}$, which is common in built-up areas and town centers in Norway. Traffic density in these streets was recorded using a radar from Amparo solutions, during June and July 2020. Information on gully pot maintenance was not available at the time of the study.

2.2. Sampling

$500\ \text{mL}$ of wet sediment was collected from each gully pot (10 in total, from 5 study sites), using a spade. The samples were consistently taken from the top of the sediment accumulated under the standing water, in an attempt to account for the most recent contaminations. All samples were dried at $105\ ^\circ\text{C}$, crushed and homogenized with mortar and pestle, and sieved at $5\ \text{mm}$ to exclude materials beyond the range of defined microplastics. From each sample, three replicates of $80\ \text{mg}$ dry sediment were placed in aluminum crucibles for STA-FTIR analysis. A standard natural soil, LUFA 2.2 (LUFA Speyer, Germany) was included in the experimental set-up as a rubber-free control, also in triplicates of $80\ \text{mg}$ dry mass. The total number of samples analyzed by STA-FTIR was 33.

2.3. STA-FTIR analysis

The acquisition of thermal and FTIR spectra involved hyphenated instruments, a simultaneous thermal analyzer STA 449 F1 Jupiter, with carrier type S (Netzsch, Germany), coupled to a Fourier transform infrared spectrometer Bruker Tensor 27 with external gas cell (Bruker, USA), as described below.



Fig. 1. (a) Overview of sampling sites and gully pots, (b) gully pots at site Sjoskogenveien (1,2), (c) gully pots at sites Raadhusplassen (3, 4), Maaltrøstveien (5, 6), and Brekkeveien (7, 8), (d) gully pots at site Nordbyveien (9, 10).

2.3.1. STA

Samples were heated from 100 to 800 °C at a rate of 10 °C/min under protective nitrogen atmosphere (flow rate 20 mL/min) for 70 min.

Evolved gases were purged continuously to the FTIR, using nitrogen as a carrier gas (at a flow rate of 50 mL/min). The thermogravimetric unit in the STA registered changes in sample mass (balance resolution

Table 1
Characteristics of sampling sites, gully pot ID and annual average daily traffic (AADT).

Site	Gully pot ID	AADT	Description
Sjoskogenveien	1	2608	Two roundabouts by the largest shopping center in the municipality, with 79 shops and restaurants open 6 days a week (Fig. 1b)
	2		
Raadhuplassen	3	N/A	Parking lot by the city hall, surrounded by shops and cafés (Fig. 1c)
	4		
Maaltröstveien	5	417	Street in a residential area with private homes only and little traffic (Fig. 1c)
	6		
Brekkeveien	7	1500	Street in a residential area with elderly care center and private homes (Fig. 1c)
	8		
Nordbyeveien	9	890	Street in an industrial and residential area (Fig. 1d)
	10		
Control	11	N/A	LUFÄ 2.2 standard natural soil (LUFÄ Speyer, Germany), used as rubber-free control sample

25 ng) every 6.83 s during the heating process, resulting in 614 mass measurements per sample, each measurement being associated to a temperature.

2.3.2. FTIR

The average signal of 8 scans of FTIR spectra in the wavenumber range of 4000–600 cm^{-1} was collected with a resolution of 1.93 cm^{-1} during the heating process, generating 1762 signal points. Each scanning took 6.83 s, which resulted in 614 spectra per sample.

2.4. PARAFAC model

Temperature was assigned to each spectrum using the time relationship between gas release and scanning, giving the FTIR dataset Wavenumber (cm^{-1}) and Temperature ($^{\circ}\text{C}$) axes with dimensions of 1762×614 values. The data from all 33 samples were then arranged as a trilinear multi-way dataset of 33 samples \times 1762 wavenumbers \times 614 temperatures, suitable for PARAFAC decomposition (Baum et al. 2016; Mengistu et al. 2019). PARAFAC models were built using 2 to 7 components, using MATLAB (The MathWorks, Inc., R2018a, Natick, USA) and a PLS Toolbox for MATLAB version 8.6 (Eigenvector Research, Inc., Wenatchee, USA). The various steps involved in PARAFAC analysis of the STA-FTIR data are detailed in S1, while the equation of the model and explanation of scores and loadings are presented in S2. The validity of the PARAFAC model was evaluated using figures of merit (core consistency, model fit and residuals) and split-half analysis, as detailed in S3. Finally, the model with the most components and the best figures of merit was selected. The outcome of PARAFAC was used for the identification and quantification of components in the samples, and more specifically to determine if rubber materials were present in the sediments, and if so, at which concentrations. PARAFAC was also applied to a spike recovery analysis, as shown in S4.

2.5. TWP identification

Rubber materials (RM), which are the core components in tires (Thorpe and Harrison 2008), are good markers to determine the presence and estimate the quantity of TWP in sediments and soils (Wagner et al. 2018). Loadings of the PARAFAC model carry information about physical and chemical properties of the substances under evaluation. Wavenumber (cm^{-1}) and temperature ($^{\circ}\text{C}$) loadings of components were evaluated against established spectra of rubber constituents in tires, e.g. styrene butadiene rubber (SBR), natural rubber (NR) and ethylene propylene diene monomer rubber (EPDM), reported in different studies (Fernández-Berridi et al. 2006; Gunasekaran et al. 2007; Januszewicz et al. 2017; Jasmínská et al. 2013; Litvinow and De 2002; Mengistu et al. 2019).

2.6. Choice of method for TWP quantification

After scores were obtained from the PARAFAC model, two alternatives were available to estimate the quantity of RM, and subsequently TWP. The first alternative was to establish a score-concentration relationship for at least one known sample, and use this relationship to calculate concentrations in unknown samples (Mengistu et al. 2019; Murphy et al. 2013). A preliminary test based on this approach, using crumb rubber, showed poor results, especially for small sample size of <1 mg crumb rubber. This might be attributed to loss of sensitivity due to small sample mass, which is common in thermal analysis (Menczel, 2009). Non-linearity between FTIR absorbance and concentration above 1% gas concentration (Schindler et al. 2013) meant that the alternative was not applicable at higher concentration either, and was thus rejected. The second alternative was based on sample mass loss during pyrolysis in STA, and the additivity and proportionality assumptions in PARAFAC (see S2, for more details). This alternative was found to be the most appropriate method to estimate the concentration of RM in gully pot sediments, and also presented the advantage of not requiring calibration with a known concentration of RM. Once a component was identified as being RM, the score of this component was used to calculate the concentration of RM in gully pot sediments, using Eq. (1).

$$C_{\text{RM}} = (\text{ml} \times a_{\text{if}}) / (\text{m} \times S_i) \quad (1)$$

where

C_{RM} = concentration of RM in a sample (mg/g)

ml = sample mass loss during pyrolysis (mg)

m = initial sample dry mass (g)

a_{if} = score of component identified as being RM in sample i

S_i = sum of scores of all components of sample i

RM constitute only a fraction of TWP, the rest being fillers, reinforcement materials, plasticizers, vulcanization and antiaging chemicals (Fernández-Berridi et al. 2006; Kreider et al. 2010; Jusli et al. 2014). While the RM fraction in TWP is variable (40–60%), 58% was used here, based on the most relevant data for the context of the study (Ragn-sells, 2020, tire crumb producer). Differences in TWP concentrations among gully pots were tested using one-way analysis of variance (ANOVA), followed by a Tukey pairwise comparison test to identify differing gully pots. The assumptions of normality and homoscedasticity were verified by normal probability plot and Levene's test, respectively, and fulfilled. The level of significance was set to 0.05.

3. Results and discussion

3.1. PARAFAC model

After testing PARAFAC models with 2 to 7 components, a model with 2 components was found to be the best to decompose the dataset, and the use of additional components did not improve the model. The model with 2 components captured 91% of the total variance in the dataset and showed good figures of merit (S3). The model showed 100% core consistency (S3a), very little overlap between model fit and unique fit (S3b), and low residuals sum of squares (S3c), indicating that the model was very stable. Split-half analysis of the dataset after running the model showed 93% similarity between the sub-datasets (S3d, e). This level of similarity confirms the validity of the model (Bro and Kiers 2003; Murphy et al. 2013).

3.2. Presence of TWP in gully pot sediments

The presence of RM in gully pot samples was revealed after concurrent assessment of the two loadings of the PARAFAC model. As presented in Fig. 2a, component 1 showed strong peaks at 2925 and 2860 cm^{-1} , and a weak peak at 3015 cm^{-1} . Even though the fingerprint

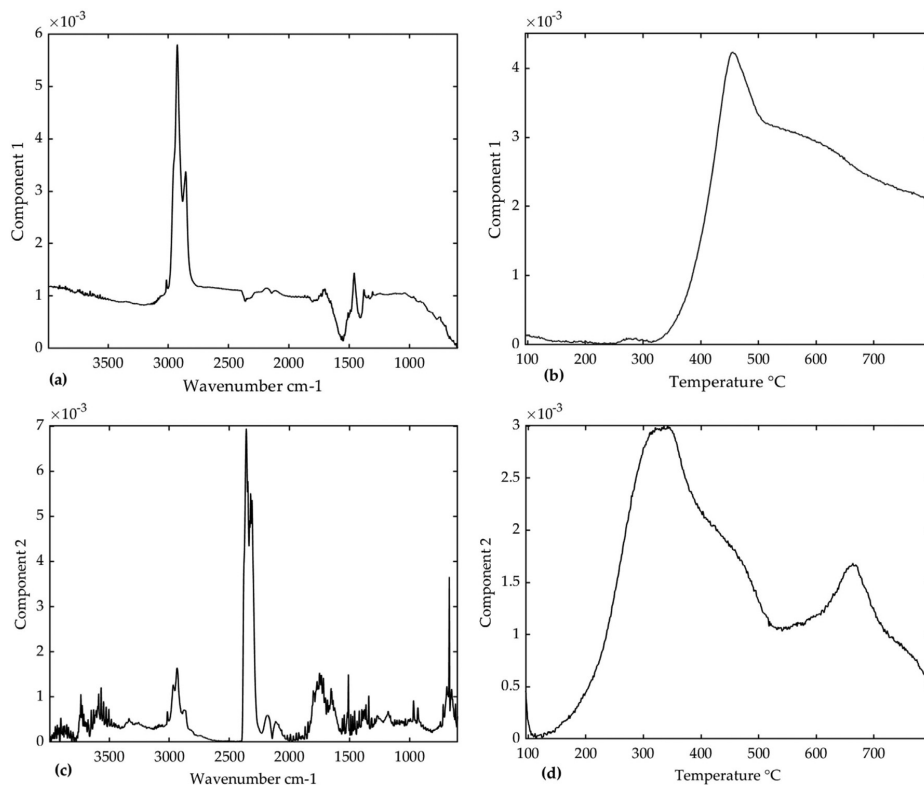


Fig. 2. Components loadings from the PARAFAC model. (a) wavenumber loading of component 1, (b) pyrolysis temperature loading of component 1, (c) wavenumber loading of component 2, (d) pyrolysis temperature loading of component 2. Component 1 corresponds to tire rubber materials and component 2 to other substances (including plant materials).

region ($<1500\text{ cm}^{-1}$) had very few clear peaks, component 1 showed weak peaks at 1450 and 1370 cm^{-1} . This spectrum was similar to those of RM identified in a study where tire crumb and tire crumb in formulated sediments were used to evaluate the applicability of PARAFAC in TWP detection and quantification (Mengistu et al. 2019). Other studies also attributed similar FTIR absorbance spectra to styrene butadiene rubber (SBR), natural rubber (NR) or ethylene propylene diene monomer rubber (EPDM) (Fernández-Berridi et al. 2006; Gunasekaran et al. 2007; Litvinow and De 2002). The thermal features shown in Fig. 2b, indicated that component 1 was a degradation product of substances pyrolyzed at temperatures starting from around $330\text{ }^{\circ}\text{C}$ and reaching a maximum at $470\text{ }^{\circ}\text{C}$. In a coupled STA-FTIR, thermal spectra may show a temperature shift up to $10\text{ }^{\circ}\text{C}$ due to transfer delay (Schindler et al. 2013), indicating that pyrolysis temperatures shown here were slightly higher than would be observed in STA alone. Compared to pyrolysis temperatures reported in literature, the thermal features of component 1 were found to be typical for pyrolysis of tires (Fernández-Berridi et al. 2006; Januszewicz et al. 2017; Jasminská et al. 2013; Jusli et al. 2014). In addition to positive matching, exclusion of components which were not rubber materials was important for the identification.

FTIR features of component 2 (Fig. 2c) were very distinct from those of component 1. Strong peaks appeared at 2360 and 670 cm^{-1} , while weaker peaks were observed at 3700 – 3500 , 3000 – 2800 , 1750 , and 1500 – 1300 cm^{-1} . The strong peaks on component 2 were attributable to CO_2 (NIST, 2011; Schindler et al. 2013; Wang and Lou 2016), while the weaker peaks at 3016 , 2950 and 2870 cm^{-1} could represent a functional group of saturated and unsaturated hydrocarbons (Fernández-Berridi et al. 2006; Gunasekaran et al. 2007; Litvinow and De 2002;

Schindler et al. 2013). The thermal features shown in Fig. 2d, indicated that component 2 was a product of pyrolysis at temperatures starting from $200\text{ }^{\circ}\text{C}$ but occurring mainly at 320 , 345 and $660\text{ }^{\circ}\text{C}$. These pyrolysis temperatures were attributable to plant organic matter and carbon black (Cambridge Polymer Group 2014; Jusli et al. 2014; Kawamoto 2017; Pantea et al. 2003; Yang et al. 2018). Therefore, both wavenumber and temperature loadings of component 2 suggested that this component was not RM.

PARAFAC is expected to decompose FTIR data from a multi-substance sample, like gully pot sediments, into multiple components. Contrarily, decomposition of the data in this study resulted in two components only, suggesting aggregation of components based on related features, the pyrolysis temperature in this case. This suggestion was strengthened by the fact that the rubber-free control samples (LUFA soil) only had one component in this model, while these samples had two components when modeled alone (CO_2 and H_2O , results not shown). The non-specificity of IR and its quality in identifying functional groups (Litvinow and De 2002) has probably contributed to the observed aggregation. This aggregation phenomenon is against the basic definition of PARAFAC modelling and prevents identification of individual polymer types (SBR, NR, EPDM) in TWP. However, given that TWP in gully pots originate from different types of tires (summer and winter tires, heavy duty vehicles and passenger cars tires) whose polymer composition is under commercial confidentiality, aggregation was here a convenient attribute, presenting all RM as one component. The aggregation may also have helped detect polymers present in smaller quantities, which may otherwise be undetectable.

The presence of similar dimers in both TWP and plant materials has recently been reported as a challenge to establish dependable markers (Eisentraut et al. 2018). Concurrent evaluation of the two loadings was therefore critical for TWP identification, as no single spectrum was robust enough to unambiguously represent the substance under investigation. For example, hydrocarbon functional groups were not only visible on wavenumber loadings of component 1 (RM), but also of component 2. This phenomenon was resolved by analyzing temperature loadings showing that the hydrocarbons in the two components were pyrolysis products of different substances. Thermal spectra (Fig. 2b and d) indicated that component 1 (RM) resulted from maximum degradation at 470 °C, while component 2 resulted from degradation of plant materials and carbon black at 330 and 660 °C, respectively.

3.3. TWP concentrations in gully pot sediments

Individual sample mass loss during pyrolysis ($7.1\% \pm 3.3\%$, mean \pm standard deviation (SD), $n = 33$) was used together with PARAFAC scores to calculate concentrations of RM, and in turn, TWP, in all sediment and control samples. The spike recovery analysis indicated a high but acceptable recovery rate of 123% (Supporting Information, S4). RM and TWP concentrations in sediments (in mg per g sediment dry weight) are presented in Table 2 and were found to differ significantly across gully pots ($F_{10,32} = 194.6$, $P < 0.001$). TWP concentration in the control soil was 0.2 ± 0.3 mg/g, which based on US EPA procedure for the determination of the method detection limit, MDL (EPA, 2016) indicates a MDL of 1.1 mg TWP per g dry sediment. Although very high compared to e.g. py-GC/MS, the detection limit is very good for a thermal-spectroscopic method with no pre-processing. The highest TWP concentration, 150 mg/g, was found in gully pot 1, in Sjoskogenveien, followed by 131 mg/g in gully pot 4 at Raadhusplassen. Gully pots 2 (Sjoskogenveien) and 3 (Raadhusplassen), with 71 and 42 mg/g, respectively, also contained significant amounts of TWP, while concentrations in gully pots 5–10 ranged from 1 to 20 mg/g, and were not found statistically different from each other and from the rubber-free control soil. The concentrations found here are in the range of those reported in roadside ditch soils, namely 0.3–117 g/kg (Vogelsang et al. 2018) and 11 g/kg in Swedish road detention systems (Wik et al. 2008). Concentrations of this magnitude are however in contrast with older studies suggesting poor TWP retention in gully pots (Cadle and Williams 1978; Fauser 1999).

The highest TWP concentration was found in the street with the highest AADT (2608, Sjoskogenveien), suggesting the influence of traffic density on TWP concentrations in gully pots. This is consistent with the results of Bondelind et al. (2020) in which higher microplastics concentrations were associated with higher traffic density. But, it was evident that AADT was not the only factor influencing TWP concentrations,

Table 2

Concentrations of rubber materials (RM) and tire wear particles (TWP) concentrations in gully pot sediments (mg/g sediment dry weight). Results are provided as mean and standard deviation (SD), $n = 3$ per gully pot and control. Means with different letters are statistically different (Tukey, $P < 0.05$).

Site	Gully pot ID	RM (mg/g sediment dw)		TWP (mg/g sediment dw)			
		Mean	SD	Mean	SD		
Sjoskogenveien	1	86.7	a	5.3	149.6	a	9.1
	2	41.4	b	1.3	71.4	b	2.2
Raadhusplassen	3	24.4	c	2.3	42.0	c	4.0
	4	75.8	a	9.9	130.7	a	17.0
Maalstrofveien	5	0.8	d	1.4	1.4	d	2.4
	6	1.6	d	2.8	2.8	d	4.8
Brekkeveien	7	0.5	d	0.5	0.8	d	0.9
	8	5.8	d	5.0	10.0	d	8.7
Nordbyveien	9	11.5	d	0.5	19.8	d	0.9
	10	1.5	d	1.5	2.7	d	2.5
Control	LUFA soil	0.1	d	0.2	0.2	d	0.3

and that driving patterns, such as braking and acceleration intensity and frequency were also contributing factors. The high TWP concentrations in gully pots at Sjoskogenveien (roundabouts) and Raadhusplassen (parking plot), where high braking activities are expected, supported this suggestion. This finding was in agreement with Knight et al. (2020), who reported an association between high level of braking and acceleration, and generation of high amounts of TWP. In addition, TWP concentrations were significantly different in the 2 gully pots of a same site at Sjoskogenveien (by a factor 2) and Raadhusplassen (by a factor 3) indicating possible effect of micro-environment on mobilization of TWP entering the gully pots. However, the influence of other factors, like management activities, could not be excluded, as not specifically evaluated here. These factors, e.g. emptying frequency, particle size and density, stormwater inflow intensity and design of the gully pots have been reported to influence particle accumulation in gully pots (Bolognesi et al. 2008; Lindholm 2015).

3.4. Implication for environmental pollution management

Gully pots are established to retain solid particles in order to facilitate the well-functioning of drainage systems and protect downstream waters against pollution. They have been found to retain a range of environmental pollutants (Lindholm 2015) and are often the only pollution control infrastructure before road runoff reaches downstream recipient water. This study demonstrated that TWP were present among the solid particles retained in gully pots, supporting the finding by (Kreider et al. 2010; Sommer et al. 2018; Wagner et al. 2018) that sedimentation may occur following heteroaggregation of TWP with higher density particles in the road environment. The presence of TWP at concentrations reaching 150 mg/g, i.e. 15% of the sediment indicated that gully pots could serve as temporary sinks to protect recipient water from pollution, yet posing an acute pollution risk if not timely emptied. The present study was conducted in streets with low traffic densities and low speed limits, but the approach would be highly relevant to road environments with more intense traffic conditions, such as highways and urban roads. Eventually, knowledge of TWP concentrations and their evolution over time would help road managers design timely and efficient emptying routines and safe disposal plans for gully pot sediment. Furthermore, the method could be applied for generating data for environmental fate and mass balance models, which would necessarily need to account for TWP trapping efficiency in stormwater.

4. Conclusion

By combining STA, FTIR and PARAFAC, rubber materials signals were identified and TWP concentrations were determined in gully pot sediments, without prior sample preparation. The model appeared to perform well, spike analysis showed good recovery rate, and the method provided a feasible way to apply FTIR to TWP. Concentrations of TWP in the studied gully pot sediments ranged from below 0.1% to 15%, showing the potential of gully pots to act as temporary sinks for TWP, while also posing an acute pollution risk for downstream water recipients, if not properly managed. The highest TWP concentrations were found at sites with higher traffic density and braking/acceleration intensity. However, to conclusively determine the influence of traffic conditions on TWP concentrations in gully pots, the approach should be applied in settings where gully pot emptying frequency and all TWP generating and mobilization factors are controlled. For sediments with low TWP concentrations (<1 mg/g), density separation might be an interesting pre-step to concentrate TWP in samples, and could also help to clarify the amount of TWP in different density classes. Another interesting pre-step might be mechanical sieving of the samples, which could also be helpful to understand capture efficiency by size in gully pots. Improving laboratory equipment and analytical procedures is another area to consider, where the use of high resolution STA, for instance, might

help individual polymer detection by improving separation between closely occurring mass loss events. Finally, by enabling quantification of TWP in gully pot sediments, the approach supports environmental monitoring of TWP and safe disposal of gully pot sediments, which is critical for environmental pollution management.

CRediT authorship contribution statement

Demmelash Mengistu: Conceptualization, Formal analysis, Methodology, Writing – original draft. **Arve Heistad:** Funding acquisition, Supervision. **Claire Coutris:** Conceptualization, Funding acquisition, Writing – review & editing.

Declaration of competing interest

The authors declare that they have no known competing financial interests or personal relationships that could have appeared to influence the work reported in this paper.

Acknowledgements

The authors wish to thank Monica Fongen for the STA-FTIR analysis of the samples.

Funding

The Norwegian Institute of Bioeconomy Research (NIBIO) financed the STA-FTIR analysis, through funding from the Norwegian Research Council (Grant number 194051). Financial support from the municipality of Ås, Norway, and the Norwegian Research Council (Grant number 272946) is also acknowledged.

Appendix A. Supporting information

Supporting information to this article can be found online at <https://doi.org/10.1016/j.scitotenv.2020.144785>.

References

Andersen, C.M., Bro, R., 2003. Practical aspects of PARAFAC modeling of fluorescence excitation-emission data. *J. Chemom.* <https://doi.org/10.1002/cem.790>.

Andersson-Sköld, Y., Johansson, M., Gustafsson, M., Järnskog, I., Lithner, D., Polukarova, M., Strömvall, A.-M., 2020. Microplastics From Tyre and Road Wear – A Literature Review. <https://doi.org/10.13140/RG.2.2.34478.54083>.

Baum, A., Hansen, P.W., Nørgaard, L., Sørensen, J., Mikkelsen, J.D., 2016. Rapid quantification of casein in skim milk using Fourier transform infrared spectroscopy, enzymatic perturbation, and multiway partial least squares regression: monitoring chymosin at work. *J. Dairy Sci.* 99, 6071–6079. <https://doi.org/10.3168/jds.2016-10947>.

Birch, G.F., Scollen, A., 2003. Heavy metals in road dust, gully pots and parkland soils in a highly urbanised sub-catchment of Port Jackson, Australia. *Aust. J. Soil Res.* 41, 1329–1342. <https://doi.org/10.1071/SR02147>.

Bolognesi, A., Casadio, A., Ciccarello, A., Maglionico, M., Artina, S., 2008. Experimental study of roadside gully pots efficiency in trapping solids washed off during rainfall events. *Int. Conf. Urban Drain* 1–10.

Bondelind, M., Sokolova, E., Nguyen, A., Karlsson, D., Karlsson, A., Björklund, K., 2020. Hydrodynamic modelling of traffic-related microplastics discharged with stormwater into the Göta River in Sweden. *Environ. Sci. Pollut. Res.* 27, 24218–24230. <https://doi.org/10.1007/s11356-020-08637-z>.

Bro, R., Kiers, H.A.L., 2003. A new efficient method for determining the number of components in PARAFAC models. *J. Chemom.* 17, 274–286. <https://doi.org/10.1002/cem.801>.

Cadle, S.H., Williams, R.L., 1978. Gas and particulate emissions from automobile tires in laboratory and field studies. *J. Air Pollut. Control Assoc.* 28, 502–507. <https://doi.org/10.1080/00022470.1978.10470623>.

Cambridge Polymer Group, 2014. *Car Tire Composition Analysis by TGA-FTIR*. Boston.

CAS, 2020. CAS Registry Support [WWW Document]. URL <https://scifinder.cas.org/scifinder/view/scifinder/scifinderExplore.jsf> (accessed 5.20.20).

Eisenbraun, P., Dümichen, E., Ruhl, A.S., Jekel, M., Albrecht, M., Gehde, M., Braun, U., 2018. Two birds with one stone - fast and simultaneous analysis of microplastics: microparticles derived from thermoplastics and tire wear. *Environ. Sci. Technol. Lett.* 5, 608–613. <https://doi.org/10.1021/acsclett.8b00446>.

EPA, 2016. Definition and procedure for the determination of the method detection limit –revision 1.11. Code of Federal Regulations, Title 40, Part 136, Appendix B. Washington, DC.

Fausner, 1999. *Particulate Air Pollution With Emphasis on Traffic Generated Aerosols*. Technical University of Denmark. Denmark. Forskningscenter Risø. Risøe-R (No. 1053).

Fernández-Berridi, M.J., González, N., Mugica, A., Bernicot, C., 2006. Pyrolysis-FTIR and TGA techniques as tools in the characterization of blends of natural rubber and SBR. *Thermochim. Acta* 444, 65–70. <https://doi.org/10.1016/j.tca.2006.02.027>.

Gunasekaran, S., Natarajan, R.K., Kala, A., 2007. FTIR spectra and mechanical strength analysis of some selected rubber derivatives. *Spectrochim. Acta - Part A Mol. Biomol. Spectrosc.* 68, 323–330. <https://doi.org/10.1016/j.saa.2006.11.039>.

ISO, 2017. Rubber – Determination of Mass Concentration of Tire and Road Wear Particles (TRWP) in Soil and Sediments – Pyrolysis-GC/MS Method [WWW Document]. <https://www.iso.org/obp/ui/#iso:std:iso:ts:21396:ed-1:v1:en>.

Januszewicz, K., Klein, M., Klugmann-Radziemska, E., Kardas, D., 2017. Physicochemical problems of mineral processing thermogravimetric analysis/pyrolysis of used tyres and waste rubber. *Physicochem. Probl. Miner. Process* 53, 802–811. <https://doi.org/10.5277/ppmp170211>.

Järnskog, I., Strömvall, A.M., Magnusson, K., Gustafsson, M., Polukarova, M., Galfi, H., Aronsson, M., Andersson-Sköld, Y., 2020. Occurrence of tire and bitumen wear microplastics on urban streets and in sweepsand and washwater. *Sci. Total Environ.* 729. <https://doi.org/10.1016/j.scitotenv.2020.138950>.

Jasmínská, N., Brestovič, T., Carnogurská, M., 2013. The effect of temperature pyrolysis process of used tires on the quality of output products. *Acta Mech. Autom.* 7, 20–25. <https://doi.org/10.2478/ama-2013-0004>.

John, C., 2000. Interpretation of infrared spectra, a practical approach. *Encycl. Anal. Chem.* 10815–10837. <https://doi.org/10.1097/00010694-197107000-00005>.

Jusli, E., Nor, H.M., Jaya, R.P., Zaiton, H., 2014. Chemical properties of waste tyre rubber granules. *Adv. Mater. Res.* 911, 77–81. <https://doi.org/10.4028/www.scientific.net/amr.911.77>.

Karlsson, K., Viklander, M., 2008. Polycyclic aromatic hydrocarbons (PAH) in water and sediment from gully pots. *Water Air Soil Pollut.* 188, 271–282. <https://doi.org/10.1007/s11270-007-9543-5>.

Kawamoto, H., 2017. Lignin pyrolysis reactions. *J. Wood Sci.* 63, 117–132. <https://doi.org/10.1007/s10086-016-1606-z>.

Knight, L.J., Parker-Jurd, F.N.F., Al-Sid-Cheikh, M., Thompson, R.C., 2020. Tyre wear particles: an abundant yet widely unreported microplastic? *Environ. Sci. Pollut. Res.* 27, 18345–18354. <https://doi.org/10.1007/s11356-020-08187-4>.

Kole, J.P., Löhr, A.J., Van Belleghem, F.G.A.J., Ragas, A.M.J., 2017. Wear and tear of tyres: a stealthy source of microplastics in the environment. *Int. J. Environ. Res. Public Health* 14. <https://doi.org/10.3390/ijerph14101265>.

Kreider, M.L., Panko, J.M., McAtee, B.L., Sweet, L.L., Finley, B.L., 2010. Physical and chemical characterization of tire-related particles: comparison of particles generated using different methodologies. *Sci. Total Environ.* 408, 652–659. <https://doi.org/10.1016/j.scitotenv.2009.10.016>.

Lindholm, O., 2015. Forurensingstilførsler fra veg og betydningen av å tømme sandfang. *Vann* 93–100.

Litvinov, V.M., De, P.P., 2002. *Spectroscopy of Rubber and Rubbery Materials*. Rapra Technology Limited, Exter, UK.

Manohar, N., Jayaramudu, J., Suchimsita, S., Rajkumar, K., Babul Reddy, A., Sadiku, E.R., Priti, R., Maurya, D.J., 2017. A unique application of the second order derivative of FTIR-ATR spectra for compositional analyses of natural rubber and polychloroprene rubber and their blends. *Polym. Test.* 62, 447–453. <https://doi.org/10.1016/j.polymertesting.2017.07.030>.

Menczel, J.D., 2009. In: Alcon, L., Prime, R.B. (Eds.), *Thermal Analysis of Polymers: Fundamentals and Applications*. John Wiley & Sons, Inc, Hoboken, New Jersey.

Mengistu, D., Nilsen, V., Heistad, A., Kvaal, K., 2019. Detection and quantification of tire particles in sediments using a combination of simultaneous thermal analysis, Fourier transform infra-red, and parallel factor analysis. *Int. J. Environ. Res. Public Health* 16. <https://doi.org/10.3390/ijerph16183444>.

Murphy, K.R., Stedmon, C.A., Graeber, D., Bro, R., 2013. Fluorescence spectroscopy and multi-way techniques. *PARAFAC*. *Anal. Methods* 5, 6557–6566. <https://doi.org/10.1039/c3ay41160e>.

NIST Chemistry WebBook, 2011. SRD 69 [WWW Document]. Natl. Stand. Technol. US Dep. Commer. <https://webbook.nist.gov/cgi/inchi?ID=C7732185&Type=IR-SPEC&Index=0>.

Panko, J.M., Chu, J., Kreider, M.L., Unice, K.M., 2013. Measurement of airborne concentrations of tire and road wear particles in urban and rural areas of France, Japan, and the United States. *Atmos. Environ.* 72, 192–199. <https://doi.org/10.1016/j.atmosenv.2013.01.040>.

Pantea, D., Darmstadt, H., Kaliaguine, S., Roy, C., 2003. Heat-treatment of carbon blacks obtained by pyrolysis of used tyres. Effect on the surface chemistry, porosity and electrical conductivity. *J. Anal. Appl. Pyrolysis* 67, 55–76. [https://doi.org/10.1016/S0165-2370\(02\)00017-7](https://doi.org/10.1016/S0165-2370(02)00017-7).

Ragn-sells, 2020. *Gummigranulat* [WWW Document]. https://www.ragnsells.no/globalassets/norge/dokumenter/dekkjgenvinning/rs_pb_granulat_fin_v5-2018-01-16.pdf.

Rhodes, E.P., Ren, Z., Mays, D.C., 2012. Zinc leaching from tire crumb rubber. *Environ. Sci. Technol.* 46, 12856–12863. <https://doi.org/10.1021/es3024379>.

Roy, C., Plante, P., De Caumia, B., 2004. Oil and carbon black by pyrolysis of used tires. *Proc. Int. Conf. Sustain. Waste Manag. Recycl. Used/Post-Consumer Tyres* 17–33.

Rumble, J., 2017. *Handbook of Chemistry and Physics* [WWW Document] URL <http://hbcponline.com/faces/contents/ContentsSearch.xhtml?%0Ajsessionid=49E72CF0E54CD060B7559A3D084CF6>.

Schindler, A., Neumann, G., Rager, A., Füglein, E., Blumm, J., Denner, T., 2013. A novel direct coupling of simultaneous thermal analysis (STA) and Fourier transform-infrared (FT-IR) spectroscopy. *J. Therm. Anal. Calorim.* 113, 1091–1102. <https://doi.org/10.1007/s10973-013-3072-9>.

- Sommer, F., Dietze, V., Baum, A., Sauer, J., Gilge, S., Maschowski, C., Gieré, R., 2018. Tire abrasion as a major source of microplastics in the environment. *Aerosol Air Qual. Res.* 18, 2014–2028. <https://doi.org/10.4209/aaqr.2018.03.0099>.
- Thorpe, A., Harrison, R.M., 2008. Sources and properties of non-exhaust particulate matter from road traffic: a review. *Sci. Total Environ.* 400, 270–282. <https://doi.org/10.1016/j.scitotenv.2008.06.007>.
- Unice, K.M., Kreider, M.L., Panko, J.M., 2012. Use of a deuterated internal standard with pyrolysis-GC/MS dimeric marker analysis to quantify tire tread particles in the environment. *Int. J. Environ. Res. Public Health* 9, 4033–4055. <https://doi.org/10.3390/ijerph9114033>.
- Vogelsang, C., Lusher, A.L., Dadkhah, M.E., Sundvor, I., Umar, M., Ranneklev, S.B., Eidsvoll, D., Meland, S., 2018. Microplastics in road dust – characteristics, pathways and measures, 173 <https://doi.org/10.1097/nnr.0000000000000034>.
- Wagner, S., Hüffer, T., Klöckner, P., Wehrhahn, M., Hofmann, T., Reemtsma, T., 2018. Tire wear particles in the aquatic environment - a review on generation, analysis, occurrence, fate and effects. *Water Res.* 139, 83–100. <https://doi.org/10.1016/j.watres.2018.03.051>.
- Wang, S., Lou, Z., 2016. *Pyrolysis of Biomass*. Walter de Gruyter GmbH, Berlin.
- Wik, A., Lycken, J., Dave, G., 2008. Sediment Quality Assessment of Road Runoff Detention Systems in Sweden and the Potential Contribution of Tire Wear 301–314. <https://doi.org/10.1007/s11270-008-9718-8>.
- Yang, X., Zhao, Y., Li, R., Wu, Y., Yang, M., 2018. A modified kinetic analysis method of cellulose pyrolysis based on TG–FTIR technique. *Thermochim. Acta* 665, 20–27. <https://doi.org/10.1016/j.tca.2018.05.008>.

Supporting Information

Tire wear particles concentrations in gully pot sediments

Demmelash Mengistu^{1*}, Arve Heistad¹ and Claire Coutris²

¹Norwegian University of Life Sciences (NMBU), Faculty of Science and Technology, Ås, Norway

²Norwegian Institute of Bioeconomy Research (NIBIO), Division of Environment and Natural Resources, Ås, Norway

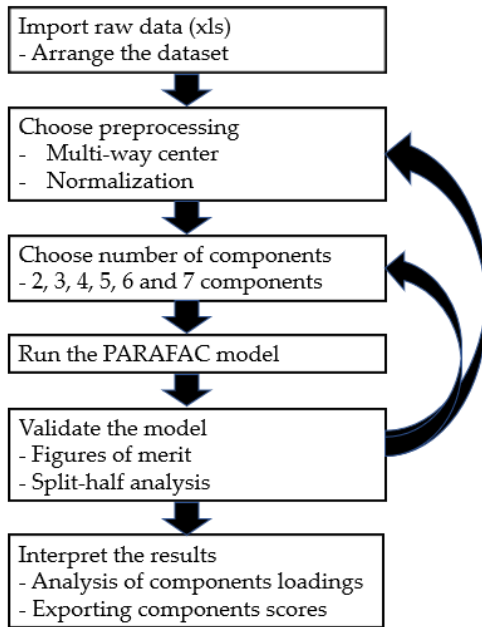
*Corresponding author: Kajaveien 5, NO-1432 Ås, Norway; demmelash.mengistu@nmbu.no

Contents

S1. Schematic of the various steps in PARAFAC analysis of STA-FTIR data.....	p.2
S2. Equation of the PARAFAC model.....	p.3
S3. Figures of merit of the PARAFAC model and split-half analysis.....	p.4
S4. Spike analysis.....	p.6
References.....	p.6

Supporting Information

S1. Schematic of the steps involved in PARAFAC analysis of STA-FTIR data of gully pot sediments. Default split method was used in the analysis.



Supporting Information

S2. A PARAFAC model decomposes the trilinear dataset into a set of trilinear terms and a residual array described in equation below (Baum et al., 2013; Murphy et al., 2013; Rasmus, 1997).

$$X_{ijk} = \sum_{f=1}^F a_{if} b_{jf} c_{kf} + e_{ijk}$$

($i = 1, \dots, I$; $j = 1, \dots, J$; $k = 1, \dots, K$; $f = 1, \dots, F$)

In equation 1, X_{ijk} is the data point corresponding to the i^{th} sample at the j^{th} wavenumber cm^{-1} on mode 2 and at the k^{th} pyrolysis temperature ($^{\circ}\text{C}$) on mode 3, and e_{ijk} is the residual representing the variability not accounted for by the model, while f represents number of components.

Each component has:

- 33 a-values, the **scores**, representing the relative magnitude of the components. These scores are represented by a_{if} and directly proportional to the concentration of the f^{th} component of sample i
- 1762 b-values, the **mode 2 loadings**, which are scaled estimates of the **wavenumber** cm^{-1} spectra, and are represented by b_{if}
- 614 c-values, the **mode 3 loadings**, which are scaled estimate of **pyrolysis temperature** $^{\circ}\text{C}$, and are represented by c_{if}

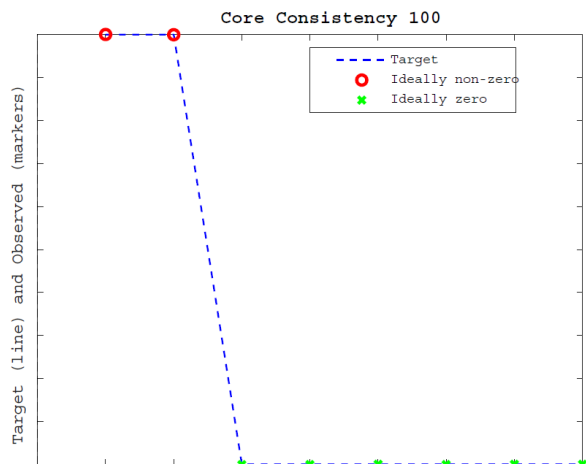
One of the assumptions in decomposing multi-way dataset with PARAFAC is additivity, which states that the total signal is due to the linear superposition of a fixed number of components (Murphy et al., 2013). This means that score of components of a sample can be added as:

$$S_i = \sum_{f=1}^F a_{if}$$

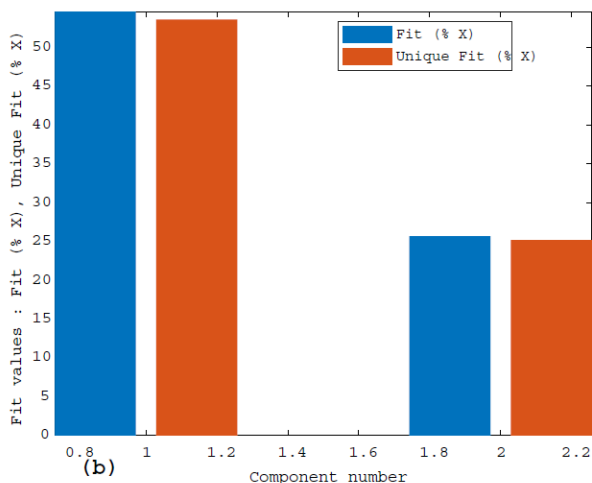
Where S_i is sum of score of components of sample i .

Supporting Information

S3. Figures of merit of the PARAFAC model and split-half analysis. (a) core consistency, (b) model fit and model unique fit, (c) residuals sum of squares, (d) similarity between FTIR data of the two split samples and (e) similarity between the pyrolysis temperature of the split samples. Default split method, which arranges samples as [A B C D], and then model the first half (AB) to compare to the last half (CD), was used.

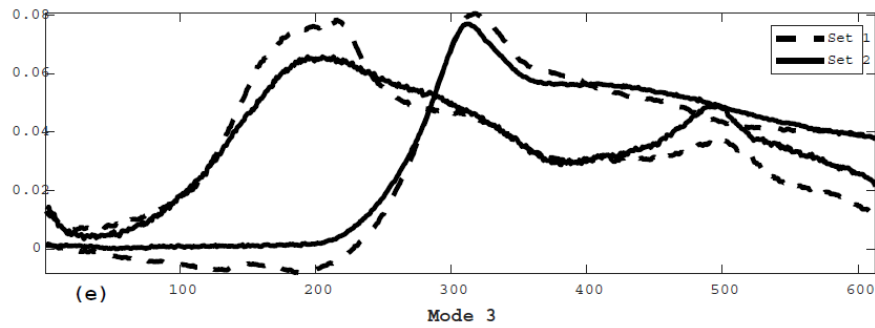
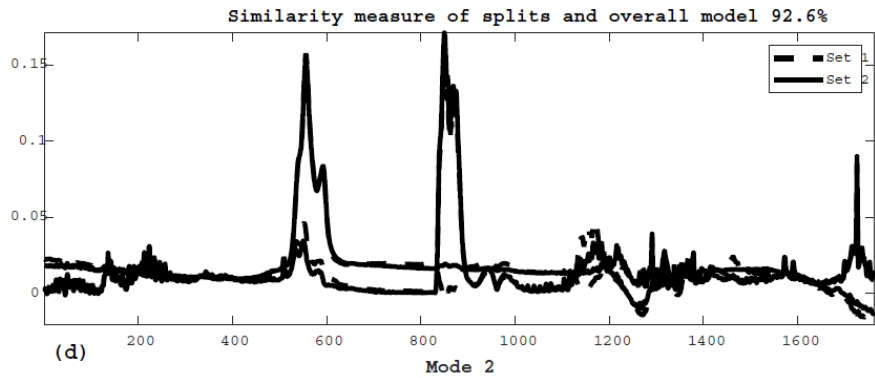
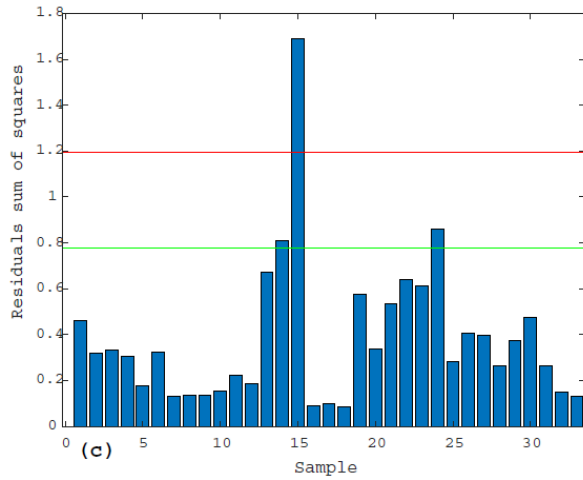


(a)



(b)

Supporting Information



Supporting Information

S4. Spike analysis

A recovery test using tire crumb from Ragn-sells (2018), and described in Mengistu et al. (2019), was conducted, where 80 mg of dry sediment from gully pot 1 were spiked with 2 mg of tire crumb, in triplicates. This mass of tire crumb (2 mg) corresponded to 1.16 mg rubber materials (RM), based on 58 % RM content in tire crumb provided by Ragn-sells. A PARAFAC model of spiked (n = 3) and non-spiked (n = 3) samples was built using similar procedures above. The model was valid and resulted in two components with spectra similar to those described in section 3.2 of the manuscript. The resulting RM mass was 1.43 mg (calculated from the difference in RM mass between the spiked and non-spiked datasets), indicating a recovery rate of 123 %. Although on the higher range, this recovery rate is in agreement with the producer's evaluation of RM content of the tire crumb.

References



- Baum, A., Waaben, P., Meyer, A.S., Dalgaard, J., 2013. Simultaneous measurement of two enzyme activities using infrared spectroscopy : A comparative evaluation of PARAFAC, TUCKER and N-PLS modeling. *Anal. Chim. Acta* 790, 14–23.
<https://doi.org/10.1016/j.aca.2013.06.039>
- Mengistu, D., Nilsen, V., Heistad, A., Kvaal, K., 2019. Detection and quantification of tire particles in sediments using a combination of Simultaneous Thermal Analysis, Fourier Transform Infra-Red, and Parallel Factor Analysis. *Int. J. Environ. Res. Public Health* 16.
<https://doi.org/10.3390/ijerph16183444>
- Murphy, K.R., Stedmon, C.A., Graeber, D., Bro, R., 2013. Fluorescence spectroscopy and multi-way techniques. *PARAFAC. Anal. Methods* 5, 6557–6566.
<https://doi.org/10.1039/c3ay41160e>
- Ragn-sells, 2018. Gummigranulat [WWW Document]. URL
https://www.ragnsells.no/globalassets/norge/dokumenter/dekkgjenvinning/rs_pb_granulat_fin_v5-2018-01-16.pdf.
- Bro, R., 1997. PARAFAC. Tutorial and applications. *Chemom. Intell. Lab. Syst.* 38, 149–171.
[https://doi.org/doi:10.1016/S0169-7439\(97\)00032-4](https://doi.org/doi:10.1016/S0169-7439(97)00032-4)
- Schindler, A., Neumann, G., Rager, A., Füglein, E., Blumm, J., Denner, T., 2013. A novel direct coupling of simultaneous thermal analysis (STA) and Fourier transform-infrared (FT-IR) spectroscopy. *J. Therm. Anal. Calorim.* 113, 1091–1102. <https://doi.org/10.1007/s10973-013-3072-9>

Paper III

Mengistu, D., Coutris, C., Paus, K. H., & Heistad, A. (2022) 'Concentrations and retention efficiency of tire wear particles from road runoff in bioretention cells', *Water* 14, 3233.
<https://doi.org/10.3390/w14203233>

Article

Concentrations and Retention Efficiency of Tire Wear Particles from Road Runoff in Bioretention Cells

Demmelash Mengistu ^{1,*}, Claire Coutris ², Kim Aleksander Haukeland Paus ¹ and Arve Heistad ¹

¹ Faculty of Science and Technology, Norwegian University of Life Sciences (NMBU), 1432 Ås, Norway
² Division of Environment and Natural Resources, Norwegian Institute of Bioeconomy Research (NIBIO), 1433 Ås, Norway
* Correspondence: demmelash.mengistu@nmbu.no

Abstract: Bioretention cells are popular stormwater management systems for controlling peak runoff and improving runoff water quality. A case study on a functional large-scale bioretention cell and a laboratory column experiment was conducted to evaluate the concentrations and retention efficiency of bioretention cells towards tire wear particles (TWP). The presence of TWP was observed in all soil fractions (<50 µm, 50–100 µm, 100–500 µm, and >500 µm) of the functional bioretention cell. TWP concentrations were higher (30.9 ± 4.1 mg/g) close to the inlet to the bioretention cell than 5 m away (19.8 ± 2.4 mg/g), demonstrating the influence of the bioretention cell design. The column experiment showed a high retention efficiency of TWP (99.6 ± 0.5%) in engineered soil consisting of sand, silty-sand, and garden waste compost. This study confirmed that bioretention cells built with engineered soil effectively retained TWP > 25 µm in size, demonstrating their potential as control measures along roads.

Keywords: stormwater; infiltration; tread wear; pollutants; soil



check for updates

Citation: Mengistu, D.; Coutris, C.; Paus, K.A.H.; Heistad, A. Concentrations and Retention Efficiency of Tire Wear Particles from Road Runoff in Bioretention Cells. *Water* **2022**, *14*, 3233. <https://doi.org/10.3390/w14203233>

Academic Editor: Jiangyong Hu

Received: 21 August 2022
Accepted: 10 October 2022
Published: 14 October 2022

Publisher's Note: MDPI stays neutral with regard to jurisdictional claims in published maps and institutional affiliations.



Copyright: © 2022 by the authors. Licensee MDPI, Basel, Switzerland. This article is an open access article distributed under the terms and conditions of the Creative Commons Attribution (CC BY) license (<https://creativecommons.org/licenses/by/4.0/>).

1. Introduction

Bioretention cells (also known as stormwater biofilters or rain gardens) have been widely used to manage stormwater from road runoff [1–3]. The objectives of bioretention cells are to reduce peak runoff, improve runoff water quality through infiltration, sedimentation, and sorption processes, increase groundwater recharge, and enhance the aesthetics of the community [4–8]. While their pollutant removal capabilities (e.g., petroleum hydrocarbon, polychlorinated biphenyls, sediments) have been demonstrated in many studies (e.g., [4,9–11]), removal efficiencies vary depending on site characteristics, design, implementation, and climatic conditions [12–14]. The hydrological performance of bioretention cells, their plant growth ability, and their pollutant removal efficiency can be optimized using engineered soil [8].

Tire wear particles (TWP) are a major source of microplastics in the environment [15,16] with potentially adverse effects on human health and aquatic and terrestrial ecosystems [17]. However, TWP are seldom found as pure tire particles in the environment because of mineral encrustations from the road surface during abrasion of tire treads; the resulting particles are therefore termed tire and road wear particles (TRWP) [18–20]. The primary entrance to the environment is runoff [15,21], which contains substantial amounts of TRWP [22]. Runoff treatment in bioretention cells removes TRWP, likely through physical filtration [23]. The removal efficiency can be affected by TRWP size, as demonstrated by [9], who studied TRWP ≥ 125 µm and showed decreasing removal efficiency with decreasing size. This can be problematic for efficient TRWP retention by bioretention cells because significant amounts of smaller TWP (≤50 µm) have been found in road dust [18,24]. The effective removal of microplastics has also been reported in bioretention cells. For example, [9,23] demonstrated a reduction of 91% of microplastic particles >125 µm in bioretention cells. Furthermore, [23] showed high removal (84%) of microplastic particles

>106 μm , including rubber fragments, in bioretention cells, while [25] reported >70% removal for larger microplastics and TRWP (>100 μm), and [26] showed >90% removal of TRWP between 20 and 100 μm in vegetated bioretention and 60% in non-vegetated filters.

The main objective of this study was to evaluate whether bioretention cells established with engineered soil retain TWP from road runoff, including finer TWP sizes. More specifically, this study aims to (1) identify and quantify TWP concentrations retained in different soil size fractions of bioretention cells (functional bioretention cells and lab-scale columns) and (2) evaluate the TWP retention efficiency and TWP concentrations in the top and bottom 5 cm of the column soil.

2. Materials and Methods

2.1. Case Study

2.1.1. Sampling Site and Sample Collection

A case study was conducted on a bioretention cell in Drammen, Southern Norway. The bioretention cell was established in 2019 using engineered soil (70% sand, 30% garden waste compost, size fractionation in Table 1) and designed to optimize hydrological conditions (lower peak flow) and plant growth [27]. The bioretention cell is located on a street with a speed limit of 50 km/h and a traffic density of 20,800 annual average daily traffic (AADT) [28]. It receives road runoff through several standardized inlets fitted to the side curb, a 13 cm high structure separating the driveway from the bioretention cell (Figure 1). These inlets are 70 m apart; they operate only during the warmer seasons and are closed during the cold winter season owing to icing (December–March) [27].

Table 1. Proportion (by mass) of each soil fraction in bulk soil collected from a functional bioretention cell in Drammen, Norway, close to the inlet (A) and 5 m away from it (B).

Soil Size Fraction (μm)	Proportion in Bulk Soil (%)	
	A	B
<50	3.8	3.3
50–100	24.6	22.6
100–500	35.6	39.0
>500	36.0	35.1



Figure 1. Left picture: the bioretention cell is the area located between the road and the sidewalk. Right picture: inlets specially designed and fitted to the side curb bring road runoff to the bioretention cell. A 13 cm high side curb (a) separates the road from the bioretention cell. Sampling spot in front of an inlet (b).

Topsoil samples (0–5 cm) were collected in April 2021 using a soil-sampling tube. Samples were collected from six different locations: three spots, each located directly in front of three different inlets and three spots each located 5 m away from these inlets. The samples were oven-dried at 105 °C for 24 h. Samples collected at the inlets were mixed and homogenized using a not sharp-edged Kenwood kitchen blender KMM770 (Kenwood, Havant, Hampshire, UK) for 5 min at high speed to prepare a composite sample A. The three samples taken 5 m away from the inlets were mixed and homogenized similarly, resulting in composite sample B.

2.1.2. Size Fractionation

After sieving soil samples with a 5 mm mesh to exclude materials beyond the range of defined microplastics, 30 g of composite samples A and B was sifted using a vibratory sieve shaker (Retac 3D, Retsch, Germany), with stainless steel mesh sizes of 50, 100, and 500 µm. The four fractions collected (<50 µm, 50–100 µm, 100–500 µm, >500 µm) were weighed using an analytical balance AT200 METTLER, (Mettler-Toledo GmbH, Giessen, Germany) and the proportion of each size fraction was determined by dividing the mass of the specific size fraction by the total mass recovered after sieving. Mass recovery of the size fractionation after dry sieving of 30 g of soil sample was 99% for sample A and 97% for sample B. The proportion of each soil fraction in the bioretention soil was similar close to the inlet and 5 m away from it, with 72 and 74% of particles >100 µm, respectively (Table 1).

The coarser fraction >500 µm was crushed with a mortar and pestle to increase the homogeneity. All samples were then analyzed in triplicate using simultaneous thermal analysis coupled with Fourier transform infrared spectrometry (STA-FTIR), followed by parallel factor analysis (PARAFAC) data modeling, as described in Section 2.3. Differences in TWP concentrations across size fractions and sampling sites were analyzed using a two-way analysis of variance, followed by a Tukey pairwise comparison test to identify different concentrations. The total TWP concentration in bulk soil was first estimated by factoring concentrations in each size fraction by the soil size fraction proportion (%) (Table 1) in a bulk sample and then adding concentrations in all size fractions. Differences in total TWP concentrations between groups A and B were analyzed using *t*-tests.

2.2. Column Experiment

2.2.1. Engineered Soil and Column Dimensions

An engineered soil was prepared in the laboratory, by mixing medium sand, silty sand, and garden waste compost collected at Lindum AS, Norway, at a ratio of 8:15:6 by mass. This engineered soil was recommended by [27] because of its infiltration efficiency and quality in promoting plant growth [29]. The physical and chemical properties of the soil used in this experiment were analyzed in a commercial laboratory, Eurofins, (Moss, Norway), and are presented in S1. Three similar cylindrical columns (C₁, C₂, C₃, diameter 3.8 cm, surface area 11.34 cm², and height 50 cm) were each filled with 40 cm of engineered soil. Dry packing of the columns was used: air-dried soil was added with a funnel into the columns and then gently pressed by hand. The column test was configured based on the dimensional parameters of the functional bioretention cells [3]. The ratio of the column diameter to the effective grain size (see Figure S1 for grain size distribution) was greater than the recommended minimum ratio (50:1) to avoid wall effects [30]. The bottom of the column was sealed with a lid with two small openings (5 mm in diameter) to release effluent water. The openings were connected to a 20 L container to collect the effluent water.

2.2.2. Influent Water and Hydraulic Load

Road runoff was collected in April 2021 from two gully pots in Ås, Southern Norway, serving as influent water to the columns. The presence and concentration of TWP in the sediments of these gully pots (Sjoskogenveien and Raadhusplassen) were demonstrated and studied in detail by [31]. Standing water and sediments from the gully pots (120 L from Sjoskogenveien and 100 L from Raadhusplassen) were collected and stored in a cold

room. During application to the columns, the water was continuously stirred to keep the particles in suspension, and applied similarly to the three columns (C₁, C₂, and C₃) using Watson peristaltic pumps, calibrated to yield a hydraulic load of 3.7 mm/min for 10 min (total water height of 37 mm). The application rate and duration were chosen to represent a Norwegian water quality design rain for a bioretention cell, sized to collect and treat runoff from a catchment 10 times the size of the bioretention cell area [32]. The pumps were programmed for 10 min on and 30 min off (10 min application, 30 min rest). The resting period was later prolonged (up to 4 h), as the high particle loads caused clogging of the soil and therefore reduced infiltration.

2.2.3. Retention Efficiency of the Columns

The TWP retention efficiency of the columns was calculated by analyzing the TWP concentrations in the influent and effluent water. For each of the three columns, 6 L of influent and their entire effluent (13.8 L, 10.3 L, and 14.2 L from C₁, C₂, and C₃, respectively) were filtered using a 25 µm mesh, and the retained particles were dried and analyzed in triplicates using STA-FTIR and PARAFAC, as described in Section 2.3, to determine TWP concentrations.

2.2.4. TWP Concentrations in Top and Bottom Soil

At the end of the experiment, the columns were left to drain for 24 h before topsoil (top 5 cm) and bottom soil (bottom 5 cm) were collected. Soil samples were oven-dried at 105 °C and subjected to density separation using 1.8 g/cm³ ZnCl₂ solution for 2 h, to get rid of heavier soil particles. As the particle density of TRWP is estimated to be 1.8 g cm⁻³ [33], they float in ZnCl₂ solution; the supernatant was decanted, rinsed with water on 25 µm mesh, and oven-dried at 105 °C. For one of the three columns, C₃, soil samples were divided into three subsamples, where the first (C₃) received the above-mentioned treatment, the second (C₃*) was analyzed without any pretreatment, and the third (C₃***) was filtered through a 25 µm mesh without density separation (only particles >25 µm were kept for analysis). Rubber material (RM) and TWP concentrations in the top 5 cm soil and bottom 5 cm soil were calculated. The differences in TWP concentrations at the top 5 cm and bottom 5 cm were analyzed using a *t*-test.

2.3. STA-FTIR Analysis and Data Modeling

Decomposition of FTIR data of environmental samples using a valid PARAFAC model provides a mechanism to detect and quantify RMs among many components [34]. Suitable data (thermal and FTIR spectra) of the samples were generated using a simultaneous thermal analyzer STA 449 F1 Jupiter with carrier type S (Netzsch, Selb, Germany), and a Bruker Tensor 27 FTIR spectrometer with an external gas cell (Bruker, Billerica, MA, USA) using the procedure described by [31]. The STA registered changes in mass during pyrolysis, as samples were heated from 40 to 800 °C and released gases to the FTIR. The FTIR scanned spectra of a wavenumber range between 4000 and 600 cm⁻¹ for gas released from the STA with a resolution of 1.93 cm⁻¹, generating 1762 signal points. The FTIR data yielded in 666 spectra per sample, giving a total of 1.1 million data points per sample. The data were arranged in a trilinear multi-way dataset as outlined in [31], to suit PARAFAC [35]. PARAFAC models were then built with components ranging from 2 to 5 using MATLAB (The MathWorks, Inc., R2018a, Natick, MA, USA) and a PLS Toolbox for MATLAB version 8.6 (Eigenvector Research, Inc., Wenatchee, WA, USA). The PARAFAC analysis steps and model validation used were described by [31].

From a valid PARAFAC model, the scores of components identified as RMs, core components of tires [36] and suitable TWP markers [21], were used to calculate the concentration of RMs [31] using Equation (1). The method detection limit (MDL) was 0.7 mg RM per g dry sediment, equivalent to 1.1 mg/g for TWP [31].

$$RM_j = \left(ml \times a_{if} \right) / (m \times S_i) \quad (1)$$

where

RM_j = concentration of RM (mg/g)

ml = sample mass loss during pyrolysis (mg)

m = initial sample dry mass (g)

a_{if} = score of the f th component of sample i extracted from PARAFAC

S_i = sum of score of components of sample i

RM constitutes a variable but significant fraction of TWP, usually between 40 and 60% [37,38]. In this study, 58% was used based on the most relevant data in the context of the study ([39], tire crumb producer). TWP concentrations were then calculated by dividing RM concentrations by 0.58. Estimation of TRWP concentrations (i.e., taking mineral encrustations into account) was not considered in this study, as a wide range (10–75%) of TWP to TRWP ratios is reported in the literature [18,24,40–42], making TRWP estimation problematic.

3. Results and Discussion

3.1. Case Study

3.1.1. Detection of TWP in the Soil of Bioretention Cells

Fitting the STA-FTIR data from all field samples in PARAFAC with three components after a preprocessing of filtering and diskiping resulted in a model that captured 85% variation, had 82% core consistency (Figure S2a) and 88% similarity in split-half analysis (Figure S2b). Models with similar figures of merit are considered valid [43,44]. The spectral signals from the wavenumber and temperature loadings of one of the components mimicked the properties of RM (Figure 2), a typical TWP marker [34]. This result confirms the presence of TWP in bioretention cells receiving road runoff and is consistent with the results obtained by [9,23,25,26], who reported the retention of rubbery fragments in bioretention cells.

3.1.2. TWP Concentrations in Soil Size Fractions Close to and Further away from the Inlet

TRWP sizes are important factors in determining their environmental fate [33,45]. In this study, TWP was observed in all soil fractions (<50 μm , 50–100 μm , 100–500 μm , >500 μm) of the bioretention cells (Figure 3). TWP concentrations in the soil (in mg per g soil dry weight) were found to differ significantly across size fractions ($F_{3,16} = 3.76$, $p < 0.001$) in A and B.

However, because of the differences in the proportion of soil size fractions in a bulk sample (Table 1), the TWP concentrations of each size fraction were different from those presented in Figure 3. The calculated TWP concentrations in each soil fraction and the total TWP concentrations are presented in Figure 4. The results showed that TWP concentrations in the finer soil fraction (<50 μm) were significantly lower than those in any of the coarser soil fractions, regardless of the sampling distance from the inlet ($F_{3,16} = 20.7$, $p < 0.001$), except in B where the difference between <50 μm and 100–500 μm was not significant. This is related to the mass of the engineered soil in this fraction (3.8 and 3.3% in A and B, respectively) compared with the other three coarser fractions (Table 1).

Studies on the size distribution of TWP retained by bioretention are scarce. However, the results of the present study are in contrast with those of [46], who covered size ranges up to 500 μm and found a decreasing trend of the TRWP concentrations with increasing sediment grain size in a sedimentation basin. The observed trend in TRWP concentration in the sedimentation basin differed from that found in the street dust analyzed in the same study, which showed no clear trend with size. [46] attributed the observed change in TRWP from coarse in runoff to fine in the sedimentation basin to processes such as easy transportability of finer particles, sedimentation of coarse particles before entering the sedimentation basin, and mechanical degradation of coarse particles. The present study, with bioretention cells close to the road, may not be affected by the processes listed above and may receive similar TRWP as present in road dust, suggesting significant amounts of TRWP below 100 μm entering the bioretention cell. Another study by [47], covering size

ranges similar to those of the present study (but with a lower limit at 10 μm), showed no clear trend but a relatively higher styrene-butadiene rubber (a TWP marker) concentration in a street runoff in the size fraction $>500 \mu\text{m}$ than in the size fraction $100\text{--}500 \mu\text{m}$. However, the studied matrices, street runoff in [47] and bioretention soil in the current study, are different and thus not directly comparable.

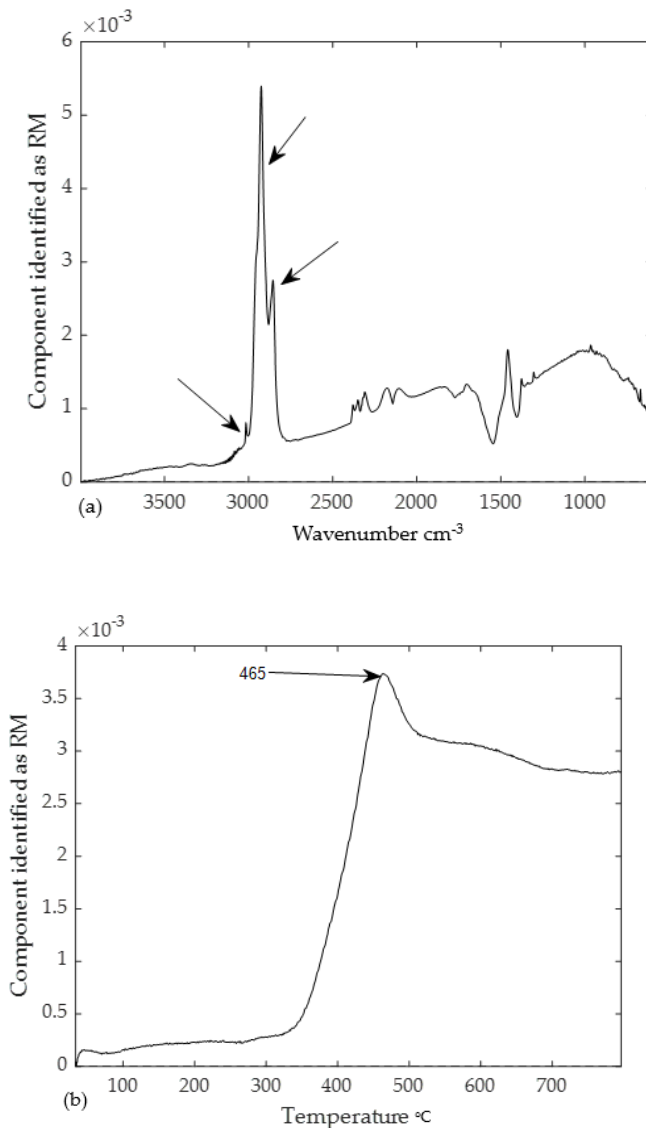


Figure 2. Wavenumber (a) and pyrolysis temperature (b) loadings from the rubber materials (RM) component in the PARAFAC model. Peaks supporting the identification of RM are indicated with arrows on the graphs.

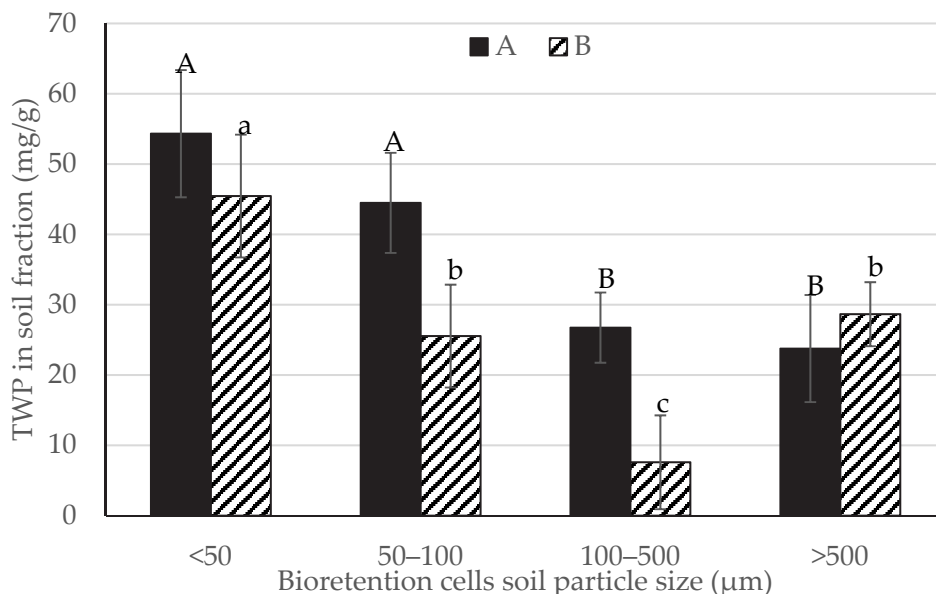


Figure 3. Tire wear particles (TWP) concentrations (mg/g, mean and one standard deviation, n = 3) per soil particle size range in soil samples collected from a functional bioretention cell in Drammen, Norway, at the inlet (A), and 5 m away from it (B). Means with different letters are statistically different (Tukey, $p < 0.05$).

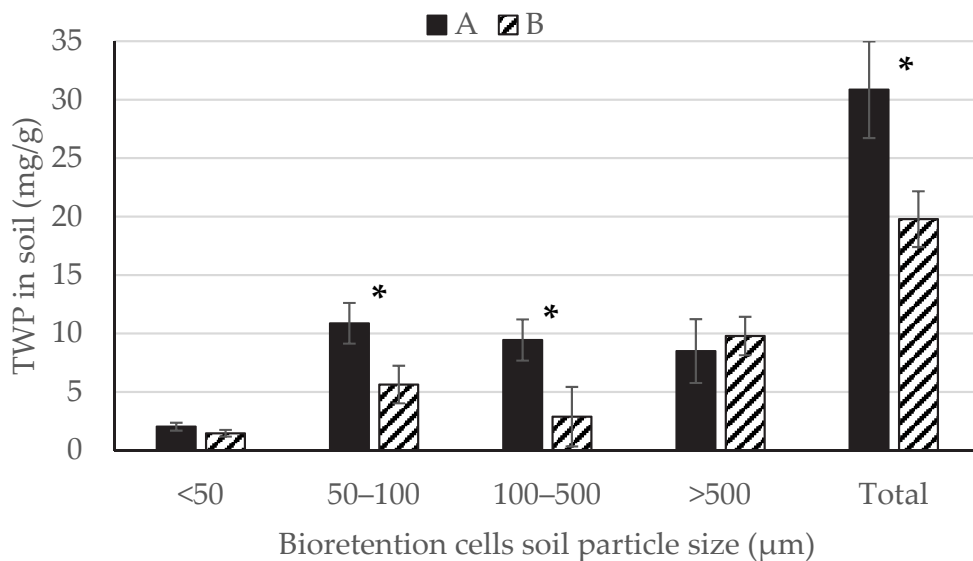


Figure 4. Tire wear particles (TWP) concentrations (mg/g, mean and one standard deviation, n = 3) factored by soil size proportion and total TWP concentrations in soil collected from a functional bioretention cell in Drammen, Norway, at the inlet (A), and 5 m away from it (B). Asterisks indicate significant differences between A and B (t -test, $p < 0.05$).

Retention efficiency could not be assessed because of a lack of data on the incoming and outgoing TWP concentrations. Therefore, it was unclear if the low contribution from the size range $<50\ \mu\text{m}$ was attributable to a lower share of small-sized TWP entering the bioretention cell, or if the bioretention cell was less efficient in retaining the finer TWP, as reported by [9]. The latter is plausible for two reasons. First, field and road simulator studies have reported that significant amounts of TWP are found in the size range $\leq 50\ \mu\text{m}$ [18,24]. Second, the main retention mechanism in bioretention cells is physical straining [23], which may allow the transfer of finer TWP down the soil profile or farther away with stormwater. Studies related to the retention efficiency of TWP in bioretention cells are scarce for direct comparison, and the few available studies are based on particle counts. For example, [9] observed up to 100% retention of microplastic particles (including rubbery fragments) larger than $500\ \mu\text{m}$. The retention efficiency decreased to 55% for the size fraction between $125\text{--}355\ \mu\text{m}$, supporting the suggestion that finer TWP particles may have moved down or away with stormwater.

Total TWP concentrations in mg per g soil dry weight (dw) (all soil fractions considered) were $30.9 \pm 4.1\ \text{mg/g}$ (mean \pm standard deviation, SD) at the inlet and $19.8 \pm 2.4\ \text{mg/g}$ 5 m away from the inlet. These concentrations were three and two times higher than the average TWP concentrations reported by [41] in roadside soils in the Seine River watershed, France. The slightly lower TWP concentrations reported in [41] may be attributed to the fact that the roadside soil was sampled at a depth of 0–15 cm (0–5 cm in the present study) and further away from the road edge (3–15 m). However, other factors not specified in the study (e.g., traffic density and service time) make comparisons difficult. [48] estimated an average TWP concentration of $20.2\ \text{mg/g}$ in roadside soil collected at 0–10 cm depth and 0.5 m away from the edge of federal roads in Germany, with an average traffic density of 24,000 AADT. This is consistent with the TWP concentrations observed in the present study. Although these studies have different TWP-generating conditions and treatment systems than the present study, the results indicate that roadside bioretention systems retain TWP. Not unexpectedly, we also showed that total TWP concentrations in soil, while of the same order of magnitude, were significantly higher at the inlet than 5 m away from it (*t*-test, $p = 0.03$).

3.2. Column Infiltration Experiment

3.2.1. Retention Efficiency of the Engineered Soil

An average of $12.8 \pm 2.1\ \text{L}$ of road runoff with a TWP concentration of $77.2 \pm 4.9\ \text{mg/L}$ passed through each column (Table 2). With a concentration of solid particles $>25\ \mu\text{m}$ of $367\ \text{mg/L}$, the influent was within the range of total suspended solids concentrations reported in highway stormwater (49–980 and 8–810 mg/L [49,50]). The physical and chemical properties of the soil used in this experiment fulfilled the requirements of bioretention applications with respect to infiltration and plant growth (Supplementary Materials Section S1). However, clogging at the column top was observed after one week of infiltration, suggesting that the initial resting period was insufficient for the hydraulic load and was therefore increased. Particle deposition, which was expected to be high in road runoff, was likely the cause of the clogging. [51] demonstrated clogging at the top of a column owing to particle deposition. Similarly, [52] found a high infiltration decline owing to clogging as a result of sediment accumulation. However, the results of the present study should be interpreted cautiously because a year and a half worth of rainfall was applied for two weeks in the column experiment. Further studies testing the influence of hydraulic loadings on the retention capacity of bioretention cells towards TRWP would be valuable, especially since high TRWP concentrations could hinder the functionality of bioretention cells. Furthermore, the absence of freeze–thaw cycles and vegetation in the columns may have made the soil more prone to clogging than what is typically observed in operative bioretention cells, which also calls for further tests using vegetated columns.

Table 2. Tire wear particles (TWP > 25 µm) concentrations in the influent and effluent of bioretention columns (C₁–C₃).

Sample	Column	Water (L)	Total Solid Particles >25 µm (mg/L)	TWP Concentration mg/L		Removal Efficiency (%)	
				Mean	SD	Mean	SD
Influent			366.7	79.9	4.9		
Effluent	C ₁	13.8	40.6	0.1	0.1	99.9	0.1
	C ₂	10.3	117.3	0.8	0.2	99.0	0.2
	C ₃	14.2	12.5	0.1	0.0	99.9	0.0

Concentrations of total solid particles >25 µm and TWP >25 µm are listed in Table 2. The effluent contained 56.8 ± 54.2 mg/L of total solid particles >25 µm, with differences observed between columns, which may be attributed to, e.g., heterogeneity of soil compaction and particle concentrations in the influent. Despite this unexpected variability in total solid particles >25 µm in the effluent, the overall TWP removal efficiency remained similar and was 99.6 ± 0.5% for TWP > 25 µm. This level of removal is high compared with that of the few available studies on the removal efficiency of microplastics (including rubber fragments) by bioretention cells [9,23,25,26]. However, these studies were conducted on field bioretention cells, which have been in operation for 2–3 years. The bioretention cells had different configurations than the column test in the current study, either in terms of the size of the catchment area they served or in their soil composition.

3.2.2. Vertical Distribution of TWP in the Columns

In this study, a test with samples that received no pretreatment, C₃^{*}, showed a TWP concentration of 5.0 ± 1.4 mg/g in the top 5 cm of the column, while the TWP concentration in the bottom 5 cm was below MDL (1.1 mg/g) (Table 3). The relatively high TWP concentration in the top 5 cm seems to originate mainly from the deposition of finer particles (<25 µm), as wet sieving of the same sample with a 25 µm mesh (C₃^{**}) showed a reduction in TWP concentration (Table 3). It is likely that these fine particles also contributed to the observed reduction in infiltration in the columns.

Table 3. Tire wear particles concentrations (TWP, in mg/g soil dw) in the 0–5 cm (Top 5 cm) and 35–40 cm (Bottom 5 cm) soil layers of bioretention columns C₁–C₃, following ZnCl₂ density separation of soil samples. In column C₃, TWP concentrations were also determined without prior filtration nor density separation (C₃^{*}), and with filtration only (C₃^{**}). N/A: not available.

Column	Top 5 cm		Bottom 5 cm	
	Mean	SD	Mean	SD
C ₃ [*]	5.0	1.4	0.0	0.0
C ₃ ^{**}	1.0	1.7	N/A	N/A
C ₁	0.9	1.0	0.4	0.5
C ₂	0.8	0.3	0.9	0.5
C ₃	0.6	0.7	0.4	0.2

TWP concentrations, determined in samples pretreated with density separation and filtration, in the top 5 cm (0.7 ± 0.7 mg/g) and bottom 5 cm (0.6 ± 0.4 mg/g) showed no statistically significant difference (*t*-test, *p* = 0.21). Considering the mass balance in the influent and effluent, sample pretreatment by density separation may have underestimated TWP concentrations due to unrecovered particles with higher density (>1.8 g/cm³). Higher TWP concentrations in the filtered top 5 cm sample (C₃^{**}, 1.0 ± 1.7 mg/g) than in the density separated top 5 cm (C₃, 0.5 ± 0.4 mg/g) also support this suggestion. This result indicates that while sample preparation by density separation using ZnCl₂ is a common

practice in microplastics and TRWP analysis [53–55], it is not optimal for TRWP, as it fails to recover TRWP denser than 1.8 g/cm^3 . Although comparing TWP concentrations at the top and bottom of the columns provided valuable results, further studies looking at TWP concentrations over the entire soil profile would enable mass balance and thereby a better understanding of TWP fate in bioretention cells.

The results of these experiments imply that bioretention cells are efficient in retaining TWP $> 25 \text{ }\mu\text{m}$. However, the observed high concentrations of TWP $< 2.5 \text{ }\mu\text{m}$ in the top 5 cm of the engineered soil suggests the entry of a high proportion of finer TWP to the bioretention system (Table 3). This warrants further study on the fate of TWP $< 25 \text{ }\mu\text{m}$ and their retention by bioretention cells, especially since our results on a large-scale functional bioretention cell showed that TWP in the finer soil fraction ($< 50 \text{ }\mu\text{m}$) only represented 7% of the top 5 cm of soil.

4. Conclusions

This study demonstrated that bioretention cells built for high infiltration and good plant growth conditions could retain TWP. A case study on a functional bioretention cell showed the presence of TWP in the top 5 cm of soil in all soil size fractions ($< 50 \text{ }\mu\text{m}$, $50\text{--}100 \text{ }\mu\text{m}$, $100\text{--}500 \text{ }\mu\text{m}$, $> 500 \text{ }\mu\text{m}$). TWP concentration was affected by the inlet fitted to the roadside curb, as TWP concentrations at the inlet were higher ($30.9 \pm 4.1 \text{ mg/g}$) than those observed 5 m away from the inlet ($19.8 \pm 2.4 \text{ mg/g}$).

The column experiment, despite varying concentrations of total solid particles $> 25 \text{ }\mu\text{m}$ in the effluent, showed high retention efficiency ($> 99\%$) of TWP $> 25 \text{ }\mu\text{m}$ in engineered soil consisting of sand, silty-sand, and garden compost.

The TWP was observed at the top and bottom of the column. Surface clogging and limited infiltration were observed during the experiment and attributed to a high particle load in a short time. A long-term study on a vegetated bioretention cell may provide more realistic wetting and drying conditions and particle loadings from the road environment to better explain the TWP dynamics in bioretention cells. A filter size smaller than $25 \text{ }\mu\text{m}$ might also help in understanding the efficiency of bioretention cells in retaining finer TWP. Finally, bioretention cells built with engineered soils not only transport high amounts of runoff water but also have been shown to retain TWP, demonstrating their potential as control measures along roads.

Supplementary Materials: The following supporting information can be downloaded at: <https://www.mdpi.com/article/10.3390/w14203233/s1>, Section S1: Particle size distribution of engineered soil; Figure S1: Grain size distribution of the engineered soil used in the column experiment; Section S2: PARAFAC model validity indicators; Figure S2: (a) core consistency of 82%, (b) similarity measure of splits 88%.

Author Contributions: D.M.: Conceptualization; Formal analysis; Methodology; Writing—original draft; C.C.: Conceptualization; Funding acquisition; Writing—review and editing; K.A.H.P.: Writing—review and editing; A.H.: Conceptualization; Supervision. All authors have read and agreed to the published version of the manuscript.

Funding: Funding from the Norwegian Research Council (Grant number 194051) is gratefully acknowledged.

Data Availability Statement: The research data is stored at Norwegian Centre for Research Data. <https://dmp.nsd.no/> (accessed on 21 August 2022).

Acknowledgments: The authors wish to thank Monica Fongen for the STA-FTIR analysis of the samples.

Conflicts of Interest: The authors declare no conflict of interest.

References

1. Ding, B.; Rezaeezhad, F.; Gharedaghloo, B.; Van Cappellen, P.; Passeur, E. Science of the Total Environment Bioretention cells under cold climate conditions: Effects of freezing and thawing on water infiltration, soil structure, and nutrient removal. *Sci. Total Environ.* **2019**, *649*, 749–759. [CrossRef]

2. Paus, K.H.; Morgan, J.; Gulliver, J.S.; Leiknes, T.; Hozalski, R.M. Assessment of the Hydraulic and Toxic Metal Removal Capacities of Bioretention Cells After 2 to 8 Years of Service. *Water Air Pollut.* **2014**, *225*, 1803. [[CrossRef](#)]
3. Kratky, H.; Li, Z.; Chen, Y.; Wang, C.; Li, X.; Yu, T. A critical literature review of bioretention research for stormwater management in cold climate and future research recommendations. *Front. Environ. Sci. Eng.* **2017**, *11*, 16. [[CrossRef](#)]
4. Khan, U.T.; Valeo, C.; Chu, A.; Van Duijn, B. Bioretention cell efficacy in cold climates: Part 2—Water quality performance. *Can. J. Civ. Eng.* **2013**, *39*, 1222–1233. [[CrossRef](#)]
5. Kim, H.; Seagren, E.A.; Davis, A.P. Engineered Bioretention for Removal of Nitrate from Stormwater Runoff. *Water Environ. Res.* **2003**, *75*, 355–367. [[CrossRef](#)]
6. LeFevre, G.H.; Paus, K.H.; Natarajan, P.; Gulliver, J.S.; Novak, P.J.; Hozalski, R.M. Review of Dissolved Pollutants in Urban Storm Water and Their Removal and Fate in Bioretention Cells. *J. Environ. Eng.* **2015**, *141*, 04014050. [[CrossRef](#)]
7. Paus, K.H.; Muthanna, T.M.; Braskerud, B.C. The hydrological performance of bioretention cells in regions with cold climates: Seasonal variation and implications for design. *Hydrol. Res.* **2016**, *47*, 291–304. [[CrossRef](#)]
8. Paus, K.H.; Braskerud, B.C. Forslag til dimensjonering og utforming av regnbed for norske forhold. *Vann.* **2013**, *1*, 54–67.
9. Gilbreath, A.; Mckee, L.; Shimabuku, I.; Lin, D. Multiyear Water Quality Performance and Mass Accumulation of PCBs, Mercury, Methylmercury, Copper, and Microplastics in a Bioretention Rain Garden. *J. Sustain. Water Built Environ.* **2019**, *5*, 1–10. [[CrossRef](#)]
10. Lefevre, G.H.; Novak, P.J.; Hozalski, R.M. Fate of naphthalene in laboratory-scale bioretention cells: Implications for sustainable stormwater management. *Environ. Sci. Technol.* **2012**, *46*, 995–1002. [[CrossRef](#)] [[PubMed](#)]
11. LeFevre, G.H.; Hozalski, R.M.; Novak, P.J. The role of biodegradation in limiting the accumulation of petroleum hydrocarbons in rain garden soils. *Water Res.* **2012**, *46*, 6753–6762. [[CrossRef](#)]
12. Roy-poirier, A.; Champagne, P.; Filion, Y. Bioretention processes for phosphorus pollution control. *Environ. Rev.* **2010**, *18*, 159–173. [[CrossRef](#)]
13. Brown, R.A.; Hunt, W.F. Improving bioretention/biofiltration performance with restorative maintenance. *Water Sci. Technol.* **2012**, *65*, 361–367. [[CrossRef](#)]
14. Roy-poirier, A.; Champagne, P.; Filion, Y. Review of bioretention system research and design: Past, present, and future. *J. Environ. Eng.* **2010**, *136*, 878–889. [[CrossRef](#)]
15. Kole, J.P.; Löhr, A.J.; Van Belleghem, F.G.A.J.; Ragas, A.M.J. Wear and tear of tyres: A stealthy source of microplastics in the environment. *Int. J. Environ. Res. Public Health* **2017**, *14*, 1265. [[CrossRef](#)]
16. Vogelsang, C.; Lusher, A.L.; Dadkhah, M.E.; Sundvor, I.; Umar, M.; Rannekleiv, S.B.; Eidsvoll, D.; Meland, S. *Microplastics in Road Dust—Characteristics, Pathways and Measures*; Norwegian Institute for Water Research: Oslo, Norway, 2018; 173p.
17. European Commission Directorate-General for Research and Innovation. *Environmental and Health Risks of Microplastic Pollution*; Publications Office of the European Union: Luxembourg, 2019. [[CrossRef](#)]
18. Kreider, M.L.; Sweet, L.I.; Panko, J.M.; McAtee, B.L.; Finley, B.L. Physical and chemical characterization of tire-related particles: Comparison of particles generated using different methodologies. *Sci. Total Environ.* **2009**, *408*, 652–659. [[CrossRef](#)]
19. Adachi, K.; Tainosho, Y. Characterization of heavy metal particles embedded in tire dust. *Environ. Int.* **2004**, *30*, 1009–1017. [[CrossRef](#)] [[PubMed](#)]
20. Cadle, S.H.; Williams, R.L. Gas and particle emissions from automobile tires in laboratory and field studies. *J. Air Pollut. Control Assoc.* **1978**, *28*, 502–507. [[CrossRef](#)]
21. Wagner, S.; Hüffer, T.; Klöckner, P.; Wehrhahn, M.; Hofmann, T.; Reemtsma, T. Tire wear particles in the aquatic environment—A review on generation, analysis, occurrence, fate and effects. *Water Res.* **2018**, *139*, 83–100. [[CrossRef](#)] [[PubMed](#)]
22. Andersson-Sköld, Y.; Johansson, M.; Gustafsson, M.; Järleskog, I.; Lithner, D.; Polukarova, M.; Strömvall, A.-M. *Microplastics from Tyre and Road Wear—A Literature Review*; Swedish National Road and Transport Research Institute: Linköping, Sweden, 2020. [[CrossRef](#)]
23. Smyth, K.; Drake, J.; Li, Y.; Rochman, C.; Van Seters, T.; Passet, E. Bioretention cells remove microplastics from urban stormwater. *Water Res.* **2021**, *191*, 116785. [[CrossRef](#)]
24. Klöckner, P.; Seiwert, B.; Weyrauch, S.; Escher, B.L.; Reemtsma, T.; Wagner, S. Comprehensive characterization of tire and road wear particles in highway tunnel road dust by use of size and density fractionation. *Chemosphere* **2021**, *279*, 130530. [[CrossRef](#)]
25. Lange, K.; Magnusson, K.; Viklander, M.; Blecken, G.T. Removal of rubber, bitumen and other microplastic particles from stormwater by a gross pollutant trap—Bioretention treatment train. *Water Res.* **2021**, *202*, 117457. [[CrossRef](#)] [[PubMed](#)]
26. Lange, K.; Österlund, H.; Viklander, M.; Blecken, G.T. Occurrence and concentration of 20–100 µm sized microplastic in highway runoff and its removal in a gross pollutant trap—Bioretention and sand filter stormwater treatment train. *Sci. Total Environ.* **2022**, *809*, 151151. [[CrossRef](#)] [[PubMed](#)]
27. Haraldsen, T.K.; Gamborg, M.; Vike, E. *Utvikling av Jordblandinger til regnbed i Drammen Pottetforsøk med Periodevis Vannmetning og Uttøking*; Norwegian Institute of Bioeconomy Research (NIBIO): Ås, Norway, 2019; Volume 5.
28. Statens Vegvesen. Vegkart. 2020. Available online: [https://vegkart-2019.atlas.vegvesen.no/#kartlag:geodata/hva:~{}\(farge:\T1\textquoteright0.id:643\)/hvor:\(kommune:~{}\(602\)\)/@243508,6627176,8/vegobjekt:1007532883:40a744:643](https://vegkart-2019.atlas.vegvesen.no/#kartlag:geodata/hva:~{}(farge:\T1\textquoteright0.id:643)/hvor:(kommune:~{}(602))/@243508,6627176,8/vegobjekt:1007532883:40a744:643) (accessed on 21 March 2021).
29. *Prosesskode 1: Standard Beskrivelse for Vegkontrakter*; Statens Vegvesen: Oslo, Norway, 2018.
30. Nilsen, V.; Christensen, E.; Myrmed, M.; Heistad, A. Spatio-temporal dynamics of virus and bacteria removal in dual-media contact-filtration for drinking water. *Water Res.* **2019**, *156*, 9–22. [[CrossRef](#)]

31. Mengistu, D.; Heistad, A.; Coutris, C. Tire wear particles concentrations in gully pot sediments. *Sci. Total Environ.* **2021**, *769*, 144785. [CrossRef]
32. Paus, K.H. Forslag til dimensjonerende verdier for trinn 1 i Norsk Vann sin tre-trinns strategi for håndtering av overvann. *Vannforeningen* **2018**, *1*, 66–77.
33. Unice, K.M.; Weeber, M.P.; Abramson, M.M.; Reid, R.C.D.; van Gils, J.A.G.; Markus, A.A.; Vethaak, A.D.; Panko, J.M. Characterizing export of land-based microplastics to the estuary—Part II: Sensitivity analysis of an integrated geospatial microplastic transport modeling assessment of tire and road wear particles. *Sci. Total Environ.* **2019**, *646*, 1650–1659. [CrossRef]
34. Mengistu, D.; Nilsen, V.; Heistad, A.; Kvaal, K. Detection and Quantification of Tire Particles in Sediments Using a Combination of Simultaneous Thermal Analysis, Fourier Transform Infra-Red, and Parallel Factor Analysis. *Int. J. Environ. Res. Public Health* **2019**, *16*, 3444. [CrossRef]
35. Baum, A.; Hansen, P.W.; Nørgaard, L.; Sørensen, J.; Mikkelsen, J.D. Rapid quantification of casein in skim milk using Fourier transform infrared spectroscopy, enzymatic perturbation, and multiway partial least squares regression: Monitoring chymosin at work. *J. Dairy Sci.* **2016**, *99*, 6071–6079. [CrossRef] [PubMed]
36. Thorpe, A.; Harrison, R.M. Sources and properties of non-exhaust particulate matter from road traffic: A review. *Sci. Total Environ.* **2008**, *400*, 270–282. [CrossRef]
37. Fernández-Berridi, M.J.; González, N.; Mugica, A.; Bernicot, C. Pyrolysis-FTIR and TGA techniques as tools in the characterization of blends of natural rubber and SBR. *Thermochim. Acta* **2006**, *444*, 65–70. [CrossRef]
38. Jusli, E.; Nor, H.M.; Jaya, R.P.; Zaiton, H. Chemical Properties of Waste Tyre Rubber Granules. *Adv. Mater. Res.* **2014**, *911*, 77–81. [CrossRef]
39. Ragn-Sells Gummigranulat. 2018. Available online: https://www.ragnsells.no/globalassets/norge/dokumenter/dekkgjenvinning/rs_pb_granulat_fin_v5-2018-01-16.pdf (accessed on 2 August 2020).
40. Panko, J.M.; Chu, J.; Kreider, M.L.; Unice, K.M. Measurement of airborne concentrations of tire and road wear particles in urban and rural areas of France, Japan, and the United States. *Atmos. Environ.* **2013**, *72*, 192–199. [CrossRef]
41. Unice, K.M.; Kreider, M.L.; Panko, J.M. Comparison of tire and road wear particle concentrations in sediment for watersheds in France, Japan, and the United States by quantitative pyrolysis GC/MS analysis. *Environ. Sci. Technol.* **2013**, *47*, 8138–8147. [CrossRef] [PubMed]
42. Sommer, F.; Dietze, V.; Baum, A.; Sauer, J.; Gilge, S.; Maschowski, C.; Gieré, R. Tire abrasion as a major source of microplastics in the environment. *Aerosol Air Qual. Res.* **2018**, *18*, 2014–2028. [CrossRef]
43. Murphy, K.R.; Stedmon, C.A.; Graeber, D.; Bro, R. Fluorescence spectroscopy and multi-way techniques. *PARAFAC. Anal. Methods* **2013**, *5*, 6557–6566. [CrossRef]
44. Bro, R.; Kiers, H.A.L. A new efficient method for determining the number of components in PARAFAC models. *J. Chemom.* **2003**, *17*, 274–286. [CrossRef]
45. Besseling, E.; Quik, J.T.K.; Sun, M.; Koelmans, A.A. Fate of nano- and microplastic in freshwater systems: A modeling study. *Environ. Pollut.* **2017**, *220*, 540–548. [CrossRef]
46. Klöckner, P.; Seiwert, B.; Eisentraut, P.; Braun, U.; Reemtsma, T.; Wagner, S. Characterization of tire and road wear particles from road runoff indicates highly dynamic particle properties. *Water Res.* **2020**, *185*, 116262. [CrossRef]
47. Eisentraut, P.; Dümichen, E.; Ruhl, A.S.; Jekel, M.; Albrecht, M.; Gehde, M.; Braun, U. Two Birds with One Stone—Fast and Simultaneous Analysis of Microplastics: Microparticles Derived from Thermoplastics and Tire Wear. *Environ. Sci. Technol. Lett.* **2018**, *5*, 608–613. [CrossRef]
48. Baensch-Baltruschat, B.; Kocher, B.; Stock, F.; Reifferscheid, G. Tyre and road wear particles (TRWP)—A review of generation, properties, emissions, human health risk, ecotoxicity, and fate in the environment. *Sci. Total Environ.* **2020**, *733*, 137823. [CrossRef] [PubMed]
49. Hallberg, M.; Renman, G. Suspended solids concentration in highway runoff during summer conditions. *Polish J. Environ. Stud.* **2008**, *17*, 237–241.
50. Thomson, N.; McBean, E.; Mostrenko, I.B.; Snodgrass, W. Characterization of Stormwater Runoff from Highways. *J. Water Manag. Model.* **1994**, *6062*, 141–158. [CrossRef]
51. Alem, A.; Elkawafi, A.; Ahfir, N.D.; Wang, H.Q. Filtration of kaolinite particles in a saturated porous medium: Hydrodynamic effects. *Hydrogeol. J.* **2013**, *21*, 573–586. [CrossRef]
52. Conley, G.; Beck, N.; Riihimäki, C.A.; Tanner, M. Quantifying clogging patterns of infiltration systems to improve urban stormwater pollution reduction estimates. *Water Res. X* **2020**, *7*, 100049. [CrossRef]
53. Hanvey, J.S.; Lewis, P.J.; Lavers, J.L.; Crosbie, N.D.; Pozo, K.; Clarke, B.O. A review of analytical techniques for quantifying microplastics in sediments. *Anal. Methods* **2017**, *9*, 1369–1383. [CrossRef]
54. Imhof, H.K.; Schmid, J.; Niessner, R.; Ivleva, N.P.; Laforsch, C.; Imhof, H.K.; Schmid, J.; Laforsch, C.; Ivleva, N.P. A novel, highly efficient method for the separation and quantification of plastic particles in sediments of aquatic environments. *Limnol. Oceanogr. Methods* **2016**, *10*, 524–537. [CrossRef]
55. Karlsson, T.M.; Ekstrand, E.; Threapleton, M.; Mattsson, K.; Nordberg, K.; Hassellöv, M. *Undersökning av mikrokräp längs bohuslänska stränder och i Sediment*; University of Gothenburg: Kristineberg, Sweden, 2019.

Supplementary Material

Concentrations and Retention Efficiency of Tire Wear Particles from Road Runoff in Bioretention Cells

Demmelash Mengistu ^{1,*}, Claire Coutris ², Kim Aleksander Haukeland Paus ¹ and Arve Heistad ¹

¹ Faculty of Science and Technology, Norwegian University of Life Sciences (NMBU), 1432 Ås, Norway

² Division of Environment and Natural Resources, Norwegian Institute of Bioeconomy Research (NIBIO), 1433 Ås, Norway

* Correspondence: demmelash.mengistu@nmbu.no

Table of Contents

Supplementary Materials Section S1. Particle size distribution of engineered soil	2
Supplementary Materials Section S2. PARAFAC model validity indicators	3
References	3

Supplementary Materials Section S1. Particle size distribution of engineered soil

The soil requirements for bioretention are unique: good infiltration capacity to drain excess water as well as water and nutrient retention to promote plant growth are required at the same time [27]. The physical and chemical properties of the soil used in the column experiment were analyzed by a commercial lab, Eurofins. The soil was classified as medium sand with pH 7.8, density of 1.4 g/cm³, low organic matter content (2 %), medium nutrient content (plant available phosphorus and potassium, as assessed by ammonium lactate (AL) extraction: P-AL 6 mg/100 g air dry soil and K-AL 10 mg/100 g air dry soil). Similar soil composition was reported in [27] to have sufficient air filled pores to drain high rainfall, making the mixture suitable for construction of bioretention cells in very wet areas with short dry periods. Grain size distribution of the engineered soil is presented in Fig. S1. A soil with this grain size distribution meets the Norwegian Road Administration guidelines (process 74.44) for constructions with soil intended for plant growth [29].

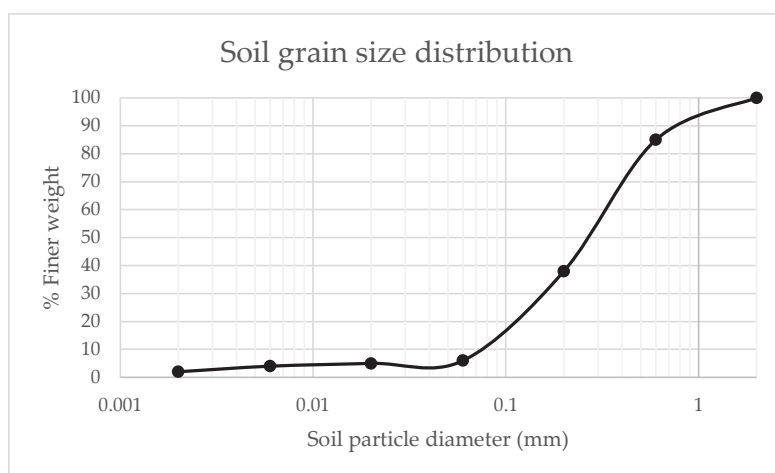


Figure S1. Grain size distribution of the engineered soil used in the column experiment prepared by mixing sand, silty-sand, and garden compost from Lindum AS, in a mass ratio of 8:15:6, respectively.

Supplementary Materials Section S2. PARAFAC model validity indicators

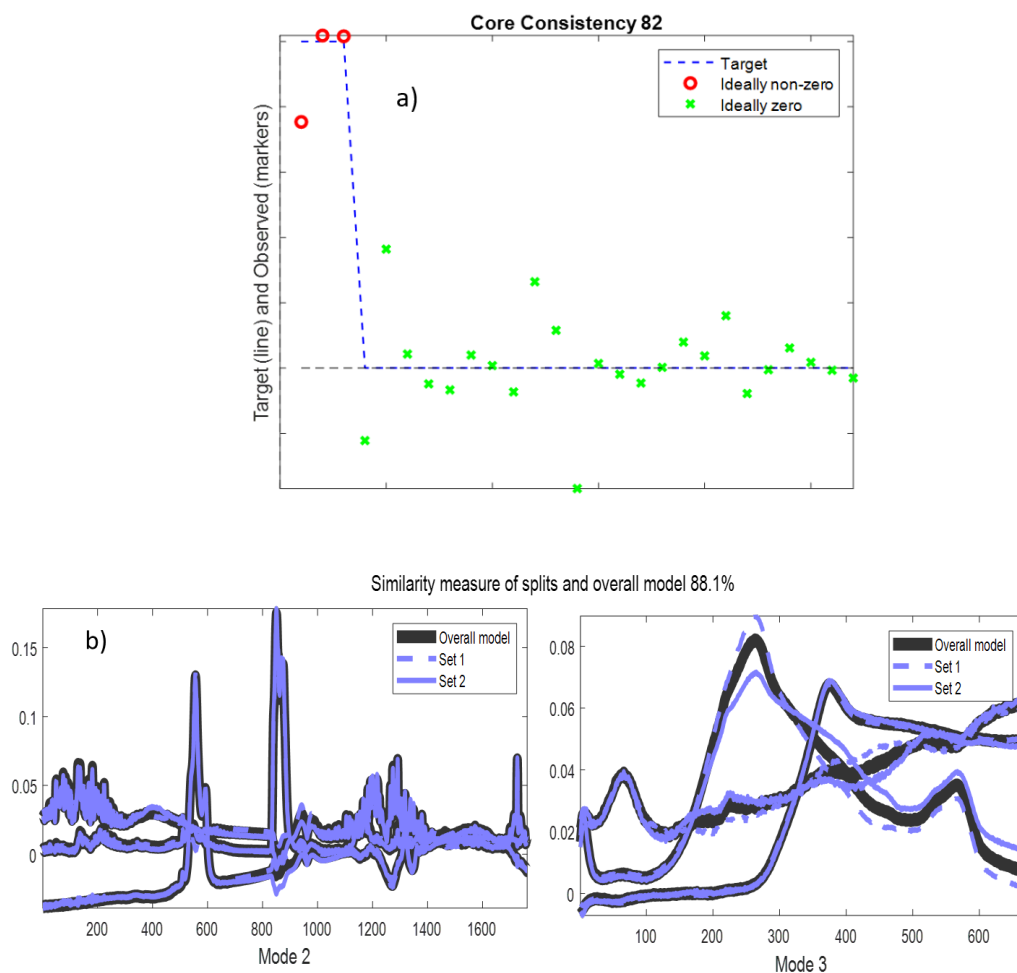


Figure S2. a) core consistency of 82 %, b) similarity measure of splits 88.1 %.

References

27. Haraldsen, T.K.; Gamborg, M.; Vike, E. *Utvikling av Jordblandinger til regnbed i Drammen Potteforsøk med Periodevis Vannmetning og Uttørring*. Norwegian Institute of Bioeconomy Research (NIBIO), Ås: 2019; Volume 5.
29. *Prosesskode 1: Standard beskrivelse for vegkontrakter, R761 Vegdir*. Oslo, 2018.

Mengistu, D., Nilsen, V., Coutris, C., Amdal, H., & Heistad, A. (2022) 'Microplastics concentration in soil along a racetrack', accepted for publication, the journal of *Water, Air, & Soil Pollution*.



Microplastics Concentrations in Soil Along a Racetrack

Demmelash Mengistu · Vegard Nilsen ·
Claire Coutris · Helena Marie Amdal ·
Arve Heistad

Received: 4 June 2022 / Accepted: 2 December 2022 / Published online: 20 December 2022
© The Author(s) 2022

Abstract Motorsport is known for its high tire wear due to speed, cornering, and high acceleration/deceleration activities. However, studies on the generation of microplastics from racetracks are rare. This study aimed at quantifying microplastics concentrations in topsoil (0–5 cm) along a racetrack. The results showed that rubber materials (RM) and tire reinforcement microplastics (TRMP) were deposited in the soil along the racetrack. Concentrations of the two microplastics were affected by the distance from the edge of the racetrack (highest concentrations within 20 cm from the track) and track alignment (highest concentrations at the start/finish area). In addition, a weak correlation was observed between the concentrations of the two microplastics, suggesting the effect of track alignment on the type of microplastics abraded. The results also showed that coarser microplastics (1000–5000 μm) dominate the size distribution of microplastics along a racetrack. The findings of this study may provide racetrack managers with basic information for designing microplastic-controlling solutions. While additional studies are required to map environmental

effects and policy measures, our initial results suggest that motorsport is of concern in terms of microplastics release to the environment.

Keywords Tire · Microplastics · Topsoil · Rubber

1 Introduction

Motorsport started in the early twentieth century, after the invention of the automobile. It occupies a highly important place in popular and sporting culture in the world (Dingle, 2009). There are about 130 local clubs and over 400 motorsport facilities registered in Norway alone (The Royal Norwegian Ministry of Culture & Equality, 2022). According to Michelin's engineers (Formula 1, 2021b), tire is an essential part of a racecar for safety and performance. Abrasion of tires is an inherent consequence of their use for all kinds of vehicles (Jekel, 2019). This process, at the interface of tires and road pavements, creates tire wear particles (TWP) (Wagner et al., 2018), which, in combination with other road particles, form tire and road wear particles (TRWP) (Panko et al., 2013). TWP generation is affected by multiple factors, like tire characteristics (size, tread depth, construction, tire pressure, and temperature, contact patch area, chemical composition, accumulated mileage, wheel alignment) and vehicle operation (speed, linear and radial acceleration, frequency and extent of braking and cornering) (Grigoratos & Martini, 2014; Gustafsson et al., 2008;

D. Mengistu (✉) · V. Nilsen · H. M. Amdal · A. Heistad
Faculty of Science and Technology, Norwegian University
of Life Sciences (NMBU), Ås, Norway
e-mail: demmelash.mengistu@nmbu.no

C. Coutris
Division of Environment and Natural Resources,
Norwegian Institute of Bioeconomy Research (NIBIO),
Ås, Norway

Jekel, 2019). High speed, fast acceleration and retardation, and high cornering speeds lead to increased tire wear (Pohrt, 2019). Dahl et al. (2006) studied the effects of speed on tire wear generation in a laboratory road simulator and found the speed to be the main factor in particle generation, as it determines mechanical stress and treads temperature. In addition, the size of the TWP generated decreased linearly with increasing temperature (Dahl et al., 2006). Therefore, it is expected that motor racing would lead to high deposition of TWP in the soil along the racetrack.

Racecar tires are composed of, among others, natural rubber (NR), styrene-butadiene rubber (SBR), carbon black or silica, sulfur, zinc oxide, antioxidants, and antiozonants (Formula 1, 2021a). Similar components constitute road tires (Grigoratos & Martini, 2014; Wik & Dave, 2009). However, race tires and road tires are very different and probably generate different TWP as car tires are made to last 40,000–50,000 km (Grigoratos & Martini, 2014; Parker-Jurd et al., 2019) while race tires, for example, Formula 1 tires, are designed to last for a maximum of 200 km (Formula 1, 2021b). Race tires are designed to withstand far larger forces than road car tires; for example, Formula 1 tires have to withstand massive forces of 6 *G* to decelerate and up to 5 *G* at cornering (Formula 1, 2021b), and potentially generate more TWP per vehicle kilometer compared to passenger cars. However, we are unaware of any prior studies on TWP concentrations in racetrack soils, the only related study being on the deposition of tire fragments from an ice racetrack (Ilgasheva et al., 2020).

This study aims to quantify the amount of TWP deposited in soils adjacent to the Rudskogen racetrack in Norway and assess whether track alignment and distance from the edge of the track influence microplastics concentrations in soil.

2 Materials and Methods

2.1 Study Area

Rudskogen racetrack is located in Southeastern Norway (Rakkestad, 59.368 N, 11.262 E) and was selected as Norway's leading motorsport facility. The main track is a 3-km-long asphalt track used for both motor racing and traffic training. The racetrack was opened for the first time in 1990 and was expanded

in 2011 to its current form. The driving direction is clockwise, and the track has a maximum elevation difference of 43 m. It has 14 corners and is 15–18 m wide. Verges along the track are made of grass-covered soil, gravel, or paved to the fence (Fig. 1). The width of the verge varies along the track, and at the selected sampling locations for this study, the width ranged from 2.8 m in the start/finish area to 40 m at the final corner. The track is swept after each race to remove tire debris.

2.2 Sampling

A total of four sampling locations were selected to represent different track alignments where TWP generation and transportation from the track surface to the verges was assumed to occur at different rates following linear speeding, radial acceleration, and braking. The sampling procedure was first described by Amdal (2021). The selected sampling locations (SF, LS, IC, and OC) are shown in Fig. 1, and the main wear-generating factors for these locations are indicated in Table 1.

At each sampling location, three sampling spots (A, B, and C) with an area of 20×20 cm each and center distances of 10, 110, and 270 cm from the edge of the track, respectively, were selected (Fig. 1). After collecting four topsoil (0–5 cm) samples from the corners of each sampling spot using a soil corer, a composite sample was prepared for each sampling spot. Samples were oven-dried at 105 °C overnight and homogenized using a not sharp-edged Kenwood kitchen blender KMM770 for 15 s. Bigger soil particles were removed by 5-mm mesh sieves before a sub-sample of 10 g was sieved sequentially with three different mesh sizes (1000 µm, 50 µm, and 25 µm) using a stainless-steel vibratory sieve shaker (Retac 3D, Retsch, Germany). After sieving, the three fractions (1000–5000 µm, 50–1000 µm, and 25–50 µm) were weighed using an analytical balance AT200 METTLER (Mettler-Toledo GmbH, Giessen, Germany) and the proportion of each size fraction was determined by dividing the mass of the specific size fraction by the total mass recovered after sieving. The majority (66.0%) of the soil sample was in the size fraction 50–1000 µm, while the size fractions 1000–5000 µm and 25–50 µm accounted for 23.4% and 2.8% by mass, respectively. Samples from the major size fraction (50–1000 µm) were analyzed in



Fig. 1 Overview of the Rudskogen racetrack with sampling locations; start/finish (SF), long straight drive (LS), inward curve (IC), and outward curve (OC). The large insert (picture) shows the three different sampling distances from the edge of

the track (A, 0–20 cm; B, 100–120 cm; C, 260–280 cm), and the small insert (schematic) shows the four sub-samples of top-soil taken for each of the three distances

Table 1 Description of the sampling locations

Code	Location	Wear-generating factors
SF	Start/finish	Acceleration/deceleration, the track is straight
LS	Long straight	Speed, no cornering
IC	Inward corner	Cornering
OC	Outward corner	Cornering

triplicate, whereas only one replicate was analyzed from size fractions 1000–5000 μm and 25–50 μm because of budget limitations—a total of 60 samples.

2.3 Data Acquisition and Modeling

Decomposition of Fourier transform infrared (FTIR) data of environmental samples using a parallel factor analysis (PARAFAC) model provides a mechanism to detect and quantify rubber materials (RM) among many components (Mengistu et al., 2019). Thermogravimetric and FTIR spectral data of the samples were generated using a simultaneous thermal analyzer STA 449 F1 Jupiter, with carrier type S (Netzsch, Germany), and a Fourier transform infrared spectrometer Bruker Tensor 27 with external gas cell (Bruker, USA) using the procedure described in (Mengistu et al., 2021). The STA registered changes

in mass while samples were heated from 40 to 800 °C and released gases to the FTIR. The FTIR scanned spectra of a wavenumber range between 4000 and 600 cm^{-1} for every batch of gas released from the STA with a resolution of 1.93 cm^{-1} , generating 1762 signal points. The FTIR data resulted in 666 spectra per sample, giving a total of 1.1 million data points per sample. The data was arranged in a trilinear multi-way dataset as outlined in Mengistu et al. (2021) to suit PARAFAC (Baum et al., 2016). PARAFAC models with 2 to 5 components were then built using MATLAB (The MathWorks, Inc., R2018a, Natick, USA) and a PLS Toolbox for MATLAB version 9.0 (Eigenvector Research, Inc., Wenatchee, USA). The PARAFAC analysis steps and model validation are presented in Mengistu et al. (2021).

From a valid PARAFAC model, scores were used to calculate the concentration of components (rubber materials (RM) and tire-reinforcing microplastics (TRMP)) in samples using Eq. 1 (Mengistu et al., 2021). RM are core components of tires (Thorpe & Harrison, 2008) and are good TWP markers (Wagner et al., 2018). Score values ≤ 0 were set to 0 in calculating concentrations. The limit of detection of the method is 0.7 mg/g, and therefore not likely to be affected by laboratory contamination for tire components.

$$C_f = (ml \times a_{if}) / (m \times S_i) \quad (1)$$

where

C_f concentration of the f^{th} component (mg/g)

ml sample mass loss during heating (mg)

m initial sample dry mass (g)

a_{if} score of f^{th} component of sample i extracted from PARAFAC

S_i sum of the score of components of sample i

2.4 Statistical Analysis

Differences in concentrations (in soil fraction 50–1000 μm) between racetrack locations and between distances from the edge of the racetrack were tested using two-way analysis of variance (ANOVA),

followed by a Tukey pairwise comparison test to identify differing locations and distances. The level of significance was set to 0.05.

3 Results and Discussion

3.1 Identifying Microplastics in Samples from the Racetrack

Microplastics along the racetrack were identified by analyzing the FTIR and pyrolysis temperature (mass loss) profiles of the components from the PARAFAC model. The PARAFAC model decomposed the data into three components, with 95% of the variation in the data captured by the variation in these components. The model showed 93% core consistency (Fig. 2a) and similarity of 71% in split-half analysis (Fig. 2b). Models with similar figures of merit are considered valid (Bro & Kiers, 2003; Murphy et al., 2013). However, the model fit and unique fit % showed differences in components 1 and 2, indicating overlap/data sharing between the two (Fig. 2c).

The FTIR spectra and pyrolysis temperature profiles of the three components are shown in Fig. 3a and b. Component 1 showed FTIR peaks typical for hydrocarbons (2927 and 2850 cm^{-1}). Other peaks (ca. 1500 and 700 cm^{-1}) were also visible. Pyrolysis temperature of component 1 showed the highest degradation at 456 °C. Another broad peak was observed at 610 °C (range 500–700 °C). Component 1 might have originated from the decomposition of other microplastics such as polyester or nylon, as they are common reinforcement synthetic fabrics in the tire industry, fitted under the tread (Tian et al., 2019). The presence of polyester or nylon is plausible because of the observed removal of pieces of rubber of different sizes and shapes shredded from tires, which might have exposed the underlying reinforcement materials. Although determining the component's identity with sufficient certainty is difficult, component 1 showed similar FTIR and pyrolysis temperature peaks to polyester (Bautista et al., 2017) than nylon (Charles et al., 2009). However, further study using gas chromatography–mass spectrometry (GC–MS) may help in achieving a more precise identification. This study uses tire-reinforcing microplastics (TRMP) to refer to this component. Component 2 mimicked the properties of RM, which is a typical marker for tires reported

Fig. 2 Figures of merit of the model: **(a)** core consistency, **(b)** similarity of split-half analysis, and **(c)** model fit and unique fit

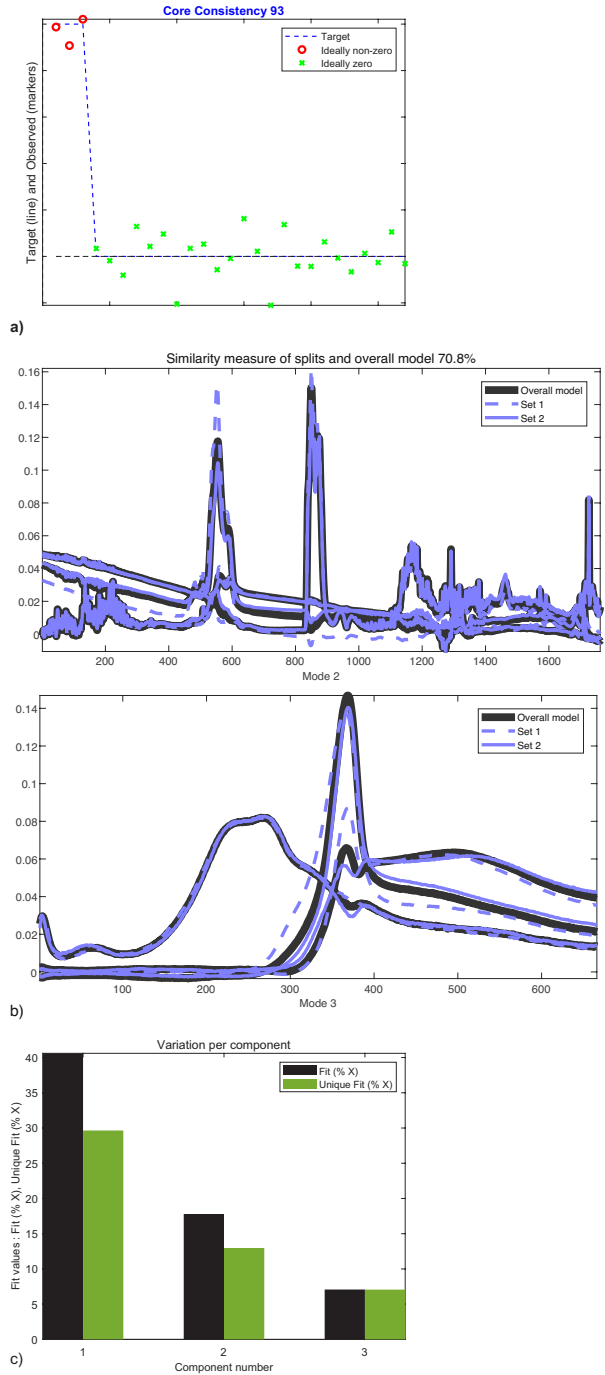
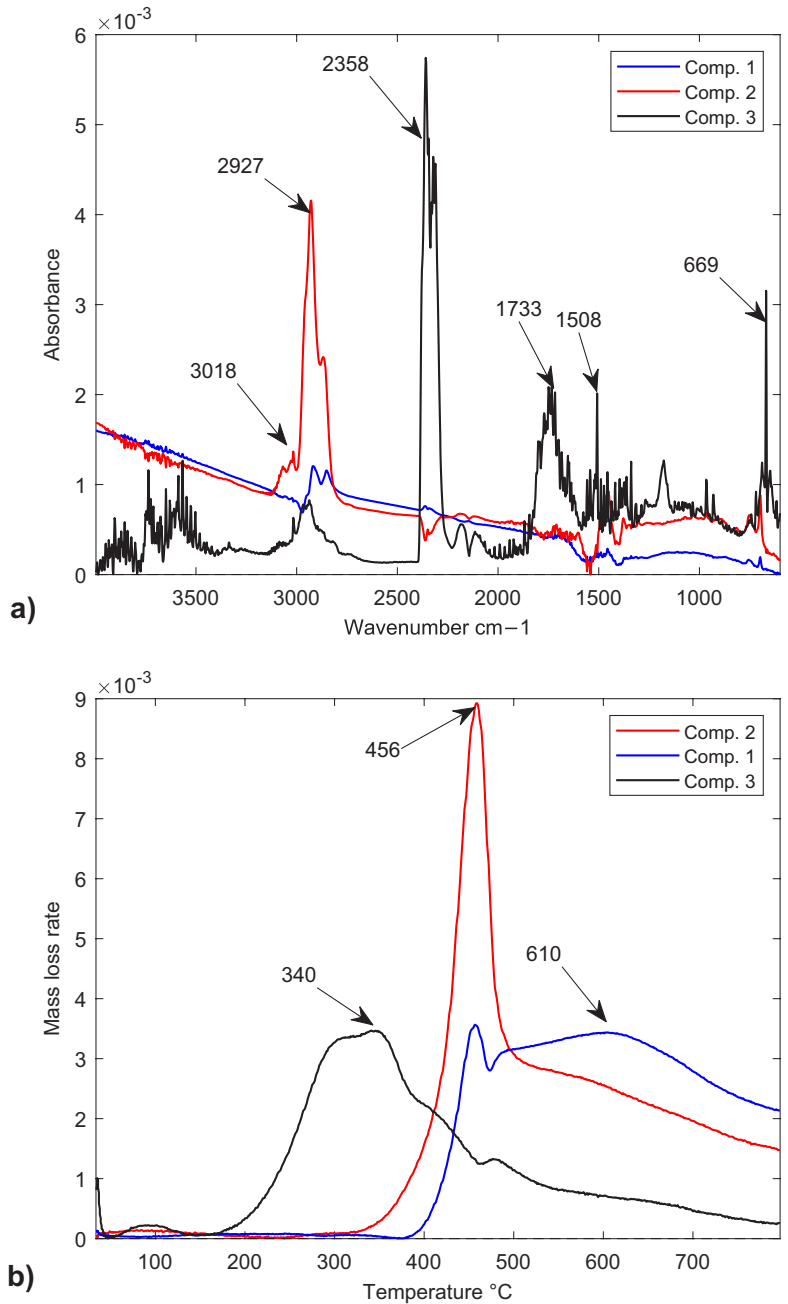


Fig. 3 Spectra for (a) FTIR and (b) pyrolysis temperature of the three components from the PARAFAC model. Component 1 (blue line) was identified as tire reinforcement microplastic (TRMP), component 2 (red line) was identified as rubber material (RM), and component 3 (black line) was identified as carbon dioxide and other substances. Peak numbers are typical identification markers



in Mengistu et al. (2019), indicating the deposition of TWP in the soil along the racetrack. Spectra of component 3 showed peaks mainly representing water and carbon dioxide. Additional signals, such as weak peaks at 3018, 2927, 2856 cm^{-1} , and a broad peak at 1733 cm^{-1} in the FTIR spectra, as well as peaks at ca. 340 and 456 $^{\circ}\text{C}$ in the mass loss profile, indicated the presence of degradation products from organic substances, likely plant materials, carbonyl-containing organic compounds, and bitumen (Kawamoto, 2017; Mohamed, 2016; Silverstein et al., 2015).

3.2 RM and TRMP Concentrations Along the Racetrack

RM and TRMP were detected at all locations (SF, LS, IC, and OC) and all distances from the edge of the racetrack (10, 110, and 270 cm). The normalized RM and TRMP concentrations (mg/g soil dw) are presented in Table 2.

RM concentrations in the soil size fraction 50–1000 μm (soil fraction analyzed in triplicates) showed statistically significant differences between the four locations ($F_{3,24}=10.56, p<0.001$), with RM concentrations significantly higher at SF, compared to the other locations (Tukey, $p<0.05$). Considering that braking and acceleration are associated with high wear generation, this finding agrees with Pohrt (2019), who reported that high-speed, fast

acceleration and retardation, and increased cornering speeds lead to increased tire wear. Mean concentrations in the soil size fraction 50–1000 μm showed statistically significant differences between the three distances from the edge of the racetrack ($F_{2,24}=19.24, p<0.001$), with higher RM concentrations 10 cm from the edge of the racetrack at locations SF and IC (Tukey, $p<0.05$).

Only 36% of the samples in soil size fraction 50–1000 μm showed detectable TRMP. The results of correlation analysis showed a weak ($R^2=0.12$) linear relationship between RM and TRMP concentrations indicating variations in factors influencing the generation of these two types of microplastics. TRMP concentrations in the soil size fraction 50–1000 μm did not show any significant differences, neither between the four locations (SF, LS, IC, and OC) ($F_{3,24}=0.18, p=0.91$) nor between distances from the edge of the racetrack ($F_{2,24}=1.56, p=0.23$).

Although the comparison cannot be evaluated statistically in the absence of replicates for the largest and lowest size fractions, it is interesting to notice that, close to the racetrack (0–20 cm), RM concentrations were the highest in the largest soil size fraction (1000–5000 μm), followed by the size fraction 50–1000 μm , and the lowest in the finest size fraction (25–50 μm), at all locations (Table 2 and Fig. 4a). Similarly, TRMP concentrations close to the racetrack were the highest in the largest size fraction, at

Table 2 Concentrations (mg/g) of rubber material (RM) and tire reinforcement microplastics (TRMP) in the three size fractions (25–50, 50–1000, and 1000–5000 μm). Concentrations in the size fraction 50–1000 μm are shown as mean \pm one stand-

ard deviation. Locations: SF, start/finish; LS, long straight; IC, inward curve; OC, outward curve. Asterisks indicate significant differences between the three distances from the edge (A, B, C), for each given location

Distance from the edge of the racetrack (cm)	Soil size fraction (μm)	Microplastics (mg/g)							
		Rubber materials (RM)				Tire-reinforcing microplastics (TRMP)			
		Locations				Locations			
		SF	LS	IC	OC	SF	LS	IC	OC
A (0–20)	1000–5000	123.9	22.9	62.9	67.9	36.4	23.1	134.0	109.1
	50–1000	66.8* \pm 25.5	5.9 \pm 3.5	28.8* \pm 6.7	8.9 \pm 5.0	0.0 \pm 0.0	10.6 \pm 18.4	0.0 \pm 0.0	2.0 \pm 3.4
	25–50	11.6	1.1	2.4	0.0	0.0	24.9	0.0	0.0
B (100–120)	1000–5000	41.2	0.0	0.0	33.8	0.0	5.9	0.0	78.1
	50–1000	2.7 \pm 1.5	2.3 \pm 0.8	1.6 \pm 3.4	19.7 \pm 2.6	22.8 \pm 18.8	1.8 \pm 3.0	10.9 \pm 9.6	6.8 \pm 11.8
	25–50	0.0	3.3	4.1	1.2	13.6	0.0	0.0	0.0
C (260–280)	1000–5000	0.0	0.0	4.4	4.1	8.3	0.0	4.9	25.5
	50–1000	8.8 \pm 3.8	2.3 \pm 2.0	3.6 \pm 2.6	25.8 \pm 10.0	0.0 \pm 0.0	0.2 \pm 0.4	10.7 \pm 14.4	8.8 \pm 15.2
	25–50	0.8	0.8	9.6	0.0	20.2	0.0	0.0	0.0

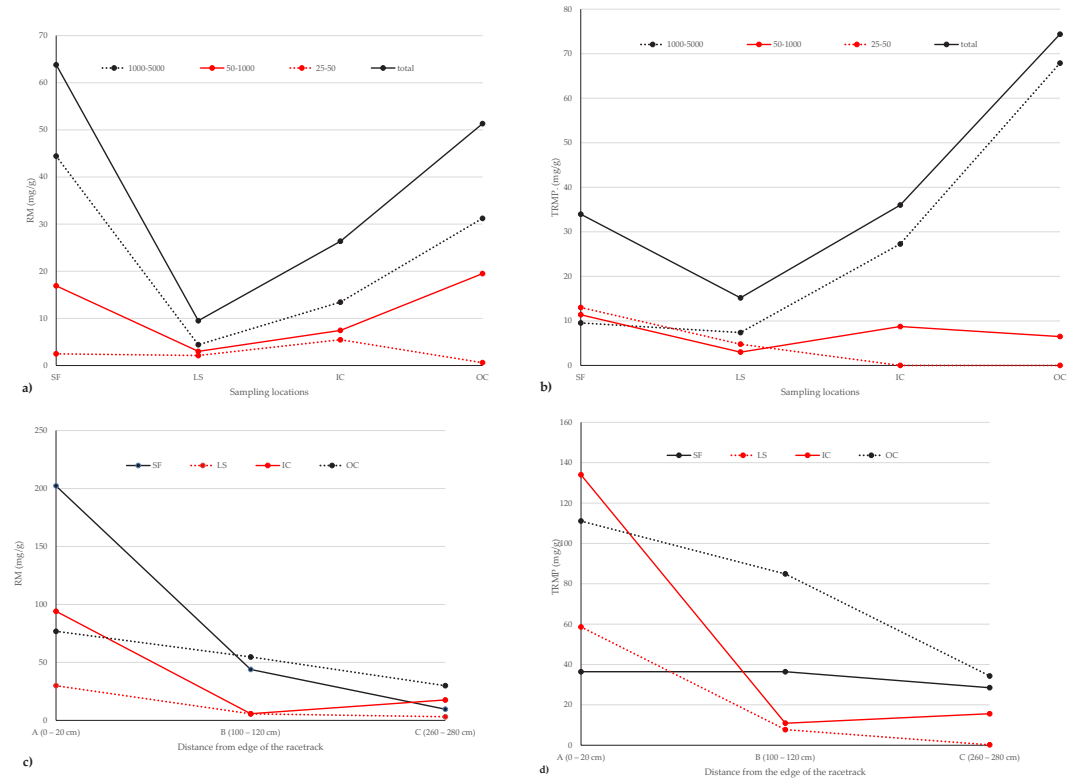


Fig. 4 Concentrations of microplastics in soil size fractions (25–50 μm , 50–1000 μm , and 1000–5000 μm) at different locations (start/finish, SF; long straight, SD; inward corner, IC; and outward corner, OC) along the Rudskogen racetrack. Distances from the edge of the racetrack: **A** (0–20 cm), **B** (100–

120 cm), **C** (260–280 cm). Concentrations of rubber material (RM) in mg/g soil dry weight are shown in (a) and (c), while concentrations of tire reinforcement microplastics (TRMP) in mg/g soil dry weight are shown in (b) and (d)

locations SF, IC, and OC (Table 2). The higher concentrations of RM and TRMP in the size fraction of 1000–5000 μm suggest that coarser particles are generated from racetrack usage than from road traffic, where TWP have been reported to be in the range of 5–350 μm (Kreider et al., 2009). The generation of coarser TWP from racing seems in line with the nature of racing itself, compared to road driving, and the composition of race tires, and was qualitatively confirmed by visual observations of marbles (pieces of rubber of different sizes and shapes shredded from tires) in the grass along the racetrack, up to 9 cm long, and with scorched surfaces. Given the presence of these large tire fragments, the reported photo- and biodegradability of TWP in the environment

(Baensch-Baltruschat et al., 2020), and the deposition of TWP over many years of racing, it is not here possible to determine the proportion of microplastics directly originating from racing from those produced by degradation and fragmentation of larger TWP. Further studies on the fate of TWP in soil along important TWP sources such as racetracks would bring valuable information.

RM concentrations, all size fractions considered, were 2.5–17 times higher at 20 cm from the edge of the racetrack than further away (Fig. 4c), suggesting that TWP mainly deposited within 20 cm from the edge of the track. The maximum RM concentration (202.4 mg/g) was observed at SF, followed by IC (94.2 mg/g) and lowest at LS (29.9 mg/g). The

decreasing trend with distance from the edge of the track was notable even though the distance studied was only 2.8 m. These results agree with the findings by Cadle and Williams (1978), who reported an exponential decrease in TRWP concentrations with distance from the edge of the road. RM concentrations at SF and IC were higher than the highest RM concentrations reported in gully pot sediments by Mengistu et al. (2021). Similarly, a decreasing concentration trend with increased distance from the edge of the racetrack was observed for TRMP (Fig. 4d).

3.3 Environmental Impact

The results showed the presence of RM in soil at concentrations 29.9–202.4 mg/g soil dw (all size classes included) within 20 cm from the edge of the racetrack (Table 2). Since, according to Grigoratos and Martini (2014) and Wik and Dave (2009), RM make 40–60% of treads, this corresponds to TWP concentrations in soil in the range 50–500 mg/g soil dw. If exposed to flooding, the soil along the racetrack could thus pose an environmental risk, as stormwater is reported to transport TWP to receiving water bodies (Johannessen et al., 2021; Kole et al., 2017; Tian et al., 2021). Acute (Khan et al., 2019; Wik & Dave, 2005, 2006) and chronic (Khan et al., 2019; Villena et al., 2017) toxic effects of TRWP are widely reported with a growing evidence of negative impacts. Some recent studies (e.g., Tamis et al., 2021) have demonstrated the environmental risk posed by TWP and other associated chemical substances from stormwater runoff in Europe. In addition, by-products of tire manufacturing additives are reported to be acutely toxic to some species. For example, the mass mortality of coho salmon (*Oncorhynchus kisutch*) in the streams of the Pacific Northwest region of the USA was attributed to 6ppd-quinone (a transformation product of N-(1,3-dimethylbutyl)-N-phenyl-p-phenylenediamine (6PPD)) (Tian et al., 2021). However, the toxicity reported might be species-specific as a recent study found no acute toxicity of 6ppd-quinone on other organisms or even other salmon species tested (chum salmon, *Oncorhynchus keta*) (McIntyre et al., 2021). The high TWP concentrations in topsoil observed in the present study suggest significant annual TWP deposition. This may lead to high inflow of microplastics into rivers, as mass flux studies in watersheds

showed that 50% of TRWP from roads reach freshwater systems if not treated (Unice et al., 2019). Since sweeping the racetrack after each race is the only treatment measure in the present case, it is possible that toxic effects could be observed in rivers receiving stormwater from the present study area, as sweeping is not considered effective in removing the finer microplastic particles (Janhäll et al., 2016). However, sweeping after the races may remove more TWP than reported in literature (Björklund et al., 2011; Janhäll et al., 2016) because of the high fraction of large-size microplastic particles observed in this study. Future studies on microplastics concentrations from race-track dust before and after sweeping as well as concentrations along the route to rivers should be considered to better understand annual fluxes.

4 Conclusion

This study demonstrated the presence of microplastics (RM and TRMP) in the soil along a racetrack. Although the two different types of microplastics were found together in most samples, the correlation observed between RM and TRMP concentrations was weak, suggesting the effect of track alignment on the type of microplastics abraded. Distance from the edge of the racetrack affected the concentrations of RM and TRMP, as concentrations decreased with increased distance, when all size fractions were considered. Track locations also affected TWP deposition, with the highest RM concentrations observed in soil alongside the Start/Finish area. The findings of this study could be of interest to racetrack managers in terms of planning microplastic management. Even though additional studies are required to map environmental effects and policy measures, our initial results suggest that motorsport is of concern in terms of microplastics release to the environment.

Acknowledgements Funding from the Norwegian Research Council (Grant number 194051), Norsk vannforening, Norges Motorsportforbund, and Notodden municipality is gratefully acknowledged. The idea for the work came from discussions with Knut Iver Skøien and Henrik Julius Frisak in Telemark Ring. The authors wish to thank Monica Fongen for the STA-FTIR analysis of the samples.

Author Contribution Conceptualization: Demmelash Mengistu, Vegard Nilsen and Helena Marie Amdal. Methodology: Demmelash Mengistu, Vegard Nilsen, and Helena Marie Amdal. Formal analysis: Demmelash Mengistu. Data curation: Demmelash Mengistu and Helena Marie Amdal. Writing—original draft preparation: Demmelash Mengistu. Writing—review and editing: Vegard Nilsen and Claire Coutris. Supervision: Arve Heistad. Funding acquisition: Vegard Nilsen, Claire Coutris, and Helena Marie Amdal.

Funding Open access funding provided by Norwegian University of Life Sciences

Data Availability The data analyzed during the current study are available from the corresponding author on reasonable request.

Declarations

Conflict of Interest The authors declare no competing interests.

Open Access This article is licensed under a Creative Commons Attribution 4.0 International License, which permits use, sharing, adaptation, distribution and reproduction in any medium or format, as long as you give appropriate credit to the original author(s) and the source, provide a link to the Creative Commons licence, and indicate if changes were made. The images or other third party material in this article are included in the article's Creative Commons licence, unless indicated otherwise in a credit line to the material. If material is not included in the article's Creative Commons licence and your intended use is not permitted by statutory regulation or exceeds the permitted use, you will need to obtain permission directly from the copyright holder. To view a copy of this licence, visit <http://creativecommons.org/licenses/by/4.0/>.

References

- Amdal, H. M. (2021) *Dekkslitasepartikler fra motorsportbaner: En første kartlegging og mulige tiltak [Tire wear particles from racetracks: A first assessment and possible measures]*. Norwegian University of Life Sciences (NMBU). Available at: <https://hdl.handle.net/11250/2833780>. Accessed May 2022
- Baensch-Baltruschat, B., et al. (2020). Tyre and road wear particles (TRWP) - a review of generation, properties, emissions, human health risk, ecotoxicity, and fate in the environment. *Science of the Total Environment*, *733*, 137823. <https://doi.org/10.1016/j.scitotenv.2020.137823>
- Baum, A., et al. (2016). Rapid quantification of casein in skim milk using Fourier transform infrared spectroscopy, enzymatic perturbation, and multiway partial least squares regression: Monitoring chymosin at work. *Journal of Dairy Science*, *99*(8), 6071–6079. <https://doi.org/10.3168/jds.2016-10947>
- Bautista, Y. et al. (2017). Thermal degradation mechanism of a thermostable polyester stabilized with an open-cage oligomeric silsesquioxane. *Materials*, *11*(22). <https://doi.org/10.3390/ma11010022>
- Björklund, K., Strömvall, A. M., & Malmqvist, P. A. (2011). Screening of organic contaminants in urban snow. *Water Science and Technology*, *64*(1), 206–213. <https://doi.org/10.2166/wst.2011.642>
- Bro, R., & Kiers, H. A. L. (2003). A new efficient method for determining the number of components in PARAFAC models. *Journal of Chemometrics*, *17*(5), 274–286. <https://doi.org/10.1002/cem.801>
- Cadle, S. H., & Williams, R. L. (1978). Gas and particle emissions from automobile tires in laboratory and field studies. *Journal of the Air Pollution Control Association*, *28*(5), 502–507. <https://doi.org/10.1080/00022470.1978.10470623>
- Charles, J., et al. (2009). FTIR and thermal studies on nylon-66 and 30% glass fibre reinforced nylon-66. *E-Journal of Chemistry*, *6*(1), 23–33. <https://doi.org/10.1155/2009/909017>
- Dahl, A., et al. (2006). Traffic-generated emissions of ultrafine particles from pavement-tire interface. *Atmospheric Environment*, *40*(7), 1314–1323. <https://doi.org/10.1016/j.atmosenv.2005.10.029>
- Dingle, G. (2009). Sustaining the race: A review of literature pertaining to the environmental sustainability of motorsport. *International Journal of Sports Marketing and Sponsorship*, *11*(1), 80–96. <https://doi.org/10.1108/ijms-11-01-2009-b006>
- Formula 1 (2021a). *Tire compound*. Available at: http://www.formula1-dictionary.net/tire_compound.html (Accessed: 12 September 2021a)
- Formula 1 (2021b). *What is the most important part of a racing car?* Available at: http://www.formula1-dictionary.net/most_important.html (Accessed: 12 September 2021b)
- Grigoratos, T. & Martini, G. (2014). Non-exhaust traffic related emissions. Brake and tyre wear PM. *Jrc Science And Policy Reports*. Luxembourg. <https://doi.org/10.2790/21481>.
- Gustafsson, M. et al. (2008). Properties and toxicological effects of particles from the interaction between tyres, road pavement and winter traction material. *Science of the Total Environment*, *393*(2–3). <https://doi.org/10.1016/j.scitotenv.2007.12.030>
- Ilgasheva, E. O. et al. (2020) Anthropogenic particles in the snow cover in the area of the ice race track. in *Minerals: Structure, Properties, Methods of Investigation*, 79–88. https://doi.org/10.1007/978-3-030-49468-1_11
- Janhäll, S. et al. (2016). *Utvärdering av städmaskiners förmåga att reducera vägdammsförrådet i gatu-och tunnelmiljöer i Trondheim [Evaluation of sweepers' ability to reduce road dust load in street and tunnel environments in Trondheim]*. Available at: <http://vti.diva-portal.org/smash/get/diva2:899278/FULLTEXT01.pdf>. Accessed April 2022
- Jekel, M. (2019). Scientific report on tyre and road wear particles, TRWP, in the aquatic environment. *Report - European Tyre & Rubber Manufacturers Association (ETRMA)*, pp. 1–35. Available at: <https://www.tyreandroadwear.com/news/scientific-report-on-tyre-and-road-wear-particles-trwp-in-the-aquatic-environment/>. Accessed May 2022
- Johannessen, C., et al. (2021). The tire wear compounds 6PPD-quinone and 1,3-diphenylguanidine in an urban

- watershed. *Archives of Environmental Contamination and Toxicology*, 0123456789, 2–10. <https://doi.org/10.1007/s00244-021-00878-4>
- Kawamoto, H. (2017). Lignin pyrolysis reactions. *Journal of Wood Science*, 63(2), 117–132. <https://doi.org/10.1007/s10086-016-1606-z>
- Khan, F. R., Halle, L. L., & Palmqvist, A. (2019). Acute and long-term toxicity of micronized car tire wear particles to *Hyalella azteca*. *Aquatic Toxicology*, 213, 105216. <https://doi.org/10.1016/J.AQUATOX.2019.05.018>
- Kole, P. J. et al. (2017). Wear and tear of tyres: A stealthy source of microplastics in the environment. *International Journal of Environmental Research and Public Health*, 14(10). <https://doi.org/10.3390/ijerph14101265>
- Kreider, M. L., et al. (2009). Physical and chemical characterization of tire-related particles: Comparison of particles generated using different methodologies. *Science of the Total Environment*, 408(3), 652–659. <https://doi.org/10.1016/j.scitotenv.2009.10.016>
- McIntyre, J. K., et al. (2021). Treading water: Tire wear particle leachate recreates an urban runoff mortality syndrome in Coho but not Chum salmon. *Environmental Science and Technology*, 55(17), 11767–11774. <https://doi.org/10.1021/acs.est.1c03569>
- Mengistu, D., Heistad, A., & Coutris, C. (2021). Tire wear particles concentrations in gully pot sediments. *Science of the Total Environment*, 769, 144785. <https://doi.org/10.1016/j.scitotenv.2020.144785>
- Mengistu, D. et al. (2019). Detection and quantification of tire particles in sediments using a combination of simultaneous thermal analysis, Fourier transform infra-red, and parallel factor analysis. *International Journal of Environmental Research and Public Health*, 16(18). <https://doi.org/10.3390/ijerph16183444>
- Mohomed, K. (2016). Thermogravimetric analysis (TGA) theory and applications. *TA Instruments*, 4–235. Available at: <http://webcache.googleusercontent.com/search?q=cache:2tG2B4rkrwJ:www.tainstruments.com/wp-content/uploads/CA-2016-TGA.pdf+&cd=20&hl=en&ct=clnk&client=firefox-b>. Accessed April 2022
- Murphy, K. R., et al. (2013). Fluorescence spectroscopy and multi-way techniques. PARAFAC. *Analytical Methods*, 5(23), 6557–6566. <https://doi.org/10.1039/c3ay41160e>
- Panko, J. M., et al. (2013). Measurement of airborne concentrations of tire and road wear particles in urban and rural areas of France Japan, and the United States. *Atmospheric Environment*, 72, 192–199. <https://doi.org/10.1016/j.atmosenv.2013.01.040>
- Parker-Jurd, F. N. F., et al. (2019). *Investigating the sources and pathways of synthetic fibre and vehicle tyre wear contamination into the marine environment*. The Department for Environment Food and Rural Affairs.
- Pohrt, R. (2019). Tire wear particles hot spots- review of influencing factors. *Mechanical Engineering*, 17(1). <https://doi.org/10.22190/FUME190104013P>. <http://casopisi.junis.ni.ac.rs/index.php/FUMechEng/article/view/4780/2923>
- Silverstein, M. R. et al. (2015). *Spectrometric identification of organic compounds*. 8th edn. Hoboken, New Jersey: John Wiley & Sons., Inc.
- Tamis, J. E., et al. (2021). Environmental risks of car tire microplastic particles and other road runoff pollutants. *Microplastics and Nanoplastics*, 1(1), 1–17. <https://doi.org/10.1186/s43591-021-00008-w>
- The Royal Norwegian Ministry of Culture and Equality (2022). *Motor sport facilities*. Available at: <https://www.anleggsregisteret.no/>. Accessed 20 April 2022
- Thorpe, A., & Harrison, R. M. (2008). Sources and properties of non-exhaust particulate matter from road traffic: A review. *Science of the Total Environment*, 400(1–3), 270–282. <https://doi.org/10.1016/j.scitotenv.2008.06.007>
- Tian, Z., et al. (2021). A ubiquitous tire rubber-derived chemical induces acute mortality in coho salmon. *Science*, 371(6525), 185–189. <https://doi.org/10.1126/science.abd6951>
- Tian, L., Wang, D., & Wei, Q. (2019). Study on dynamic mechanical properties of a nylon-like polyester tire cord. *Journal of Engineered Fibers and Fabrics*, 14(1800). <https://doi.org/10.1177/1558925019868807>
- Unice, K. M., et al. (2019). Characterizing export of land-based microplastics to the estuary - part I: Application of integrated geospatial microplastic transport models to assess tire and road wear particles in the Seine watershed. *Science of the Total Environment*, 646, 1639–1649. <https://doi.org/10.1016/j.scitotenv.2018.07.368>
- Villena, O. C., et al. (2017). Effects of tire leachate on the invasive mosquito *Aedes albopictus* and the native congener *Aedes triseriatus*. *PeerJ*, 9, 1–15. <https://doi.org/10.7717/peerj.3756>
- Wagner, S., et al. (2018). Tire wear particles in the aquatic environment - a review on generation, analysis, occurrence, fate and effects. *Water Research*, 139(March), 83–100. <https://doi.org/10.1016/j.watres.2018.03.051>
- Wik, A., & Dave, G. (2005). Environmental labeling of car tires—toxicity to *Daphnia magna* can be used as a screening method. *Chemosphere*, 58(5), 645–651. <https://doi.org/10.1016/J.CHEMOSPHERE.2004.08.103>
- Wik, A., & Dave, G. (2006). Acute toxicity of leachates of tire wear material to *Daphnia magna*—variability and toxic components. *Chemosphere*, 64(10), 1777–1784. <https://doi.org/10.1016/J.CHEMOSPHERE.2005.12.045>
- Wik, A., & Dave, G. (2009). Occurrence and effects of tire wear particles in the environment – a critical review and an initial risk assessment. *Environmental Pollution*, 157(1), 1–11. <https://doi.org/10.1016/J.ENVPOL.2008.09.028>

Publisher's Note Springer Nature remains neutral with regard to jurisdictional claims in published maps and institutional affiliations.

ISBN: 78-82-575-2045-8

ISSN: 1894-6402



Norwegian University
of Life Sciences

Postboks 5003
NO-1432 Ås, Norway
+47 67 23 00 00
www.nmbu.no